Aus der Klinik und Poliklinik für Mund-, Kiefer- und plastische Gesichtschirurgie
an der Universitätsmedizin Rostock

Translationale Ansätze im Screening neuer Anti-Tumor-Wirkstoffe zur Identifizierung metabolischer Tumormarker

Kumulative Habilitationsschrift
zur
Erlangung des akademischen Grades
rerum naturalium habilitatus / habilitata (Dr. rer. nat. habil.)
an der Universitätsmedizin Rostock

vorgelegt von Dr. rer. nat. Nadja Engel
geboren am 03.09.1979 in Rostock
Wohnhaft in Moltenow
Rostock, den 27.02.2019

https://doi.org/10.18453/rosdok_id00002631

Gutachter:

Prof. Dr. med. Dr. med. dent. Bernhard Frerich, Universitätsmedizin Rostock, Klinik und Poliklinik für Mund-, Kiefer- und Plastische Gesichtschirurgie

Prof. Dr. Michael Keusgen, Philipps-Universität Marburg, Institut für Pharmazeutische Chemie

Prof. Dr. Andreas Hensel, Westfälische Wilhelms-Universität Münster, Institut für Pharmazeutische Biologie und Phytochemie

Jahr der Einreichung: 2019

Jahr der Verteidigung: 2019

Jahr der Lehrprobe: 2020

Inhaltsverzeichnis

Synopsis

Die aktuellen Zahlen des deutschen Krebsinformationsdienst (www.krebsinformationsdienst.de/) dokumentieren rückwirkend für das Jahr 2014 476.120 Krebsneuerkrankungen in Deutschland. Für 2018 werden ca. 493.600 Neuerkrankungen prognostiziert. Aktuell steht Krebs als Todesursache an vierter Stelle in Deutschland. Angeführt wird die Liste der Krebsinzidenzen von dem Lungen-, Brust-, Kolonrektum- und Prostatakrebs, obwohl hier zwischen den Geschlechtern differenziert werden muss. Die globale Krebsstatistik spiegelt die deutsche Inzidenzverteilung wider (Bray et al., 2018). Eine Schätzung für das Jahr 2018 beschreibt 18,1 Millionen neue Fälle und 9,6 Millionen Krebstodesfälle.

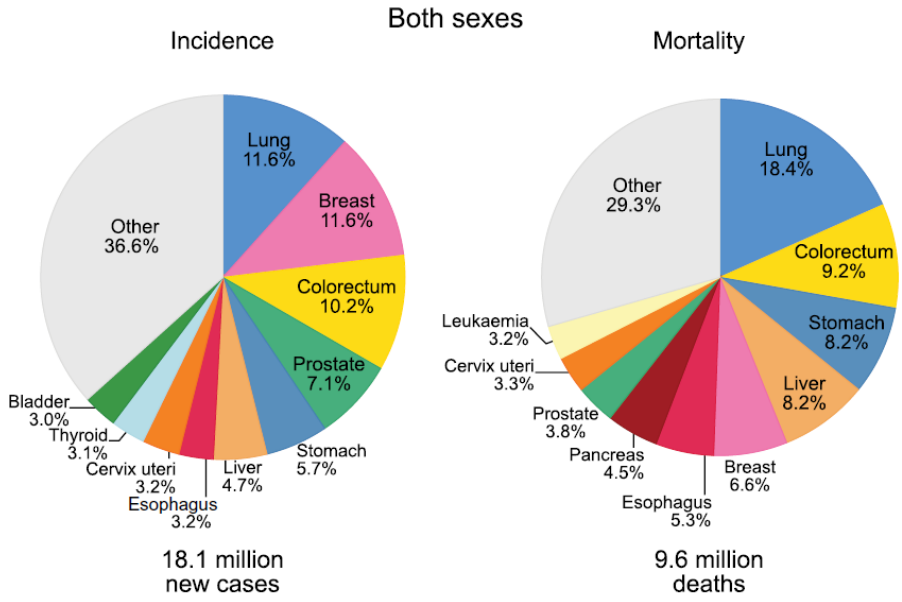

Abb. 1 Verteilung der Inzidenz- und Mortalitätsraten der häufigsten Krebsarten beider Geschlechter weltweit. Quelle: GLOBOCAN 2018 (Bray et al., 2018).

Neben der chirurgischen Intervention, der radiologischen Behandlung und immer bedeutsamer werdenden Immuntherapie ist die Chemotherapie eine Hauptsäule der Krebsbehandlung. Die antineoplastische Chemotherapie ist meistens eine zytostatische Behandlung von Krebserkrankungen, die kurativ, adjuvant oder palliativ angewendet wird. Zytostatika sind Monosubstanzen natürlichen oder synthetischen Ursprungs, die die Proliferation der Tumorzellen inhibieren. Zum Beispiel werden Substanzen der Gruppe der Taxane, die durch ein großangelegtes Screening am US-amerikanischen Nationalen Krebsinstitut (National Cancer Institute) von 35.000 Pflanzengattungen in 1960er Jahren entdeckt wurden (Wall und Wani, 1995), zunehmend bei der Therapie von Brust-, Prostata- und Lungenkrebs und Hautkrebs eingesetzt (www.krebsgesellschaft.de). Deren Wirkmechanismus beruht auf der Störung der Mikrotubuli-Degradation, wodurch das Zytoskelett stabilisiert wird und die Zellen

teilungsunfähig sind (https://www.bionity.com/en/encyclopedia/Paclitaxel.html#_note-2/). Aber auch sich schnell teilende gesunde Zellen, wie z. B. Epithelzellen werden teilungsunfähig, wodurch schwere Nebenwirkungen, wie Knochenmarksuppression (Thrombozytopenie, Neutropenie, Anämie), Neuropathien, Myalgien, Haarausfall, gastrointestinale Nebenwirkungen (z. B. Übelkeit, Erbrechen, Durchfall) auftreten können (Alves et. al., 2018). Somit besteht die Notwendigkeit, neue Wirkungsstoffe mit anti-tumorigenen Potential zu identifizieren, um zum einen Nebenwirkungen zu reduzieren und zum anderen das personalisierte Therapiekonzept zu optimieren. Der ideale Anti-Tumorwirkstoff beschreibt eine selektive Wirkung auf den Tumor mit einem Minimum an zytotoxischen Eigenschaften für das gesunde Gewebe und/oder negativer Einflussnahme auf das humane Immunsystem. Bisher wurden weltweit nur 15 % der höheren Pflanzen bezüglich ihrer bioaktiven Inhaltsstoffe untersucht. Somit ist ein systematisches Anti-Tumor-Screening traditionell genutzter Heilpflanzen sehr bedeutsam für die Identifizierung neuer Anti-Tumor-Wirkstoffe in der Therapie und Prävention von neoplastischen Erkrankungen. Diese Arbeit beschreibt die Optimierung von Screeningverfahren, um selektiv wirksame Monosubstanzen und Mehrstoffgemische zu isolieren. Weiter wird die Wirkungsweise durch zelluläre, biochemische und molekularbiologische Methoden beschrieben, um die zellulären Targets der Substanzen zu ermitteln. Dadurch lassen sich auch potenzielle neue Tumormarker ableiten. Daraus ergeben sich die drei Hauptziele dieser Arbeit:

1. Die Optimierung der *in vitro* Anti-Tumor-Screening-Verfahren zur ersten Abschätzung der allgemeinen Zytotoxizität und Anti-Tumor Eigenschaften.
2. Vom pflanzlichen Vielstoffgemisch zur Einzelsubstanz: Isolierung neuer, spezifischer und selektiver Anti-Tumor-Wirkstoffe mit dem Potential, als Chemotherapeutikum zugelassen zu werden.
3. Die Identifizierung validierbarer, metabolischer Tumormarker zur Bewertung des Patienten-Outcomes.

Um diese ambitionierten Ziele zu erreichen, war es notwendig, ein Konsortium an Kooperationspartnern unterschiedlicher Fachrichtungen zusammenzuführen. Das Fundament für die Errichtung eines groß-vernetzten Kooperationskonsortiums legten wir durch einen Forschergruppenantrag (Projektnummer: 107820), der 2010 durch die Deutsche Krebshilfe „Mildred Scheel“ gefördert wurde. Dieses Projekt war darauf ausgerichtet, einheimische Heilpflanzen, wie z. B. Sanddorn, Lein, Brennnessel hinsichtlich ihrer antineoplastischen Wirkung durch *in vitro* Studien zu untersuchen. Durch die Vernetzung mit der Naturheilkunde (Frau Prof. Dr. K. Kraft), der Technischen und Organischen Chemie (Herr Prof. Dr. Kragl, Herr Prof. Dr. Langer), der Biochemie (Frau Prof. Dr. Piechulla), der Frauenklinik (Herr Prof. Dr. Briese) und der Zellbiologie (Frau Prof. Dr. Nebe) der Universität und Universitätsmedizin Rostock konnten wir ein multidisziplinäres Team etablieren, das

durch eine große Anzahl an gemeinsamen Veröffentlichungen den Erfolg dieses Projektes dokumentiert. Durch persönlich initiierte Kooperationen mit der Pharmazeutischen Chemie in Benin, Nigeria (Herr Prof. Dr. Falodun), der Chemischen Fakultät in Gilgit-Baltistan, Pakistan (Herr Prof. Dr. Iftikhar Ali), der Allgemeinen und Speziellen Botanik der Universität Rostock (Herr Prof. Dr. Porembski) sowie der Abteilung für Agrarkultur in Neapel, Italien (Herr Dr. Rosario Nicoletti) gelang es mir, die Screenings auf internationale Heilpflanzen auszudehnen. Auf Empfehlung von traditionellen „Heilern", Pharmazeuten und Komplementärmedizinern aus benannten Ländern wurde ein großes Panel an Pflanzenextrakten hinsichtlich ihrer Anti-Tumor Eigenschaften untersucht.

Um die anti-kanzerogene Wirkung von Monosubstanzen und Vielstoffgemischen zu evaluieren, werden sehr oft *in vitro* Schnelltests, wie MTS (z. B. Cell Titer Promega), LDH und BrdU eingesetzt. Diese Tests eignen sich als Vorscreening-Methoden, geben aber keinen direkten Rückschluss auf die Wirkungsweise der zu testenden Substanz. Auch die auf der Grundlage dieser Tests berechneten IC_{50}-Werte variieren stark und weichen oft von der tatsächlichen inhibitorischen Konzentration ab. 2011 veröffentlichten McGowan et al. einen fundamentalen Übersichtsartikel zu den „Pitfalls of the MTS Assay". Durch eine vergleichende Betrachtung von günstigen, handelsüblichen *in vitro* Schnelltests zur Beurteilung der Zellvitalität, -proliferation und Apoptose konnte McGowan et al. belegen, dass eine Kombination aus metabolischen Analysen und DNA-Markierungsexperimenten für ein effizientes Anti-Tumor-Screening am besten geeignet ist. Meine Empfehlung für ein valides Anti-Tumor-Screening wird noch erweitert und umfasst das Messen der metabolischen Aktivität, die prozentuale Bestimmung der Zellzyklusphasen, der Nachweis der Apoptose/Nekrose sowie die morphologische Analyse. Aktuell empfehle ich folgende Vorgehensweise im Anti-Tumor-Screening unbekannter Wirkstoffe und Wirkstoffgemische:

i. Behandlungskonzeption

Im initialen Vorscreening mit den potenziellen Wirkstoffen sollten die Tumorzellen in Zellkulturmedium ohne Phenolrot und mit Aktivkohle-absorbierten Serum inkubiert werden. Das Phenolrot, das in der Regel dem Zellkulturmedium als pH-Indikator zugesetzt wird, kann durch die phenolische Struktur Östrogen-ähnliche Reaktionen auslösen (Welshons et al., 1988). In der Regel wird fötales Kälberserum zur Supplementierung des Zellkulturmediums verwendet. Da die Wirkungsweise des neuen Wirkstoffes noch nicht bekannt ist, ist es sinnvoll, die im Serum enthaltenen Hormone, z. B. durch Aktivkohle zu entfernen. Große Schwankungen, z. B. im Östrogengehalt in den jeweiligen Serum-Chargen wurde in Kooperation mit der Technischen Chemie, Universität Rostock ermittelt. Eine nicht-tumorigene Kontrollzelllinie oder primäre Kontrollzellen sollten als Negativreferenz immer mitgeführt werden.

ii. Methoden

Für das initiale Screening sollten mindestens vier zelluläre Prozesse untersucht werden (Abb. 2).

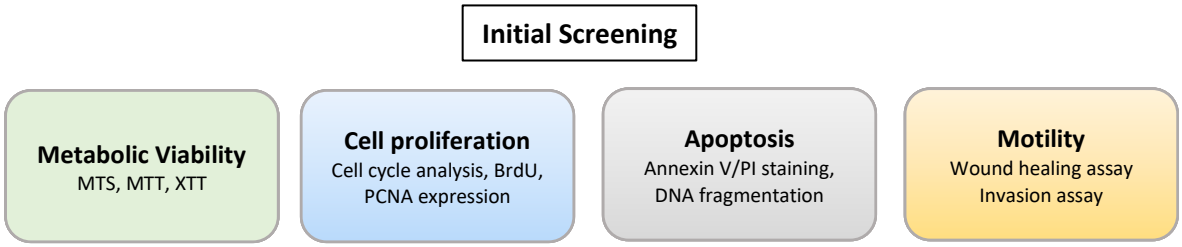

Abb. 2 Übersicht der vier zellulären Prozesse, die beim initialen Anti-Tumor-Screening untersucht werden sollten. Mögliche Methoden sind dazu annotiert.

1. Der Zellstoffwechsel - dafür eignen sich kostengünstige Schnelltests, wie z. B. der MTS-Assay. Eine Kontrollgruppe ohne das Vorhandensein der Tumorzellen muss immer mitgeführt werden, um das oxidative/reduktive Potential des Wirkstoffes zu ermitteln.
2. Die Zellproliferation kann durch Ermittlung der Zellzyklusphasen, BrdU-Markierung oder PCNA-Expression bestimmt werden. Durch die Interkalation der DNA mit Propidium-Jodid (PI) und sich anschließender Berechnung der Zellzyklusphasen am Durchflusszytometer ist eine gleichzeitige Determinierung G2-Aresten und DNA-Strangbrüchen in der sub-G1-Phase möglich.
3. Die Apoptose (der induzierte Zelltod) kann durch Bestimmung der DNA-Fragmentierung am Durchflusszytometer, Hoechst-Färbung oder DNA-Gelelektrophorese nachgewiesen werden. Auch Lebend-Tod-Färbungen mit Annexin V/PI eignen sich zur Detektion apoptotischer Tumorzellen.
4. Die Zellbeweglichkeit, die u. a. das Migrations- und Invasionspotential einer Tumorzelle beschreibt, kann initial durch einfache Wound-healing- (Scratch-Assay) oder Invasions-Assays (Transwell) dokumentiert werden.

Eine Betrachtung dieser vier zellulären Parameter ermöglicht ein umfassendes *in vitro* Anti-Tumor-Screening zur ersten Abschätzung des zytotoxischen und anti-tumorigenen Potentials der verwendeten Substanz oder des Vielstoffgemisches. Darüber hinaus kann eine erste Eingrenzung der Wirkungsweise erfolgen. Daraus leiten sich anschließende Experimente zur Identifizierung der zellulären Wirkungsweise ab.

Im Rahmen dieser Habilitation wurden u. a. drei Vielstoffgemische (Pflanzenextrakte) und eine Einzelsubstanz isoliert, die das Potential als Wirkstoff in der standardisierten Tumortherapie besitzen:

<u>Pflanzenextrakte:</u>

- der ethanolische Wurzelextrakt des einheimischen Gemeinen Leins (*Linum usitatissimum*) (Engel et al., 2015)
- der methanolische Wurzelextrakt des pakistanischen Strauchs *Berberis orthobotrys* Bien. ex Aitch (Engel et al., 2016)
- der methanolische Wurzelextrakt des pakistanischen Strauchs *Vincetoxicum arnottianum* (Engel et al., 2016)

Einzelsubstanz:

- 4-hydroxy-5-methylene-3-undecyclidenedihydrofuran-2(3H)-one aus der Wurzel des nigerianischen Avocadobaums (*Persea americana*) (Engel et al., 2011; Falodun et al., 2013)

Der Leinwurzelextrakt in seiner gesamten Wirkstoffkomposition stabilisiert das Zytoskelett von Mammakarzinomzellen und bewirkt dadurch das Aufbrechen des Tumorzellverbandes (Engel et al., 2015). Das Alken-Lakton der Avocadowurzel induziert bereits in sehr geringen Konzentrationen (0,1 - 1 µg/ml) Apoptose bei verschiedensten Tumorarten (Engel et al., 2011; Falodun et al., 2013). Auch der Berberis-Wurzelextrakt führt zum induzierten Zelltod bei Knochenkrebszellen, allerdings durch die Lysosomen-vermittelten Signalkaskaden (Engel et al., 2016). Der Vincetoxicum-Pflanzenextrakt vermittelt einen G2/M-Arrest im Zellzyklus, hervorgerufen durch eine gesteigerte Aktin-Stressfaser-Polymerisierung, so dass die Tumorzellen nicht mehr teilungsfähig sind (Engel et al., 2016). Diesen drei pflanzlichen Vielstoffgemischen und der beschriebenen Einzelsubstanz ist gemein, dass die Vitalität der gesunden Kontrollzellen gar nicht oder nur in sehr hohen Konzentrationen negativ beeinflusst wird. Durch das Screening von hunderten Pflanzenextrakten kristallisierte sich unter anderem heraus, dass insbesondere die Extrakte aus den heterotrophen Pflanzenorganen, wie z. B. die Wurzel, die Kotyledonen oder auch die Rinde ein hohes anti-tumorigenes Potential besitzen. Dies liegt darin begründet, dass die Wurzel als Fraßschutz, zu der Abwehr vor Parasitenbefall und zur Kompensation von abiotischem Stress höhere Konzentrationen an sekundären Wirkstoffen synthetisieren muss (Harborne, 1983). Weiter zeigte sich, dass die meisten Pflanzenextrakte nur in ihrer natürlichen Zusammensetzung anti-tumorigenes Potential zeigen. Durch chemische Analysen konnte nachgewiesen werden, dass die sekundären, chemischen Modifikationen, wie z. B. Glykosylierungen durch pflanzliche Enzyme entscheidend zu der anti-tumorigenen Aktivität der Wirkstoffe beitragen. Außerdem konnten wir zeigen, dass biphasische Wirkungen, wie z. B. die konzentrationsabhängige Proliferationsstimulation und -repression von dem Hauptsojainhaltstoff Genistein durch die Verwendung eines Genistein-haltigen natürlichen Pflanzenextraktes, wie z. B. dem Leinwurzelextrakt vermieden werden können (Engel et al., 2015).

Die in Kooperation mit Herrn Prof. Falodun (Pharmazeutisches Institut, Universität Benin, Nigeria) identifizierte Einzelsubstanz 4-hydroxy-5-methylene-3-undecyclidenedihydrofuran-2(3H)-one ist das einzige Isolat, das auch in isolierter Form eine sehr starke anti-tumorigene Aktivität verursacht. Der IC_{50}-Wert wurde für hormonabhängige Brustkrebszellen mit einem Wert von 20,48 µg/µl determiniert: entspricht einer starken spezifischen Zytotoxizität (Falodun et al., 2013). Diese Zytotoxizität konnte aber nicht für nicht-tumorigenen Kontrollzellen nachgewiesen werden. Im Gegenteil, es zeigte sich ein positiv stimulierender Effekt. Dieses neuartige Alken-Lakton empfiehlt sich daher für weitere Studien am murinen Xenograftmodell.

Um die spezifische Wirkungsweise ausgewählter Substanzen (Genistein) und Vielstoffgemische (Leinwurzelextrakt) noch detaillierte zu bestimmen, wurden metabolische Untersuchungen mittels Metabolomics ergänzt (Engel et al., 2012, 2017; Lisec et al., 2006). Diese Untersuchungen ermöglichen die Analyse verschiedener Stoffwechselwege durch Erfassung primärer und sekundärer Stoffwechselmetabolite. Diese Metabolite stellen auch putative Tumormarker dar, die im Tumorgewebe, im Blut oder Urin nachgewiesen werden können. Denn zum heutigen Zeitpunkt ist die Schwachstelle vieler etablierter Tumormarker, dass diese erst bei fortgeschrittener Erkrankung detektiert oder durch weitere Erkrankungen und/oder Lebensgewohnheiten, z. B. durch Rauchen für CEA (Kolorektale Karzinome) oder Alkoholabusus für CA 125 (Ovarialkarzinom), erhöht werden. Auch das PSA: „prostate specific antigen“, das zur Messung von Prostatakrebs bei Männern verwendet wird, hat den Nachteil, dass es sowohl bei benignen als auch tumorigenen Konditionen erhöht vorliegen kann. Die meisten Männer mit erhöhten PSA-Gehalt haben allerdings keinen Prostatakrebs, und bis zu 30 % aller Männer mit normalen PSA-Werten haben Prostatakrebs (Perkins et. al., 2003). Daraus resultieren viele Falsch-positive oder -negative Befunde. Letztlich konnten zwei große, randomisierte Studien belegen, dass das PSA-Screening die Sterblichkeit durch Prostatakrebs nur minimal reduziert (Taneja, 2015; Bublak, 2014). Die Identifizierung neuer Tumormarker mit hoher Spezifität zur Tumor-Prädiktion, Verlaufskontrolle und Bewertung der Patienten-Outcome nimmt einen besonderen Stellenwert in der onkologischen Forschung ein.

Metabolische Tumormarker treten immer mehr in den Fokus der onkologischen Forschung, denn die metabolische Re-Programmierung ist ein Meilenstein des Tumordifferenzierungsprozesses. Dadurch rückte z. B. der Glycin-Stoffwechsel von Tumorzellen, insbesondere die Glycin-Serin-Interkonversion und der damit assoziierte C1-Metabolismus zur Generierung von Purinen in den Fokus der onkologischen Forschung. Dies belegt eindrucksvoll die Arbeit von Jain et al. (2012), die bei 60 Tumorzelllinien (NCI-60 panel; CORE Profile von 219 Metaboliten) eine Präferenz für einen gesteigerten Glycin-Verbrauch nachweisen konnten. Daraus abgeleitet konnten sie auf eine gesteigerte Mortalitätsrate bei Mammakarzinom-Patientinnen mit einer überdurchschnittlich hohen

Expression der in der mitochondrialen Glycin-Biosynthese involvierten Enzyme schließen (Metaanalyse von sechs Datensätzen mit einer Hazard-Ratio von 1,82; 95% CI:143-2.31), welche mit weiteren Faktoren wie Lymphknotenstatus und Tumorgrad kongruent waren und so den Rückschluss auf eine schlechte Prognose bestätigte. Auf ähnliche Weise identifizierten Zhang et al. (2012) Enzyme des Glycin-Decarboxylase System als zentrale Schaltstelle für TICs (tumor initiating cells) im Nicht-kleinzelligen Bronchialkarzinom. Auch hier konnten die *in vitro* Untersuchungen durch die Analyse von Gewebematerial bestätigt werden: eine aberrante Aktivierung der Glycindecarboxylase korreliert mit einer schlechten Überlebensrate bei Lungenkrebspatienten. In einer kürzlich erschienenen Studie wurden auch neue potenzielle Biomarker zur Unterscheidung verschiedener Sarkom-Subtypen (hochgradiges Osteosarkom, Leiomyosarkom, Myxofibrosarkom und undifferenziertes pleomorphes Sarkom) mittels MALDI-MSI (Matrix-assisted laser desorption ionization mit MS imaging) untersucht. Hierbei wurden 20 Proteine (z. B. Acyl-CoA-Bindeproteine, Galectin-1) identifiziert, die spezifisch für die einzelnen Subtypen, und 9 Proteine (Proteasom-Aktivator-Komplex, Histon-H4-Varianten) die spezifisch mit dem Gesamtüberleben assoziiert sind (Lou et al., 2016).

Für die Identifizierung potenzieller, metabolischer Tumormarker bedienten wir uns der Metabolomics-Technologie. Insbesondre Metabolite des Sphingolipid-Stoffwechsels, wie das Sphingosin, Sphingosin-1-Phopshat (S1P) oder Ethanolamin wurden während der Tumorigenese stark reguliert (Engel et al., 2012, 2017; Warsow et al., 2013). In weiterführenden Arbeiten, konnten wir zeigen, dass primär die Sphingosin-1-Phosphat Lyase (SGPL1) ein Regulator bei der Metastasierung von verschiedenen Tumorentitäten eine essentielle Rolle spielt. Dieses Enzym katalysiert die irreversible Degradierung des „second messenger“ S1P zu Ethanolamin-Phosphat und Hexadecenal (Abb. 3).

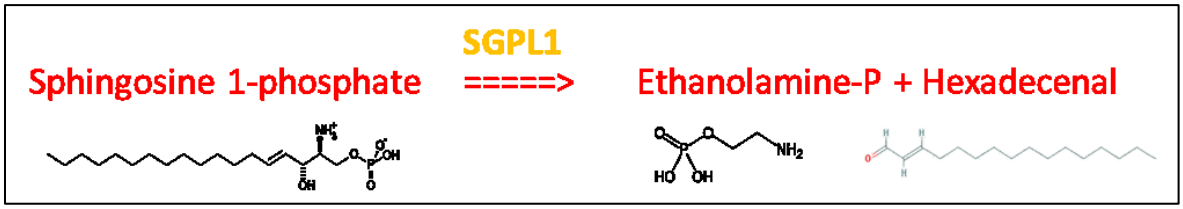

Abb. 3 Irreversible Sphingosin-1-Phosphat (S1P) Degradation zu Ethanolamin-Phosphat und Hexadecenal durch die Sphingosin-1-Phosphat-Lyase. Strukturformeln unter der Gleichung. (Adaptiert von https://www.genome.jp/kegg-bin/show_pathway?hsa04071+8879)

Weiter konnten wir nachweisen, dass die SGPL1 in nicht-tumorigenen Mammaepithelzellen und –geweben stark exprimiert und in Mammakarzinomen reprimiert vorliegt. Fluoreszenz-Markierungsexperimente belegten, dass in den nicht veränderten Kontrollzellen die SGPL1 neben der intrazellulären Lokalisation in dem endoplasmatischen Retikulum auch eine mit der Zytoplasmamembran-assoziierte Expression detektierbar war (Abb. 4).

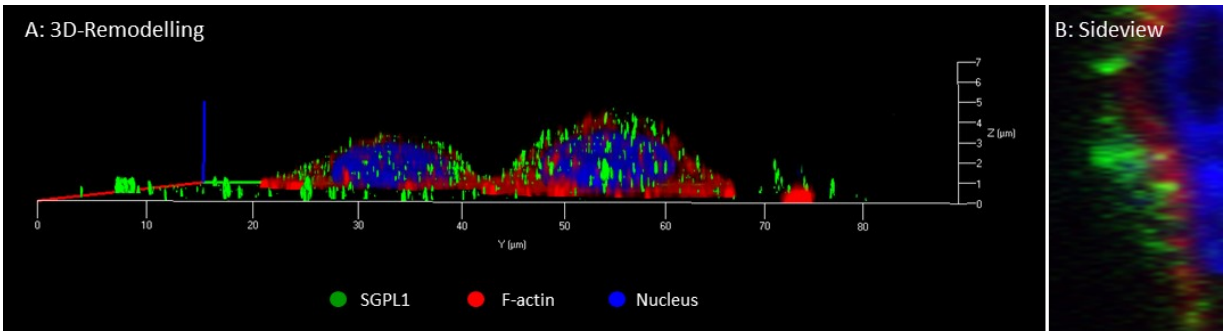

Abb. 4 Konfokal-Mikroskopische Aufnahmen nicht-tumorigener Mammaepithelzellen unter Normalbedingungen in der 3D-Rekonstruktion (A) und im Seitenquerschnitt (B). Grün: SGPL1; rot: F-Aktin Zytoskelett; blau: Zellkern. Engel et. al., 2018.

Dadurch ist eine direkte Degradation des Tumor-stimulierenden „second messengers“ S1P durch die auf der Zellmembran befindlichen SGPL1 denkbar. Aktuell wird der genetische Hintergrund der differentiellen SGPL1-Expression evaluiert. Darüber hinaus werden „Rescue“-Experimente zur Wiederherstellung des nicht-mutierten Phänotyps experimentell umgesetzt.
Letztlich könnte die SGPL1-Expressionsstärke, die intrazelluläre Verteilung und genetische Varianz der SGPL1 (z. B. in der Promotor- und/oder Transitpeptidsequenz) als neuer, potenzieller Marker in Hinblick auf das Metastasierungsvermögen der Tumorzellen Anwendung finden.

Zusammenfassend geben die hier dargestellten Studien zum einen eine Empfehlung für ein zielgerichtetes *in vitro* Screening zur Abschätzung des anti-tumorigenen Potentials eines Vielstoffgemisches oder einer Einzelsubstanz und zum anderen wurde ein neuer, potenzieller Tumormarker, die SGPL1 identifiziert. Sowohl das SGPL1-Expressionsmuster als auch die SGPL1-Mutationshäufigkeit sollten unabhängig von der Tumorentität zur Abschätzung des Metastasierungsrisikos in sich anschließenden Arbeiten untersucht werden.

Nachstehend entnehmen Sie bitte die kurzen Zusammenfassungen der Publikationen, die das Fundament dieser Habilitationsschrift bilden.

Referenz I

Engel N, Oppermann C, Falodun A*, Kragl U. Proliferative effects of traditional Nigerian medicinal plant extracts on human breast and bone cancer cell lines. J Ethnopharmacol. 2011 Sep 2;137(2):1003-10. NCBI-Link: https://www.ncbi.nlm.nih.gov/pubmed/21782919

Zusammenfassung:

In dieser ersten Publikation aus dem Jahre 2011 wurden fünf nigerianische Pflanzenextrakte für ein initiales *in vitro* Anti-Krebs-Screening bei Osteosarkom- (MG-63, Saos-2) und Mammakarzinomzelllinien (MCF-7, BT-20) eingesetzt. Diese Extrakte wurden aus vier traditionell medizinisch verwendeten Pflanzen (bzw. -teilen), namens *Hunteria umbellata* (HUL), *Cola lepidota* (CCL), *Persea americana* leaf (PAL), Root bark of *Persea americana* (RPA) und *Plukenetia conophora* (PCL) isoliert. Die Anti-Tumor-Evaluierung erfolgte durch Proliferations- und Apoptose-Messungen nach 48 h Extrakt-Inkubation in einer finalen Konzentration von 10 µg/ml im Zellkulturversuch. Im Vergleich mit nicht veränderten Primärzellen zeigte der Wurzelextrakt von *Persea americana* (RPA, Avocadowurzel) die stärkste Proliferationsreduktion (18 %) und Apoptose-Induktion (27 %) in den MCF-7 Brustkrebszellen. Da es sich bei MCF-7 um hormon-abhängige Tumorzellen (insb. für Östrogen und Progesteron) handelt, wurde ein Einfluss von pflanzlichen Hormonen (Phytoöstrogenen) in dem RPA Extrakt vermutet. In einer sich anschließenden Arbeit (Falodun et al., 2013) wurde durch Fraktionierung und chemische Charakterisierung des RPA-Extraktes eine Einzelsubstanz isoliert, die die zytotoxischen Eigenschaften auf MCF-7 vermittelt. Dabei handelt sich allerdings nicht um ein Phytoöstrogen, sondern ein Alken-Lakton mit der chemischen Nomenklatur: 4-hydroxy-5-methylene-3-undecyclidenedihydrofuran-2 (3H)-one. Der IC_{50}-Wert mit 20,48 µg/ml beschreibt eine moderate Zytotoxizität für die MCF-7 Brustkrebszellen, die sich durch einen Adhäsionsverlust innerhalb des Zellverbandes und damit verbundenem Apoptose-Eintritt darstellt. In den epithelialen Kontrollzellen konnte keine zytotoxische Wirkung nachgewiesen werden. Dieses Alken-Lakton weißt selektive, spezifische Anti-Krebseigenschaften auf, die weiter untersucht werden.

Falodun A*, **Engel N**, Kragl U, Nebe B, Langer P. Novel anticancer alkene lactone from Persea americana. Pharm Biol. 2013 Jun;51(6):700-6. doi: 10.3109/13880209.2013.764326. Epub 2013 Apr 9.

Journal of Ethnopharmacology 137 (2011) 1003–1010

Contents lists available at ScienceDirect

Journal of Ethnopharmacology

journal homepage: www.elsevier.com/locate/jethpharm

Proliferative effects of five traditional Nigerian medicinal plant extracts on human breast and bone cancer cell lines

N. Engel[a], C. Oppermann[c], A. Falodun[b,*], U. Kragl[c]

[a] Department of Cell Biology, Biomedical Research Center, University of Rostock, Schillingallee 69, 18057 Rostock, Germany
[b] Department of Pharmaceutical Chemistry, Faculty of Pharmacy, University of Benin, Nigeria
[c] Institute of Chemistry, University of Rostock, Albert-Einstein-Str. 3A, 18059 Rostock, Germany

ARTICLE INFO

Article history:
Received 22 April 2011
Received in revised form 14 June 2011
Accepted 6 July 2011
Available online 18 July 2011

Keywords:
Plant extracts
Herbal medicine
Anticancer
Flow cytometry

ABSTRACT

Ethnopharmacological relevance: The medicinal plants *Hunteria umbellata* (HUL), *Cola lepidota* (CCL), *Persea americana* leaf (PAL), Root bark of *Persea americana* (RPA) and *Plukenetia conophora* (PCL) are used in Nigerian traditional medicine for the treatment of cancer and cancer related diseases.
Aim of the study: To scientifically evaluate the cell proliferative and apoptotic effects of the plants extracts using breast and osteocarcinoma cell lines, and also to identify the possible components via LC–MS to have a kind of chemical fingerprint.
Materials and methods: The antiproliferative and apoptotic effects of methanolic extracts (10 μg/ml) of the five medicinal plants were subjected to in vitro evaluation using four cancer cell lines (breast-MCF-7 and BT-20; Osteocarcinoma-MG-63 and Saos-2) measured by flow cytometry. Non-tumorigenic controls MCF-12A and primary isolated osteoblasts (POB) were chosen to eliminate negative influence on healthy tissue.
Results: Of the five extracts RPA demonstrated a significant ($P < 0.05$) anti-proliferative activity against estrogen receptor positive breast cancer cell lines (MCF-7). The proliferative phase was decreased by 18%, whereas, a significant increase in cell proliferation (about 27%) was observed for RPA at a concentration of 10 μg/ml. PCL, CCL, HUL and PAL did not show marked inhibition of the proliferation of cell line MCF-7.
Conclusion: These results give suggestive evidence that the plant extracts exhibit some correlation between the claimed ethnomedicinal uses and the cell proliferative activity. RPA extract includes chemical compounds with estrogen-like activity and validates its potential use as anticancer agent, particularly against breast carcinoma; provided important information potentially helpful in drug designing and discovery. Further studies will involve the isolation of anti tumour compounds in RPA by LC–MS and detailed mechanism of anticancer activities.

1. Introduction

Natural products have historically and continually been investigated for promising new leads in pharmaceutical development.

Cancer is a major public health problem worldwide with millions of new cancer patients diagnosed each year and many deaths resulting from this disease. Chemotherapy remains the principal mode of treatment for various cancers. Tamoxifen, a non-steroidal anti-estrogen drug, is used in the treatment of estrogen receptor (ER) – positive breast cancer patients and as chemoprevention in high risk women (Fisher et al., 2005), but is not effective against ER negative breast tumors (Gupta and Kuperwasser, 2006). Cancer cells are characterized by unregulated growth, as well as insufficient and inappropriate vascular supply (Tomida and Tsuruo, 1999). Moreover, a core of cells was subjected to micro environmental stress conditions, and has decreased apoptotic potential through genetic alterations, thereby resulting in resistance to apoptosis (Kaufman et al., 2002). Breast cancer is a cancer that starts in the tissue of the breast. It could be invasive or non invasive. The incidence of breast cancer in developing countries is on the increase due to many underlying factors such as birth control, sliding to Western culture, lifestyle, lack of facilities for early detection, poor funding by government and international bodies. Adjuvant hormonal treatments such as tamoxifen are an essential part of the treatment regimen for early breast cancer, used to prevent recurrence. Hot flashes and night sweats are the most frequently occurring side effects, with up to 80% of women taking tamoxifen reporting them as troublesome. With nearly 46,000 new diagnoses of breast cancer annually in the United Kingdom and over 1 million worldwide, the problem is widespread, with estimates of over 100,000 women in the UK experiencing these symptoms at any given time (Love et al., 1991; Langer, 1996; Hunter et al., 2004). The use of plants or plant

* Corresponding author. Tel.: +234 8073184488.
E-mail address: faloabi@uniben.edu (A. Falodun).

0378-8741/$ – see front matter © 2011 Elsevier Ireland Ltd. All rights reserved.
doi:10.1016/j.jep.2011.07.023

products for cancer treatment could be due to several reasons such as availability of the materials, affordability, relatively cheap and little or no side effects. For these reasons, World Health Organization (WHO) supports the use of traditional medicines provided they are proven to be efficacious and non toxic. It is well established that plants have been a useful source of clinically relevant antitumor compounds (Cragg et al., 1994). Indeed, there have been worldwide efforts to discover new anticancer agents from plants. The diagnosis of cancer and related tumors by trado medical practitioners is not clearly understood (Cragg et al., 1994). However, traditional Nigerian medicinal herbs have been used in the treatment of different diseases in the country for centuries. There have been claims that some traditional healers in Nigeria can successfully treat cancer using herbal preparations. Hence, the need to look inwards for the discovery of new or lead drugs for the treatment of the disease cannot be over-emphasized. Furthermore, in Nigeria, as in other developing countries, traditional medicines are in widespread use; with the practitioners formulating and dispensing the recipes to their patients. The medicaments are prepared most often from a combination of two or more plant products which may contain active chemical constituents with multiple physiological and pharmacological activities and could be used in treating various disease conditions. The discovery of effective herbs and elucidation of their underlying mechanisms could lead to the development of an alternative and complementary method for cancer prevention and/or treatment. Based on an analysis of published literature, we selected five traditional Nigerian plants with medicinal value to evaluate their anticancer efficacy. Such plants as *Cola lepidota* (CCL), *Hunteria umbellata* (HUL), *Plukenetia conophora* (PCL), *Persea americana* (PAL) and *Persea americana* root bark (RPA). *Cola lepidota* is a tree of about 1.8 m high. It is commonly used in the treatment of various ailments such as cancer, and is also consumed regularly as a part of the daily diet. *Plukenetia conophora* (family Euphorbiacae) is a climbing shrub that is common in the South western part of Nigeria. The seeds are eaten like wallnuts often along with maize. The leaves are edible and are often eaten with rice. The leaves are also used traditionally for curing headache and the fresh nuts are used for curing snakebites (Hutchinson and Dalziel, 1958). The fruits have a bitter flavour unlike the kola nut and are considered to be tonic, and aphrodisiac. The leaves of the plant are used in traditional medicine as remedy against cancer, sexual impotence, headache and inflammation, antitussive, coronary heart disease (Iwu et al., 1999). *Hunteria umbellata* K. Schum (Apocynaceae) is a tree, about 15–22 m in height, found in West and Central Africa. Biological investigations include antibacterial, oxytocic, antinflammatory, antiobesisty and antidiabetic (Ejimadu and Falodun, 2002; Falodun et al., 2006; Igbe et al., 2010).

Persea americana Mill (family: Lauraceae), commonly known as: 'avocado', 'avocado pear', 'Mexican avocado' and so on, is a medium-sized, single-stemmed, terrestrial, erect, perennial, deciduous, evergreen tree of 15–20 m in height. The leaves and other morphological parts of *Persea americana* possess medicinal properties, and are widely used in traditional medicines of many African countries. In Nigeria, the leaves of *Persea americana* have been used as an effective antitussive, antidiabetic, antihypertensive; and as analgesic and anti-inflammatory remedies (Adeboye et al., 1999; Adeyemi et al., 2002; Antia et al., 2005; Owolabi et al., 2005). The aqueous decoction of the leaves is used locally for the treatment of tumors and tumour related diseases.

In the course of our screening studies for the anticancer compounds from plants, we undertook the present study to evaluate the in vitro proliferative activity of five plant extracts that are used in Nigerian traditional medicine as anticancer herbal drugs. Using two human breast (MCF-7, BT-20) and bone (MG-63, Saos-2) cancer cell lines, the plant extracts were screened via analysis of the cell cycle phases. As a kind of control, non-tumorigenic cell lines of the breast (MCF-12A) and bone (POB) were included in the screening.

Despite their widespread use, however, no scientific assessment for anticancer effect has been conducted in most cases. Considering their increasing recognition and consumption, the present study was undertaken to evaluate the anticancer potential of these plant extracts in the inhibition of cell proliferation and induction of cell death in human breast and bone cancer cell lines.

2. Materials and methods

2.1. Plant materials

All plant samples (wild type) were collected from Southern part of Nigeria around January, 2011. The plants were identified and authenticated by Prof M. Idu, and their respective voucher specimens are deposited at the Faculty of Pharmacy of Pharmacy, University of Benin, Benin City, Edo State, Nigeria.

2.2. Preparation of extracts

For each plant sample, plant materials were dried at room temperature and grounded. Dried powdery plant samples were exhaustively extracted with methanol by maceration. Dried methanolic extracts were obtained after removing the solvent by evaporation under reduced pressure. We dissolved 10 mg dry methanolic extracts in 1 ml absolute ethanol to have the measuring extracts for the LC–MS analysis and to give the desired stock solutions of the extracts for the cancer activity tests.

2.3. Chemicals

Absolute ethanol from MERCK, with the purity ACS, ISO, Reag. PhEur was used as extraction solvent. The LC–MS Chromasolv® grade solvents, methanol with 0.1% formic acid and water with 0.1% formic acid were obtained by FLUKA.

2.4. LC–MS-analysis

The extracts and possible phytoestrogens were identified on a Thermo Scientific HPLC-LTQ system (Thermo Scientific, Dreieich, Germany) comprising of a Surveyor Plus™ HPLC system equipped with a three simultaneous channel PDA detector and a linear trap quadropol mass spectrometer (LTQ) fitted with an electronicspray ionization source. Data were evaluated and interpreted with Xcalibure software (Thermo Scientific, Dreireich, Germany) and a special interpretation HighChem©: Mass Frontier™ Software (Thermo Scientific, Dreireich, Germany). The separation was performed on a Discovery® HS-C18 column (15 cm × 2.2 cm, 3 μm) produced by Supelco. The column temperature was kept at 35 °C and the mobile phases consisted of solvent A methanol with 0.1% formic acid (LC–MS Chromasolv®, Fluka) and B water with 0.1% formic acid (LC–MS Chromasolv®, Fluka). Elution of the extracts were performed by the following solvent gradient: 40% A to 95% A (10 min), 95% A isocratic (10 min), 95% A to 80% A (10 min), 80% A to 40% A (5 min) and 40% A isocratic (5 min). The flow rate was 0.15 ml/min and the injection volume amount 5 μl. MS spectra were recorded in both positive and negative modes and in the range m/z 90.00–2000.00. The compounds were identified by ion trap technology and the mass spectrometric detection was realized with electron spray ionization (ESI).

2.5. Cell culture

All cell lines except for the primary isolated osteoblasts were obtained from the American Type Culture Collection (Manassas,

VA, USA) and maintained at 37 °C and in a 5% CO_2 atmosphere in a monolayer. Confluent cells were passaged by treating them with 0.05% trypsin–0.02% EDTA. The medium was changed every two days.

2.6. Human mammary epithelial cell lines

The estrogen-sensitive human breast adenocarcinoma cell line MCF-7 (ATCC no. HTB-22) and the estrogen-independent adenocarcinoma cell line BT-20 (ATCC no. HTB-19) were cultured in Dulbecco's modified Eagle's medium (Invitrogen, Germany) with 10% fetal bovine serum (PAN Biotech GmbH, Germany) and 1% gentamycin (Ratiopharm, Germany). As kind of control functions the non-tumorigenic epithelial breast cell line MCF-12A (ATCC no. CRL-10782) which was grown in Dulbecco's modified Eagle's medium Ham's F12 without phenol red (Invitrogen, Germany) containing 10% horse serum (PAA Laboratories GmbH, Germany), the Mammary Epithelial Cell Growth Medium SupplementPack (Promo Cell, Germany) including Bovine Pituitary Extract 0.004 ml/ml, Epidermal Growth Factor (recombinant human) 10 ng/ml, Insulin (recombinant human) 5 μg/ml, Hydrocortisone 0.5 μg/ml and 1% gentamycin (Ratiopharm, Germany).

2.7. Human osteoblast cell lines

The two osteosarcoma cell lines MG-63 (ATCC no. CRL-1427) and Saos-2 (ATCC no. HTB-85) were cultured in Dulbecco's modified Eagle's medium (Invitrogen, Germany) with 10% fetal bovine serum (PAA Laboratories GmbH, Germany) and 1% gentamycin (Ratiopharm, Germany). Normal human osteoblasts (POB), isolated from a patient's cancellous bone were grown in Dulbecco's modified Eagle's medium (Invitrogen, Germany) with 10% fetal bovine serum (PAN Biotech GmbH, Germany) and 1% gentamycin (Ratiopharm, Germany).

2.8. Treatment with plant extract

For all experiments 0.5×10^6 cells were seeded in a 6-well plate in regular culture medium for one day. Subsequently, cells were washed with phosphate buffered saline (PBS) and adapted to phenol-red-free Dulbecco's modified Eagle's medium (PAA Laboratories GmbH, Germany) with 10% charcoal stripped fetal bovine serum (PAN Biotech GmbH, Germany) for 48 h to avoid unspecific stimulation of endogenous hormones in the serum (assay medium). Treatment with plant extracts (final concentration 10 μg/ml) or established phytoestrogens like genistein (4, 5, 7-trihydroxyisoflavone) and daidzein (7, 4-dihydroxyisoflavone), both purchased from Sigma (Germany) with a final concentration of 100 μM was carried out for 48 h in assay medium. As negative control substance the vehicle ethanol (0.1%) was used in the same manner.

2.9. Flow cytometric measurement of cell proliferation

The extent of cell cycle progression and apoptosis in the cells was estimated by flow cytometric analysis after propidium iodide (Roche Diagnostics, IN, USA) staining of the cells as already described (Nebe et al., 2006). After plant extract treatment cells were trypsinized with 0.05% trypsin–0.02% EDTA for 5–10 min. The reaction was stopped with assay medium. Cells suspension was transferred to FACS tubes (BD Biosciences, USA) and fixed in 70% ethanol for 12 or more hours at −20 °C. Briefly, after washing with PBS cells were incubated with RNase (1 mg/ml) at 37 °C for 30 min. Finally, cells were re-suspended in propidium iodide (50 mg/ml) for at least 3 h at +2 to +8 °C protected from light until flow-cytometric analysis.

Flow cytometric measurements were performed on the flow cytometer BD FACSCalibur, equipped with an argon-ion laser of the wavelength 488 nm (BD Biosciences, USA). For data acquisition, the software CellQuest Pro 4.0.1 (BD Biosciences, USA) was used. A minimum of 15,000 ungated events were recorded. Doublets and clumps were excluded by gating on the DNA pulse width versus pulse area displays. For the analysis of cell proliferation, the cell cycle phases G0/G1, S and G2/M were calculated in percentage using ModFIT LT 3.0 for Power Mac G4 (BD Biosciences, USA). For statistical evaluation, the S-phase and G2/M-phase cells were defined as proliferative cells.

2.10. Immunofluorescence staining of estrogen receptors

Cells were seeded on glass coverslips and let them adhere for 24 h. Fixation was carried out with 4% paraformaldehyde (PFA) for 15 min, followed by three washings with PBS. Then, cells were permeabilized with 0.1% Triton X-100 for 15 min. After carefully washing, cells were incubated with the rabbit anti-human estrogen receptor antibodies (ERα; sc-542 and ERβ; sc-8974; both from Santa Cruz, USA) in a 1:50 dilution for 1 h at room temperature. Afterwards cells were washed three times with PBS and incubated with 488-labeled secondary goat anti-rabbit antibody (Molecular Probes, USA, 1:100) for 1 h at room temperature in the dark. After washing the cells were incubated with DAPI (Roche Diagnostics GmbH, Germany) for 15 min. Finally the cells were washed four times with PBS and embedded. Visualization and imaging was carried out with the Axio Scope. A1 fluorescence microscope (Carl Zeiss, Germany). Notably all pictures were taken at the same exposure time to guarantee comparable results.

2.11. Statistical analysis

Every experiment was replicated three times with individual passaged cells and data sets were expressed as means ± standard deviations (SD). Statistical significance was determined by the unpaired *t*-test (***$P < 0.001$, **$P < 0.005$, *$P < 0.05$).

3. Results and discussion

The list of the investigated plants, the parts used and their known medicinal uses according to the Handbook of African Medicinal Plants (Iwu, 1993), *Ethnobotany Desk Reference* (Johnson, 1999) and direct information obtained by Dr A. Falodun (Department of Pharmaceutical Chemistry, Faculty of Pharmacy, University of Benin, Benin City, Nigeria) through interviewing local traditional healers, are presented in Table 1. Based on this information, five medicinal plants were screened. Ethno pharmacological data (information based on the medicinal traditional use of plants) has been one of the common useful ways for the discovery of biologically active compounds from plants (Cordell et al., 1991). The big advantage of the ethno pharmacological information is that the extensive literature may already allow for some rationalization with respect to the biological potential of a reputed use.

In this study, ethanolic extracts of *Cola lepidota* (CCL), *Hunteria umbellata* (HUL), *Plukenetia conophora* (PCL), *Persea americana* leaves (PAL) and root bark (RPA) were used to analyze the chemical composition of the plant extracts by LC–MS. We used this technique to get a chemical fingerprint for each plant. As shown in the chromatograms (Fig. 1) by the different compositions of the base peaks all extracts are complex mixtures of different compounds like phytoestrogens which are often conjugated to one or more carbohydrate moieties and other polar principles. Further work is ongoing to reveal the identity and the structures principles of some of these compounds by MS measurements and other analytical methods like NMR spectroscopy or elemental analysis.

Table 1
List of screened plant species common names, used parts and known ethno-medicinal uses.

Plant species	Family	Common name	Parts of plant use	Ethnomedicinal uses
Plukenetia conophora Müll Arg. (PCL)	Euphorbiaceae	African walnut	Leaves	Cancer, stomach pain, infertility
Cola leptdota (CCL)[a]	Sterculiaceae	Cockroach kola	Seeds	Cancer, bacterial infections, infertility
Hunterta umbellata(*HUL*)	Apocynaceae	Osun	Leaves	Cancer, cough, diabetes, inflammations
Persea americana (PAL)	Lauraceae	Avocado pear	Leaves	Cancer, inflammation
Persea americana (RPA)[a]	Lauraceae	Avocado pear	Root	Cancer, threatened abortion, ulcer

[a] Anticancer information obtained from interaction with tradomedical practitioners; others obtained from literature sources.

Traditional healers who were interviewed on how they prepared the extracts before administering to the patients indicated that it was the water decoction that was administered, meaning that it is the polar compounds that were responsible for the reported anticancer activity. Since it is known that different cell lines might exhibit different sensitivities towards a cytotoxic compound, the use of more than one cell line is therefore considered necessary in the detection of cytotoxic compounds. Bearing this in mind, six human cell lines of different histological origins were used in the present study.

In order to evaluate the anticancer property of five medicinal plant extracts that are used in Nigerian traditional medicine, cell cycle analysis with two breast adenocarcinoma (MCF-7, BT-20) and two osteosarcoma (MG-63 and Saos-2) cell lines were performed. As control lines function the non-tumorigenic mammary epithelial cell line, MCF-12A, and primary osteoblasts (POB), isolated patient's cancerous bone, to exclude a negative influence on normal/healthy tissue. The variety of cell lines especially the usage of estrogen-receptor-positive (MCF-7) and negative (BT-20) cell lines helps to get an idea of the mechanisms of action. However, potential sub-

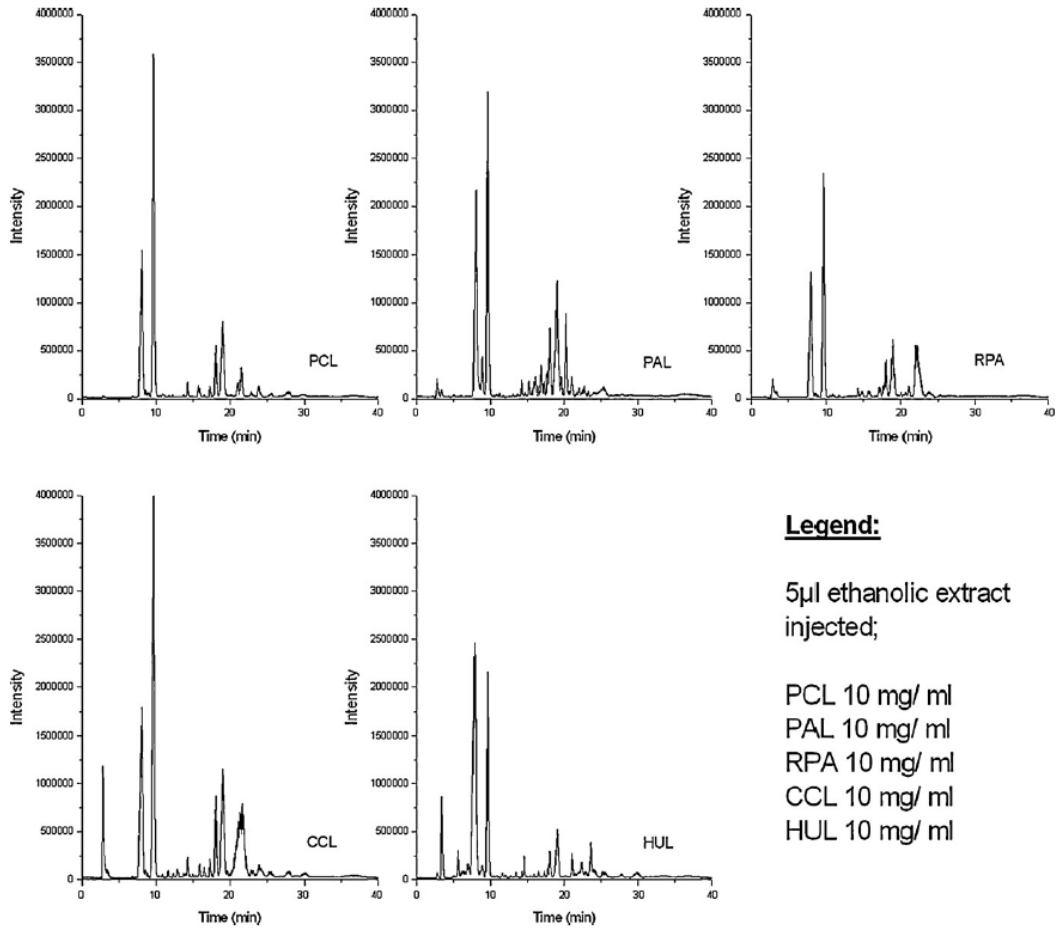

Fig. 1. Overview about the LC–MS chromatograms of five Nigerian plant extracts in ethanol; *Cola leptdota seed* (CCL), *Hunterta umbellata* leaves (HUL), *Plukenetia conophora* leaves (PCL), *Persea americana* leaves (PAL) and root bark (RPA); Base Peak.

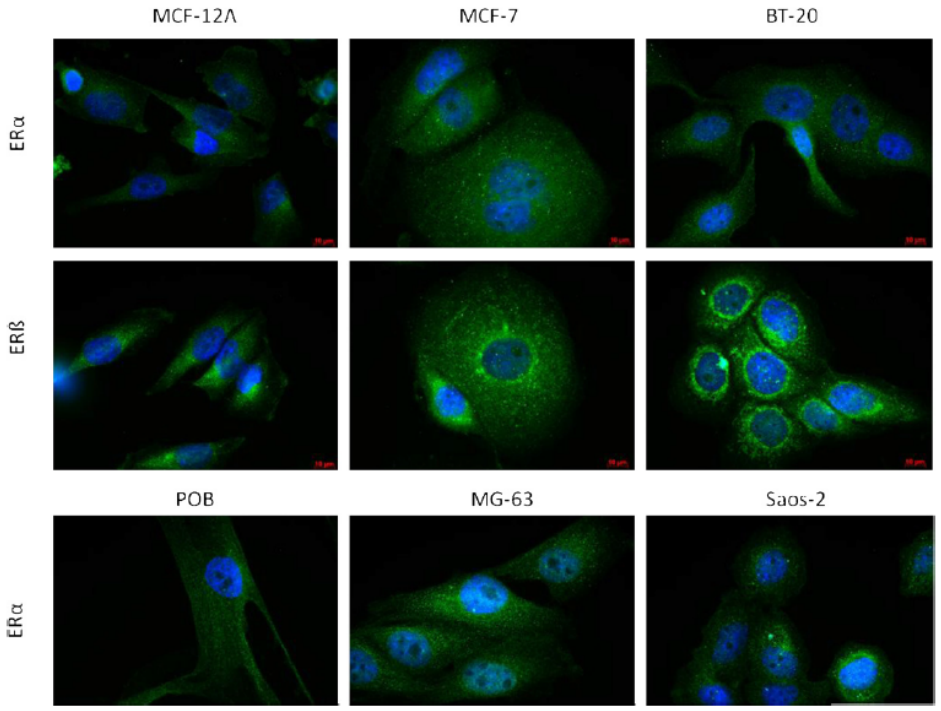

Fig. 2. Immuno fluorescence staining of the estrogen receptors α and β (ERα/β) of all human cell lines used in this study. Estrogen receptors (green). Nuclear staining with DAPI (blue) Exposure time was maintained at 5.6 s to guarantee identical excitation. (For interpretation of the references to color in this figure legend, the reader is referred to the web version of the article.)

stances or compound mixtures of the chosen plant extracts with estrogen-receptor-dependent or -independent effects could be identified in adjacent projects. But so far the estrogen receptor (ER) status of all cell lines was tested by immune-fluorescence against the ERα and ERβ isoforms (Fig. 2). Simultaneous staining with DAPI and identical exposure times enable information about the localization and the expression intensity of these isoforms. Every cell line harbors ERα as well ERβ in different contents. The estrogen receptor expression was mainly detected in the cytoplasmic matrix of all cell lines. The cell lines MCF-12A and POB exhibit the lowest ER expression levels confirming their non-tumorigenic status. The breast as well as the bone cancer cell lines showed an increased expression of especially ERβ. The expression levels of ERα were not that dramatically altered in comparison to the non-tumorigenic controls. Even the so called estrogen-receptor-negative cell line BT-20 harbors clearly visible contents of both estrogen receptors. This finding matches with results presented by Castles et al. (1993), demonstrating the expression of a constitutively active estrogen receptor variant in this cell line. This immunofluorescence staining gives an overview of the overall expression of all estrogen receptor isoforms but not allows quantitative information of the expression levels of single ER isoforms. However, the positive estrogen receptor status of all cell lines enables the binding and reaction of plant compounds with estrogen-like activity.

Cell cycle analysis via flow cytometry distinguishes between different cell cycle phases and detects apoptotic DNA fragmentation, simultaneously, so that the proliferative (S + G2/M) as well as the apoptotic (degraded DNA) effects of the crude plant extracts can be measured (Nunez, 2001). First, a percentage comparison of cell cycle phases including apoptotic rates of all cell lines under non-treated conditions is given in Fig. 3. Therefore, the cells were harvested by a confluence of approximately 70% to allow a proliferative as well as anti-proliferative effect of the plant extracts. As expected, the non-tumorigenic cell lines MCF-12A (Breast) and POB (primary osteoblast) showed low proliferative potential as shown in Fig. 3. Only 3–5% of all cells were in G2/M or S phase. These low percentages of proliferating cells are enough to guarantee the self-renewal of the tissue. Contrary, the breast as well the bone cancer cell lines are marked by increased proliferative phases (G2/M + S) about 25%, 27%, 40% (MCF-7; MG-63; Saos-2), respectively. Even the

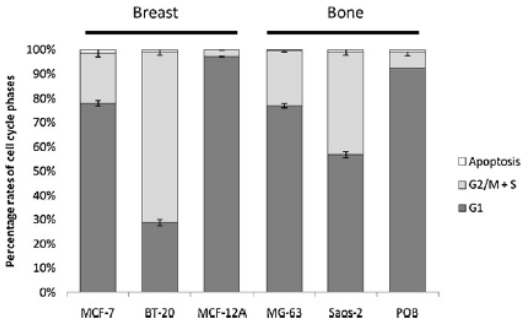

Fig. 3. Comparative analysis of the cell cycle phases and apoptotic rates of non-treated mammary cell lines MCF-7, BT-20, MCF-1 2A and osteo cell lines MG-63, Saos-2 and primary osteoblasts (POB). G1 phase (darker grey); S + G2/M phase (lighter grey); Apoptotic cells (white).

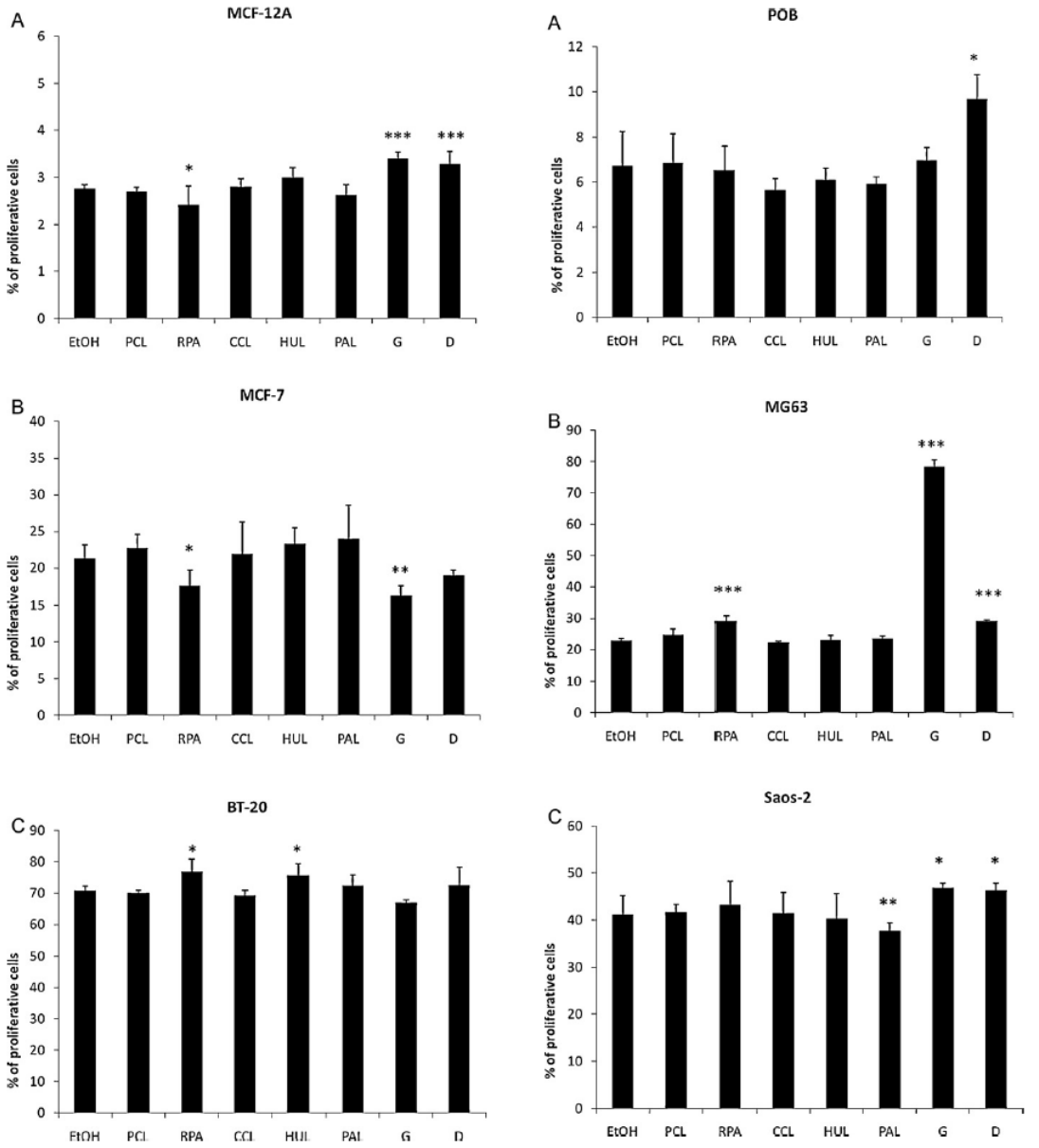

Fig. 4. (A–C) Effect of the five plant extracts and the phytoestrogens genistein (G) and (D) on breast (cancer) cell proliferation. As proliferative cells the sum of G2/M + S phases was determined in percentages. Cell cycle distribution was monitored by flow cytometry. Only the RPA extract at a final concentration of 10 μg/ml caused significant alterations in the cell cycle phases of the mammary cell lines. Note that the vertical axes differ in their calibration. Columns, mean; bars, SE ($n = 3$). ***$P < 0.001$, **$P < 0.005$, *$P < 0.05$, significantly different compared with EtOH-treated control (unpaired t-test).

Fig. 5. (A–C) Effect of the five plant extracts and the phytoestrogens genistein (G) and daidzein (D) on bone (cancer) cell proliferation. As proliferative cells the sum of G2/M + S phases was determined in percentages. Cell cycle distribution was monitored by flow cytometry. Note that the vertical axes differ in their calibration. Columns, mean; bars, SE ($n = 3$). ***$P < 0.001$, **$P < 0.005$, *$P < 0.05$, significantly different compared with EtOH-treated control (unpaired t-test).

Table 2
Summary of all cell cycle phases including the apoptotic fraction of cell lines induced by the fraction RPA. Changes of the proliferative phases (G2/M + S) in comparison to the vehicle treated control were determined in percent. Significant alterations were signed with asterisks.

Cancer type	Cell line	G1	G2/M	S	Apoptotic cells	Proliferation (%)
Breast	MCF-12A	97.30 ± 0.40	1.91 ± 0.15	0.50 ± 0.07	0.15 ± 0.05	87.75 ± 6.60*
	MCF-7	79.99 ± 0.31	9.50 ± 2.38	8.40 ± 0.28	1.23 ± 0.76	82.66 ± 12.23*
	BT-20	23.07 ± 4.06	29.99 ± 4.28	46.93 ± 8.21	0.33 ± 0.14	108.49 ± 5.28*
Bone	POB	93.47 ± 1.06	4.18 ± 1.13	2.35 ± 0.07	0.70 ± 0.03	97.17 ± 16.24
	MG-63	70.84 ± 1.53	13.87 ± 0.40	15.27 ± 1.16	0.14 ± 0.05	127.47 ± 5.28*
	Saos-2	54.60 ± 0.83	19.38 ± 2.44	23.79 ± 2.73	0.14 ± 0.07	104.91 ± 11.57

breast cancer cell line BT-20 harbors about 60% proliferating cells indicating its invasive potential. The cell physiologic apoptotic rates of all cell lines were between 0.5 and 1.5%.

For validating the anticancer potential of the five plant extracts, cells were incubated for 48 h with in ethanol diluted extracts up to a final concentration of 10 μg/ml. This relatively low concentration reflects a possibly reachable concentration within the human body. Higher concentrations are hardly to achieve via specific plant-based diets. Fig. 4(A–C) shows the proliferation activity of the breast (cancer) cell lines after treatment with the plant extracts in comparison with established phytoestrogens like genistein and daidzein. Only the root of the *Persea americana* (RPA) extract causes significant alterations ($P < 0.05$) in the proliferative status of all breast cell lines when compared with the control. The proliferative phases of the non-tumorigenic cell line MCF-12A as well as the tumorigenic one, MCF-7, were decreased about 12% and 18% respectively (see Table 2). By comparing the LC–MS chromatograms of *Persea americana* leaf (PAL) and root bark (RPA) extracts (Fig. 1) we find some differences. RPA seems to be the most active which could probably be due to phytoestrogens with high molecular weight. This revealed that *Persea americana* plant possess anticancer property which is demonstrated by the root (RPA) part of the plant. Surprisingly, PCL, CCL, HUL and PAL did not show any marked inhibition of the proliferation of the cell line MCF-7. On the other hand the invasive breast cancer cell line BT-20 showed an increased proliferative rate of approximately 8% after treatment with the RPA extract. In comparison with the influence of the well established phytoestrogen genistein and daidzein in high concentrations (final concentration 100 μM) the RPA extract causes a reduction of the G2/M + S phase in MCF-7 in almost the same manner whereas MCF-12A showed an increased proliferation after treatment with genistein as well as daidzein. Genistein is a natural isoflavone phytoestrogen sensitive to estrogenic receptors and has been reported to have an inhibitory effect on the proliferation of cells induced by a non steroidal estrogenic mycotoxin-zearalenone in MCF-7 (Wang et al., 1996; Heisel, 1998; Dingfa et al., 2010). It therefore has a potential as anticancer agent (Sirtori, 2001; Somekawa et al., 2001; Messina, 2003; Munro et al., 2003; Howes et al., 2006). These results indicate that the extract of *Persea americana* includes components that affect the cell cycle phases of breast cancer cell lines in a different way like genistein or daidzein do. Beside the action of the RPA extract only the *Hunteria umbellata* (HUL) extract showed an exclusive influence on the proliferation of BT-20. The proliferative phases increased up to 6%. Probably the exclusive effect on BT-20 attributes to the special ER variants in this cell type. However, research is ongoing in our lab to determine the chemical phytoestrogens or other active components in RPA using LC–MS and other spectroscopic methods.

The results of the cell proliferative activity of the extracts on osteo cancer cell lines are shown in Fig. 5. A significant increase in cell proliferation about 27% was observed for RPA at a concentration of 10 μg/ml on the osteosarcoma cell line MG-63 (Fig. 5A) whereas the non-tumorigenic osteoblast (POB) as well as the bone cancer cell line Saos-2 remained unaffected (Fig. 5B and C). But in comparison to the control substance genistein, the increase of proliferation induced by the RPA extract was relatively slight. Genistein caused an increase of the proliferative phases in MG-63 and Saos-2 about 400% and 25% respectively. The other four plant extracts showed no significant alteration in the cell cycle phases in any bone cell line. This indicates that the RPA plant extract can inhibit breast cancer proliferation on one hand and enhance bone cancer on the other. However, the RPA extract or isolated components could be potential anticancer agents in the treatment of breast cancer.

Phyto-chemicals have been shown to induce cell cycle arrest, cause apoptosis and affect the differentiation and proliferation of cells mediated by the effect of intracellular reactive oxygen species on the signal transduction pathway (Hu and Kong, 2004). These cytotoxic natural products may be able to play a significant role in treating breast and osteo cancer by working in concert with conventional chemotherapeutic drugs thereby improving their efficacy or reducing their toxicity. Taken together only the RPA extract showed an influence on the cell cycle phases of breast and bone cancer cell lines. The research work is ongoing with a view to isolating the identified compounds, and characterizes the structure of the still unknown anticancer components in the most active plant extract (RPA) by LC–MS and GC–MS and other analytical methods.

4. Conclusion

A large number of novel anticancer drugs have been discovered from natural products in the past and new ones are continually being developed. The studies have shown that the five Nigerian plant extracts are full of several compounds which are similar to the phytoestrogens genistein and daidzein. Comparative analysis of the five extracts showed that RPA possessed the most potent and significant anticancer activity at the concentration tested. This lends support to the ethnomedicinal uses of the plants for which they are known and used for, and could therefore, potentially be sources for pharmacologically active products suitable for development as chemotherapeutic or chemopreventive agents. Future work will focus on the isolation of identified compounds (phytoestrogens), and also elucidation of the precise in vitro and in vivo bio molecular mechanisms.

Acknowledgements

We are grateful to DFG-TWAS (2010/11) for the award of a visiting scientist to Dr. A. Falodun. Special appreciation to Institute of Chemie, University of Rostock, Germany. University of Benin, Benin City, Nigeria is also acknowledged. We would like to thank Deutsche Krebshilfe (FKZ: 107821) for the funding of our work as well. We acknowledge the technical help of Petra Seidel, Dept. of Cell Biology, University of Rostock.

References

Adeboye, J.O., Fajonyomi, M.O., Makinde, J.M., Taiwo, O.B., 1999. A preliminary study on the hypotensive activity of *Persea americana* leaf extracts in anaesthetized, normotensive rats. Fitoterapia 70, 15–20.

Adeyemi, O.O., Okpo, S.O., Ogunti, O.O., 2002. Analgesic and anti-inflammatory effects of *Persea americana* Mill (Lauraceae). Fitoterapia 73, 375–380.
Antia, B.S., Okokon, J.E., Okon, P.A., 2005. Hypoglycaemic activity of aqueous leaf extract of thoracic rat aorta. *Persea americana* Mill. Indian Journal of Pharmacology 37, 325–326.
Castles, C.G., Fuqua, S.A.W., Klotz, D.M., Hill, S.M., 1993. Expression of a constitutively active estrogen receptor variant in the estrogen receptor-negative BT-20 human breast cancer cell line. Cancer Research 15, 5934–5939.
Cragg, G.M., Boyd, M.R., Cardellina, J.H., Newman, D.J., Snader, K.M., McCloud, T.G., 1994. Ethnobotany and drug discovery: the experience of the US National Cancer Institute. In: Ethnobotany and Search for New Drugs, Ciba Foundation Symposium 185. Wiley, Chichester, pp. 178–196.
Cordell, G.A., Beecher, C.W., Pezzuto, J.M., 1991. Can Ethnopharmacology contribute to the development of new anticancer drugs? Journal of Ethnopharmacology 32, 117–133.
Dingfa, W., Qingshan, Ma, Z., Desheng, Q., 2010. Genistein inhibit the proliferation induced by zearalenone in MCF-7 cells. Molecular Cell Toxicology 6, 25–31.
Ejimadu, I.M., Falodun, A., 2002. Biological and Chemical studies of *Hunteria umbellata* seed K. Schum. International Journal of Chemistry 12, 241–248.
Falodun, A., Nworgu, Z.A.M., Ikponmwosa, M.O., 2006. Phytochemical components of *Hunteria umbellata* and its effect on Non-pregnant at uterus. Pakistan Journal of Pharmaceutical Sciences 19, 256.
Fisher, B., Costantino, J.P., Wickerham, L.D., Cecchini, R.S., Croni, W.M., Robidoux, A., Bevers, T.B., Kavanah, M.T., Atkins, J.N., Margolese, R.G., Runowicz, C.D., James, J.M., Ford, L.G., Wolmark, N., 2005. Tamoxifen for the prevention of breast cancer: current status of the National Surgical Adjuvant Breast and Bowel Project P-1 Study. Journal of National Cancer Institute 97, 1652–1662.
Gupta, P.B., Kuperwasser, C., 2006. Contributions of estrogen to ER-negative breast tumor growth. Journal of Steroid Biochemistry and Molecular Biology 102, 71–78.
Howes, L.G., Howes, J.B., Knight, D.C., 2006. Isoflavone therapy for menopausal flushes: a systematic review and meta-analysis. Maturitas 55, 203–211.
Hu, R., Kong, A.H.T., 2004. Activation of MAP kinases, apoptosis and nutrigenomics of gene expression elicited by dietary cancer prevention compounds. Nutrition 20, 83–88.
Hunter, M., Grunfeld, E.A., Mittal, S., Sikka, P., Ramirez, A.J., 2004. Menopausal symptoms in women with breast cancer: prevalence and treatment preferences. Psychooncology 13, 769–778.
Hutchinson, J., Dalziel, J.M., 1958. Flora of West Tropical Africa, Part 2, vol. 1., second ed. Keay R.W.J. Crown Agents, London, pp. 365–367, 396–397.
Iwu, M.M., 1993. Handbook of African Medicinal Plants. CRC Press, Boca Raton, FL.
Iwu, M.M., Angela, R., Duncan, C., Okunji, O., 1999. In: Janick, J. (Ed.), New Antimicrobials of Plant Origin in Perspectives of New Crops and Uses. ASHS Press, Alexandra, VA.
Igbe, I., Ching, F.P., Eromon, A., 2010. Anti-inflammatory activity of aqueous fruit pulp extract of *Hunteria umbellata* K. schum in acute and chronic inflammation. Acta Poloniae Pharmaceutica – Drug Research 67, 81–85.
Johnson, T., 1999. Ethnobotany Desk Reference. CRC Press, Boca Raton, FL.
Kaufman, R.J., Scheuner, D., Schroder, M., Shen, X., Lee, K., Liu, C.Y., Arnold, S.M., 2002. The unfolded protein response in nutrient sensing and differentiation. Nature Reviews Molecular Cell Biology 3, 411–421.
Langer, A.S., 1996. Talking with the breast cancer patient about tamoxifen. In: Jordan, V.C. (Ed.), Tamoxifen: A Guide for Clinicians and Patients. PRR, Huntington, NY, pp. 127–134.
Love, R.R., Cameron, L., Connell, B.L., Leventhal, H., 1991. Symptoms associated with tamoxifen treatment in postmenopausalwomen. Archives of Internal Medicine 151, 1842–1847.
Messina, M.J., 2003. Emerging evidence on the role of soy in reducing prostate cancer risk. Nutrition Review 61, 117–131.
Munro, I.C., Harwood, M., Hlywka, J.J., Stephen, A.M., Doull, J., Flamm, H., 2003. Soy isoflavones: a safety review. Nutrition Review 61, 1–33.
Nebe, B., Peters, A., Duske, K., Richter, D.U., Brieste, V., 2006. Influence of Phytoestrogens on the proliferation and expression of adhesion receptors in human and epithelial cells in vitro. European Journal of Cancer Prevention, 405–415.
Nunez, R., 2001. DNA measurement and cell cycle analysis by flow cytometry. Current Issues Molecular Biology 3, 67–70.
Owolabi, M.A., Jaja, S.I., Coker, H.A.B., 2005. Vasorelaxant action of aqueous extract of the leaves of *Persea americana* on isolated rat uterus. Fitoterapia 76, 567–573.
Sirtori, C.R., 2001. Risks and benefits of soy phytoestrogens in cardiovascular diseases, cancer, climacteric symptoms and osteoporosis. Drug Safety 24, 665–682.
Somekawa, Y., Chiguchi, M., Ishibashi, T., Aso, T., 2001. Soy intake related to menopausal symptoms, serum lipids, and bone mineral density in postmenopausal Japanese women. Obstetrics and Gynecology 97, 109–115.
Tomida, A., Tsuruo, T., 1999. Drug resistance mediated by cellular stress response to the mircroenvironment of solid tumors. Anticancer Drug Design 14, 169–177.
Wang, T.T., Sathyamoorthy, N., Phang, J.M., 1996. Molecular effects of genistein on estrogen receptor mediated pathways. Carcinogenesis 17, 271–275.

Referenz II

Engel N, Falodun A*, Kragl U, Langer P, Nebe JB. Anti-proliferative and anti-adhesive effects of four plant extracts on the breast cancer cell line MCF-7. BMC Complementary and Alternative Medicine 2014; 14:334 doi:10.1186/1472-6882-14-334.

NCBI-Link: https://www.ncbi.nlm.nih.gov/pmc/articles/PMC4177160/

Zusammenfassung:

Aus einem großen Pool an nigerianischen Pflanzenmaterial wurden vier Extrakte der Pflanzen *Jatropha curcas* (JCP1), *Pyrenacantha staudtii* (PS), *Picralima nitida* (ZI) und *Jatropha gossypifolia* (JCP2) ausgewählt und hinsichtlich ihres Anti-Tumor-Potentials an der Brustkrebszelllinie MCF-7 in einer Konzentrationsreihe (1 - 50 µg/ml) evaluiert. Dazu wurde die Proliferationsrate mit Hilfe von Zellzyklusmessungen, der Apoptose-Induktion via Annexin V/PI-Färbung und Western Blots sowie Adhäsions-/Konfluenzveränderungen mittels Durchflusszytometrie, Integrin-Rezeptor-Expression und Fluoreszenzmikroskopie untersucht. Alle vier Extrakte induzierten Apoptose beginnend mit einer finalen Konzentration von 10 µg/ml und wiesen moderate IC_{50}-Werte im Bereich von 23–38 µg/ml auf (Abb. 5).

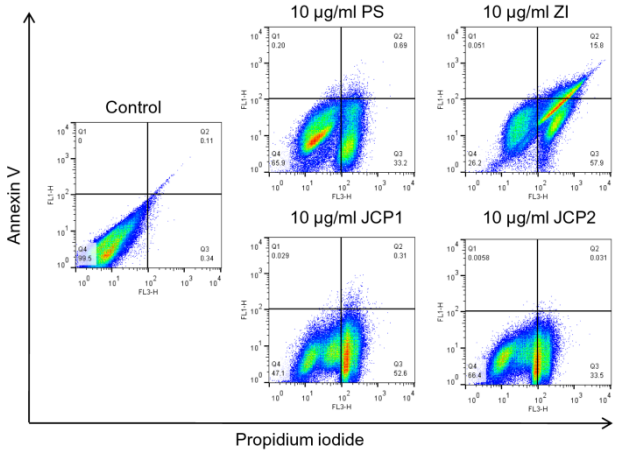

Abb. 5 Bestimmung der apoptotischen Zellen mittels Annexin V/PI Färbung nach der Behandlung mit 10 µg/ml PS, ZI, JCP1 und JCP2 im Vergleich zur Kontrollgruppe (Engel et al., 2014)

Weiterführende zellbiologische Untersuchungen zur Beschreibung der detaillierten Extraktwirkung zeigten, dass die zytotoxische Wirkung durch Aktivierung unterschiedlicher Signalkaskaden induziert wurde. Durch die Behandlung mit PS, JCP1 und JCP2 wurde ein Adhäsionsverlust der Zellen aus dem Zellverband und zu der extrazellulären Matrix induziert, wodurch die Zellen in Suspension gingen und der Zelltod über die Caspasenaktiverung erfolgte. Die zytotoxische Wirkung von Zi war nicht mit einer Adhäsionsreduktion assoziiert. Im Gegenteil die Zell-Zellkontakte wurde durch eine erhöhte ß1-Intergrin-Expression verstärkt. Die Apoptose-Initiierung erfolgte über die Aktivierung der MAPK-

Signalweges. Diese Arbeit belegt eindrucksvoll, dass verschiedene stoffwechselphysiologische Wirkungen zur Inhibierung des Tumorwachstums aktiviert werden können. Perspektivisch soll die detaillierte metabolische Wirkung von Zi in Kontrast zu den anderen drei Extrakten mittels Proteomics und Metabolomics evaluiert werden.

Erharuyi O, **Engel-Lutz N**, Ahomaforb J, Imiejec V, Falodun A, Nebe B, Langer P. Anticancer activity of five Forest crops used in African folklore: antiproliferative and proapoptotic effects. Nat Prod Res. 2014 Feb 26. DOI: 10.1080/14786419.2013.879475.

Oriakhi K, Erharuyi O, Oikeh EI, **Engel-Lutz N**, Falodun A. Free radical scavenging and cytotoxic effects of methanol extract of Theobroma cacao L. (Sterculiaceae) seed. West Afr J Pharm 2015; 26(2):83-91.

Engel et al. BMC Complementary and Alternative Medicine 2014, 14:334
http://www.biomedcentral.com/1472-6882/14/334

BMC Complementary & Alternative Medicine

RESEARCH ARTICLE Open Access

Pro-apoptotic and anti-adhesive effects of four African plant extracts on the breast cancer cell line MCF-7

Nadja Engel[1], Abiodun Falodun[2*], Juliane Kühn[1], Udo Kragl[3], Peter Langer[3] and Barbara Nebe[1]

Abstract

Background: *Jatropha curcas* (JCP1), *Pyrenacantha staudtii* (PS), *Picralima nitida* (ZI) and *Jatropha gossypifolia* (JCP2) are plants used in the African folklore for the treatment of various cancers.

Methods: This study investigated the *in vitro* anticancer effects of the ethanol extracts against human epithelial MCF-7 breast cancer cells in a dose-dependent manner (1–50 μg/ml) by using cell cycle analysis, viability assay, annexin V/PI staining, TUNEL method and expression determination of apoptotic and adhesion relevant proteins. Adhesion processes were monitored by detachment via flow cytometry, β1-integrin expression and formation of the actin cytoskeleton.

Results: The three extracts, termed PS, JCP1 and JCP2 at a concentration of 10 μg/ml induced cell death in MCF-7 breast cancer cells verified by high amounts of PI-positive cells in the cell cycle analysis, Annexin V/PI staining and DNA fragmentation measurements. In parallel cell detachment was accompanied by decreased β1- integrin expression and phosphorylation of the focal adhesion kinase at Tyr397. ZI extract was the exception by the increasing β1-integrin expression and strengthening the cortical actin cytoskeleton. However, all four plant extracts mediated strong anti-cancer properties with IC_{50} values between 23–38 μg/ml.

Conclusion: PS, JCP1 and JCP2 were found to be very active against MCF-7 cells by inducing anoikis and therefore possessing vast potential as medicinal drugs especially in estrogen receptor positive breast cancer treatment. ZI mediated their anti-cancer action by different signaling mechanisms which should be analyzed in future studies. Our results further supported the idea that medicinal plants can be promising sources of putative anticancer agents.

Keywords: Traditional medicine, Breast cancer, Plant extraction, Cell cycle, Apoptosis, Integrin, Adhesion, Anoikis

Background

The use of natural products including medicinal plants has become more and more important in primary health care especially in developing countries. Many pharmacognostical and pharmacological investigations are carried out to identify new drugs or to find new lead structures to develop novel therapeutic agents for the treatment of human diseases such as cancer [1]. In developing countries and particularly in Yemen, a large segment of the population still rely on folk medicine to treat serious diseases including infections, cancer and different types of inflammations.

Currently, there is insufficient scientific research on the plants from Nigeria. Previous studies described the anticancer investigations of some endemic and non-endemic plants from Nigeria [2]. This study was carried out as a part of our continued exploration of Nigerian medicinal plants for interesting biological activities. Thus, the main aim of the present project was to carry out a phytochemical and cell biological investigation on selected plants from the southern part of Nigeria, especially on those that are endemic and those that find a use in traditional medicine as anticancer agents. In this study, four plants were collected for evaluation of their antitumor activities with respect to pro-apoptotic and anti-adhesive properties.

* Correspondence: faloabi@uniben.edu
[2]Department of Pharmaceutical Chemistry, Faculty of Pharmacy, University of Benin, Benin City, 300001, Nigeria
Full list of author information is available at the end of the article

Picralima nitida (Stapf.) Th. & H. Durand (Flowering plant family: *Apocynaceae*) has widely varied applications in Nigeria folk medicine for antipyretic, antihypertensive, gastro-intestinal disorders, as an antimalarial, aphrodisiac, antitrypanocidal, and as a remedy against hyperglycemia [3-6]. The plant is used in Nigeria and West Africa as remedy against breast cancer [7].

Pyrenacantha staudtii Hutch and Dalz (Tropical forest tree family*: Icacinaceae*) is a medicinal plant widely used in tropical Africa for the treatment of various ailments such as stomach disorders, intestinal colic, menstrual disorders, and as anticancer and antiabortificient agents [8,9].

Jatropha gossypifolia L (*Euphorbiaceae*) is widely distributed in many tropical countries [10,11]. It has antibacterial, antiinflammatory, analgesic and anticancer activities [12]. It was known in ancient medicine for its ethnomedicinal uses in the treatment of cancerous growth and for its pesticidal activity [13,14].

Jatropha curcas Linnaeus (*Euphorbiaceae*) is a small tree or large shrub that can reach a height up to 5 m. It is used in traditional medicine as remedy against cough, cancer, and human immunodeficiency virus [15]. The local populace in the eastern part of Nigeria uses the ethanol extract for the treatment of breast cancer. In some cases, traditional herbal practitioners use the aqueous decoction to cure cancer [15]. The search for anticancer agents via activity directed identification and characterization lead to the present study with a view to validating the claimed ethno-medicinal property of these plants as anticancer remedy. Hence, this study is focused totally on the exposure of the ethanol root bark extracts of the plants to MCF-7 cancer cell line in a dose-dependent manner.

Methods

Collection and identification of plant materials

The plant parts (listed in Table 1) were collected from different locations of Nigeria in the rainy season (March-June) of 2011 and identified by Mr. A. Sunny of the Department of Pharmacognosy, Faculty of Pharmacy, University of Benin, Benin City. Voucher specimens are deposited at the Faculty of Pharmacy, University of Benin, Nigeria.

Preparation of plant extracts

The powdered plant samples (100 g) were each extracted by maceration, with ethanol (250 ml) at room temperature, and concentrated to dryness using a rotary evaporator at reduced pressure. The% yield (10, 23, 40 and 51 for JCP1, PS, ZI and JCP2, respectively) was obtained. Dried samples were stored at −20°C until further use. Finally, all plant extracts were dissolved in dimethylsulfoxide (DMSO) to give a desired stock solution of 50 mg/ml, which was aliquoted and stored at −80°C.

Phytochemical composition of extracts

The ethanol extracts were subjected to photochemical screening in order to identify the secondary metabolites and nature of the extracts. The method employed, was from Trease and Evans [16].

Cell culture

Human breast adenocarcinoma cell line MCF-7 (ATCC no. HTB-22) was obtained from the America Type Culture Collection (Manassas VA, USA). Cells were maintained at 37°C and in a 5% CO_2 atmosphere in a monolayer in Dulbecco's modified Eagle's medium (DMEM, Invitrogen, Germany) with 10% fetal bovine serum (PAA Laboratories GmbH, Germany) and 1% gentamycin (Ratiopharm, Germany). Confluent cells were passaged by treating them with 0.05% trypsin/ 0.02% EDTA. The medium was changed every two days. MCF-7 cells were authenticated by morphology and growth rate and were mycoplasma free. Cultivation conditions were described previously [17].

Treatment with plant extracts

Treatment conditions were previously described [17]. Treatments with the four plant extracts (final concentrations of 1, 10, 25, 50 μg/ml) were carried out for 48 h in assay medium. As negative control substance the vehicle dimethylsulfoxide (DMSO, 0.1%) was used in the same manner.

Cell cycle analysis

To determine proliferation and apoptosis alterations, the cell cycle analysis via flow cytometry (FACSCalibur, BD

Table 1 Properties of the four Nigerian plants used in this study

Plant	Abbr.	Family	Parts used	Medical uses	Location	$IC_{50\ MCF-7}$ (μg/ml)
**Jatropha curcas* Linn	JCP1	Euphorbiaceae	RB	cough, wound healing, HIV, cancer	Benin City	36.55
**Pyrenacantha staudtii* Hutch & Dalz	PS	Icacinacaeae	L	threatened abortion, malaria, GIT and cancer	Benin City	37.36
**Picralima nitida* Th. & H. Durand	ZI	Apocynaceae	RB	malaria, hyperglyaceamia, antiseptic etc.	NIFOR	22.76
**Jatropha gossypifolia* Linn	JCP2	Euphorbiaceae	RB	cancer, pesticides	Owan	25.55

Overview of the four plant extracts including its medical uses, IC_{50} values at 48 h for MCF-7 cells. RB; Root bark; L; leaf; * Most of the information of traditional use has been taken from native people.

Biosciences) after propidium iodide staining (50 mg/ml) of the MCF-7 cells was carried out [17,18]. For data acquisition, the software FlowJo version 7.6.5 (Tree Star; www.flowjo.com) was used. A minimum of 15,000 ungated events were recorded. For statistical analysis, the S-phase and G2/M-phase cells of the cell cycle were defined as proliferative cells and the sub-G1-peak of the histogram as apoptotic ones.

Annexin V/PI apoptosis detection

In this assay, Annexin-V detects the translocation of phosphatidylserine from the inner leaflets to the outer leaflets of the plasma membrane, which is a key feature of apoptotic cells, whereas PI detects necrotic cells with permeabilized plasma membrane. Labeling of early apoptotic and dead cells was performed according to the manufacturer's instructions from the Alexa Fluor488 Annexin V/Dead Cell Apoptosis Kit (Thermo Fisher Seintific Inc., Germany). Cells were treated with 10 μg/ml plant extract for 48 h. After treatment detached as well as adherent cells were washed twice with cold PBS. The cell pellet was resuspended in 100 μl of annexin binding buffer at a density of 1×10^6 cells per ml and incubated with 5 μl of Alexa488-conjugated Annexin-V and 5 μl of PI for 15 min at room temperature in the dark. 400 μl of 1× binding buffer was added to each sample tube, and the samples were immediately analyzed by flow cytometry. Histograms and statistics were designed with the software FlowJo Version 7.6.5.

Calculation of cell detachment

400,000 MCF-7 cells were seeded in 6-well plates (Greiner, Germany). After treatment with the four plant extracts (10 μg/ml) and the DMSO control detached cells were counted by flow cytometry.

Measurement of integrin expression

Measurement and calculation of β1-integrin expression at the cell surface by flow cytometry (FACSCalibur) was described previously [18]. Anti-integrin antibody β1 (CD29; Immunotech, 0.2 mg/ml, mouse anti-human 4B4, Isotype: IgG1) was secondarily labeled with fluorescein isothiocyanate-conjugated anti-mouse IgG (Fab_2) fragment (Sigma). Ten thousand events were recorded for each measurement and each measurement was repeated three times.

Immunofluorescence and microscopy

Filamentous (F)-actin was selectively labeled with BODIPY® FL phallacidin emitting green fluorescence (Invitrogen, Germany). Nuclei were stained with Hoechst dye (Invitrogen, Germany). Bright field and all fluorescence images were obtained using Axio Scope A1 fluorescence microscope (Carl Zeiss, Germany). Individual fluorophores were imaged in black and white for maximum sensitivity and pseudocolored and overlaid using AxioVision Imaging Software Release 4.8.2. (Carl Zeiss, Germany).

Western blotting procedure

After treatment with the plant extracts for at least 48 h the cells were trypsinized, washed with PBS and lysed in ice-cold lysis buffer (Bio-Plex Cell Lysis Kit, Bio-Rad, USA). Cells were homogenized by brief sonification at 4° C and centrifuged at 10,000 g for 2 min at 4°C. Protein concentrations of the supernatants were estimated by Bradford protein assay so that equal amounts (10 μg) of total soluble protein could be separated by Criterion TGX Stain-Free precast gels (Bio-Rad, Germany) and blotted on PVDF membranes. After SDS-PAGE, protein content per lane as well separation quality was additionally controlled with the Criterion Stain FreeTM gel imaging system (Bio-Rad, Germany). After the protein transfer membranes were blocked with 5% skim milk in Tris buffered saline (TBS) and washed six times in TBS. For protein detection primary antibodies (β1 integrin: sc-374429; PCNA: sc- sc-56; both from Santa Cruz, USA; caspase 7, 8, 9 from the Apoptosis sampler kit #9915; FAK antibodies within the sampler kit #9330; Akt #4691; pAkt (S473) #9271; p44/42 MAPK #9102; P-p44/42 MAPK (T202/204) #4377; β-Actin #4970: all from Cell Signaling, USA) were incubated overnight at 4°C followed by labeling with a horseradish peroxidase (HPR)-conjugated secondary antibody (Dako, Glostrup, Denmark) for 1 hour at room temperature. Protein signals were visualized by using SuperSignal West Femto Chemiluminescent Substrate (Pierce Biotechnology, Rockford, USA) for detection of peroxidase activity from HRP-conjugated antibodies (Thermo Fisher Scientific Inc., Rockford, USA). Band intensity was analyzed densitometrically with the Molecular Imager ChemiDoc XRS and Image Lab 3.0.1 software (Bio- Rad, USA). Protein detection was repeated at least three times with individual prepared cell lysates from independent passaged cells.

Tunel assay

Apoptotic DNA degradation was stained using the terminal deoxynucleotidyl transferase (TdT)-mediated dUDP-biotin nick end labeling (TUNEL) method. In this study, the In Situ Cell Death Detection Kit, Fluorescein (Roche, USA) was used for this purpose according to the manufacturer's protocol. Briefly, MCF-7 cells (1.5×10^6 cells/well) were cultured on cover glasses in 6-well plates. After exposure to the plant extracts, cells were washed with PBS, fixed with 4% paraformaldehyde solution for 1 h at 15–25°C, and incubated in permeabilisation solution for 2 min on ice. After washing with PBS cells were incubated with the TUNEL reaction mixture

for 60 min at 37°C in a humidified atmosphere in the dark.

Fluorescence of the stained cells was observed using a Carl-Zeiss confocal laser scanning microscope (LSM 780, Jena, Germany) with an excitation wavelength of 488 nm.

Calculation of IC_{50} values

The half maximal inhibitory concentrations (IC_{50}) values were calculated by colorimetric measurements of mitochondrial metabolic activity with the CellTiter MTS/PES assay following to the manufacturer's instructions (Promega Corp., Madison, WI). MTS is a tetrazolium compound [3-(4,5-dimethylthiazol-2-yl)-5-(3-carboxymethoxyphenyl)-2-(4-sulfophenyl)-2H-tetrazolium] which is combined with an electron coupling reagent (phenazine ethosulfate; PES) to form a stable solution. The conversion to formazan is bioreduced by cells which is presumably accomplished by NADPH or NADH produced by dehydrogenase enzymes in metabolically active cells. The measured mitochondrial metabolic activity also reflects the cell cytotoxicity directly and the cell viability indirectly.

Cells were seeded in 96-well plates at a density of 2000 cells/well in 100 μl medium and left to attach for 24 h. Treatment with plant extracts at final concentrations of 1, 10, 25, and 50 μg/ml was carried out as described previously. In parallel, control approaches were carried out with medium only and 0.1% of the solvent DMSO to calculate background absorbance. No background absorbance was obtained for the extracts and MTS in the absence of cells, as some extracts are capable of reducing the MTS. After an initial incubation for 24 h cells were assayed with MTS according to the manufacturer's instructions (Promega Corp., Madison, WI). Colorimetric changes were measured at 490 nm and raw data was transferred to Microsoft Excel and analyzed. At least 8 replicates corrected with the background absorbance were performed. Reduction of cell viability at each concentration was plotted as a dose response curve. The IC_{50} of the active extracts were calculated using nonlinear regression to fit data to the dose–response.

Live/dead cell staining

Live/Dead cell staining was performed following the manufacturer's instructions (Live/Dead Cell Staining Kit II, PromoCell GmbH, Germany).

Statistical analysis

All data were analyzed by the Students *t*-test using Microsoft Excel 2010. Every experiment was done in triplicate with individual passaged cells and data sets were expressed as means ± standard deviations (SD). Statistical significance was represented as $^{***}P < 0.001$, $^{**}P < 0.01$, $^{*}P < 0.05$.

Results and discussion

The list of the investigated plants, the parts used and their known medicinal uses are represented in Table 1. These informations were sorted out in accordance with the recommendation of the *Handbook of African Medicinal Plants* [4]. *Ethnobotany Desk Reference* [19], and direct information obtained by Dr. A. Falodun (Department of Pharmaceutical Chemistry, Faculty of Pharmacy, University of Benin, Benin City, Nigeria) through interviewing local traditional healers. Ethno pharmacological data (information based on the medicinal traditional use of plants) has been one of the common useful ways for the discovery of biologically active compounds from plants [20]. The phytochemical composition of the extracts showed the presence of alkaloids, tannins, saponins, flavonoids in JCP1, PS and ZI. Only tannins and flavonoids were present in JCP2 (Table 2).

Proliferation and apoptosis events after treatment with the plant extracts

First, the anti-cancer properties of these four extracts were examined by cell cycle analysis. Therefore, we chose the breast cancer cell line MCF-7, a model for hormone-dependent non-invasive cancer types. This model fits for initial screening experiments with these untested extracts. Cell cycle analysis via flow cytometry allowed us to distinguish between alterations in proliferation and apoptosis. Distribution of cell cycle phases (histograms) of MCF-7 cells after treatment with different concentrations (1, 10, 25 and 50 μg/ml) of the plant extract are mentioned in Figure 1A. In untreated, exponentially growing MCF-7 cells the G1- and G2/M-phases were well defined with a large number of dividing cells (S-phase between G1- and G2/M-peaks). Demonstrated were the most prominent histograms of all measurements (Figure 1A).

All four plant extracts caused a significant influence on the proliferation phases of the MCF-7 cells, which turned out to be concentration dependent but not always linear. To quantify proliferation we defined the cell cycle phases S and G2/M as proliferative phases so that the sum of it describes the proliferation rate. In parallel, the apoptotic rates were measured by determination of

Table 2 Determined substance classes

Phytochemical compositions	*J. curcas* (JCP1)	*P. staudtii* (PS)	*P. nitida* (ZI)	*J.gossypifolia* (JCP2)
Alkaloids	+	+	+	-
Saponins	+	+	+	-
Tannins	+	+	+	+
Flavonoids	+	+	+	+

Phytochemical compositions of the root bark extracts of four medicinal plants. + presence of components; – absence of components.

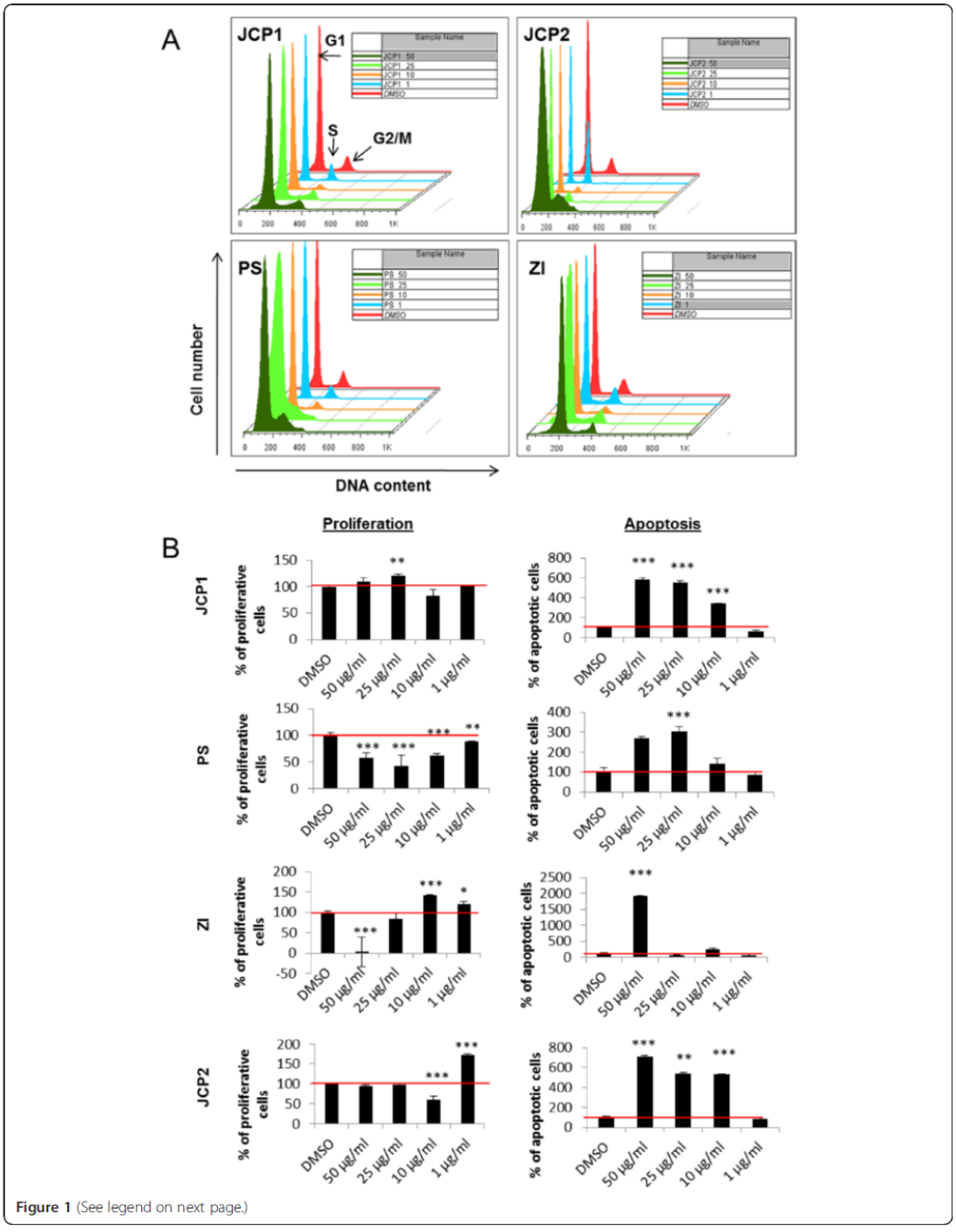

Figure 1 (See legend on next page.)

(See figure on previous page.)
Figure 1 Cell cycle analysis of MCF-7 cells. A: Histograms of the cell cycle distribution of MCF-7 cells after treatment with the control substance DMSO and the plant extracts JCP1, PS, ZI, JCP2 at concentrations of 1, 10, 25 and 50 μg/ml for 48 hours. G1, S and G2/M phases are marked with black arrows. Represented were the most prominent samples of 3–5 individual replicates. **B**: Calculation of proliferation and sub-G1 phase. Measurement of proliferation and apoptosis via cell cycle analysis after treatment with the vehicle DMSO (equates to 100%) and the plant extracts JCP1, PS, ZI, JCP2 at concentrations of 1, 10, 25 and 50 μg/ml for 48 h. As proliferative phases the sum of S and G2/M phases were calculated in percentages. As apoptotic fraction the sub G1-peak was measured. (mean ± SD, n = 5, ***P < 0.001, **P < 0.01, *P < 0.5, significantly different compared to control, unpaired *t*-test).

the sub G1-peak showing DNA fragmentation events. Both results were displayed in Figure 1B. As negative control the DMSO treated cells were set to 100%. As positive controls genistein was used which results were previously reported [17]. Only the PS extract mediated an almost linear reduction in proliferation. In contrast, the ZI extract showed a biphasic effect. Low concentrations (1–10 μg/ml) caused an increase in the proliferative phases and at a concentration >25 μg/ml, the proliferation was significantly reduced. JCP1 induced only a slight proliferation induction after an exposure of 25 μg/ml accompanied by a significant elevation of sub-G1 positive cells. This effect of proliferation and apoptosis induction at the same time is noted by a number of studies have which have shown that cell-cycle regulators could interconnect with proliferation and apoptosis [21]. In contrast, JCP2 displayed a bi-phasic effect on the distribution of the MCF-7 cell cycle phases. At the lowest concentration of 1 μg/ml the content of the G2/M phase nearly doubled in comparison to the DMSO

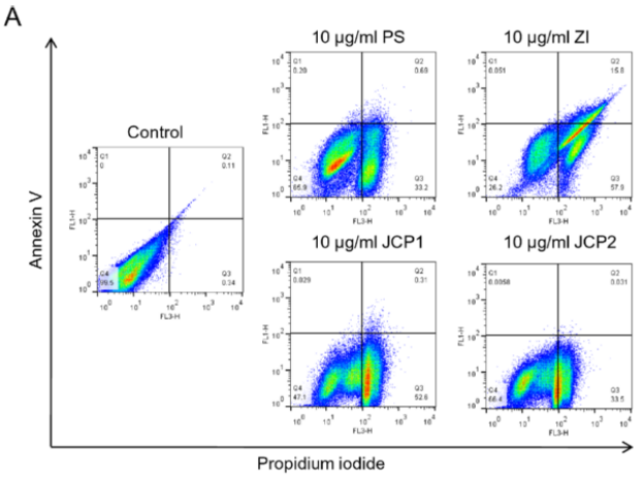

B

	Annexin V	PI	Annexin V/PI	Sub G1
Control	0.7% ± 0.13	1.68% ± 0.78	0.3% ± 0.24	1.35 %
JCP1	0.33% ± 0.29	46.54% ± 15.77	0.31% ± 0.01	40.40%
PS	1.52% ± 0.97	33.05% ± 9.08	0.61% ± 0.21	2.69%
ZI	0.16% ± 0.11	34.43% ± 17.82	7.05% ± 9.34	2.21%
JCP2	0.15% ± 0.13	47.80% ± 14.32	0.0% ± 0.4	65.49%

Figure 2 Apoptosis determination via Annexin V/PI staining. A: Histogramms of Annexin V/PI- stained MCF-7 cells after treatment with 10 μg/ml of the four plant extracts in comparison with the control treatment for 48 h. Annexin V in conjunction with PI staining was used to distinguish early apoptotic (Annexin V- positive, PI negative; quadrant 1 of each panel) from late apoptotic or necrotic cells (Annexin V positive, PI positive; quadrant 2 of each panel). **B**: Table of quantitative analysis of single Annexin V or PI positive and double positive stained MCF-7 cells. Notably, sub-G1 phase positive cells from the cell cycle measurement were listed for comparison. Results are representative of three separate experiments.

control. Analogously to the PS extract, a JCP2 concentration of 10 μg/ml caused also a significant reduction of G2/M phase and an arrest in G0/G1 phase.

But ultimately, all four extracts mediate a significant increase in sub-G1 phase. The extracts JCP1 and JCP2, already caused at the low concentration of 10 μg/ml a significant increase in the sub-G1 phase. In summary, all four plant extracts were able to influence the proliferation rates of the estrogen receptor-positive cell line MCF-7 depending on the concentrations used. This phenomenon is not uncommon for some effective anticancer extracts. For example, soy ingredients like genistein causes biphasic effects on hormone-dependent cancer cell lines [22]. At low concentrations (1–10 μM), genistein stimulates cell proliferation whereas higher concentrations are able to induce a block in G2/M phase. This result suggests that the plant extracts contain substances that trigger similar biphasic effects, known as phytoestrogens such as genistein. In subsequent experiments, the exact ingredients of the extracts by high-performance liquid chromatography (HPLC) and gas chromatography–mass spectrometry (GC-MS) will be analyzed to obtain a deeper insight into the existing drug classes.

However, to confirm the results of the cell cycle analysis, three additional methods were used to verify the influence on proliferation and apoptosis: Annexin V/PI labeling, TUNEL assay and western blotting experiments of relevant proteins. Beside the calculation of the sub-G1-peak by cell cycle analysis, apoptosis/necrosis induction was determined by using Alexa Fluor488 Annexin V/PI staining (Figure 2). Treatment with 10 μg/ml JCP1 and JCP2 resulted in the highest levels of dead MCF-7 cells (46% and 47%) which were positive for the PI labeling. These values are comparable with the apoptosis data obtained from the determination of the sub-G1 phase in the cell cycle measurement which indeed showed the highest percentages in sub-G1 phase. The treatment with 10 μg/ml PS and ZI resulted in approximately 33% cell death compared to the control. Surprisingly, only the treatment with 10 μg/ml ZI showed a moderate Annexin V/PI labeling, as an indication of late apoptosis induction. PS, and especially JCP1 and JCP2 induced only necrotic events, verified by high amounts of PI-positive cells. These results are similar to those of the TUNEL measurements (Additional file 1: Figure S1). At concentrations of 10 μg/ml PS, JCP1 as well as JCP2 caused DNA fragmentation within the cell nucleus, whereas ZI induced signals within the cytoplasm, indicating for extrinsic death signals.

Furthermore, the induction of apoptosis was verified by western blot analysis with apoptosis relevant specific

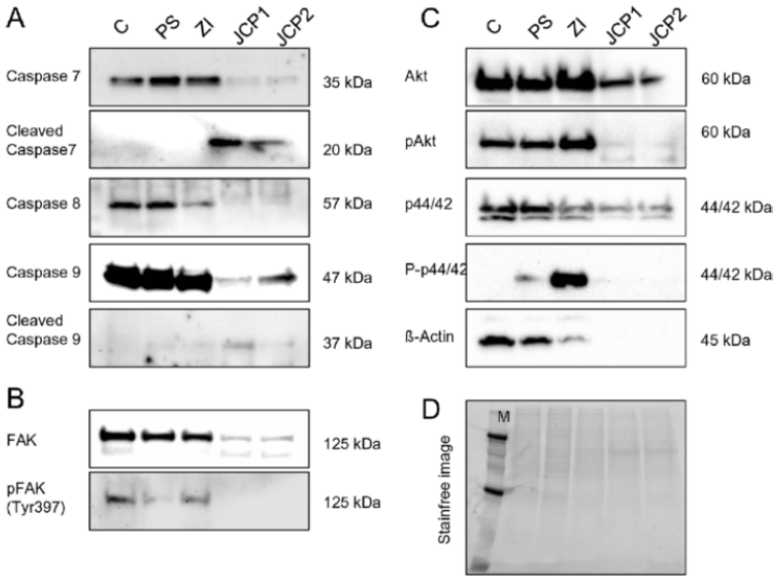

Figure 3 Protein expression analysis of MCF-7 cells by Western blotting after treatment with 10 μg/ml of the four plant extracts in comparison with the control treatment for 48 h. A: Determination of caspase 7, 8, and 9 cleavage. Detected were the pro-caspases as well as the cleaved proteins. **B**: Expression of total focal adhesion kinase (FAK) protein and phosphorylated FAK protein at residue Tyr397. **C**: Protein content of kinases: total Akt, phosphorylated Akt at residue S473 (pAkt), total MAPK p44/42, phosphorylated MAPK p44/42 at residues T202/204 (P-p44/42) and β-Actin which did not function as housekeeping protein. **D**: Stain-free image of separated proteins after SDS-PAGE to ensure equal protein amounts on each polyacrylamide gel used.

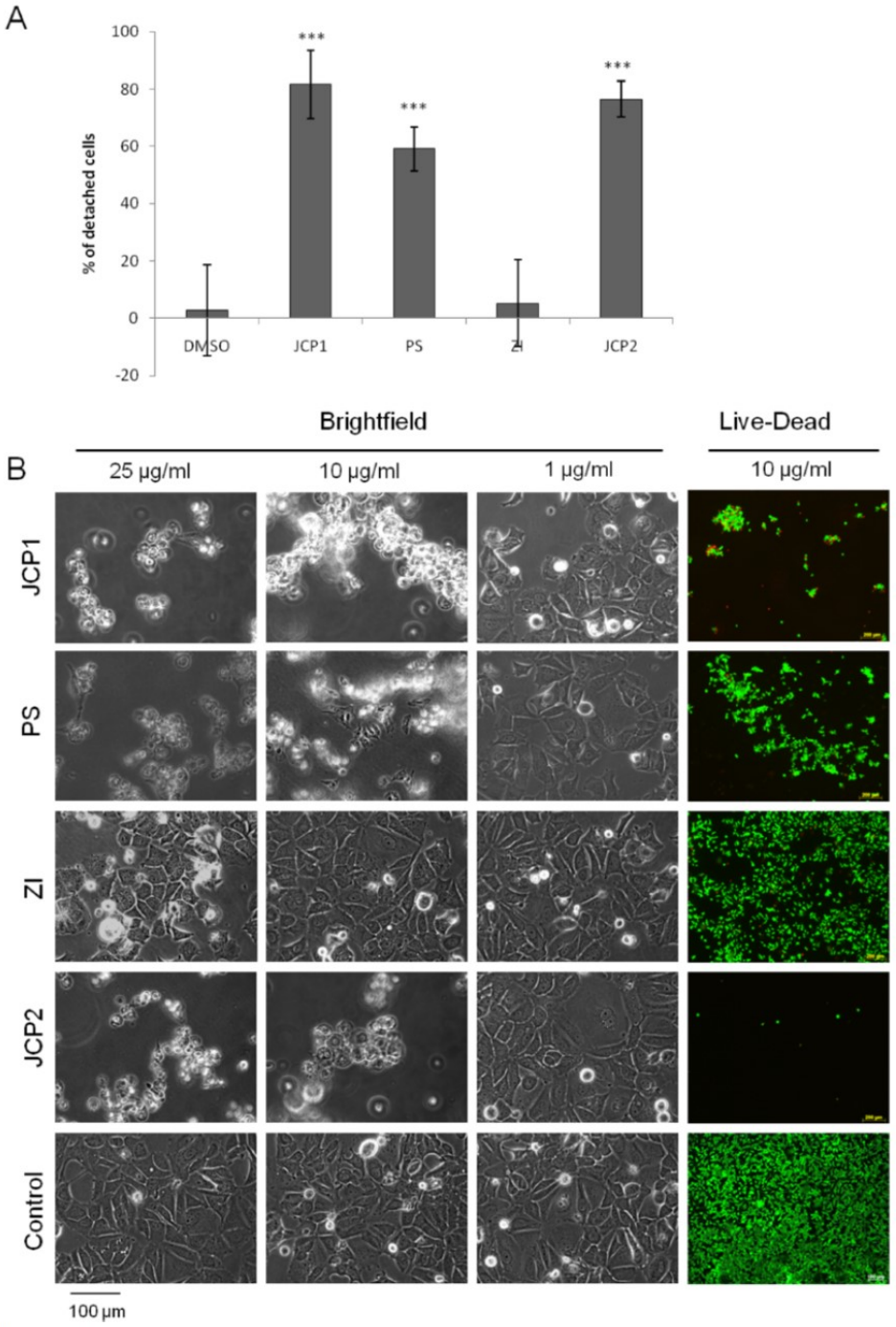

Figure 4 (See legend on next page.)

(See figure on previous page.)
Figure 4 Measurement of cell detachment and morphological alterations. A: Cell detachment was calculated by flow cytometry after 48 h after exposure to 10 μg/ml of the plant extracts and 0.1% DMSO. (mean ± SD, n = 8, **P < 0.01, *P < 0.05, significantly different compared to control, unpaired *t*-test). **B**: Bright field microscopy to monitor morphological alterations after treatment with the four plant extracts JCP1, PS, ZI, JCP2 in a concentration dependent manner on MCF-7 cells. Even the lowest concentration of 1 μg/ml caused a significant detachment of the MCF-7 cells from the plate surface. At a concentration of 10 μg/ml almost 70 - 80% of all cells treated with PS, JCP1 and JCP2 were detached. Detachment correlates with induction of apoptosis which was determined by two-color fluorescent Live/Dead-Staining. Green: viable cells; red: dead cells.

antibodies (Figure 3A). The treatment with 10 μg/ml JCP1 and JCP2 revealed a cleavage of caspase 7 and caspase 9 so that pro-caspases 7 and 9 were hardly to detect which also applies also to caspase 8. Interestingly, neither the PS nor the ZI extract lead to caspase cleavage. The proliferation results of the cell cycle analysis were validated by the expression analysis of PCNA (Proliferating Cell Nuclear Antigen) (Additional file 2: Figure S2). At a concentration of 10 μg/ml ZI induced an increase of the proliferative phases whereas the JCP1 and JCP2 decreased the expression of PCNA. Ultimately, these results demonstrate that the cell cycle analyses were well performed and comparable with Annexin V/PI labeling as well as with expression analysis of PCNA. The JCP1 and JCP2 extracts mediated the strongest decrease in proliferation with a simultaneous induction of cell death.

Plant extracts induced cell detachment mediated by decreased β1 integrin expression

Morphological alterations under treatment conditions were verified by bright field microscopy (Figure 4B). The plant extracts PS, JCP1 and JCP2 at concentration of 10 μg/ml or higher induced a loss of cell-cell and cell-matrix adhesion accompanied by rounding of the cells. Treatment with ZI induced no visual cell detachment. Incubation with 1 μg/ml plant extract resulted in a few detached cells while the typical cell cluster of MCF-7, called domes, were not affected. To calculate detachment rates, detached MCF-7 cells after exposure to 10 μg/ml plant extract were counted by flow cytometry (Figure 4A). The extracts JCP1 and JCP2 induced significant increased cell detachment with rates of 81% and 76%, respectively. Exposure with the PS extract resulted in 59% detached cells. The ZI extract caused no significant cell detachment in comparison to the control.

Detachment from the extracellular matrix or lost contact with the neighbor cells is a clear indication of induction of an apoptotic process that is termed anoikis [23]. This observation confirmed the results of the cell cycle measurements that showed a significant increase of apoptotic cells after treatment with 50 μg/ml of the four plant extracts. To confirm the induction of anoikis, which is accompanied by cell detachment, we performed live/dead staining of the cell after exposure to 10 μg/ml of the extracts. These staining demonstrated that only attached cells were viable (green fluorescence) while detachment by the extracts caused cell death (red fluorescence). Moreover, this test showed that the concentration of 10 μg/ml of each extract led to a different degree of cell detachment. Treatment with JCP1 and JCP2 resulted in the highest cell detachment rates (approximately 60 - 90%), so that nearly no viable cells were attached to the cell culture plates. The ZI extract exhibited the lowest rate of cell detachment and only a few dead cells, which correlated with the results of the cell cycle measurements where the ZI extract at a concentration of 10 μg/ml showed a significantly increased proliferative phase.

The ability of epithelial cells to survive through suppression of anoikis depends on their engagement to the extracellular matrix through a family of heterodimeric transmembrane receptors named integrins. Anoikis in mammary epithelial cell can be initiated by direct inhibition of β1-integrins [24,25]. Therefore, the β1 integrin expression by flow cytometry analysis was measured (Figure 5A). Although the three plant extracts, JCP1, JCP2 and PS lead to cell detachment at a concentration of 10 μg/ml, only JCP2 lowered the β1-integrin expression in MCF-7 cells, significantly. PS and JCP1 revealed only a slight decrease in β1-integrin expression while ZI increased the β1-integrin level significantly up to 9%. Because the flow cytometry data only represent the levels of membrane associated β1-integrin expression, western blotting was performed with a β1-integin specific antibody. Additional file 2: Figure S2 shows the expression pattern of β1-integrin in the soluble and membrane protein fractions. Consistent with flow cytometry results the exposure with 10 μg/ml ZI revealed a significant increase of β1-integrin in the membrane fraction, while the soluble content was markedly reduced. The extracts JCP1 and JCP2 convey no significant change in β1-integrin expression, neither in the soluble nor the membrane fraction. The PS extract is the exception. Compared with the flow cytometry data 10 μg/ml PS extract caused a significant increase in β1-integrin expression in the membrane fraction while the soluble protein content was reduced. This phenomenon may be attributable to the fact that different antibodies were used for the flow cytometry analysis. The antibody suitable for western blotting detection of β1-integrin was raised against amino acids 375–480 mapping within an extracellular domain of β1-integrin of human origin (sc-374429,

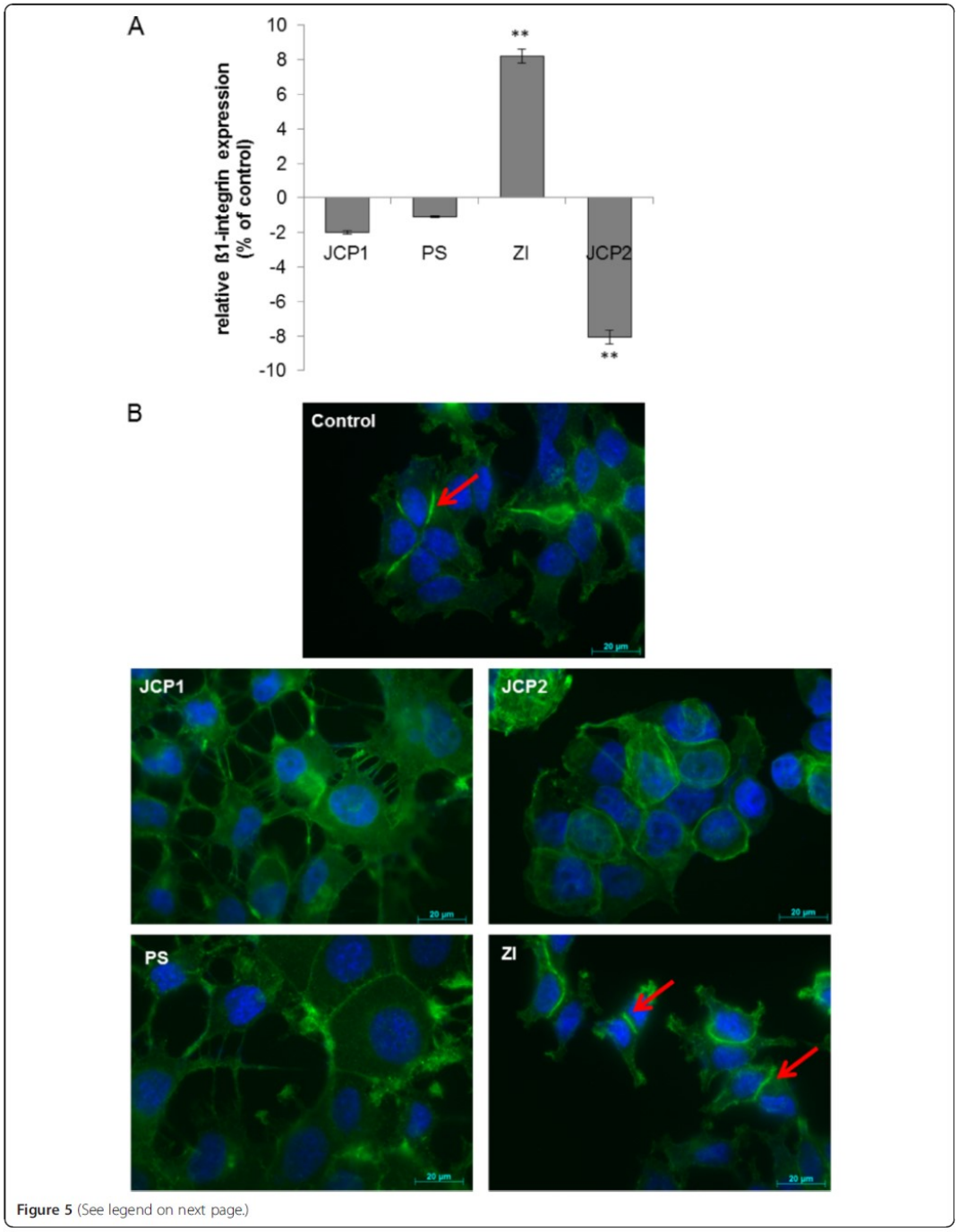

Figure 5 (See legend on next page.)

(See figure on previous page.)
Figure 5 Monitoring of adhesion related proteins. A: Cell membrane associated (cell surface) β1-integrin expressions of plant extract treated (10 μg/ml) MCF-7 cells in percent of control measured by flow cytometry. As control DMSO treated cells were used. (mean ± SD, n = 3, **P < 0.01, *P < 0.05, significantly different compared to control, unpaired *t*-test). **B**: Fluorescence microscopy of F-actin (green) alterations after treatment with 10 μg/ml of the plant extract. Nuclei are marked in blue. Arrows point to the increased actin accumulation at sides of cell-cell contacts.

Santa Cruz). The flow cytometric antibody (CD29, Immunotech) was raised against the entire amino acid sequence, making it more specific for β1-integrin detection. Thus, it is possible that there will be slight differences in the recognition of the β1-integrin protein. Accordingly, the western blot results are only a general review of the flow cytometry data. However, it could be confirmed that the ZI extract mediates a clear overexpression of β1-integrin in the cell membrane. In contrast, JCP1 and JCP2 caused a slight reduction in β1-integrin expression.

Additionally, the expression levels of the focal adhesion kinase (FAK), a widely expressed cytoplasmic protein tyrosine kinase involved in integrin-mediated signal transduction and its phosphorylation status was checked (Figure 3B). Consistent with the lowered β1-integrin expression levels after treatment with JCP1 and JCP2, the expression of total FAK and the phosphorylation at residue Tyr397 decreased. Also the exposure to PS caused a slight decrease in the autophosphorylation of FAK indicating for the deactivation of FAK and lowered adhesion to the extracellular matrix.

These findings suggest that the plant extracts target different signaling pathways in the MCF-7 cells and thus initiate various mechanisms of cell detachment. Loss of integrin binding to extracellular matrix proteins results in impairment of cell spreading which depends on the integrity of the internal actin cytoskeleton formation [26]. This assertion is supported by the fact that the formation of the actin cytoskeleton is affected differently by the plant extracts (Figure 5B). Under control conditions MCF-7 cells form a diffuse actin cytoskeleton without any visible stress fibers. The actin filaments are short and find to be enriched at sides of cell-cell contacts (Figure 5B; red arrows). JCP1, JCP2 and PS revealed a distinct alteration of the actin organization. No strong accumulation of actin in adjacent cells could be observed in comparison with controls. By treatment with the PS and JCP1 strong cellular contacts were diminished. Cells seem to be enlarged in their areas and express filopodia. Consistent with the increased β1-integrin expression by ZI increased formation of actin filaments was observed between neighboring cells (Figure 5B, red arrows). In addition, the western blot results confirm that after treatment with JCP1 and JCP2 the β-actin filaments were degraded: further evidence for the induction of anoikis (Figure 3C).

However, the three plant extracts (JCP1, JCP2 and PS) harbor anticancer potential, which should be analyzed in further studies. Especially the signaling mechanisms should be identified because initial analysis of central signaling molecules like the serine/threonine-specific protein kinase Akt and mitogen-activated protein kinases (MAPKs) showed alterations in their expression levels (Figure 3C).

Plant extracts harbor IC_{50} values between 23 and 38 μg/ml

Finally, the IC_{50} values of the plant extracts for MCF-7 via MTS assay was determined (Figure 6). Data of the MTS measurements were plotted on dose response curve and IC_{50} values were calculated by non-linear regression. The IC_{50} values for JCP1, PS, ZI and JCP2 for MCF-7 cells were 36.55, 37.36, 22.76 and 25.55 μg/ml, respectively. These values describe a moderate potential as an anti-cancer agent but colorimetric test were not that convincing and require confirmation by additional experiments [27]. Also, because the cell cycle analysis, bright field microscopy and β1-integrin expression revealed a markedly lower effective concentrations (1–10 μg/ml) of the plant extracts. However, further investigation is needed to explore the detailed anticancer potential of these plant extracts and the corresponding signaling pathways.

Conclusion

Anticancer screening experiments for bioactive agents from natural products are in focus of current research. But effective screening methods are rare and sometimes difficult to interpret. Therefore in this study standard methods were chosen for the interpretation of the influence on proliferation (cell cycle measurement, PCNA expression by Western blotting), apoptosis (cell cycle measurement, Annexin V/PI labeling, TUNEL assay, live-dead staining, caspase claevage), morphology (bright field imaging), metabolism (MTS assay) and adhesion (β1-integrin expression, F-actin staining, cell detachment). These methods allow an overview of the potential effectiveness of the extracts on the key mechanisms of cancer cells, but do not allow a clear identification of signaling pathways. All four plant extracts displayed distinct alterations on these major cellular mechanisms in the breast cancer cell line MCF-7. These results reveal an anti-tumorigenic potential of the four plant extract. But the dose response curves and calculated IC_{50} values also indicate a general cytotoxic activity. This could be

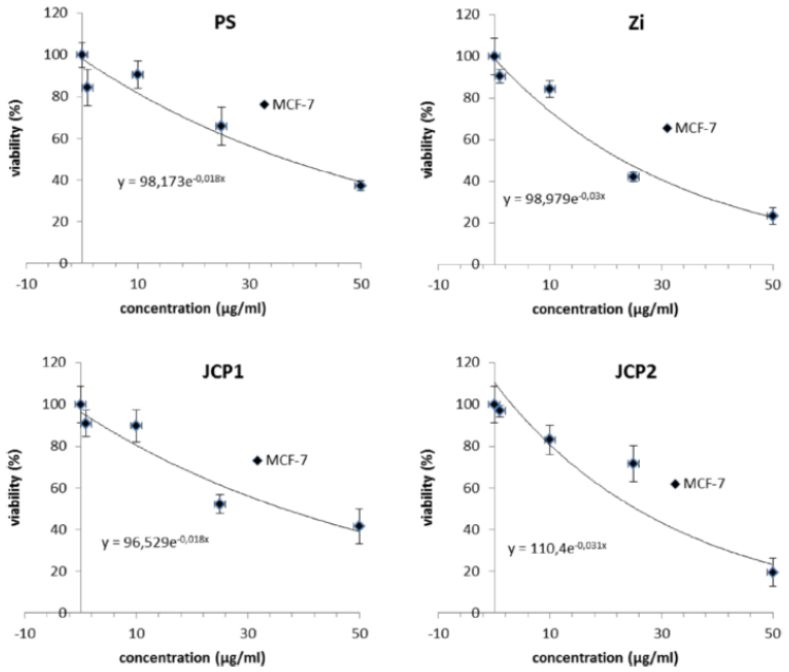

Figure 6 Determination of IC_{50} values. The 50% inhibition concentration (IC_{50}) values of the four plant extracts JCP1, PS, ZI, JCP2 on MCF-7 cancer were measured by MTS assay. The four extracts reduced viability of MCF-7 cells in a dose dependent manner. IC_{50} values (see Table 1) were calculated from the dose response curves by nonlinear regression. Background absorbance was corrected against MTS reaction without cells and control treatment (0.1% DMSO).

due to the mixture of ingredients within the extracts. Accordingly, in subsequent experiments the active substance classes will be identified and fractionated. The overall goal for future work is to isolate the active compounds and their testing on different cancer cell lines.

Interestingly, the PS, JCP1 and JCP2 plant extracts induced cell rounding and cell detachment at concentrations ≥10 µg/ml. Cell detachment could be caused by several processes. One protein relevant for cancer cell progression and metastasis is the β1-integrin [28]. This finding implicates that the ZI extracts influences different cellular pathway compared with other extracts. However, the four tested plant extracts exert cytotoxic and anticancer potential which should be investigated in further studies.

In conclusion, the results in the present study coincide to some extent with the traditional uses of the plants investigated. Our results further supported the idea that medicinal plants can be promising sources of potential anticancer, antimicrobial and antioxidants agents. The present results will form the basis for selection of plant species for further investigation in the potential discovery of new natural bioactive compounds. Studies aimed at the isolation and structure elucidation of anticancer chemical constituents are in progress.

Additional files

Additional file 1: Figure S1. DNA fragmentation by TUNEL assay. Late apoptotic effects induced by 1 and 10 µg of the four plant extracts on MCF-7 cells were analyzed by TUNEL assay to measure the extent of DNA fragmentation visualized by confocal laser scanning microscopy (LSM 780, Carl Zeiss, Jena, Germany). Green fluorescence within the cell nucleus of PS, JCP1 and JCP2 (10 µg/ml) reflect DNA damage. Notably, ZI extract causes cytosolic labeling, an indication for extrinsic apoptotic pathways.

Additional file 2: Figure S2. PCNA and integrin expression by western blotting. Expression analysis of β1 integrin and Proliferating Cell Nuclear Antigen (PCNA) of the soluble and membrane fraction of MCF-7 cells after treatment with 10 µg/ml plant extract in comparison with the DMSO control. Loading controls were visualized by stain-free imaging of the SDS-PAGEs prior blotting procedure. Note that β1 integrin expression is demonstrated twice. Upper panel shows the normal exposure, lower panel the overexposed variant.

Competing interests

The authors declare that they have no competing interests.

Authors' contributions

Cell biological experimental work was done by NE and JK. Plant collection, extraction preparation and chemical studies were performed by AF. The first draft of the paper was written by NE and reviewed by AF, JK BN. All authors participated in the design of the study data, read and approved the final manuscript.

Acknowledgements
We would like to thank Deutsche Krebshilfe (FKZ: 107821) and the habilitation scholarship program of University of Rostock for the funding of our work. Special thanks to the University of Benin for the facilities. Funding from DFG-TWAS 2010–12 is highly acknowledged.

Author details
[1]Department of Cell Biology, University Medical Center Rostock, Schillingallee 69, 18057 Rostock, Germany. [2]Department of Pharmaceutical Chemistry, Faculty of Pharmacy, University of Benin, Benin City, 300001, Nigeria. [3]Institute of Chemistry, University of Rostock, Albert-Einstein-Str. 3A, 18059 Rostock, Germany.

Received: 6 December 2013 **Accepted:** 27 August 2014
Published: 9 September 2014

References

1. Cragg GM, Newman DJ: **Antineoplastic agents from natural sources: achievements and future directions.** *Expert Opin Investig Drugs* 2000, **9:**2783–2797.
2. Falodun A, Qadir MI, Choudhary MI: **Isolation and characterization of xanthine oxidase inhibitory constituents of Pyrenacantha staudtii.** *Acta Pharm Sin* 2009, **44:**390–394.
3. Dalziel JM: *The Useful Plants of West Tropical Africa.* London: In The Crown Agents; 1961.
4. Iwu MM: *Hand book of African Medicinal Plants.* U.S.A: CRC Press Inc; 1993:219–221.
5. Oliver B: **Medical plants in Nigeria.** *Ibadan: Nigerian College of Arts, Science and Tech* 1960, 23.
6. Wosu LO, Ibe CC: **Use of extracts of Picralima nitida bark in the treatment of experimental trypanosomiasis: A preliminary study.** *J Ethnopharmacol* 1989, **25:**263–268.
7. Gill LS: *Ethnomedical Uses of Plants in Nigeria.* Benin-City, Nigeria: In University of Benin Press; 1992.
8. Falodun A, Usifoh CO, Nworgu ZAM: **Phytochemical analysis and inhibitory effect of Pyrenacantha staudtii leaf extract on isolated rat uterus.** *Pak J Pharm Sci* 2005, **18:**31–35.
9. Falodun A, Nworgu ZAM, Usifoh CO: **Smooth muscle relaxant effect of 3-carbomethoxylpyridine from P. staudtii leaf on isolated rat uterus.** *Afri J Biotech* 2006, **5:**1271–1273.
10. Csurhes SM: **Bellyache Bush (Jatropha Gossypifolia) in Queensland, Pest Status Review Series - Land Protection.** In *Queensland Government Department of Natural Resources.* Brisbane: Qld; 1999.
11. Sastri BN: **The Wealth of India.** In *Raw Materials*, Volume 5. New Delh: CSIR; 1959:295.
12. Das B, Das R: **Medicinal properties and chemical constituents of Jatropha gossypifolia Linn.** *Ind Drugs* 1994, **31:**562–567.
13. Chatterjee A, Das B, Aditya Chaudhury N, Dabkirtaniya S: **Jatrodien, a lignan from stems of Jatropha gossypifolia.** *Ind J Agric Sci* 1980, **50:**637–638.
14. Chopra RN, Nayar SL, Chopra IC: *Glossary of Indian Medicinal Plants.* New Delhi: CSIR; 1956:149.
15. Muanza DN, Euler KL, Williams L, Newman DJ: **Screening for antitumor and anti-HIV activities of nine medicinal plants from Zaire.** *Int J Pharmacog* 1995, **33:**98–106.
16. Evans WC: **Phytochemical Screening and in Vitro Bioactivity of Medicinal Plants.** In *Trease and Evans Pharmacognosy.* 15th edition. London: W.B. Sanders; 2002:214–393.
17. Engel N, Oppermann C, Falodun A, Kragl U: **Proliferative effects of five traditional Nigerian medicinal plant extracts on human breast and bone cancer cell lines.** *J Ethnopharmacol* 2011, **137:**1003–1010.
18. Nebe B, Peters A, Duske K, Richter DU, Briese V: **Influence of phytoestrogens on the proliferation and expression of adhesion receptors in human and epithelial cells in vitro.** *Eur J Cancer Prev* 2006, **15:**405–415.
19. Johnson T: *Ethnobotany Desk Reference.* Boca Raton, FL: In CRC Press; 1999.
20. Cordell GA, Beecher CW, Pezzuto JM: **Can ethnopharmacology contribute to the development of new anticancer drugs?** *J Ethnopharmacol* 1991, **32:**117–133.
21. Alenzi FQ: **Links between apoptosis, proliferation and the cell cycle.** *Br J Biomed Sci* 2004, **61:**99–102.
22. Cappelletti V, Fioravanti L, Miodini P, Di Fronzo G: **Genistein blocks breast cancer cells in the G(2)M phase of the cell cycle.** *J Cell Biochem* 2000, **79:**594–600.
23. Frisch SM, Francis H: **Disruption of epithelial cell-matrix interactions induces apoptosis.** *J Cell Biol* 1994, **124:**619–626.
24. Boudreau N, Sympson CJ, Werb Z, Bissell MJ: **Suppression of ICE and apoptosis in mammary epithelial cells by extracellular matrix.** *Science* 1995, **267:**891–893.
25. Pullan S, Wilson J, Metcalfe GM, Edwards N, Goberdhan J, Tilly JA, Hickman C, Dive CH, Streuli H: **Requirement of basement membrane for the suppression of programmed cell death in mammary epithelium.** *J Cell Sci* 1996, **109:**631–642.
26. Meredith JE, Fazeli B, Schwartz MA: **The extracellular matrix as a cell survival factor.** *Mol Biol Cell* 1993, **4:**953–961.
27. Wang P, Henning SM, Heber D: **Limitations of MTT and MTS-based assays for measurement of antiproliferative activity of green tea polyphenols.** *PLoS One* 2010, **16:**e10202.
28. Desgrosellier JS, Cheresh DA: **Integrins in cancer: biological implications and therapeutic opportunities.** *Nat Rev Cancer* 2010, **10:**9–22.

doi:10.1186/1472-6882-14-334
Cite this article as: Engel *et al.*: Pro-apoptotic and anti-adhesive effects of four African plant extracts on the breast cancer cell line MCF-7. *BMC Complementary and Alternative Medicine* 2014 **14:**334.

Referenz III

Engel N*, Adamus A, Ali I, Dad A, Ali S, Nebe B, Atif M, Ismail M, Langer P, Ahmad VU. Antitumor evaluation of four selected pakistani plants on human bone and breast cancer cell lines. BMC Complementary and Alternative Medicine.2016, 16:244. DOI: 10.1186/s12906-016-1215-9.

NCBI-Link: https://www.ncbi.nlm.nih.gov/pubmed/27457235

Zusammenfassung:

Ein weiterer Kooperationspartner in diesem internationalen Konsortium zur Identifizierung neuer, pflanzlicher Anti-Tumor-Wirkstoffe ist Prof. Dr. Iftikhar Ali (Department of Chemistry, Karakoram International University, 15100 Gilgit-Baltistan, Pakistan), der auch dieses Projekt initiiert hat und mit dem aktuell eine großanlegte Studie zu der Wirksamkeit von pakistanischen, pflanzlichen Wirkstoffen auf Hals-Kop-Tumore begonnen hat. Auch für diese Arbeit stand uns ein großes Reservoir an traditionell genutzten Heilpflanzen aus Pakistan und Kamerun zur Verfügung, aus dem wir schöpfen konnten. In dieser Arbeit wurden vier pakistanische Pflanzen: *Vincetoxicum arnottianum* (VSM), *Berberis orthobotrys* (BORM), *Onosma hispida* (OHRM and OHAM) und *Caccinia macranthera* (CMM) im Anti-Tumor-Screening bei humanen Knochen- und Brustkrebszelllinien eingesetzt. Der methanolische Wurzelextrakt von BORM induzierte bereits in geringen Konzentrationen Apoptose in den Tumorzellen, primär über einen lysosomalen Signalweg. BORM bewirkte nach der Applikation eine sofortige Reduktion der mitochondrialen Respiration (Abb. 6), begleitet von der gesteigerten Expression des pro-apoptotischen Moleküls BCL-2.

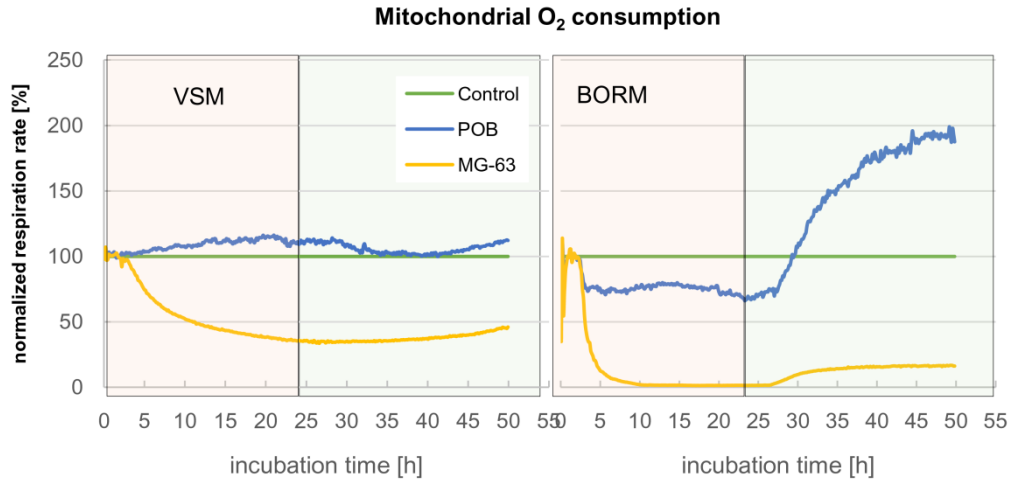

Abb. 6 Messung der mitochondrialen Respiration am Bionas® 2500 Analyzing System, welches mit dem metaboischen Chip Bionas DisocveryTM SC1000 kombiniert wurde. Sowohl der VSM als auch der BORM-Extrakt reduzieren die mitochondriale Respiration bei der Osteosarkomzelllinie MG-63.Hingegen beeinflusste VMS die Respiration der Kontrollzelllinie (POB – primary osteoblasts) nicht. Der BORM-Extrakt reduziert ebenfalls die Respiration der Kontrollzelllinie, aber nur um ca. 20 %. Diese Reduktion wurde nach dem Stoppen der BORM-Applikation revertiert und mehr noch, signifikant gesteigert.

Der methanolische Extrakt von VSM verursachte einen Zellzyklus-Arrest in der G2/M-Phase und eine Stabilisierung des Aktin-Zytoskeletts durch eine gesteigerte Stressfaser-Formierung. Dadurch wurde eine reduzierte Migrations- und Invasionsfähigkeit der Tumorzellen erzielt.

Durch diese Arbeiten konnten wir zwei Pflanzenextrakte mit starker anti-kanzerogener Wirkung identifizieren, die zum einem auf eine metabolische Beeinträchtigung (BORM) oder zytoskeletale Reprogrammierung (VSM) der Tumorzellen zurückzuführen ist. Aktuell erfolgt die chemische Charakterisierung der Inhaltstoffe durch Herrn Prof. Ali. Erste chemische Charakterisierungen liegen in einer aktuellen Publikation vor:

Dad A, Ali I, **Engel N**, Atif M, Hussain H, Ahmad VU, Langer P. The Phytochemical Investigation and Biological Activities of Berberis Orthobotrys. Int J Phytomed. 2017 July; 9(2):213-8. doi: 10.5138/09750185.1899.

Engel et al. BMC Complementary and Alternative Medicine (2016) 16:244
DOI 10.1186/s12906-016-1215-9

BMC Complementary and Alternative Medicine

RESEARCH ARTICLE Open Access

Antitumor evaluation of two selected Pakistani plant extracts on human bone and breast cancer cell lines

Nadja Engel[1,4*], Iftikhar Ali[2,3], Anna Adamus[4], Marcus Frank[5,6], Akber Dad[2], Sajjad Ali[2], Barbara Nebe[4], Muhammad Atif[5,6], Muhammad Ismail[2], Peter Langer[3] and Viqar Uddin Ahmad[7]

Abstract

Background: The medicinal plants *Vincetoxicum arnottianum* (VSM), *Berberis orthobotrys* (BORM), *Onosma hispida* (OHRM and OHAM) and *Caccinia macranthera* (CMM) are used traditionally in Pakistan and around the world for the treatment of various diseases including cancer, dermal infections, uterine tumor, wounds etc. The present study focuses on the investigation of the selected Pakistani plants for their potential as anticancer agents on human bone and breast cancer cell lines in comparison with non-tumorigenic control cells.

Methods: The antitumor evaluation was carried out on human bone (MG-63, Saos-2) and breast cancer cell lines (MCF-7, BT-20) in contrast to non-tumorigenic control cells (POB, MCF-12A) via cell viability measurements, cell cycle analysis, Annexin V/PI staining, microscopy based methods as well as migration/invasion determination, metabolic live cell monitoring and western blotting.

Results: After the first initial screening of the plant extracts, two extracts (BORM, VSM) revealed the highest potential with regard to its antitumor activity. Both extracts caused a significant reduction of cell viability in the breast and bone cancer cells in a concentration dependent manner. The effect of VSM is achieved primarily by inducing a G2/M arrest in the cell cycle and the stabilization of the actin stress fibers leading to reduced cell motility. By contrast BORM's cytotoxic properties were caused through the lysosomal-mediated cell death pathway indicated by an upregulation of Bcl-2 expression.

Conclusions: The antitumor evaluation of certain medicinal plants presented in this study identified the methanolic root extract of *Berberis orthobotrys* and the methanolic extract of *Vincetoxicum arnottianum* as promising sources for exhibiting the antitumor activity. Therefore, the indigenous use of the herbal remedies for the treatment of cancer and cancer-related diseases has a scientific basis. Moreover, the present study provides a base for phytochemical investigation of the plant extracts.

Keywords: Traditional herbal remedies, Plant extracts, Antitumor evaluation, Actin cytoskeleton

Background

Natural products have historically and continually been investigated for promising new leads in pharmaceutical development. Cancer is a major public health problem worldwide with millions of new cancer patients diagnosed each year and many deaths resulting from this disease. Chemotherapy remains the principal mode of treatment for various cancers. Researchers have focused on the anticancer activity of the plants because the medicinal plants are used in different countries for the treatment and prevention of cancer [1, 2]. For example, Traditional Chinese medicine (TCM) is used as an adjuvant therapy to alleviate cancer symptoms at the terminal stages when Western medicine treatments cannot offer any other treatment options [3, 4].

In Pakistan, as in other developing countries, traditional medicines are in widespread use; with the practitioners

* Correspondence: nadja.engel-lutz@gmx.de
[1]Department of Pediatric Surgery, University Hospital Marburg, Baldingerstraße, Marburg 35034, Germany
[4]Department of Cell Biology, University Medical Center Rostock, Schillingallee 69, Rostock 18057, Germany
Full list of author information is available at the end of the article

formulating and dispensing the recipes to their patients. The medicaments are prepared most often from a combination of two or more plant products which may contain active chemical constituents with multiple physiological and pharmacological activities and could be used in treating various disease conditions. The discovery of effective herbs and elucidation of their underlying mechanisms could lead to the development of an alternative and complementary method for cancer prevention and/or treatment. Based on an analysis of published literature, we selected four traditional Pakistani plants with medicinal value to evaluate their anticancer efficacy. In search of the target plant extracts for the development of anticancer drugs, here we have investigated *Vincetoxicum arnottianum*, *Berberis orthobotrys*, *Onosma hispida* and *Caccinia macranthera* of Pakistan origin.

Vincetoxicum arnottianum Wight (Syn: *Cyanchum arnottianum* Wight) is a perennial plant of the Apocynaceae family found in different parts of Pakistan including Hazara, Swat, Kaghan, Shinkiari, Kashmir etc. [5]. The family Apocynaceae is one of the largest angiosperm family comprising 375 genera and over 5100 species. Plants of the family Apocynaceae have been reported to be extensively used for the treatment of the skin diseases, pimples [6], malaria, diabetes and diarrhea and most importantly some species have been used in cancer chemotherapy [7]. Some species of *Vincetoxicum* have exhibited very high cytotoxicity against brine shrimps [16], antidiarrheal and antispasmodic [8], antibiotic [9], anti-inflammatory [10], antidiabetic and antioxidant [11] activities etc. Alkaloids are normally reported from various *Vincetoxicum* species [12, 13]. The plant *V. arnottianum* (syn. *C. arnottianum*) has been reported for the treatment of maggots in wounds of cattle, horses and sheep [14], wounds and injuries [15] etc.

Berberis orthobotrys Bien ex Aitch. is a shrub that belongs to the family Berberidaceae. Berberidaceae family comprises 13 genera and 650 species [25] and it is represented in Pakistan by 3 genera and 22 species. Various species of the genus *Berberis* are reported from different parts of Pakistan i.e. Gilgit, Baltistan, Chitral, Skardu, Astor etc. Hussain et al. [16] have studied the diversity and ecological characteristics of different plants including *B. orthobotrys*. Mokhber-Dezfuli et al. [17] and Srivastava et al. [18] have reviewed on the chemical and biological diversity in *Berberis*. The plant *B. orthobotrys* has been reported for the treatment of ulcer, stomach problems, kidney stones, uterine tumor, wounds [19], blood purification, jaundice, urine problem, diarrhea [20], gastrointestinal diseases [21] etc. Moreover the plant *B. orthobotrys* has revealed various biological activities including antihypertensive [22], cardiac depressant [23], antihyperlipidemic [24] etc. The chemical constituents that are reported from *B. orthobotrys* include alkaloids [25].

Onosma hispida Wall. ex G. Don. is a perennial herb of the Boraginaceae family found in different localities in Pakistan including Gilgit, Chitral, Baluchistan, Swat, Hazara etc. Kumar et al. [26] have reviewed the genus for its phytochemical and pharmacological aspects. The genus *Onosma* L. is one of the largest and most species-rich genera of the family Boraginaceae comprising more than 150 species [27–29]. *O. hispida* is used as a medicinal herb [30, 31] exhibiting various biological properties including antibacterial activity [32]. The plant *O. hispida* has been reported to be used as blood purifier and for cuts, swells, wounds [33]. And it has also been reported for the treatment of abdominal ulcers, hair problems, bladder and kidney stones and rheumatism [34], pneumonia, typhoid fever and also used for dyeing hairs [35]. A number of chemical constituents including benzoic acid derivatives, apigenin derivatives, flavones and flavanone derivatives have been isolated from *O. hispida* [26].

Caccinia macranthera (Banks & Sol.) Brand (Syn: *Borago macranthera* Banks & Sol.) is a leafy perennial plant of the Boraginaceae family found in Baluchistan province in Pakistan [36]. The roots of *C. macranthera* have been reported to be used for the treatment of dermal infections, liver disorders and dyspepsia and some other traditional uses [37, 38], sedative, treatment of cough, expectorant [39]. Moreover, the leaves of *C. macranthera* have also been reported for its medicinal properties [40]. The Boraginaceae is a large family that comprises approximately 205 genera and 2500 species worldwide [41]. The root extract of *C. macranthera* was studied for induction of phage production [42]. Different chemical constituents including glycosides [43], pyrrolizidine alkaloids [44], triterpenoid sapogenin [45] have been reported from the species of the genus *Caccinia* other than *C. macranthera*. However El-Shazly & Wink have reported that pyrrolizidine alkaloids are commonly found in Boraginaceae family. However, the overview about the medicinal plants *Vincetoxicum arnottianum*, *Berberis orthobotrys*, *Onosma hispida* and *Caccinia macranthera* of Pakistan origin is given in Table 1.

Despite their widespread use, however, no scientific assessment for anticancer effect has been conducted in most cases. Considering their increasing recognition and consumption, the present study was undertaken to evaluate the anticancer potential of these plant extracts in the inhibition of cell proliferation, induction of cell death, metabolic alterations and structural modifications in human breast (MCF-7, BT-20) and bone (MG-63, Saos-2) cancer cell lines. As a kind of control, non-tumorigenic cell lines of the breast (MCF-12A) and bone (POB) were included in the screening.

Table 1 Overview of the selected Pakistani plants used in this study

Plant name	Sample code	Description	Family	Medicinal uses
Vincetoxicum arnottianum Wight	VSM	Methanolic extract of the plant.	Apocynaceae	Wounds, Injuries, Maggots in wounds of cattle, horses etc.
Berberis orthobotrys Bien. ex Aitch.	BORM	Methanolic root extract of the plant.	Berberidaceae	Uterine tumor, wounds, gastrointestinal problems, ulcer, blood purification, jaundice, urine problem, diarrhea, antihypertensive, cardiac depressant, antihyperlipidemic etc
	BOFM	Methanolic extract of the flowers of the plant		
	BO-5	Ethylacetate soluble oily substance extracted from the methanolic fruit extract of the plant.		
	BO-23	n-hexane soluble oily substance extracted from the methanolic fruit extract of the plant.		
Onosma hispida Wall. ex G. Don.	OHRM	Methanolic root extract of the plant.	Berberidaceae	Wounds, cuts, swells, abdominal ulcer, antibacterial, blood purifier, hair problems, dying hair, bladder and kidney stones, rheumatism, pneumonia, typhoid fever etc.
	OHAM	Methanolic extract of the aerial parts of the plant.		
Caccinia macranthera (Banks & Sol.) Brand	CMM	Methanolic extract of the plant.	Boraginaceae	Dermal infections, liver disorders, dyspepsia, sedative, cough, expectorant, induction of phage production etc

Methods

Plant material collection and identification

Four plants were employed in the present study. *Vincetoxicum arnottianum* and *Caccinia mancranthera* were collected from Baluchistan (Pakistan) and *Berberis orthobotrys* and *Onosma hispida* were collected from Gilgit-Baltistan (Pakistan) in 2014 (Table 1). The plants were identified by Dr. Sher Wali Khan and reference specimens were deposited at the Department of Biological Sciences, Karakoram International University, Pakistan.

Preparation of extracts

Each plant sample including the aerial part of *V. arnottianum* (VSM), root (BORM) and fruit (BOFM) parts of *B. orthobotrys*, root (OHRM) and aerial (OHAM) parts of *O. hispida*, and the aerial part of *C. macranthera* (CMM) were air dried in shade and mechanically ground to fine powder. The finely-powdered material of each plant was soaked in methanol for several days and extracted. The dried methanolic extracts were obtained by removing the methanol by evaporation under reduced pressure. Furthermore, the fruit extract (BOFM) of *B. orthobotrys* was fractionated using solvent-solvent extraction and yielding n-hexane soluble oily substance (BO-23) and ethylacetate soluble oily substance (BO-5). Finally, eight samples i.e. VSM, BORM, BOFM, BO-5, BO-23, OHRM, OHAM and CMM were obtained and used for further study. Then, 50 mg of each dry sample was dissolved in 1 ml DMSO, EtOH or MeOH for the antitumor activity tests.

Chemicals

For soaking and extraction purposes, the commercial grade solvents were used. For preparation of the samples for the antitumor activity, absolute ethanol, DMSO, and absolute methanol from Sigma Aldrich were employed.

Cell lines, culturing and treatment conditions

Human osteosarcoma cell lines MG-63 (CRL-1427), Saos-2 (HTB-85) and human breast adenocarcinoma cell lines MCF-7 (ATCC: HTB-22), BT-20 (HTB-19) as well as non-tumorigenic human epithelial breast cell line MCF-12A (CRL-10782) were purchased from ATCC (http://www.lgcstandards-atcc.org/) under the given numbers. The human non-tumorigenic, primary osteoblast cells (POB) were chosen as control cells. Briefly, cells were isolated from the spongiosa of the femoral heads of patients undergoing primary total hip replacement. The samples were collected with patient agreement and approval by the Local Ethical Committee (registration number: A 2010-10). Human primary osteoblasts were already used and isolation procedure was already described [46]. Except for MCF-12A, all other cell lines and the primary POB cells were cultivated in Dulbecco's modified Eagle's medium (Invitrogen, Germany) with 10 % fetal bovine serum (PAN Biotech GmbH, Germany) and 1 % gentamycin (Ratiopharm, Germany). MCF-12A was grown in Dulbecco's modified Eagle's medium Ham's F12 without phenol red (Invitrogen, Germany) containing 10 % horse serum (PAA Laboratories GmbH, Germany), the Mammary Epithelial Cell Growth Medium SupplementPack (PromoCell, Germany) including Bovine Pituitary Extract 0.004 nl/ml, Epidermal Growth Factor (recombinant human) 10 ng/ml, Insulin (recombinant human) 5 g/ml, Hydrocortisone 0.5 g/ml and 1 % gentamycin (Ratiopharm, Germany).

Prior treatment with the plant extract cells were adapted to phenol-red-free Dulbecco's modified Eagle's medium (PAA Laboratories GmbH, Germany) with 10 % charcoal stripped fetal bovine serum (PAN Biotech GmbH, Germany) for 48 h to avoid unspecific stimulation of endogenous hormones in the serum (assay medium). Treatment with plant extracts (final concentration 1, 10,

25, 50, and 100 μg/ml) was carried out for 48 h in assay medium. As negative control substance the vehicle DMSO, ethanol or methanol (0.1 %) was used in the same manner.

Viability assay and calculation of IC_{50} values

MTS (3-(4, 5-dimethylthiazol-2-yl)-5-(3-carboxymethoxyphenyl)-2-(4-sulfophenyl)-2H-tetrazolium) assay to determine cell viability was performed according to manufactures protocol (CellTiter 96® AQueous One Solution Cell Proliferation Assay; Promega Corp., Madison, WI, USA). Briefly, cells were seeded in 96-well plates at a density of 2000 cells/well in 100 μl medium and left to attach for 24 h. Treatment with plant extracts at final concentrations of 1, 10, 25, 50 and 100 μg/ml was carried out as described previously [47]. In parallel, control approaches were carried out with medium only and 0.1 % of the solvent DMSO, EtOH or MeOH to calculate background absorbance. No background absorbance was obtained for the extracts and MTS in the absence of cells, as some extracts are capable of reducing the MTS. After an initial incubation for 24 h cells were assayed with MTS. Colorimetric changes were measured at 490 nm and raw data was transferred to Microsoft Excel and analyzed. At least 8 replicates corrected with the background absorbance were performed. Reduction of cell viability at each concentration was plotted as a dose response curve. The IC_{50} values were calculated using nonlinear regression to fit data to the dose–response.

Cell cycle analysis

Proliferation alterations as well as apoptosis induction under the exposure of the plant extracts were estimated by cell cycle analysis via flow cytometry (FACS Calibur, BD Biosciences) after propidium iodide (Roche Diagnostics, IN, USA) staining (50 mg/ml) of the cells as already described [47, 48]. For data acquisition and histogram preparation, the software FlowJo version 7.6.5 (Tree Star; www.flowjo.com) was used. A minimum of 15,000 ungated events were recorded. Doublets and clumps were excluded by gating on the DNA pulse width versus pulse area displays. For statistical evaluation, the sum of cells in S- and G2/M-phase was defined as proliferative events and the sub-G1-peak of the histogram as apoptotic ones.

Annexin V/PI apoptosis detection

Annexin-V detects the translocation of phosphatidylserine from the inner leaflets to the outer leaflets of the plasma membrane, which is a key feature of apoptotic cells, whereas PI detects necrotic cells with permeabilized plasma membrane. Labeling of early apoptotic and dead cells was performed according to the manufacturers' instructions from the Alexa Fluor488 Annexin V/Dead Cell Apoptosis Kit (Thermo Fisher Scientific Inc., Germany). Cells were treated with 100 μg/ml plant extract for 48 h. After treatment detached as well as adherent cells were washed twice with cold PBS. The cell pellet was resuspended in 100 μl of annexin binding buffer at a density of 1×10^6 cells per ml and incubated with 5 μl of Alexa488-conjugated Annexin-V and 5 μl of PI for 15 min at room temperature in the dark. 400 μl of 1× binding buffer was added to each sample tube, and the samples were immediately analyzed by flow cytometry. Histograms and statistics were designed with the software FlowJo Version 7.6.5.

Microscopy

For bright field as well as fluorescence microscopic imaging, cells were seeded on glass cover slips and cultured for 24 h. After treatment with plant extracts bright field images were obtained using Axio Scope A1 microscope and the software AxioVision Imaging Software Release 4.8.2. (Carl Zeiss, Germany). For fluorescence imaging cell were fixed with 4 % paraformaldehyde for 15 min, followed by three washings with PBS and then permeabilized with 0.1 % Triton X-100 for 15 min. After carefully washing, cells were incubated with 100 μl 6.6 μM Alexa Fluor594 phalloidin (Invitrogen, Germany) for 60 min in the dark at room temperature, washed again, counterstained with DAPI (Roche Diagnostics GmbH, Germany) for 15 min. Finally, cell were washed four times with PBS and embedded in mounting medium. Lysosomes were labeled with LysoTracker® Green DND-26 (Molecular Probes, Carlsbad, CA, USA) following the protocol supplied. The other cell compartments: mitochondria (MitoTracker® Mitochondrion-Selective Probes Green FM), Golgi complex (BODIPY® FL C5-ceramide complexed to BSA), endoplasmic reticulum (ER-Tracker™ Green BODIPY® FL glibenclamide), neutral lipids (4,4-difluoro-1,3,5,7,8-pentamethyl-4-bora-3a,4a-diaza-s-indacene BODIPY® 493/503), all from Molecular Probes, Germany were labeled following the manufactures' instructions. All fluorescence signals were investigated with an inverted confocal laser scanning microscope (LSM780, Carl Zeiss, Germany) equipped with a helium/neon-ion laser and a ZEISS 63 × oil immersion objectives. The confocal images (1024 × 1024 pixel) were optimized using the ZEN software (Carl Zeiss, Germany).

Scanning electron microscopy

For scanning electron microscopy (SEM) cells grown on glass cover slips were fixed with 2 % glutaraldehyde and 1 % PFA in 0.1 M phosphate buffer pH 7.3. After washes in 0.1 M phosphate buffer the cells were dehydrated with a graded series of ethanol and were processed for critical point drying using CO_2 as intermedium (Emitech K850 critical point dryer, Emitech Ltd. Ashford, UK).

The cover slips were mounted on SEM stubs with adhesive carbon tape (Plano, Wetzlar, Germany) and sputter-coated with a gold layer (approximately 15–20 nm thickness) using a Bal-Tec SCD004 sputter coater (Balzers Union Ltd., Balzers, Liechtenstein). Specimens were viewed in a field-emission SEM operated at 5 kV (Merlin VP compact, Carl Zeiss Microscopy, Jena, Germany) and images with a size of 1024 x 768 pixels were recorded. Morphometric measurements of cell body axis length and width were taken with the free line measurement tool on calibrated pictures imported into iTEM imaging software (Olympus Soft Imaging Solutions, Münster, Germany).

Mitochondrial O_2-consumption

Mitochondrial O_2-consumption as a measure for respiratory activity was determined by the Bionas® 2500 analyzing system combined with the metabolic chip Bionas DisocveryTM SC1000 equipped with Clark-type oxygen sensors. Prior experiments, chips were cleaned with 70 % ethanol for 10 min, washed with PBS and were adapted to the measurement medium for 5 min. Measurement medium was composed of DMEM without NaHCO3 (Invitrogen, Germany), 0.1 % charcoal stripped fetal bovine serum (PAN Biotech GmbH, Germany) and 1 % gentamycin (Ratiopharm, Germany), pH value 7.4 and sterile filtered. On each chip $2x10^6$ cells were seeded and let them adhere over night at 37 °C and in 5 % CO_2 so that 80 % sub-confluence on the sensor chips was reached. Bionas measurements were carried out with a pump rate of 56 ml/min [49]. After an adaption phase of 2 h to the new culture conditions, extracellular oxygen consumption of MG-63 cells after application of 25 μg/ml BORM or VSM was measured continuously for 20 h. Thereafter the recovery status (measurement medium without plant extracts) of the cells was monitored for additional 24 h. Data sets were evaluated and normalized with the software Bionas15002 Data analyzerV1.07.

Migration and invasion

Influence on migration was conducted on MG-63 cells, pre-incubated in assay medium for 48 h adaption in 6-well plates (Greiner, Germany). A scratch wound was made by Ibidi culture inserts (μ-Dish 35 mm; Ibidi GmbH, Martinsried, Germany) following the instructors recommendations. When cell layers reached confluence, the culture insert was removed and cells were treated with VSM (25–50 μg/ml) extract or control (vehicle, DMSO). Gap closure was analyzed as described previously [50]. Cell invasion assay was performed with the CytoSelect™ 24 –Well Cell Invasion Assay (Basement Membrane, Fluorometric Format) from Cell Biolabs, Inc., CA, USA. Briefly, $1x10^6$ MG-63 cells with the plant extracts were seeded in the membrane insert for 48 h. Fluorescence of invaded cells was counted with a plate reader at 480/520 nm.

Western blotting procedure

The general steps of the Western blot procedure have been described previously [49]. Briefly, after treatment with the plant extracts VSM and BORM for at least 48 h the cells were trypsinized, washed with PBS and lysed in ice-cold lysis buffer (Bio-Plex Cell Lysis Kit, Bio-Rad, USA). After SDS-PAGE, protein content per lane as well separation quality was controlled with the Criterion Stain FreeTM gel imaging system (Bio-Rad, Germany). For protein detection primary antibodies (PCNA: sc-56, from Santa Cruz, USA; BCL-2: B3170, from Sigma) were incubated overnight at 4 °C followed by labeling with a horseradish peroxidase (HPR)-conjugated secondary antibody (Dako, Glostrup, Denmark) for 1 h at room temperature. Protein signals were visualized by using SuperSignal West Femto Chemiluminescent Substrate (Pierce Biotechnology, Rockford, USA). Band intensity was analyzed densitometrically with the Molecular Imager ChemiDoc XRS and Image Lab 3.0.1 software (Bio-Rad, USA). Protein detection was repeated at least three times with individually prepared cell lysates from independently passaged cells.

Statistical analysis

Every experiment was replicated three times with individually passaged cells and data sets were expressed as means ± standard deviations (SD). Statistical significance was determined by the unpaired one-way ANOVA or *t*-test (***$P < 0.001$, **$P < 0.005$, *$P < 0.05$).

Results

Initial screening on cell viability

To evaluate the anticancer properties of the Pakistani plant extracts two bone (MG-63, Saos-2) and two breast (BT-20, MCF-7) cancer cell lines in comparison with primary osteoblasts (POB-110) and non-tumorigenic mammary epithelial cells (MCF-12A) were selected. The osteosarcoma cell line MG-63 represents an early osteoblastic type while Saos-2 cells exhibited the most mature osteoblastic phenotype [51]. The breast cancer cell line MCF-7 represents the luminal, estrogen and progesterone receptor-positive subtype whereas BT-20 cells are invasive, triple-negative breast cancer cells [52]. For the initial screening all cells were treated with 50 μg/ml of each plant extract for 48 h and cell viability was measured right after (Fig. 1). The extracts VSM and BORM caused the greatest significant reduction (40–60 %) of cell viability in the osteosarcoma cell lines MG-63 and Saos-2. On primary osteoblast cells (POB-110) VSM induced only a slight decrease in cell viability while BORM

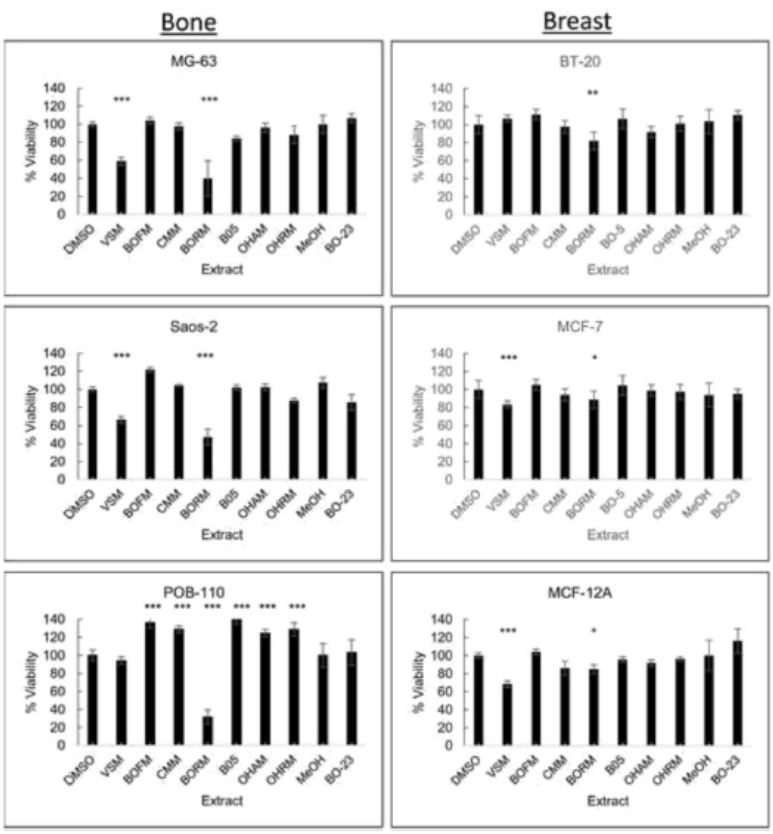

Fig. 1 Determination of cell viability. Measurement of cell viability via MTS assay after exposure to 50 μg/ml plant extract for 48 h on respective bone (MG-63, Saos-2) and breast (BT-20, MCF-7) cancer cell lines in comparison with primary osteoblasts (POB) and non-tumorigenic mammary epithelial cells (MCF-12A). As control treatment the vehicle DMSO and MeOH were used at a final concentration of 0.1 % (w/v). Samples were compared using one-way ANOVA. Error bars indicated mean ± SD, $n = 8$, ***$P < 0.001$, **$P < 0.01$, *$P < 0.5$, significantly different compared to control

lowered the viability up to 80 %. Beside VSM and BORM, only the treatment with BO-5 on MG-63 cells as well as OHRM on Saos-2 cell revealed a significant viability decrease of 10–15 %. These results illustrate that the VSM extract has anticancer potential on bone cancer cells, since it selectively reduced the vitality of osteosarcoma cells and only exerts a minimal effect on the primary osteoblasts. Similar results were achieved for the treatment of the breast cancer cell lines. On BT-20, hormone-independent and invasive carcinoma cells, only the BORM extract caused a slight viability reduction of approximately 20 %. On MCF-7 cells, VSM as well as BORM induced decreased vitality rate in a range of 10–20 %. This vitality reduction was also measured on the non-tumorigenic control cell line MCF-12A indicating that the extracts VSM and BORM displayed strong cytotoxic effects which will be analyzed in the next sections.

Influence on cell cycle phases of MG-63 osteosarcoma cells

Besides the vitality measurements, the influence on cell growth and the induction of apoptosis are important parameters to evaluate the respective anticancer properties of the plant extracts. Therefore, cell cycle analyses were performed to determine the influence on the proliferation behavior (G2/M + S phase) and apoptosis initiation by DNA strand breaks (sub G1 phase), simultaneously (Fig. 2). Exemplarily, for all cell lines used, Fig. 2 demonstrates the DNA histogram (Fig. 2a), proliferation alterations (Fig. 2b) and the number of apoptotic cells (Fig. 2c) after 48 h treatment with 50 μg/ml plant extract on MG-63 osteosarcoma cell line.

Both, in the histogram and in the proliferation diagram is clearly evident that the extracts OHRM, VSM, BO-5 and BO-23 accelerate the cell number in the proliferative phases G2 and M. Only BORM caused a slight significant

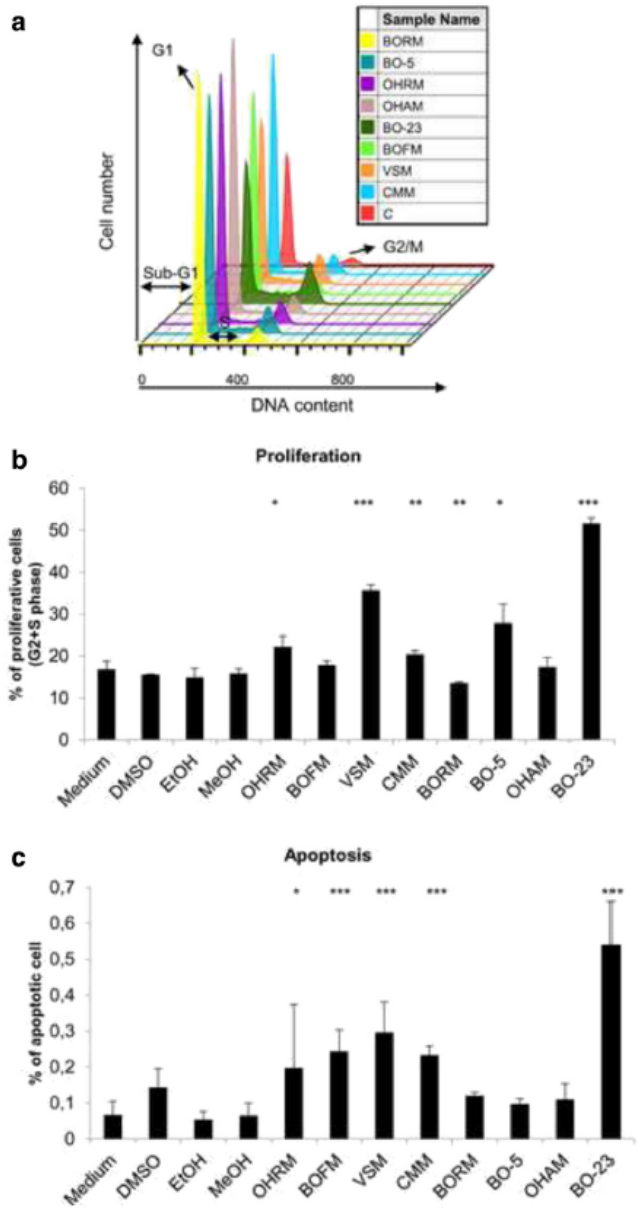

Fig. 2 Cell cycle alterations of MG-63 cells. **a** Histogram of the cell cycle distribution of MG-63 cells after treatment with the control substance (**c**) and the eight samples of plant extracts at a concentration of 50 μg/ml for 48 h. G1, S, G2/M and sub-G1 phases are marked with black arrows. Represented were the most prominent samples of 3–5 individual replicates. **b** Calculation of proliferation after treatment with the vehicle (DMSO, EtOH, MeOH; equates to 100 %) and the plant extracts at a concentration of 50 μg/ml for 48 h. As proliferative phases the sum of S and G2/M phases were calculated in percentages. **c** As apoptotic fraction the sub G1-peak was measured. (mean ± SD, $n = 3–5$, $^{***}P < 0.001$, $^{**}P < 0.01$, $^{*}P < 0.5$, significantly different compared to control, one-way ANOVA)

reduction in the proliferative phases (20 %). The number of apoptotic cells increased after treatment with 50 µg/ml of BOFM, VSM, CMM and BO-23, significantly. In summary, some of the plant extracts display an effect on the proliferative phases G2/M and S, but do not affect the sub-G1 phase. The DNA-histograms of the control treatments with medium, DMSO, EtOH and MeOH (final concentration: 0.1 µg/ml) are given in Additional file 1: Figure S1, showing no alterations in the cell cycle phases.

Concentration dependent effects of BORM and VSM

As BORM and VSM caused the most significant effects on all bone and breast cancer cell lines, both extracts were examined in concentration series ranging from 0.1 to 100 µg/ml to evaluate the concentration dependent effects (Figs. 3 and 4) on cell viability and to calculate the IC_{50} values (Table 2). Therefore, all the cell lines were used in non-confluent cell cultures (confluence at treatment beginning: 60–80 %).

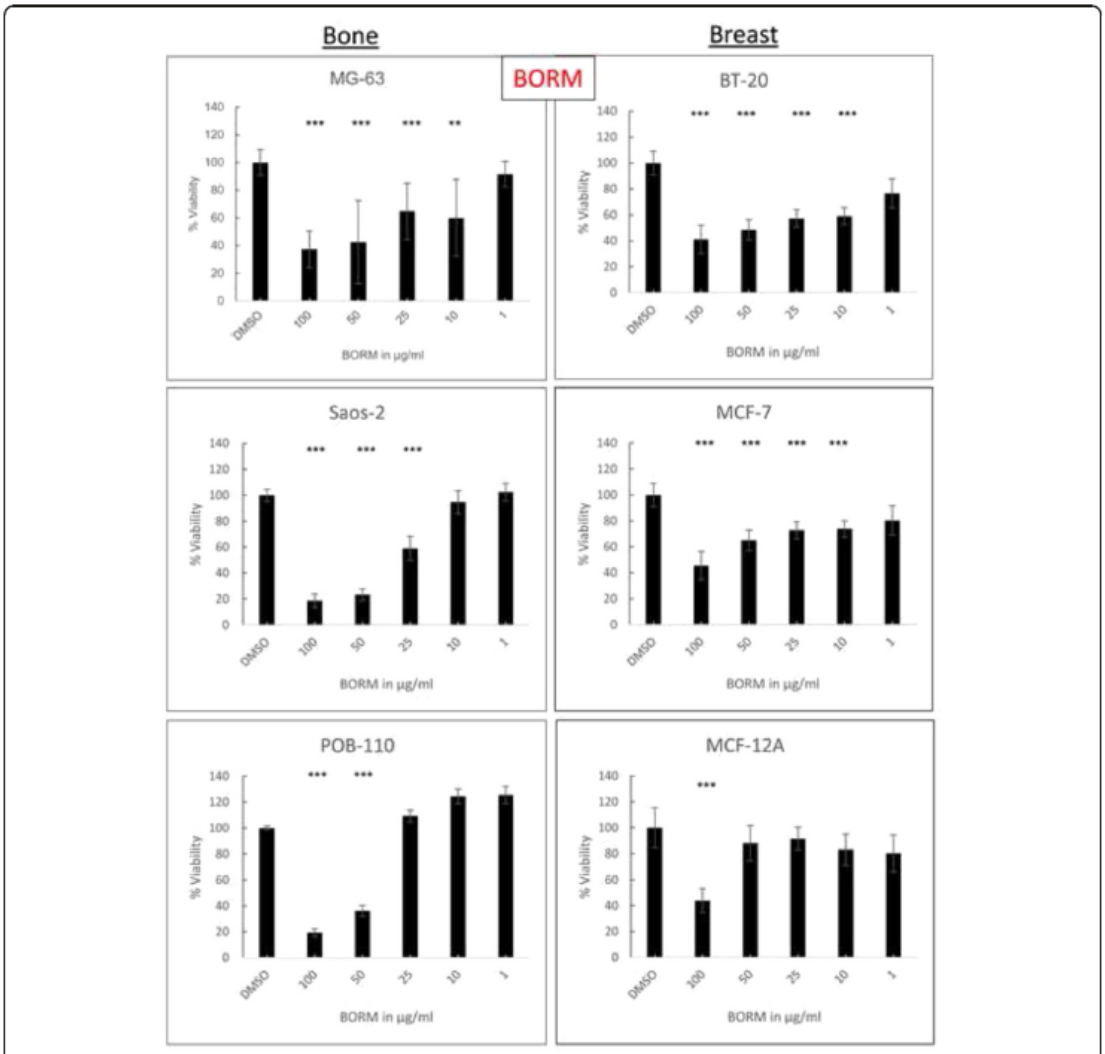

Fig. 3 Concentration dependent effects of BORM. Cell viability measurement in concentration series of BORM in a range from 1 to 100 µg/ml after exposure of 50 µg/ml plant extract for 48 h on respective bone (MG-63, Saos-2) and breast (BT-20, MCF-7) cancer cell lines in comparison with primary osteoblasts (POB) and non-tumorigenic mammary epithelial cells (MCF-12A). The solvent DMSO was used as a negative control. Mean ± SD, $n = 6–8$, ***$P < 0.001$, **$P < 0.01$, *$P < 0.5$, significantly different compared to control, one-way ANOVA

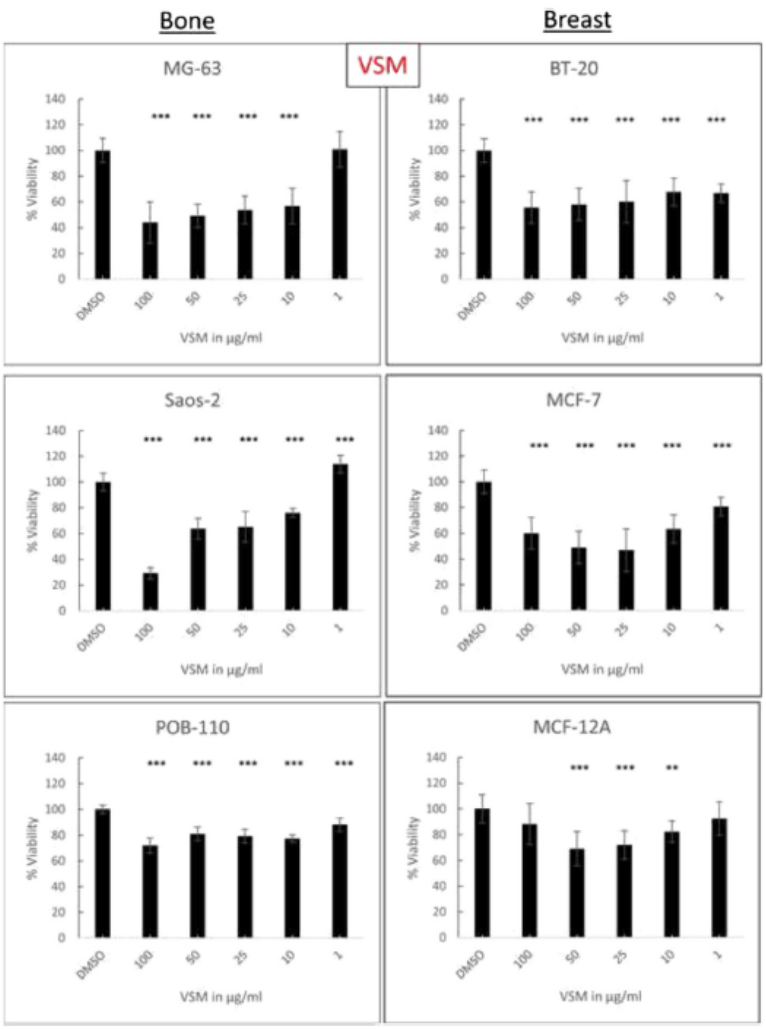

Fig. 4 Concentration dependent effects of VSM. Cell viability measurement in concentration series of VSM in a range from 1 to 100 µg/ml after exposure of 50 µg/ml plant extract for 48 h on respective bone (MG-63, Saos-2) and breast (BT-20, MCF-7) cancer cell lines in comparison with primary osteoblasts (POB) and non-tumorigenic mammary epithelial cells (MCF-12A). The solvent DMSO was used as a negative control. Mean ± SD, $n = 6–8$, ***$P < 0.001$, **$P < 0.01$, *$P < 0.5$, significantly different compared to control, one-way ANOVA

BORM induced linear concentration dependent effects on the osteosarcoma cell lines MG-63 and Saos-2 as well as on the breast cancer cell lines BT-20 and MCF-7 (Fig. 3). The highest concentration of 100 µg/ml reduced the cell viability by 60–80 % in all tumorigenic and control cells. However, in comparison with cancer cells, the control cells POB-110 and MCF-12A were not that strongly affected by BORM in concentrations below 50 µg/ml. This is confirmed by the calculation of the IC_{50} values: BORM exhibited the lowest values for BT-20 and Saos-2 (~60 and 34 µg/ml), indicating a pronounced cytotoxicity (Table 2). In contrast, VSM caused only a linear concentration dependent effect on the bone cancer cell lines MG-63 and Saos-2 leading to IC_{50} values of 62.53 and 57.09 µg/ml, respectively. The IC_{50} value for the control primary osteoblasts POB was significantly higher (515.76 µg/ml) indicating that VSM mediates a stronger cytotoxic impact on the bone cancer cell lines. The vitality of the non-tumorigenic mammary epithelial cell line MCF-12A was only minimally affected

Table 2 Overview of the calculated IC_{50} values. IC_{50} values of the plant extracts BORM and VSM on the bone and breast cancer cell lines in comparison with the non-tumorigenic control cells determined by viability measurements after 48 h treatment

	Cell line	BORM (µg/ml)	VSM (µg/ml)
Breast	MCF-12A	105.87	Incalculable (>5000)
	MCF-7	81.35	116.82
	BT-20	60.48	132.67
Bone	POB	49.65	515.76
	MG-63	52.01	62.53
	Saos-2	34.02	57.09

by VSM leading to a no calculable IC_{50} value. On the other hand VSM displayed moderate IC_{50} values for BT-20 and MCF-7 (132.67, 116.82). These results illustrate that the plant extract VSM has anti-tumor potential, primarily because the viability of the cancer cells is reduced and the influence on the non-tumorigenic control cells is low.

These dose dependent effects were verified by cell cycle measurements (Fig. 5a, b) and apoptosis detection (Fig. 5c) on the osteosarcoma cell line MG-63, exemplarily. In comparison with the control treatments BORM induced a slight increase of the proliferative phase G2/M, starting at a concentration of 10 µg/ml. In contrast, the VSM extract caused a linear, concentration-dependent increase in the proliferative phase G2/M and S, indicating for a G2-arrest. At a concentration of 100 µg/ml VSM more than half of the analyzed cells were detected in the G2/M phase. To verify the apoptosis induction an Annexin V/PI staining was performed (Fig. 5c, Additional file 2: Figure S2). 100 µg/ml BORM induced an increase in early and late apoptotic events up to 50 %. By contrast, VSM caused a slight shift in early apoptotic events (~ 20 %). All together, these results suggest that BORM and VSM exhibit anti-tumorigenic potential. The precise mode of action is to be analyzed in the next chapters.

Morphological, cytoskeletal and cell compartment alterations

To characterize morphological and cytoskeletal changes (F-actin and ß-tubulin), MG-63 cells were cultured in the presence of BORM and VSM (0.1–100 µg/ml) or vehicle control (0.1 % DMSO) for 48 h, and monitored by bright field, scanning electron and laser scanning microscopy (Fig. 6; Additional file 3: Figure S3, Additional file 4: Figure S4). Under control conditions MG-63 cells form a confluent monolayer with the typical fibroblast-like cell structure (Fig. 6a). Confocal imaging revealed that untreated MG-63 cells possess cortical actin, some well-defined stress fibers, and cell polarity as shown by the presence of lamellipodia (Fig. 6c). VSM caused a remarkable change in cell shape: cells are wider and have a larger cell surface (Fig. 6b). Furthermore, a reduced formation of the cortical cytoskeleton and a solid reinforcement of actin stress fibers through the entire cell area are visible. The stress fibers are much longer, thicker and stabilize the entire cell, so that the cell contacts are partially broken. Exposure to BORM resulted in a strong increase of vesicles in the cell nucleus environment, observed both in the bright field image as well as in the F-actin staining (Fig. 6a-c). The cells are much more stretched and spindle-shaped, resulting in a smaller cell area (Fig. 6b). The formation of the actin fibers as well as the distribution of cortical actin did not change, substantially. The formation of tubulins is neither changed after treatment with BORM nor VSM. The increased formation of vesicles after exposure to BORM as well as the strengthening of the actin skeleton after treatment with VSM can be due to metabolic alteration or cell compartment disorders. Therefore, primary cell compartment alterations were monitored by live cell imaging (Fig. 7). The number and distribution of mitochondria as well as the appearance of the endoplasmic reticulum remained almost unchanged. But in contrast, the exposure to BORM revealed an accumulation and augmentation of lysosomes while treatment with VSM reduced the amount of lysosomes, significantly. Already at a starting concentration of 1 µg/ml the number of

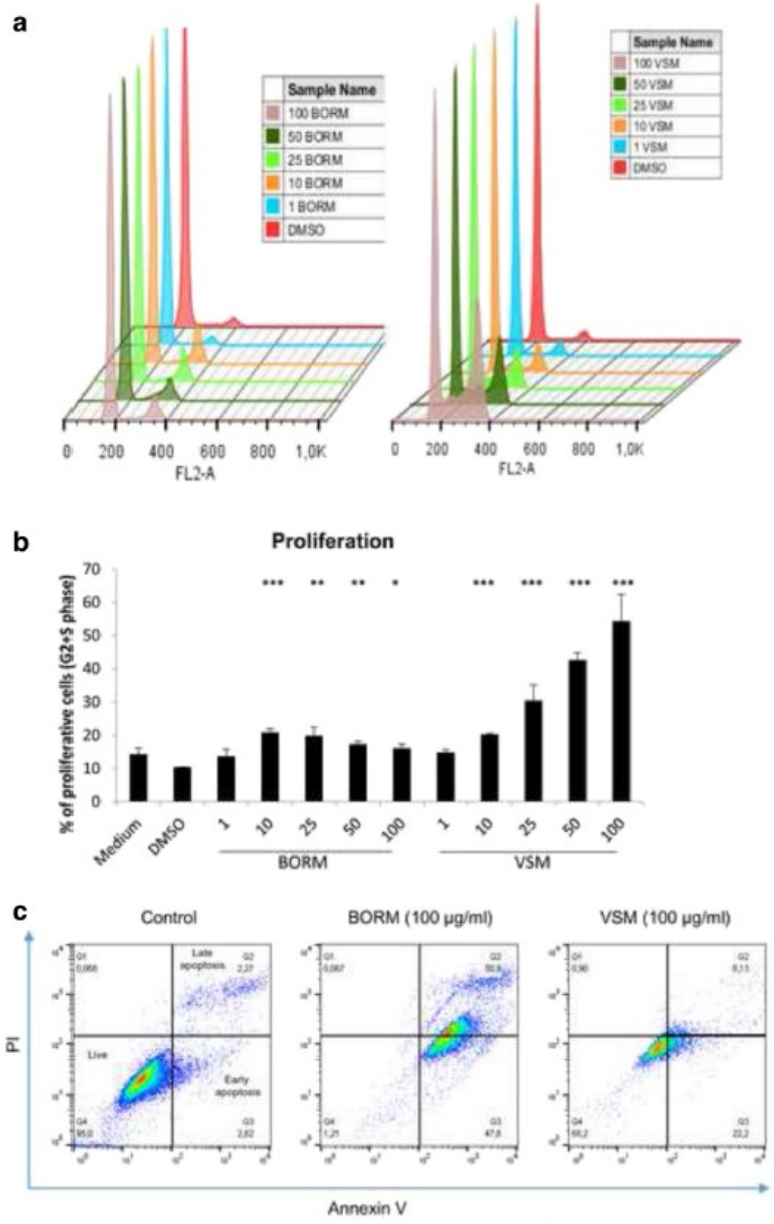

Fig. 5 Cell cycle phases, proliferation and apoptosis events. Cell cycle analysis of VSM and BORM treated MG-63 cells (48 h) in concentration series ranging from 1 to 100 µg/ml in comparison with the control treatment (DMSO). **a** Histograms of the cell cycle distribution. **b** Calculation of proliferation. As proliferative phases the sum of S and G2/M phases were calculated in percentages. Mean ± SD, $n = 3–4$, ***$P < 0.001$, **$P < 0.01$, *$P < 0.5$, significantly different compared to control, one-way ANOVA. **c** Annexin V/PI staining to label living, early and late apoptotic events after treatment with the control (DMSO), 100 µg/ml BORM or VSM measured via flow cytometry

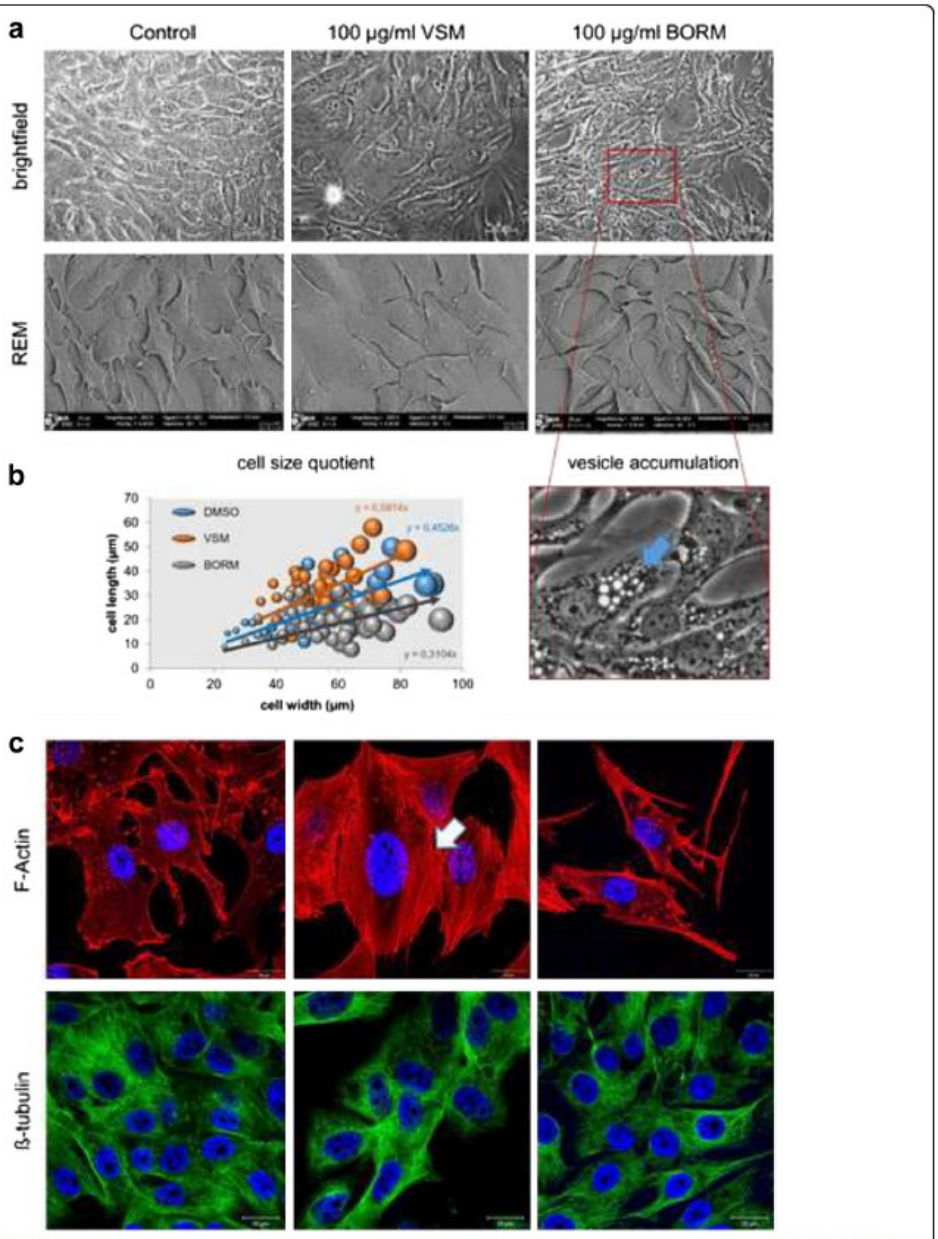

Fig. 6 Morphological and cytoskeletal alterations of MG-63 cells analyzed by different microscopic techniques. **a** Morphological alterations of MG-63 cells after treatment with DMSO (control) or 100 µg/ml VSM and BORM by bright field imaging (*upper panel*) and scanning electron microscopy (*lower panel*). **b** Calculation of the cell size quotients by length and width measurements of the cells in the scanning electron micrographs (*left*). $n = 30$. Enlarged section of BORM treated MG-63 cells. Distinctly, the vesicles accumulation can be detected around cell nucleus (*right*). **c** Laser scanning microscopic images of F-actin (*red*) and ß-tubulin (*green*) stained MG-63 cells. Cells were counterstained with Hoechst to label the cell nuclei (*blue*). Notably, VSM induced an increased Actin stress fiber formation through the entire cell, leading to a greater cell surface area. In contrast, treatment with BORM caused an increased production of vesicle-like structures and a spindle-shaped cell shape. Magnification bars = 20 µm

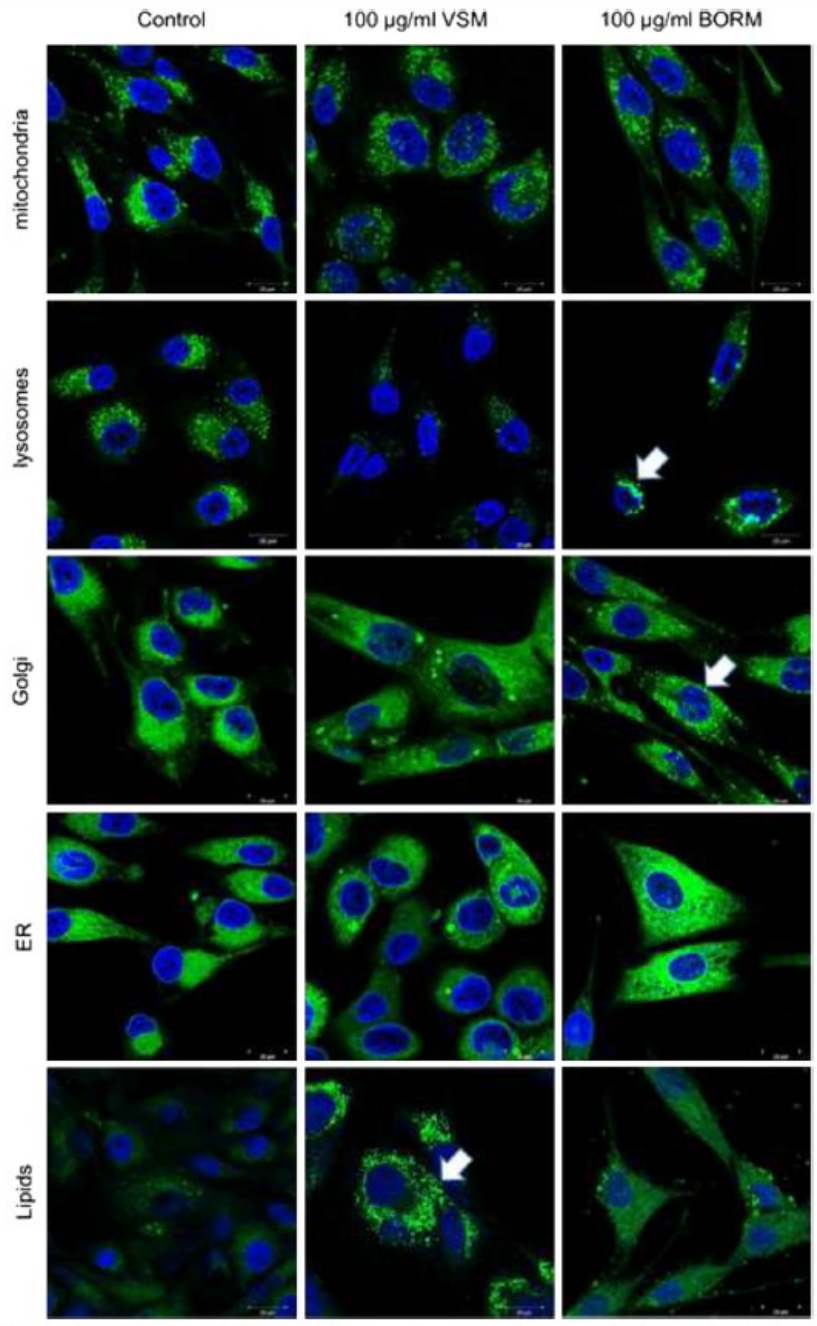

Fig. 7 Structural cell compartment alterations of MG-63 cells. Laser scanning microscopic analysis of cell compartments (mitochondria, lysosomes, Golgi apparatus, endoplasmic reticulum, and neutral lipids) within MG-63 cells treated with 100 µg/ml BORM or VSM in comparison to the control (DMSO). Cells were counterstained with Hoechst to label the cell nuclei (*blue*). Notably, exposure to VSM caused a reduced production of lysosomes and a strong increase of neutral lipids. In contrast, BORM treatment revealed an accumulation and augmentation of lysosomes, stronger granularization and formation of Golgi vesicles and a diffuse distribution of neutral lipids

lysosomes increased, and reached the highest number at a concentration of 25 μg/ml BORM. Higher concentrations of BORN did not further elevate the amount of lysosomes but caused a merger of lysosomes so that the size increased up to the 3–5 fold (Additional file 5: Figure S5). Similarly, treatment with BORM caused a change of the Golgi apparatus: a stronger granularisation and formation of Golgi vesicles can be observed. The staining of neutral lipids, which was only very slightly visible in the untreated cells, was strongly upregulated after VSM exposure. Many small dots of lipids could be verified around the nucleus and in the cytoplasmic area. In contrast, treatment with BORM resulted in a diffuse distribution of neutral lipids in the cell without any specific dot distribution. Up to this state, it can be concluded that BORM and VSM mediate cytotoxic effect by affecting different metabolic pathways. To discuss this more profound, various metabolic and motility-specific investigations were carried out.

Influence on O_2 consumption, motility and selected protein marker expression

To examine the cell specific mode of action of the two plant extracts, the influence on cell metabolism was investigated, firstly. Therefore, live cell monitoring of three metabolic parameters (cell impedance, O_2-consumption and extracellular acidification) was performed (Fig. 8a, Additional file 6: Figure S6). Both, the treatment with VSM and BORM for 24 h resulted in a strong reduction (VSM: 75 %, BORM: 99 %) of the mitochondrial O_2-consumption in MG-63 cells (Fig. 8a). This decrease in respiratory capacity cannot be reverted after the discontinuation of the plant extracts. In contrast, the effect on primary osteoblasts (POB) was different: VSM did not alter the respiration capacity; BORM induced a slight decrease in O_2-consumption (~ 20 %) which could not only be reverted but enhanced up to 100 % after discontinuation of the plant extract. Beside this strong effect on cellular energy metabolism, the effect on cell motility was investigated. Because VSM induced an increased formation of stress fibers (Fig. 6), the influence on cell migration and invasion was determined (Fig. 8b, c). Concentrations of 25–50 μg/ml VSM decreased the migratory activity (90 %) and the invasiveness (35 %) of MG-63 cells. BORM did not alter the cell motility, significantly but induced apoptotic signals by enhanced BCL-2 expression and proliferation reduction by PCNA repression (Fig. 8d).

Discussion

In this study, eight samples from four Pakistani plant extracts were evaluated for their potential as anticancer agents in selected human bone and breast cancer cell lines in comparison with non-tumorigenic control cells via cell viability measurements, cell cycle analysis, live cell imaging and monitoring of metabolic as well as motility features. After the first initial screening, BORM and VSM revealed the highest potential with regard to its antitumor activity. Both extracts caused a significant reduction of cell viability in the breast and bone cancer cells. However, BORM also induced a strong reduction of cell viability in the primary osteoblasts (POB), as well as VSM lowered the cell vitality in the non-tumorigenic breast cell line MCF-12A. But, VSM caused no negative influence on POBs wherein the bone cancer cell lines were strongly influenced (Fig. 1). These results suggest that the therapeutic use of VSM particularly for the treatment of bone cancer would be possible. For the treatment of breast cancer the BORM extract may be suitable on the basis of the vitality studies. Because BORM caused only a marginal effect on the vitality of the control cell line MCF-12A and induces a significant vitality reduction in both, the estrogen receptor-positive breast cancer cell line MCF-7 and in the triple-negative cell line BT-20.

Subsequent cell cycle analysis revealed a substantial increase of the proliferative phases G2/M and S after exposure to 50 μg/mg VSM whereas BORM slightly lowered the proliferation (Fig. 2a-b; exemplarily illustrated at the bone cancer cell line MG-63). Although VSM especially increases the G2/M phase in MG-63 cells, a simultaneous increase in DNA strand breaks, to be mentioned in the sub-G1 phase (Fig. 2c), could be observed. This suggests that the VSM extract induces apoptotic changes which are often associated with elevated proliferation rates in order to obtain the cell layer. Another possibility is a G2/M arrest of the cell population similar to the effect of paclitaxel which stabilizes tubulin polymerization resulting in arrest in mitosis and apoptotic cell death [53].

So far, the obtained results imply that the extracts VSM and BORM mediate different cellular responses which lead to cytotoxic events. In order to identify these cellular mechanisms, dose-response curves were created first (Figs. 3 and 4). From these curves it can be concluded that both extracts exert concentration-dependent effects on both, breast as well as bone cancer cells. The calculated IC_{50} values (Table 2) show that VSM primarily affects the bone cancer cells and only minimally impaired the vitality of healthy osteoblasts. The IC_{50} values of BORM illustrate that this extract reduces the vitality of the breast cancer cell, predominantly. For the non-tumorigenic control cell line MCF-12A a considerably higher IC_{50} value was determined.

However, bright field, scanning electron and laser scanning microscopy observations revealed morphological and structural alterations of MG-63 osteoblastic cells after exposure to 100 μg/ml VSM or BORM (Fig. 6). In comparison to the control, VSM treated MG-63 cells

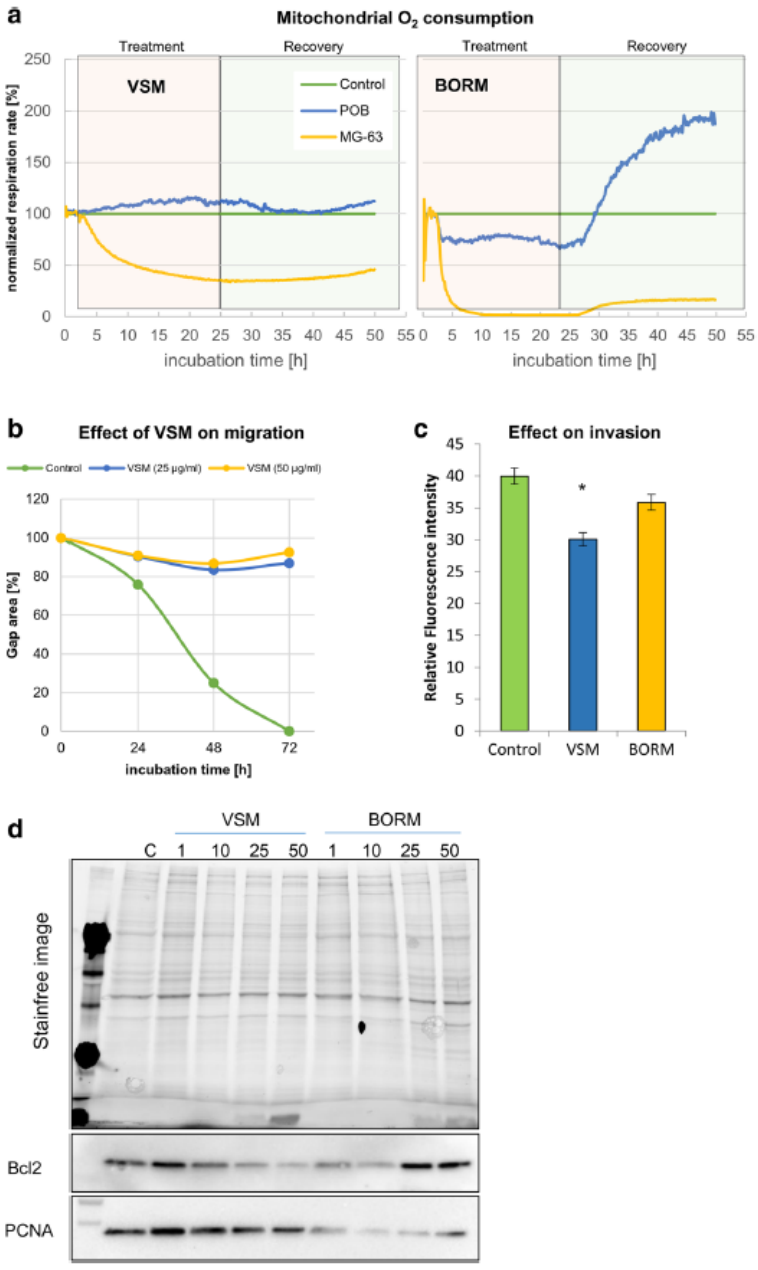

Fig. 8 (See legend on next page.)

(See figure on previous page.)
Fig. 8 Influence on O_2 consumption, motility and selected protein marker expression. **a** Mitochondrial O_2 consumption (respiration) in MG-63 cells and primary osteoblasts (POB) during exposure to 25 μg/ml VSM or BORM in comparison to the control (which was set to 100 %) determined by the Bionas® 2500 analyzing system combined with the metabolic chip Bionas DisocveryTM SC1000 equipped with Clark-type oxygen sensors. Both BORM and VSM reduce the respiration rate dramatically (99 and 60 % reduction, respectively) in tumorigenic osteoblasts. **b** Effect of VSM (25, 50 μg/ml) on MG-63 migration behavior in comparison to the control treatment (DMSO) in a 72 h time period in a wound healing assay (raw data available in Additional file 7: Figure S7). Notably, exposure to VSM prevents migration of MG-63 cells so that the cell lawn cannot be closed. **c** Invasion assay of BORM and VSM treated MG-63 cells. Only VSM reduced the invasion capacity, significantly. Mean ± SD, $n = 3$, $^*P < 0.5$, significantly different compared to control, unpaired *t*-test. **d** Western blot analysis of proliferation (PCNA) and apoptosis (Bcl-2) marker expression in VSM or BORM treated (concentration series 1–50 μg/ml) MG-63 cells in comparison to the control (**c**). The stain free image of the polyacrylamide gel functions as loading control

exhibit a prolonged shape accompanied with reduced cell-cell contacts. F-actin staining revealed a strong induction of stress fiber formation through the entire cells. Along with the reduced cell viability, the mediated G2/M arrest in the cell cycle phases and increased actin fiber formation can be assumed that the VSM extract causes a stabilization of the tumor cells, thus causing the cytotoxic properties. In contrast, the BORM extract promotes the formation of vesicle-like structures in the cell which can be due to a stimulation of the lysosomal activity or aggregation of lysosomal vesicles. Even at low concentration (1–10 μg/ml BORM) an increased formation of lysosomes was observed (Fig. 7). The higher the BORM concentrations, the greater the expansion of the lysosomal compartments. At the highest concentration (100 μg/ml) the lysosomes are large clusters around the nucleus (Fig. 7). This means that the cytotoxic effect of BORM is due to the activation of lysosomes which can selectively activate programmed cell death [54]. Briefly, lysosomal ROS generation can cause lysosomal membrane permeabilization, whereby lysosomal cathepsins, as well as other hydrolytic enzymes, are released from the lysosomal lumen to the cytosol, and can trigger programmed cell death [55, 56]. In addition, BORM caused a stronger granularisation and formation of Golgi vesicles as well as a diffuse distribution of neutral lipids. This is not surprising, because it is thought that the reservoir of chemicals in the lysosome can be 'topped up' by supplies from the Golgi apparatus. The chemicals are manufactured in the endoplasmic reticulum, modified in the Golgi apparatus and transported to the lysosomes in vesicles (sealed droplets). Modification in the Golgi apparatus includes 'destination labeling' at a molecular level ensuring that the vesicle is delivered to a lysosome and not to the plasma membrane or elsewhere. The 'label' is returned to the Golgi apparatus for re-use (http://bscb.org/ Society for Cell Biology.org). This suggests that BORM primarily affects cell metabolism by the disruption of lysosomal function and thus initiating cell death. This view is supported by the changes in the apoptotic signaling cascades, i.e. the upregulation of Bcl-2 expression and further confirmed by a nearly complete reduction of mitochondrial O_2 consumption (Fig. 8). Although the treatment with VSM also resulted in a significant reduction in respiration rate, the underlying mechanisms are different. Because of the stabilization of the actin cytoskeleton, the MG-63 cells are limited in their motility and can no longer divide, so that a G2/M arrest is forced.

Conclusions

In this study two Pakistani plant extracts, namely VSM and BORM could be identified as potential anti-tumor agents at least on the bone and breast cancer cell lines in vitro. The mechanism of action of VSM is achieved by a cell cycle arrest in the G2/M phase and the stabilization of the cell by increased actin stress fiber formation. The antitumor effect of BORM is mediated by activating the lysosomal induced cell death pathway. However, both plant extracts exhibit strong cytotoxic potential in a concentration dependent manner. In this case VSM displayed the least impact on primary osteoblast functioning as non-tumorigenic cells whereas BORM showed the lowest cytotoxic effect on the mammary control cell line. Therefore, based on these results, we can postulate that VSM can be of interest for the treatment of bone tumors and BORM for the treatment of breast cancer. To prove this assertion, future work is on the identification of potential antitumor ingredients of these extracts and the evaluation of the dose-response relationships, in vitro and in vivo.

Additional files

Additional file 1: Figure S1. Control cell cycle analysis. Histogram of cell cycle phases in MG-63 cells after treatment with 0.1 % of the control substances (DMSO, MeOH, EtOH) in comparison with untreated cells, cultivated in assay medium. No significant effect on the cell cycle phases, mediated by the solvents used in this study could be observed. (TIF 645 kb)

Additional file 2: Figure S2. Bright field imaging of cell morphology. Bright field images of MG-63 cells after exposure to VSM or BORM (concentration series ranging from 1 to 100 μg/ml) for 48 h in comparison with the control treatment. (TIF 12518 kb)

Additional file 3: Figure S3. Imaging of actin cytoskeleton. Laser scanning microscopic images of F-actin (red) and Hoechst (blue) stained MG-63 cells after exposure to VSM or BORM (concentration series ranging from 1 to 100 μg/ml) for 48 h in comparison with the control treatment. (TIF 12140 kb)

Additional file 4: Figure S4. Live cell imaging of lysosomes. Laser scanning microscopic images of lysosomes (green) in MG-63 cells after

treatment with 1–100 μg/ml BORM. Lysosomes were labeled with LysoTracker® Green DND-26 (Molecular Probes, Carlsbad, CA, USA). Cell nuclei (blue) were labeled with Hoechst. Notably, lysosome amount increased with rising BORM concentration. (TIF 6162 kb)

Additional file 5: Figure S5. Metabolic live cell monitoring. Live cell monitoring of three metabolic parameters (extracellular acidification, mitochondrial O_2 consumption and cell impedance) in MG-63 cells and primary osteoblasts (POB) during exposure to 25 μg/ml VSM or BORM in comparison to the control (which was set to 100 %) determined by the Bionas® 2500 analyzing system combined with the metabolic chip Bionas DisocveryTM SC1000. (TIF 1735 kb)

Additional file 6: Figure S6. Wound healing assay. Raw data of the wound healing assay of VSM (25, 50 μg/ml) treated MG-63 cells. (TIF 10288 kb)

Additional file 7: Figure S7. Apoptosis detection. Annexin V/PI labeling of VSM and BORM (50, 100 μg/ml) treated MG-63 cells. (TIF 1742 kb)

Abbreviations

ANOVA, one-way analysis of variance; Bcl-2/BCL-2, B-cell lymphoma 2; BORM, *Berberis orthobotrys* roots; BOFM, *Berberis orthobotrys* fruits; BO-5, ethylacetate soluble oily substance of *Berberis orthobotrys* fruits; BO-23, n-hexane soluble oily substance of *Berberis orthobotrys* fruits; CMM, *Caccinia macranthera* aerial part; DAPI, 4',6-diamidino-2-phenylindole; DMSO, dimethyl sulfoxide; DNA, Deoxyribonucleic acid; EtOH, ethanol; IC_{50}, inhibitory concentration of 50 % population; MeOH, methanol; MTS, 3-(4, 5-dimethylthiazol-2-yl)-5-(3-carboxymethoxyphenyl)-2-(4-sulfophenyl)-2H-tetrazolium; OHRM, *Onosma hispida* roots; OHAM, *Onosma hispida* aerial parts; PCNA, Proliferating cell nuclear antigen; PI, propidium iodide; POB, primary osteoblast cells; SEM, standard error of mean or scanning electron microscopy; TCM, Traditional Chinese medicine; VSM, *Vincetoxicum arnottianum*

Acknowledgements

We wish to express thanks to Prof. V. U. Ahmad for providing the plant extracts (VSM & CMM). Moreover Prof. P. Langer is highly acknowledged for inviting IA to his sophisticated chemical labs.

Funding

We would like to thank the BMBF habilitation scholarship program of the University of Rostock for the funding of Nadja Engels work.

Availability of data and materials

The data sets supporting the conclusions of this article are presented in this main paper. Plant materials used in this study have been identified by Dr. Sher Wali Khan and reference specimens were deposited at the Department of Biological Sciences, Karakoram International University, Pakistan. The supporting materials can be obtained upon request via email to the corresponding author.

Authors' contributions

Cell biological experimental work was done by NE, AA and MF. Plant collection, extraction preparation and chemical studies were performed by IA, AD, SA, VUA. The first draft of the paper was written by NE, IA, AA, and BN and reviewed by PL, VUA. All authors participated in the design of the study data, read and approved the final manuscript.

Authors' information

Not relevant.

Competing interests

The authors declare that they have no competing interests.

Consent for publication

Not relevant.

Ethics approval and consent to participate

Not relevant.

Financial disclosure

None.

Author details

[1]Department of Pediatric Surgery, University Hospital Marburg, Baldingerstraße, Marburg 35034, Germany. [2]Department of Chemistry, Karakoram International University, Gilgit-Baltistan 15100, Pakistan. [3]Institut für Chemie, Universität Rostock, Albert-Einstein-Str. 3a, Rostock 18059, Germany. [4]Department of Cell Biology, University Medical Center Rostock, Schillingallee 69, Rostock 18057, Germany. [5]Medical Biology and Electron Microscopy Centre, University Medical Center Rostock, Strempelstraße 14, Rostock 18057, Germany. [6]University of Education Vehari Campus, Punjab, Pakistan. [7]HEJ Research Institute of Chemistry, ICCBS, University of Karachi, Karachi 75270, Pakistan.

Received: 5 November 2015 Accepted: 14 July 2016
Published online: 26 July 2016

References

1. Madhuri S, Pandey G. Some anticancer medicinal plants of foreign origin. Curr Sci. 2009;96:779–83.
2. Cragg GM, Newman DJ. Plants as a source of anti-cancer agents. J Ethnopharmacol. 2005;100(1-2):72–9.
3. Ling CQ, Yue XQ, Ling C. Three advantages of using traditional Chinese medicine to prevent and treat tumor. J Integr Med. 2014;12(4):331–5.
4. Zhai XF, Chen Z, Li B, Shen F, Fan J, Zhou WP, Yang YK, Xu J, Qin X, Li LQ, Ling CQ. Traditional herbal medicine in preventing recurrence after resection of small hepatocellular carcinoma: a multicenter randomized controlled trial. J Integr Med. 2013;11(2):90–100.
5. Nasir E, Ali SI (eds) 1980-2005 Flora of Parkistan. Department of Botany. University of Karachi. Karachi: Karachi University Printing Press.
6. Rana MS, Samant SS. Diversity, indigenous uses and conservation status of medicinal plants in Manali wildlife sanctuary, north western Himalaya. Ind J Trad Knowl. 2011;10:439–59.
7. Middleton DJ. Apocynaceae (subfamilies Rauvolfioideae and Apocynoideae). Flora Malesiana, ser. I, seed plants. Vol. 18. Leiden: The National Herbarium of the Netherlands. p. 474.
8. Shah AJ, Zaidi MA, Sajjad H, Hamidullah, Gilani AH. Antidiarrheal and antispasmodic activities of Vincetoxicum stocksii are mediated through calcium channel blockade. Bangladesh J. Pharmacol. 2011;6:46-50.
9. Mogg C, Petit P, Cappuccino N, Durst T, McKague C, Foster M. Tests of the antibiotic properties of the invasive vine Vincetoxicum rossicum against bacteria, fungi and insects. Biochem Systemat Ecol. 2008;36:383–91.
10. Estakhr J, Javadian F, Ganjali Z, Dehghani M, Heidari A. Study on the anti-inflammatory effects of ethanolic extract of Cynanchum acutum. Curr Res J Bio Sc. 2012;4:630–2.
11. Fawzy GA, Abdallah HM, Marzouk MSA, Soliman FM, Sleem AA. Antidiabetic and antioxidant activities of major flavonoids of Cynanchum acutum L. (Asclepiadaceae) growing in Egypt. Z Naturforsch. 2008;63:658–62.
12. Staerk D, Nezhad KB, Asili J, Emami SA, Ahi A, Sairafianpour M, et al. Phenanthroindolizidine alkaloids from Vincetoxicum pumilum. Biochem Systemat Ecol. 2005;33:957–60.
13. Gibson DM, Krasnoff SB, Biazzo J, Milbrath L. Phytotoxicity of antofine from invasive swallow-worts. J Chem Ecol. 2011;37:871–9.
14. Beigh SY, Nawchoo IA, Iqbal M. Traditional veterinary medicine among the tribes of Kashmir Himalaya. J Herbs Spices Med Plants. 2004;10:121–7.
15. Zaidi MA, Crow Jr SA. Biologically active traditional medicinal herbs from Balochistan, Pakistan. J Ethnopharmacol. 2005;96:331–4.
16. Hussain F, Shah SM, Badshah L, Durrani MJ. Diversity and ecological characteristics of flora of Mastuj valley, district Chitral, Hindukush range, Pakistan. Pak J Bot. 2015;47:495–510.
17. Mokhber-Dezfuli N, Saeidnia S, Gohari AR, Kurepaz-Mahmoodabadi M. Phytochemistry and pharmacology of Berberis species. Pharmacogn Rev. 2014;8:8–15.
18. Srivastava S, Srivastava M, Misra A, Pandey G, Rawat AKS. A review on biological and chemical diversity in Berberis (Berberidaceae). EXCLI J. 2015;14:247–67.
19. Khan SW, Khatoon S. Ethnobotanical studies on useful trees and shrubs of Haramosh and Bugrote valleys in Gilgit, northern areas of Pakistan. Pak J Bot. 2007;39:699–710.
20. Noor A, Khatoon S, Ahmed M, Razaq A. Ethnobotanical study on some useful shrubs of Astore valley, Gilgit-Baltistan, Pakistan. Bangladesh J Bot. 2014;43:19–25.

21. Abbas Q, Khan SW, Khatoon S, Hussain SA, Hassan SN, Hussain A, et al. Floristic biodiversity and traditional uses of medicinal plants of Haramosh valley Central Karakoram National Park of Gilgit district, Gilgit-Baltistan, Pakistan. J Bio Env Sci. 2014;5:75–86.
22. Alamgeer MS Akhtar, Jabeen Q, Akram M, Khan HU, Karim S, Malik MNH, et al. Antihypertensive activity of aqueous-methanol extract of Berberis orthobotrys Bien. Ex. Aitch. in rats. Trop. J. Pharm. Res. 2013;12:393-399.
23. Alamgeer MS Akhtar, Jabeen Q, Bashir S, Malik MNH, Karim S, Mushtaq MN, et al. Possible mechanism of cardiac depressant activity of Berberis orthobotrys roots in isolated rabbit heart. Acta Poloniae Pharmaceutica – Drug Research 2014a;71:667-675.
24. Alamgeer, Ghuffar A, Ahmad T, Mushtaq MN. Antihyperlipidemic effect of Berberis orthobotrys in hyperlipidemic animal models. Bangladesh J. Pharmacol. 2014b;9:377-382.
25. Hussain SF, Khan L, Sadozai KK, Shamma M. New alkaloids from Berberis orthobotrys. J Nat Prod. 1981;44:274–8.
26. Kumar N, Kumar R, Kishore K, Onosma L. A review of phytochemistry and ethnopharmacology. Pharmacogn Rev. 2013;7:140–51. and references therein.
27. Al-Shahbaz I. The genera of Boraginaceae in the Southeastern United States. J Arnold Arbor Suppl. 1991;1:1–169.
28. El-Shazly A, Abdel-Ghani A, Wink M. Pyrrolizidine alkaloids from Onosma arenaria (Boraginaceae). Biochem Syst Ecol. 2003;31:477–85.
29. Kolarcik V, Zozomova-Lihova J, Martonfi P. Systematics and evolutionary history of the Asterotricha group of the genus Onosma (Boraginaceae) in central and southern Europe inferred from AFLP and nrDNA ITS data. Pl Systemat Evol. 2010;290:21–45.
30. Ahmad H, Khan SM, Ghafoor S, Ali N. Ethnobotanical study of upper Siran. J Herbs Spices Med Pl. 2009;15:86–97.
31. Sher H, Elyemeni M, Hussain K, Sher H. Ethnobotanical and economic observations of some plant resources from the northern parts of Pakistan. Ethnobot Res Appl. 2011;9:027–41.
32. Naz S, Ahmad S, Ajaz RS, Asad SS, Siddiqi R. Antibacterial activity directed isolation of compounds from Onosma hispidum. Microbiol Res. 2006;161:43–8.
33. Sharma PK, Thakur SK, Manuja S, Rana RK, Kumar P, Sharma S, et al. Observations on traditional phytotherapy among the inhabitants of Lahaul valley through Amchi System of Medicine – A cold desert area of Himachal Pradesh in North Western Himalayas, India. Chin Med. 2011;2:93–102.
34. Gairola S, Sharma J, Bedi YS. A cross-cultural analysis of Jammu, Kashmir and Ladakh (India) medicinal plant use. J Ethnopharmacol. 2014;155:925–86. and references therein.
35. Khan SW, Khatoon S. Ethnobotanical studies on some useful herbs of Haramosh and Burgote valleys in Gilgit, northern areas of Pakistan. Pak J Bot. 2008;40:43–58.
36. Czerepanov, SK. Sosud. Rast. SSSR. Leningrad: Nauka, Leningradskoe Otd-nie. p. 509.
37. Ghorbani AB, Mosaddegh M, Naghibi F. Ethnobotanical and ethnopharmaceutical study of Tturkmens of Golestan and Khorasan provinces, north of Iran. Ir J Pharmaceut Res. 2004;2:20.
38. Sahranavard S, Naghibi F, Mosaddegh M, Esmaeili S, Sarkhail P, Taghvaei M, et al. Cytotoxic activities of selected medicinal plants from Iran and phytochemical evaluation of the most potent extract. Res Pharmaceut Sc. 2009;4:133–7.
39. Amiri MS, Joharchi MR. Ethnobotanical investigation of traditional medicinal plants commercialized in the markets of Mashhad, Iran. Avicenna J Phytomed. 2013;3:254–71.
40. Asl MB, Talebpour A, Alijanpour R. Introducing of medicinal plants in Maragheh, Eastern Azerbaijan Province (Northwestern Iran). J Med Pl Res. 2012;6:4208–20.
41. Stapf MNS. Neotropical Boraginaceae. In: Milliken, W. Klitgård, B. & Baracat, A. (2009 onwards), Neotropikey - Interactive key and information resources for flowering plants of the Neotropics. http://www.kew.org/science/tropamerica/neotropikey/families/Boraginaceae.htm (accessed on 3 May 2015).
42. Taghvaei M, Naghibi F, Mosaddegh M, Moazzami N, Ghorbani A, Fakhari A. Prophage induction in Escherichia coli K-12(λ) by some plants from Iran. Ethno-Med. 2009;3:57–9.
43. Arora HRK, Arora RB. Pharmacological investigation of the glucoside and aglucone isolated from Caccinia glauca. J Pharm Sci. 1962;51:1040–2.
44. Siddiqi MA, Suri KA, Suri OP, Atal CK. A new pyrrolizidine alkaloid from Caccinia glauca. Phytochem. 1978;17:2049–50.
45. Ayengar KNN, Rangaswami S. Structure of caccigenin, a new triterpenoid sapogenin from Caccinia glauca Savi. Tetrahed Lett. 1966;7:1947–52.
46. Lüthen F, Lange R, Becker P, Rychly J, Beck U, Nebe JG. The influence of surface roughness of titanium on beta1- and beta3-integrin adhesion and the organization of fibronectin in human osteoblastic cells. Biomaterials. 2005;26(15):2423–40.
47. Engel N, Falodun A, Kühn J, Kragl U, Langer P, Nebe B. Pro-apoptotic and anti-adhesive effects of four African plant extracts on the breast cancer cell line MCF-7. BMC Compl Alt Med. 2014;14:334.
48. Engel N, Oppermann C, Falodun A, Kragl U. Proliferative effects of five traditional Nigerian medicinal plant extracts on human breast and bone cancer cell lines. J Ethnopharmacol. 2011;137:1003–10.
49. Engel N, Kraft K, Müller P, Duske K, Kühn J, Oppermann C, Nebe B. Actin cytoskeleton reconstitution in MCF-7 breast cancer cells initiated by a native flax root extract. Adv Med Plant Res. 2015;3(3):92–105.
50. Engel N, Lisec J, Piechulla B, Nebe B. Metabolic profiling reveals sphingosine-1-phosphate kinase 2 and lyase as key targets of (phyto-) estrogen action in the breast cancer cell line MCF-7 and not in MCF-12A. PLoS One. 2012;7(10):e47833. doi:10.1371/journal.pone.0047833.
51. Pautke C, Schieker M, Tischer T, Kolk A, Neth P, Mutschler W, et al. Characterization of osteosarcoma cell lines MG-63, Saos-2 and U-2 OS in comparison to human osteoblasts. Anticancer Res. 2004;24:3743–8.
52. Neve RM, Chin K, Fridlyand J, Yeh J, Baehner FL, Fevr T, et al. A collection of breast cancer cell lines for the study of functionally distinct cancer subtypes. Cancer Cell. 2006;10:515–27.
53. Wahl AF, Donaldson KL, Fairchild C, Lee FY, Foster SA, Demers GW, et al. Loss of normal p53 function confers sensitization to Taxol by increasing G2/M arrest and apoptosis. Nat Med. 1996;2(1):72–9.
54. Hamacher-Brady A, Stein HA, Turschner S, Toegel I, Mora R, Jennewein N, et al. Artesunate activates mitochondrial apoptosis in breast cancer cells via iron-catalyzed lysosomal reactive oxygen species production. J Biol Chem. 2011;286(8):6587–601.
55. Boya P, Kroemer G. Lysosomal membrane permeabilization in cell death. Oncogene. 2008;27(50):6434–51.
56. Liu Z, Wang Y, Zhao S, Zhang J, Wu Y, Zeng S. Imidazole inhibits autophagy flux by blocking autophagic degradation and triggers apoptosis via increasing FoxO3a-Bim expression. Int J Oncol. 2015;46(2):721–31. doi:10.3892/ijo.2014.2771.

Referenz IV

Engel N*, Lisec J, Piechulla B, Nebe B. Metabolic profiling reveals sphingosine-1-phosphate kinase 2 and lyase as key targets of (phyto-) estrogen action in the breast cancer cell line MCF-7 and not in MCF-12A. PLoS One. 2012;7(10):e47833. doi:10.1371/journal.pone.0047833. Epub 2012 Oct 24.
NCBI-Link: https://www.ncbi.nlm.nih.gov/pubmed/23112854

Zusammenfassung:

Zur Wirkung von Phytoöstrogenen (sekundäre Pflanzeninhaltsstoffe, die strukturell den humanen Östrogenen ähneln) auf Tumorzellen gibt es zahlreiche Arbeiten, die aber niemals die metabolischen Downstream-Prozesse der Tumorzelle betrachten. Dies scheint aber sinnvoll, denn Metabolit-veränderungen ermöglichen Rückschlüsse auf die initiale Wirkungsweise der applizierten Substanz auf den Tumorstoffwechsel. Daher wurde mit der Technologie der Metabolomics die Identifizierung neuer metabolischer Tumormarker nach der Behandlung mit sekundären Pflanzeninhaltstoffen etabliert. Die zellulären Metabolite der Brustkrebszelllinie MCF-7 wurde vergleichend mit denen der Kontrollzelllinie MCF-12A mittels Gaschromatographie separiert und anschließend mit Massenspektrometrie analysiert. Sowohl das endogene 17ß-Östradiol als auch das Phytoöstrogen Genistein bewirkten signifikante Metabolitveränderungen im Lipid-, Aminosäure- und Kohlenhydratstoffwechsel. Besonders auffällig waren die Alterationen dreier Metabolite des Sphingolipidstoffwechsels: Sphingosin, Dihydro-Sphingosin und Ethanolamin-Phosphat. Die assoziierten katabolen und anabolen Enzyme wurden detailliert untersucht, so dass eine differentielle Regulation der Sphingosin-1-Phosphat-Kinase und der Sphingosin-1-Phosphat-Lyase (SGPL1) durch humane und pflanzliche Östrogene nachgewiesen werden konnte. Dadurch wird in den MCF-7 Brustkrebszellen der „second messenger“ Sphingosin-1-Phosphat (S1P) überexprimiert. S1P kann intra- und extrazellulär als Proliferations-, Apoptose-, Angiogenese- und Motilitätsregulator wirken und so die Tumorigenese entscheidend lenken. Durch die Behandlung mit dem pflanzlichen Hormon Genistein wird die S1P-abbauende Lyase (SGPL1) verstärkt exprimiert, so dass das stimulierende Signalmolekül S1P sowohl intra- als auch extrazellulär reduziert vorliegt. Diese neuen Erkenntnisse deuten darauf hin, dass durch eine Supplementation mit Phytoöstrogenen oder eine entsprechende Umstellung der Ernährung auf Phytoöstrogen-haltige Lebensmittel die Tumorigenese beeinflusst werden kann.

OPEN ACCESS Freely available online

PLOS ONE

Metabolic Profiling Reveals Sphingosine-1-Phosphate Kinase 2 and Lyase as Key Targets of (Phyto-) Estrogen Action in the Breast Cancer Cell Line MCF-7 and Not in MCF-12A

Nadja Engel[1]*, Jan Lisec[2], Birgit Piechulla[3], Barbara Nebe[1]

1 University of Rostock, Department of Cell Biology, Rostock, Germany, **2** Max Planck Institute for Molecular Plant Physiology, Potsdam-Golm, Germany, **3** University of Rostock, Department of Biochemistry, Rostock, Germany

Abstract

To search for new targets of anticancer therapies using phytoestrogens we performed comparative metabolic profiling of the breast cancer cell line MCF-7 and the non-tumorigenic breast cell line MCF-12A. Application of gas chromatography-mass spectrometry (GC-MS) revealed significant differences in the metabolic levels after exposure with 17ß-estradiol, genistein or a composition of phytoestrogens within a native root flax extract. We observed the metabolites 3-(4-hydroxyphenyl)-lactic acid, cis-aconitic acid, 11-beta-hydroxy-progesterone, chenodeoxycholic acid and triacontanoic acid with elevated levels due to estrogen action. Particularly highlighted were metabolites of the sphingolipid metabolism. Sphingosine and its dihydro derivate as well as ethanolaminephosphate were significantly altered after exposure with 1 nM 17ß-estradiol in the cell line MCF-7, while MCF-12A was not affected. Treatment with genistein and the flax extract normalized the sphingosine concentrations to the basic levels found in MCF-12A cells. We could further demonstrate that the expression levels of the sphingosine metabolizing enzymes: sphingosine-1-phosphate kinase (Sphk) and lyase (S1P lyase) were significantly influenced by estrogens as well as phytoestrogens. The isoform Sphk2 was overexpressed in the tumorigenic cell line MCF-7, while S1P lyase was predominantly expressed in the non-tumorigenic cell line MCF-12A. Importantly, in MCF-7 the weak S1P lyase expression could be significantly increased after exposure with 10 µM genistein and 1 µg/ml root flax extract. Here, we present, for the first time, an analysis of metabolic response of phytoestrogens to breast cancer cell lines. The contrasting regulation of sphingolipid enzymes in MCF-7 and MCF-12A render them as preferred targets for future anticancer strategies.

Citation: Engel N, Lisec J, Piechulla B, Nebe B (2012) Metabolic Profiling Reveals Sphingosine-1-Phosphate Kinase 2 and Lyase as Key Targets of (Phyto-) Estrogen Action in the Breast Cancer Cell Line MCF-7 and Not in MCF-12A. PLoS ONE 7(10): e47833. doi:10.1371/journal.pone.0047833

Editor: Toshi Shioda, Massachusetts General Hospital, United States of America

Received May 31, 2012; **Accepted** September 17, 2012; **Published** October 24, 2012

Funding: The authors greatly appreciate the financial support from the Deutsche Krebshilfe Mildred-Scheel (FKZ: 107820; www.krebshilfe.de/dr-mildred-scheel-stiftung.html) and University of Rostock (habilitation scholarship under the program of the Federal Ministry for Education and Research (BMBF)). The funders had no role in study design, data collection and analysis, decision to publish, or preparation of the manuscript.

Competing Interests: The authors have declared that no competing interests exist.

* E-mail: nadja.engel-lutz@uni-rostock.de

Introduction

Phytoestrogens are plant-derived phytochemicals which can react like the endogenous steroid hormone 17ß-estradiol because of their structural similarity. Especially flavonoids, such as daidzein and genistein, initially isolated from soybean, are well studied phytoestrogens with the potential to prevent cancer development and progression [1]. It was shown that some phytoestrogens e.g. genistein mediate estrogenic effects at low concentrations (<10 µM) whereas higher concentrations (≥10 µM) cause anti-estrogenic activity [2]. This biphasic role for genistein has been studied primarily in the human breast cancer cell line MCF-7 [3,4]. Genistein at high concentrations has the ability to induce growth arrest and apoptosis in ER-positive cell line MCF-7 most likely by inhibiting the intrinsic tyrosine kinase activities of growth factor receptors [5]. However, the reason why endogenous estrogen hormones or synthetic xenoestrogens can increase breast cancer risk and phytoestrogens appear to exert a preventive effect is still not fully understood.

Until now, research was focused on genome-wide gene expression profile studies to enlighten the transcriptional regulation properties of phytoestrogens. Only recently, one group evaluated the transcriptional responsiveness of breast cancer cells to soy phytoestrogens using a whole-genome microarray based approach [6]. They identified 334 differentially expressed genes after treatment with 18.5 µM genistein or 78.5 µM daidzein which belong to completely different metabolic pathways. In addition to transcriptional analysis, downstream mechanisms, often referred to as non-genomic estrogenic pathways, became more and more in focus during the search for new phytoestrogen targets.

Here, we report for the first time on the influence of phytoestrogens on the metabolome of breast cancer cells. To this end, comparing GC-MS analyses of MCF-7, a well established breast cancer cell line, and MCF-12A, a non-tumorigenic epithelial breast cell line, allowed to distinguish between the metabolic features of breast cancer cells in contrast to their healthy counterparts. Both cell lines were positive for ERα and –ß expression [7]. To gain deeper insights in the mode of action of

phytoestrogens and how they can diminish the proliferation-promoting action of 17ß-estradiol, we treated the cells with 17ß-estradiol, genistein and a natural blend of phytoestrogens extracted from the native root of *Linum usitatissimum* [8,9]. This flax extract is composed of a variety of classical isoflavones and lignanes which potentially leads to synergistic effects on breast cancer cells in such a combination. This approach allows comparing tumor-relevant metabolic effects of cancerous cells and normal cells under tumor-promoting (17ß-estradiol) and tumor-regressing (phytoestrogens) modes and, therefore, enables the identification of new targets for anticancer treatment.

The combination of transcriptomics, metabolomics and intelligent pattern recognition methods for tumor metabolism recently allowed advances in breast cancer profiling [10,11]. As a result, metabolic pathways, like the biosynthesis of bile acids, extracellular matrix synthesis or sphingolipid metabolism, are progressively gaining research attention. Bioactive sphingolipids play a key role in cancer progression, especially for proliferation, migration and tamoxifen resistance [12,13]. The balance between ceramide, sphingosine and sphingosine-1-phosphate (and also their dihydro derivates) is thought to regulate cellular processes, including cell survival, growth and differentiation. Especially sphingosine-1-phosphate (S1P) which is controlled by S1P kinases (isoforms: Sphk1, Sphk2; biosynthesis) and S1P lyases (degradation) is a well established pro-survival molecule [14]. It was shown that S1P promotes the migration of MCF-7 cells, suggesting a role for Sphks in metastasis [15]. The biological effects of S1P are mediated by five specific G-protein-coupled receptors located on the cell surface (named $S1P_{1,2,3,4,5}$). The functional $S1P_1$ antagonist FTY720 and inhibitor of Sphk1 activity decreases breast cancer proliferation and metastasis in mouse models [12]. Several growth factors and steroid hormones, such as TGF-ß and 17ß-estradiol could be related to up-regulation of Sphk1. The role of Sphk2 in cancer remains somewhat unclear and the irreversible conversion of S1P to ethanolamine and hexadecanol by S1P lyase is unstudied so far.

Materials and Methods

Cell Culture and Treatment Conditions

Cell culture conditions of cell lines MCF-7 and MCF-12A, purchased from ATCC (www.atcc.org/) were described previously [7]. At a sub-confluence of approximately 80% the cell monolayer was washed with PBS and adapted to phenol-red-free Dulbecco's Modified Eagle's Medium (PAA Laboratories GmbH, Germany) with 10% charcoal stripped fetal bovine serum (PAN Biotech GmbH, Germany) for 48 hours to avoid unspecific stimulation of endogenous hormones in the serum. Treatments with the flax extract (L; final concentrations: 0.01, 1 and 50 µg/ml), the phytoestrogen genistein (G; 5,7,40 trihydroxyisoflavone; final concentration: 1, 10 and 100 µM) and 17ß-estradiol (E; final concentration: 1 nM), last two purchased from Sigma, Germany, was carried out for 48 hours. Extract preparation from flax roots of *Linum usitatissimum* (L) was described previously [8,9]. Lignan/isoflavone contents of the flax extract according to Luyengi extract preparation were about 1.25–4.25 mg/g fresh weight (0.125%–0.425%) [8]. As negative control substances the respective vehicle (C; final concentration: 0.1%) was used in the same manner.

Flow Cytometric Measurements of Cell Proliferation and Apoptosis

Flow cytometric measurements and calculation of proliferation and apoptosis was done as described in detail [7,16].

Metabolic Profiling via GC-MS

The metabolite profiles were measured by gas chromatography–mass spectrometry (GC–MS). For each sample, 200,000 MCF-7 and 460,000 MCF-12A cells were harvested with 0.05% trypsin-0.02% EDTA, washed three times with ice-cold PBS and cell pellet was frozen in liquid nitrogen after centrifugation (14,000 rpm, 4°C, 2 min). Sample extraction and derivatization followed the procedure described previously [17]. Metabolite signals were obtained from raw data and compared against a reference database using the TargetSearch package [18]. Some samples were removed after inspection of their chromatograms due to overall lower peak intensities, leaving four to six replicates per group (all samples of the same genotype and subjected to the same treatment). Out of all putative metabolic traces only 106 were retained in the resulting raw data matrix that met the following criteria: (i) the peak was present in all samples of at least one replicate group (genotype/treatment combination); (ii) the median peak height exceeded a value of 250 (well above the detection limit); (iii) the peak mass spectra showed a similarity of >75% to the respective library entry and a retention time deviation of <2s (can be considered as correctly identified). All data were log10-transformed to improve normality and normalized to show similar median peak intensity within replicate groups as described previously [19].

Western Blot

After treatment with phytoestrogens for at least 48 h the cells were trypsinized, washed with PBS and lysed in ice-cold lysis buffer (Bio-Plex Cell Lysis Kit, Bio-Rad, USA). Cells were homogenized by brief sonification at 4°C and centrifuged at 10,000 g for 2 min at 4°C. Protein concentrations of the supernatants were estimated by Bradford protein assay [20] and verified by Coomassie staining [21] so that equal amounts (10–30 µg) of total soluble protein could be separated by SDS-PAGE and blotted on PVDF membranes, subsequently. After the protein transfer membranes were blocked with 5% skim milk in Tris-buffered saline (TBS) and washed six times in TBS. For protein detection primary antibodies (Sphk1: sc-48825; Sphk2: sc-22704; S1P-lyases: sc-67368, all from Santa Cruz, USA) were incubated overnight at 4°C followed by a labeling with a horseradish peroxidase (HPR)-conjugated secondary antibody (Dako, Glostrup, Denmark) for 1 hour at room temperature. Protein signals were visualized by using SuperSignal West Femto Chemiluminescent Substrate (Pierce Biotechnology, Rockford, USA) for detection of peroxidase activity from HRP-conjugated antibodies (Thermo Fisher Scientific Inc., Rockford, USA). Band intensity was analyzed densitometrically with the Molecular Imager ChemiDoc XRS and Image Lab 3.0.1 software (Bio-Rad, USA). Protein detection was repeated at least three times with individual prepared cell lysates from independent passaged cells.

Immunofluorescence Staining

For immunofluorescence staining 1×10^5 cells were seeded on glass cover slips (20×20 mm) and let them adhere for 24 hours. Thereafter treatment with phytoestrogens for 48 h and control substances followed as described above. Cover slips were washed twice with Dulbecco's PBS without Ca and Mg, fixed with 4% paraformaldehyde for 15 min, washed again and permeabilized with 0.1% Triton X-100 for 15 min. After a washing step with phosphate buffered saline (PBS) cells were incubated with the primary antibody (see Western blotting procedure) in a dilution of 1:50 at 4°C overnight. Afterwards cells were washed three times with PBS and incubated with 488Alexa Fluor-labeled secondary

antibody (Molecular Probes, USA, 1:100) for 1 hour at room temperature in the dark. After washing cells were incubated with DAPI (Roche Diagnostics GmbH, Germany) to stain nuclei for 15 min. Finally the cells were washed four times with PBS, embedded and stored in the dark at 4°C. Visualization and imaging was carried out with the Axio Scope.A1 fluorescence microscope (Carl Zeiss, Germany) using AxioVision Imaging Software 4.8.2.0 (Carl Zeiss, Germany). Notably, photomicrographs stained with the same primary antibody were taken at identical exposure times to guarantee comparable results.

Live Cell Monitoring of Adhesion, Acidification and Respiration

Online monitoring of the adhesion, acidification, respiration under the influence of sphingosine-1-phosphate (S1P) and D-sphingosine (D-S) was performed with the Bionas® 2500 analyzing system with the metabolic chip SC 1000 (Bionas GmbH, Rostock, Germany) and the measurement software Bionas15002 CS1.47 [22]. Prior experiments, chips were cleaned with 70% ethanol for 10 minutes, washed with PBS and were adapted to the measurement medium for 5 minutes. Measurement medium was composed of DMEM without $NaHCO_3$ (Invitrogen, Germany), 0.1% charcoal stripped fetal bovine serum (PAN Biotech GmbH, Germany) and 1% gentamycin (Ratiopharm, Germany), pH value 7.4 and sterile filtered. On each chip 2×10^6 cells were seeded and let them adhere over night at 37°C and in 5% CO_2 so that 80% sub-confluence on the sensor chips was reached. Bionas measurements were carried out with a pump rate of 56 µl/min for 24 hours [22,23]. Within the first 4 hours cells could adapt to the new measurement medium. Thereafter cells were treated with the vehicle substance (control), 1 µM S1P (Sigma, Germany) or with 1 µM D-S (Sigma, Germany) for 20 h. Every measurement was repeated three times. Data set was evaluated and normalized with the software Bionas1500[2] Data analyzerV1.07.

Statistical Analysis

Flow cytometry, western blotting and immunofluorescence experiments were replicated at least three times with individual passaged cells and data sets were expressed as means ± standard deviations (SD). Statistical significance was determined by the student's t-test (** $P<0.001$, * $P<0.01$).

All statistical tests on metabolite profiles have been conducted in R (www.r-project.org) using the respective functions. To facilitate comparison of treatment effects in MCF-7 and MCF-12A, two further normalization strategies have been followed for metabolic values, applying the following formula:

$$x'_{m,g,t} = \log 2\left(\frac{x_{m,g,t}}{\overline{x}_{m,g,ctrl}}\right)$$

$\overline{x}$ the observed, normalized and mean value and m, g and t are metabolite, genotype and treatment, respectively. Basically this transformation expresses all values relative to a control group mean and centers the deviations on zero (due to log2). For $\overline{x}$ctrl we choose either the control group mean of the same genotype as the sample (strategy one) or consistently the control group mean of MCF-12A (strategy two). While the first strategy removes any differences between the control samples of MCF-12A and MCF-7, therefore highlighting the treatment effects, the second strategy maintains between line differences. To investigate which metabolite levels are stronger affected in MCF-7 compared to MCF-12A after treatment with E, we conducted t-tests between control (C) and estradiol (E) treatment for both lines. Instead of selecting all metabolites showing non-significant P-values in MCF-12A and significant P-values in MCF-7, we decided to select candidates based on the P-value ratio of both tests being larger than 100. That means we also selected metabolites that had a (significant) P-value of 0.01 in MCF-12A if the observed P-value for MCF-7 was lower than 0.0001. Because this is rather intuitive than statistically sound, we confirmed this ranking by manual inspection of the data using boxplots. For principal component analysis we used the pcaMethods package [24], applying the nipals algorithm on pareto normalized data. For analysis of variance (ANOVA) we considered genotype and treatment as factors and allowing for interactions. The resulting P-values were Bonferroni corrected. Heatmaps were produced using the pheatmap package.

Results and Discussion

Determination of the Effective Phytoestrogen Concentrations

Prior to metabolic profiling experiments we determined the most effective concentrations of genistein (G) and a native root flax extract (L) for our treatment conditions via cell cycle analysis in flow cytometry studies. First, the proliferative phases (S+G2/M) and the apoptotic rates (sub-G1) were calculated for the cell lines MCF-7 and MCF-12A under control conditions (Fig. 1A). The non-tumorigenic cell line MCF-12A showed low proliferative potential indicating that only 2–4% of all measured cells were in G2/M or S phase. In contrast, the tumorigenic cell line MCF-7 is marked by higher proliferative phases in the sum of about 27%. The apoptotic cells of both cell lines were below 0.5%, typical for a subconfluent, continuously growing cell culture (Fig. 1B). For validating the most effective concentrations of the phytoestrogens both cell lines were treated with either EtOH or 17ß-estradiol (C, E), both are regarded as control experiments, or three concentrations of genistein (G) or the flax extract (L) for 48 hours. Determination of the apoptotic rates revealed no significant alterations in both cell lines except at the highest concentration of the flax extract (50 µg/ml) for the MCF-7 (Fig. 1B). The detailed analysis (Fig. 1C) illustrated that the applied concentrations of genistein and flax extract are not cytotoxic, even for the non-tumorigenic cell line MCF-12A. This important to note because the MCF-12A cells are considered as a control cell line representing healthy, normal breast epithelial tissue. The proliferative rates in MCF-12A cells revealed that the highest concentration of the flax extract (50 µg/ml) lead to a moderate but significant impairment of the dividing activity of MCF-12A, while the other concentrations did not significantly affect the cell cycle phases of MCF-12A (Fig. 1C). Therefore, the highest concentration of the flax extract was excluded from further experiments because healthy tissue could be affected detrimentally. Treatment with E and showed stronger proliferative response in the cell line MCF-7 (Fig. 1D). The addition of 17ß-estradiol resulted in a strong increase of the proliferative phases of the estrogen-sensitive cell line MCF-7 (40–45%) indicating that nearly half of all MCF-7 cells were in the G2 or S phase. The application of G caused a concentration-dependent biphasic effect on the proliferation of MCF-7 cells, as already described [25–27]. The lowest concentration of 1 µM genistein yielded in 10–15% elevated rates of G2+ S phase compared to the control. The intermediate concentration of 10 µM showed no alteration of the cell cycle phases and the highest concentration of 100 µM led to a 20–30% reduction of the proliferative phases in MCF-7 *in vitro* (Fig. 1D). In contrast to the effects obtained after genistein application, the native flax extract significantly decreased proliferation of MCF-7 at all tested concentrations. The highest

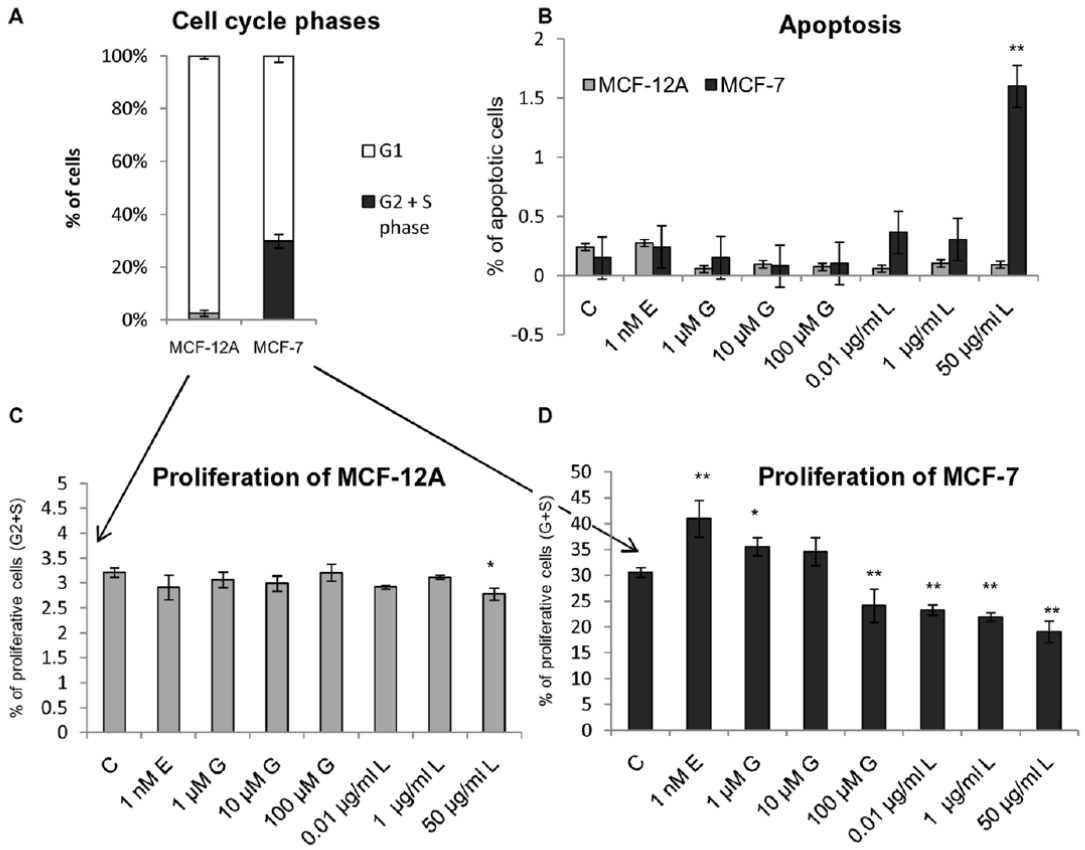

Figure 1. Cell cycle analysis to determine proliferation and apoptosis. Determination of effective 17ß-estradiol (E), genistein (G) and flax extract (L) concentration on the cancerous cell line MCF-7 and the non-tumorigenic cell line MCF-12A via cell cycle analysis by flow cytometry. Control (C) treatment was carried out with the vehicle ethanol (EtOH). **A**: Percentage distribution of cell cycle phases in both cell lines under un-treated conditions. Proliferative phases were summed as G2+S. Notably, the MCF-7 cells line harbors a more than 10fold greater proliferative potential with up to 30% cells in G2+S phase. **B–D**: Dose dependent effects of genistein and flax extract on apoptosis and proliferation (G2+S) on the cell lines MCF-7 and MCF-12A. All results are indicated in overall percentage. Mean ± SD values (n = 5–7). * = $p<0.01$; ** = $p<0.001$ as compared to EtOH control (unpaired *t* test).
doi:10.1371/journal.pone.0047833.g001

concentration of 50 µg/ml native flax extract resulted in the strongest inhibition (10–15%) of MCF-7 proliferation.

On the basis of these proliferation results we decided to use the low and intermediate concentrations of 1 µM and 10 µM of genistein for the following metabolic profiling experiments. As expected the low concentration revealed more estrogenic effect on MCF-7 cells. A concentration of 10 µM genistein could be reached in the human body after a phytoestrogen-rich diet and therefore support the transition to an anti-estrogenic action [28]. Since concentrations of 100 µM most likely do not appear in the human body these test concentrations are considered unphysiologically. Regarding the native flax root concentrations, 0.01 and 1 µg/ml were used for metabolic measurements because the highest concentration of 50 µg/ml caused a significant decrease in cell proliferation of MCF-12A. Apparently, the mixture of various phytoestrogens in a plant extract appears to be more effective for the inhibition of cell proliferation of MCF-7 than a moderately dosed, single isolated phytoestrogen like genistein.

Metabolic Profiling of Mammary Epithelial Cell Lines (MCF-12A, MCF-7)

In a preliminary experiment, 200,000 MCF-7 and MCF-12A cells under normal culture conditions were harvested in five replicates. Comparison of the GC-chromatograms and mass spectra revealed drastic changes in the pool sizes of most metabolites, allowing a discrimination of tumorigenic and non-tumorigenic cells (data not shown). We further observed that metabolite levels were generally twice as high in MCF-7 compared to MCF-12A. This finding suggested that the MCF-7 cells are bigger or, less likely, contain proportionally larger amounts of primary metabolites, which are predominantly measured using GC-MS. We then determined the fresh weight of both cell lines and found MCF-7 cells to be approximately 2.3-fold heavier than MCF-12A cells (data not shown). Therefore, we decided to adjust the imbalanced metabolite levels by using 200,000 MCF-7 and

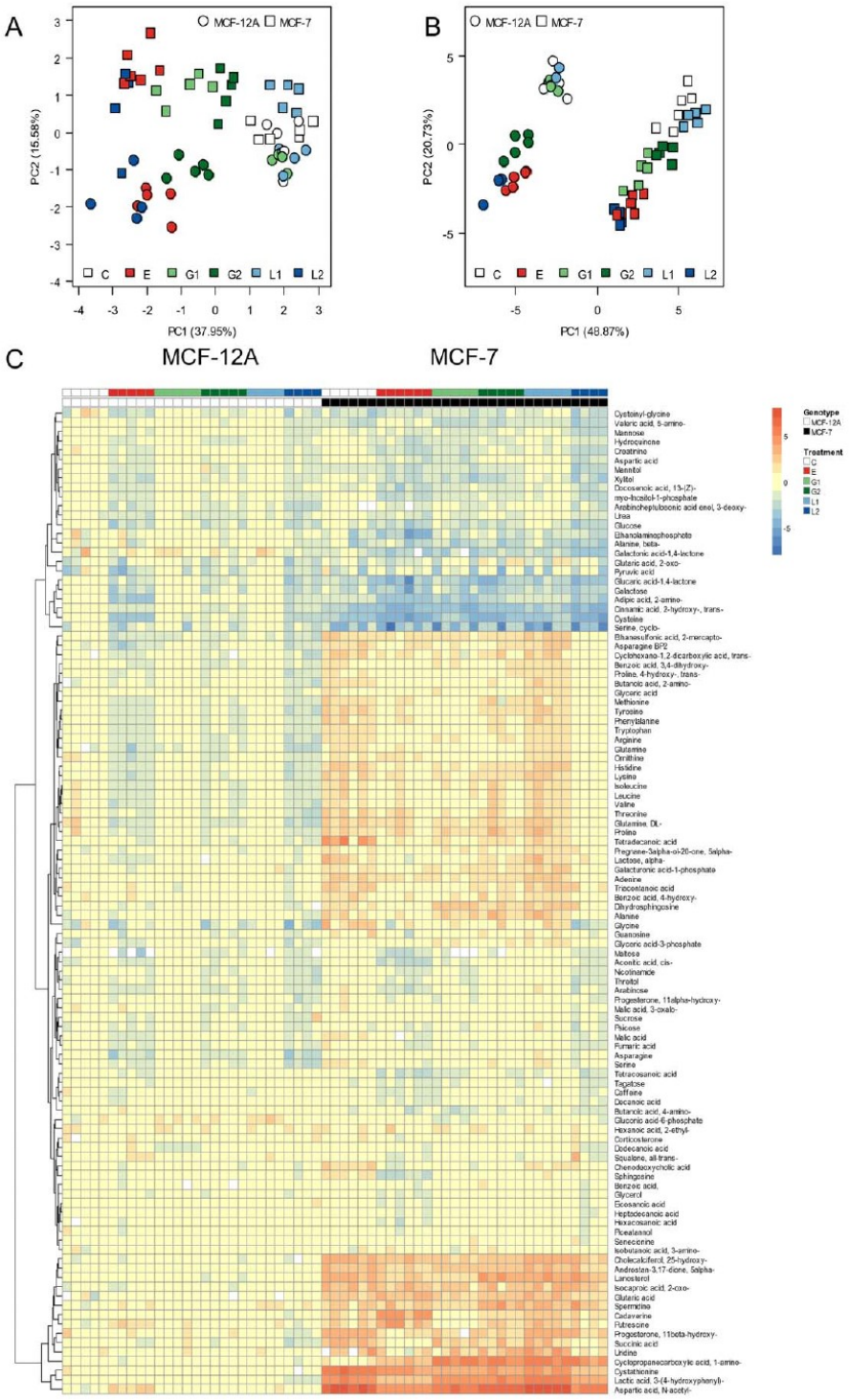
A
MCF-12A
MCF-7
PC2 (15.58%)
PC1 (37.95%)
C
E
G1
G2
L1
L2
B
PC2 (20.73%)
PC1 (48.87%)
C
MCF-12A
MCF-7
Genotype
MCF-12A
MCF-7
Treatment
C
E
G1
G2
L1
L2
Cysteinyl-glycine
Valeric acid, 5-amino-
Mannose
Hydroquinone
Creatinine
Aspartic acid
Mannitol
Xylitol
Docosanoic acid, 13-(Z)-
myo-Inositol-1-phosphate
Arabinoheptulosonic acid enol, 3-deoxy-
Lysine
Glucose
Ethanolaminephosphate
Alanine, beta-
Galactonic acid-1,4-lactone
Glutaric acid, 2-oxo-
Pyruvic acid
Glucaric acid-1,4-lactone
Galactose
Adipic acid, 2-amino-
Cinnamic acid, 3-hydroxy-, trans-
Cysteine
Serine, cyclo-
Ethanesulfonic acid, 2-mercapto-
Asparagine BP2
Cyclohexane-1,2-dicarboxylic acid, trans-
Benzoic acid, 3,4-dihydroxy-
Proline, 4-hydroxy-, trans-
Butanoic acid, 2-amino-
Glycolic acid
Methionine
Tyrosine
Phenylalanine
Tryptophan
Arginine
Glutamine
Ornithine
Histidine
Lysine
Isoleucine
Leucine
Valine
Threonine
Glutamine, DL-
Proline
Tetradecanoic acid
Pregnane-3alpha-ol-20-one, 5alpha-
Lactose, alpha-
Galacturonic acid-1-phosphate
Adenine
Tricontanoic acid
Benzoic acid, 4-hydroxy-
Dihydrosphingosine
Alanine
Glycine
Guanosine
Glycolic acid-3-phosphate
Maltose
Aconitic acid, cis-
Nicotinamide
Threitol
Arabinose
Progesterone, 11alpha-hydroxy-
Malic acid, 3-oxalo-
Sucrose
Phlorose
Malic acid
Fumaric acid
Asparagine
Serine
Tetracosanoic acid
Tagatose
Caffeine
Decanoic acid
Butanoic acid, 4-amino-
Gluconic acid-6-phosphate
Hexanoic acid, 2-ethyl-
Corticosterone
Dodecanoic acid
Squalene, all-trans-
Chenodeoxycholic acid
Sphingosine
Benzoic acid,
Glycerol
Eicosanoic acid
Heptadecanoic acid
Hexacosanoic acid
Ficealanaol
Senecionine
Isobutanoic acid, 3-amino-
Cholecalciferol, 25-hydroxy-
Androstan-3,17-dione, 5alpha-
Lanosterol
Isocaproic acid, 2-oxo-
Glutaric acid
Spermidine
Cadaverine
Putrescine
Progesterone, 11beta-hydroxy-
Succinic acid
Uridine
Cyclopropanecarboxylic acid, 1-amino-
Cystathionine
Lactic acid, 3-(4-hydroxyphenyl)-
Aspartic acid, N-acetyl-

Figure 2. Heat map of metabolites comparing between MCF-12A and MCF-7. Principal component analysis (PCA) and heat map presentation of metabolite profiles from MCF-7 cells (squares) and MCF-12A (circles) treated with 0.1% EtOH (C, white), 1 nM 17β-estradiol (E, red), 1 μM genistein (G1, light green), 10 μM genistein (G2, dark green), 0.01 μg/ml *Linum usitatissimum* (L1, light blue) and 1 μg/ml *Linum usitatissimum* (L2, dark blue) for 48 hours. **A**: For log10-transformed values the main sources of variance are cell type (PC1, 49%) and treatment (PC2, 21%). **B**: For data expressed relative to the respective control samples the main sources of variance are treatment (PC1, 38%) and treatment within cell type (PC2, 16%). **C**: Heat map presentation of all identified metabolites by GC-MS based profiling under the treatment with 17ß-estradiol (E), genistein (G) and flax extract (L) in the cell lines MCF-12A and MCF-7 (see color bar for scale; blue color indicates down regulated metabolites; red color indicates up regulated metabolites). The data were normalized to the untreated control of MCF-12A to identify significantly altered metabolites in the tumorigenic cell line MCF-7. Metabolites were grouped according to cell line and each treatment condition (indicated with specific colors in the upper panel) and hierarchically clustered. Correlation coefficients were calculated by applying the Pearson algorithm using R software.
doi:10.1371/journal.pone.0047833.g002

460,000 MCF-12A cells for every further metabolic measurement to ensure comparable results.

Subsequently to sample preparation, we could detect 106 metabolites that were identified based on retention times, characteristic ions and mass spectra, comprising mainly amino acids, organic acids and mono- and disaccharides. Initially, we applied principal component analysis (PCA) on the data to evaluate the major differences between the individual groups. As shown in Fig. 2A most of the variance is attributed to differences between the two cell lines (PC1, 49%), while treatment effects also contribute strongly (PC2, 21%). The differences between the lines are not caused by differences in cell weight. In contrast to our preliminary experiment we observed about 40% of all metabolites to show higher levels in MCF-12A compared to MCF-7. This was expected as we controlled for the total sample amount by cell number (see above). It can be seen that higher concentrations (E, L2, G2) generally modulate the metabolic profile of both lines stronger, while cells treated with lower concentrations (L1, G1) tend to closer resemble the metabolic profile of the control samples. An interesting exception is the treatment with G1, which shows no effect in MCF-12A but does show an effect on MCF-7. To render treatment effects more comparable between cell lines, we expressed metabolic profiles relative to the control samples of the respective cell line (cf. Material and Methods). This procedure removed most genotypic differences and allowed to checking if metabolic changes of similar treated samples were consistent or different between MCF-7 and MCF-12A. As can be seen in Fig. 2B, metabolic changes due to different treatments were not contrasting between the two cell lines but do show differences. Differences in metabolic profiles were further quantified by an analysis of variance (ANOVA) for each metabolite including the two factors genotype and treatment as well as an interaction term (Fig. S1). These results confirm the PCA by showing that most metabolites are found to be significantly different between genotypes (74 metabolites with Bonferroni corrected P-values <0.05) and treatments (82 metabolites).

To give a more intuitive representation of differences for individual metabolites a heatmap of metabolic levels was established (Fig. 2C). To optimally visualize genotypic and treatment effects in one plot, all metabolite intensities were normalized to the respective mean values of the MCF-12A controls (0.1% EtOH) since these data represent the metabolite levels of the unaffected, normal epithelial breast tissue cell line. A log2-transformation centers the values around zero, such that values of one and two indicate a two and four-fold increase compared to the control. Minus one and two indicate a two and four-fold decrease, respectively, compared to the control. Up- and down-regulated metabolites in comparison to MCF-12A are indicated by red and blue colors, respectively. As expected several metabolite levels were up-regulated in the breast cancer cell line MCF-7 under both, treated and untreated conditions in contrast to MCF-12A, with N-acetyl-aspartic acid, 3-(4-hydroxyphenyl)-lactic acid and cystathionine (dark red color) being the most prominent examples. We found metabolites significantly down-regulated in MCF-7 cells like cyclo-serine, 2-hydroxy-trans-cinnamic acid and cysteine (blue color).

While per se differences between the metabolism of cancerous and non-cancerous cells were investigated previously [29,30] we focused our work on the metabolic alterations in these cell lines treated with 17ß-estradiol and phytoestrogens. Consequently, we searched for metabolites which were significantly influenced in the tumor line MCF-7 and not in the non-tumorigenic cell line MCF-12A after an exposure of 1 nM 17ß-estradiol. We ranked all metabolites according to their stronger alteration in MCF-7 versus MCF-12A after exposure of 1 nM 17ß-estadiol (Table 1). Sphingosine was ranked first and followed by the 3-(4-hydroxyphenyl)-lactic acid, 1-amino-cyclopropanecarboxylic acid, succinic acid, chenodeoxycholic acid and N-acetyl-aspartic acid. The ranking of the 29 metabolites fulfilling our criteria is given in Table 1 and box plots of their normalized levels can be found in Fig. S2. The 29 compounds are annotated to different cellular pathways, e.g. lipid metabolism, amino acid metabolism, steroid hormone synthesis, indicating that different targets were addressed by 17ß-estradiol treatment in cancer cells. Astonishingly, strongly effected metabolites appeared in lipid and steroid biosynthetic pathways. Furthermore, we noticed that three metabolites of the sphingolipid pathway (sphingosine, ethanolaminephosphate, dihydrosphingosine) were part of the ranking and, therefore, potentially main targets of 17ß-estradiol in the breast cancer cell line MCF-7 (highlighted in Table 1).

In Fig. 3 these three metabolites were analyzed in detail regarding all treatment conditions. Sphingosine was found in higher concentrations in the cell line MCF-7 under control conditions but after exposure 17ß-estradiol the levels were significantly reduced. The treatment with genistein as well as with the phytoestrogen mixture in form of the flax extract normalized the sphingosine levels in MCF-7 while the amounts in MCF-12A were not significantly affected. Similar results were obtained for dihydrosphingosine and ethanolaminephosphate with the exception that genistein and the flax extract could not normalize the expression of dihydrosphingosine in the cell line MCF-7 to gain the level of MCF-12A under control conditions, like it is was observed for sphingosine and ethanolaminephosphate. Our experiments clearly demonstrate that metabolites of the sphingolipid metabolism are one of the main targets for the action of 17ß-estradiol and phytoestrogens with similar structural properties like genistein.

Expression of Sphingosine Kinase and Lyase is Influenced by Phytoestrogen Action

The metabolites sphingosine, dihydrosphingosine and ethanolaminephosphate are linked with each other via enzymatic steps including several enzymes. An overview of the sphingolipid metabolism is indicated in a modified KEGG pathway and schematic representation (Fig. S3, S4). Alterations in the protein content and distribution of three involved enzymes (Sphk1, Sphk2,

Table 1. List of the ranked metabolites.

No.	Metabolite	Related pathway	KEGG/pubchem no.
1	**Sphingosine**	**Lipid metabolism**	**C00319/cid: 5280335**
2	3-(4-hydroxyphenyl)-Lactic acid	Glycolysis	C01432/cid: 612
3	1-amino-Cyclopropanecarboxylic acid	Amino acid metabolism	C01234/cid:535
4	Succinic acid	Tricarboxyclic acid cycle (TCA)	C00042/cid: 1110
5	Chenodeoxycholic acid	Lipid metabolism	C02528/cid: 5645
6	N-acetyl-Aspartic acid	Amino acid metabolism	C01042/cid:97508
7	Cystathionine	Amino acid metabolism	C00542/cid: 834
8	**Dihydrosphingosine**	**Lipid metabolism**	**C00836/cid: 91486**
9	11-beta-hydroxy-Progesterone	Steroid hormone synthesis	C05498/cid: 92750
10	2-amino-Butanoic acid	Amino acid metabolism	Cid:6657
11	All-trans-Squalene	Steroid hormone synthesis	C00751/cid: 638072
12	Cis-Aconitic acid	Tricarboxyclic acid cycle (TCA)	C00417/cid: 643757
13	Threitol	Sugar alcohols	C16884/cid:169019
14	Corticosterone	Steroid hormone synthesis	C02140/cid: 5753
15	5-alpha-Androstan-3,12-dione	Steroid hormone synthesis	C00674/cid:3943
16	Triacontanoic acid	Lipid metabolism	Cid: 10471
17	Cadaverine	Amino acid metabolism	C01672/cid: 273
18	Malic acid	Tricarboxyclic acid cycle (TCA)	D04843/cid:525
19	Creatinine	Amino acid metabolism	C00791/cid: 588
20	Lanosterol	Steroid hormone synthesis	C01724/cid:4861
21	Piceatannol	Stilbenoid, diarylheptanoid and gingerol biosynthesis	C05901/cid:667739
22	4-hydroxy-, trans-Proline	Amino acid metabolism	C01015/cid:5810
23	Glutaric acid	Fatty acid metabolism; lysine degradation	C00489/cid:743
24	**Ethanolaminephosphate**	**Lipid metabolism**	**C00346/cid: 1015**
25	Caffeine	Purine metabolism; calcium signaling pathway	D00528/cid:2519
26	11-alpha-hydroxy-Progesterone	Steroid hormone synthesis	C03747/cid:6508
27	Galactonic acid-1,4-lactone	Ascorbate and aldarate metabolism	C01040/cid:97165
28	4-hydroxy-Benzoic acid	Amino acid metabolism	C00156/cid: 105001
29	5-amino-Valeric acid	Amino acid metabolism	C00431/cid:3720

Ranking of the 29 metabolites affected stronger by 17ß-estradiol in the tumorigenic cell line MCF-7 compared to the non-tumorigenic cell line MCF-12A. Related pathways and the KEGG and/or PubChem number are given.
doi:10.1371/journal.pone.0047833.t001

S1P lyase) were analyzed by western blotting and immunofluorescence staining. Western blotting experiments revealed a significant decrease in the amount of Sphk1 and Sphk2 enzyme in the breast cancer cell line MCF-7 after 48 h exposure with G and L in a concentration dependent manner (Fig. 4A, B; Fig. 5A, B). Especially treatment with the flax extract resulted in a 2–3fold reduction of both kinases. Furthermore, we could observe a slight increase of Sphk1 and Sphk2 expression in MCF-7 after treatment with 1 nM 17ß-estradiol. In MCF-12A Sphk1 expression was decreased nearly by half after treatment with 17ß-estradiol and phytoestrogen exposure revealed boosted Sphk1 amounts (Fig. 4B). In contrast, western blots of MCF-12A cells showed poor, nearly undetectable expression rates of Sphk2 even when 20–30 µg soluble protein was loaded on the SDS-gel (Fig. 4D). Negligible alterations in the expression of Sphk2 were measured in MCF-12A after treatment with 17ß-estradiol and phytoestrogens (Fig. 4E). All western blot results were confirmed by immunofluorescence stainings with identical antibodies (Fig. 4C; Fig. 4F). Proteins of interest were secondary labeled with AlexaFluor488 (green color). Additionally, nuclei were stained with DAPI (blue) for better local orientation of the protein expressions within the cell. To guarantee quantitative comparable results we have ensured that photographs were taken with identical settings, e.g. exposure time. Representative pictures of Sphk1 expression in MCF-7 and MCF-12A were displayed in Fig. 4C. As in the western blots already indicated, phytoestrogens are able to decrease Sphk1 expression in the breast cancer cell line MCF-7 and enhance its expression in the non-tumorigenic cell line MCF-12A (Fig. 4C). When strong and constitutive expression was reached the cell nuclei were overlaid with the green dye indicating current protein biosynthesis at the surface of the rough endoplasmic reticulum. We conclude that 17ß-estradiol and phytoestrogens have opposite effects on the Sphk1 expression in MCF-7 and vice versa for MCF-12A. For Sphk2 we obtained similar results in the cell line MCF-7 (Fig. 4D). In contrast Sphk2 is expressed weakly in MCF-12A like it was shown by western blot result previously (Fig. 4E). Nearly no green fluorescence is visible inside the cell only the blue-glowing nuclei can be mentioned. These findings led us to the assumption that SPHK1 is expressed in cancerous as well as non-tumorigenic cells

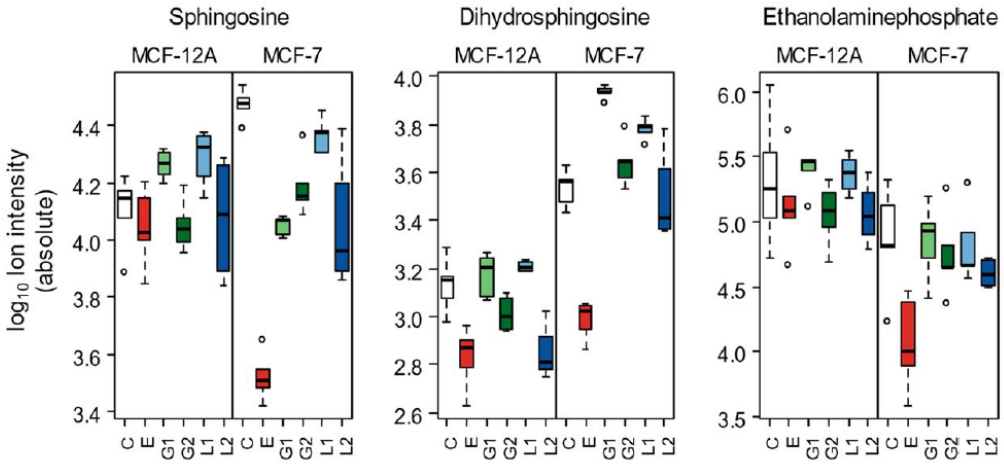

Figure 3. Alterations in sphingolipid metabolites. Boxplots of absolute metabolite levels for sphingosine, dihydrosphingosine and ethanolaminephosphate under the treatment of 17ß-estradiol (E), genistein (G) and flax extract (L) in the cell lines MCF-12A and MCF-7. Each box plot shows the median, and upper and lower quartiles. Outlier values are indicated by individual data points.
doi:10.1371/journal.pone.0047833.g003

while SPHK2 is overexpressed in MCF-7 and, therefore, an important regulator of sphingosine phosphorylation.

The degradation of sphingosine-1-phosphate (S1P) to phosphoethanolamine and (2E)-hexadecenal is mediated by S1P lyase. Western blot analysis revealed a weaker expression in MCF-7 than in MCF-12A (Fig. 5A). But after exposure with genistein and the flax extract the amounts of S1P lyase increased dramatically in MCF-7. Up to 4–5 fold higher levels were reached, especially after treatment with 10 µM genistein. Similar results were obtained in immunofluorescence staining experiments. The strongest fluorescence in MCF-7 cells was seen after exposure with 10 µM genistein which correlated with significant elevated enzyme levels in western blot (Fig. 5B). In the non-tumorigenic cell line MCF-12A we observed constant expression levels of S1P lyase after treatment with 17ß-estradiol and genistein while both concentrations of the flax extract increased the S1P lyase amount up to 30% (Fig. 5B). While most results were confirmed by immunofluorescence staining, no confirmation with the western blotting results was observed in experiments with 10 µM genistein and 1 µg/ml flax extract (Fig. 5B, C). These experiments suggests that Sphk2 and S1P lyase may be useful targets for cancer therapy drugs, as decreasing or increasing its expression during tumorigenesis may help to regulate cell proliferation.

Online Monitoring of Cellular Metabolism during Stimulation with Sphingolipids

To prove the influence of S1P and sphingosine on cell metabolism we used the Bionas® 2500 analyzing system and Bionas® metabolic chip SC1000 to monitor existing adhesion/impedance, O_2 consumption (respiration) and the extracellular acidification of living MCF-7 cells under the exposure of either 1 µM S1P or D-sphingosine (D-S) in the course of 24 hours (Fig. 6). The exposure with S1P reduced the adhesion in all three replicates up to 40%. The respiration was increased in all cases whereas the acidification rates are subject to large fluctuations and in two measurements was slightly increased. As expected the treatment with D-S revealed completely different results for these three parameters. Sphingosine itself is known for its apoptotic and anti-proliferative affects [13]. Treatment with D-S revealed a significant increase of cell impedance/adhesion in two cases, while the respiration rates were not influenced. The acidification rates were lowered in two cases. These online monitoring studies regarding three relevant parameters of cell metabolism are reflecting the influence of the sphingolipids on the estrogen-receptor positive breast cancer cell line MCF-7. Despite the fact that flow cytometry measurements of proliferation and apoptosis indicated for no great alteration after exposure with neither S1P nor D-sphingosine the more sensitive method with the Bionas system confirmed the contrary effects of both sphingolipids on MCF-7 cells. Exposure with S1P caused greater acidification rates in the surrounding medium, while D-sphingosine lowered these levels. Therefore, we concluded that energy production by glycolysis was reduced and less lactate was produced. Apparently higher acidification rates in cancer cells are primarily traced to the lactate production and secretion, primarily. It is known that higher fluxes through glycolysis and increased lactate production are associated with tumor progression even when oxygen levels are abundant [29]. In addition the boosted respiration rates after treatment with S1P were indicating higher energy production via oxidative phosphorylation in the TCA (citric acid cycle) cycle. Taken together S1P exposure caused higher glycolysis as well as TCA fluxes in MCF-7 and therefore increasing the energy production dramatically. Lowered impedance of MCF-7 cells after exposure with S1P does not consequently imply that cells lose their contacts to the surface but changing shape and a reduced formation of focal adhesion might explain that effect as well. Conversely, the opposite reactions are applying for the rising impedance after treatment with D-sphingosine.

Conclusions

Our metabolic profiling reveals members of the sphingolipid pathway as one of the main targets of estrogen and phytoestrogen action. A summary of the relationship between the three highlighted sphingolipids and their metabolic functions are shown in Fig. S4. The hormone 17ß-estradiol and the phytoestrogens execute contrasting reactions on the Sphks. While 17ß-estradiol

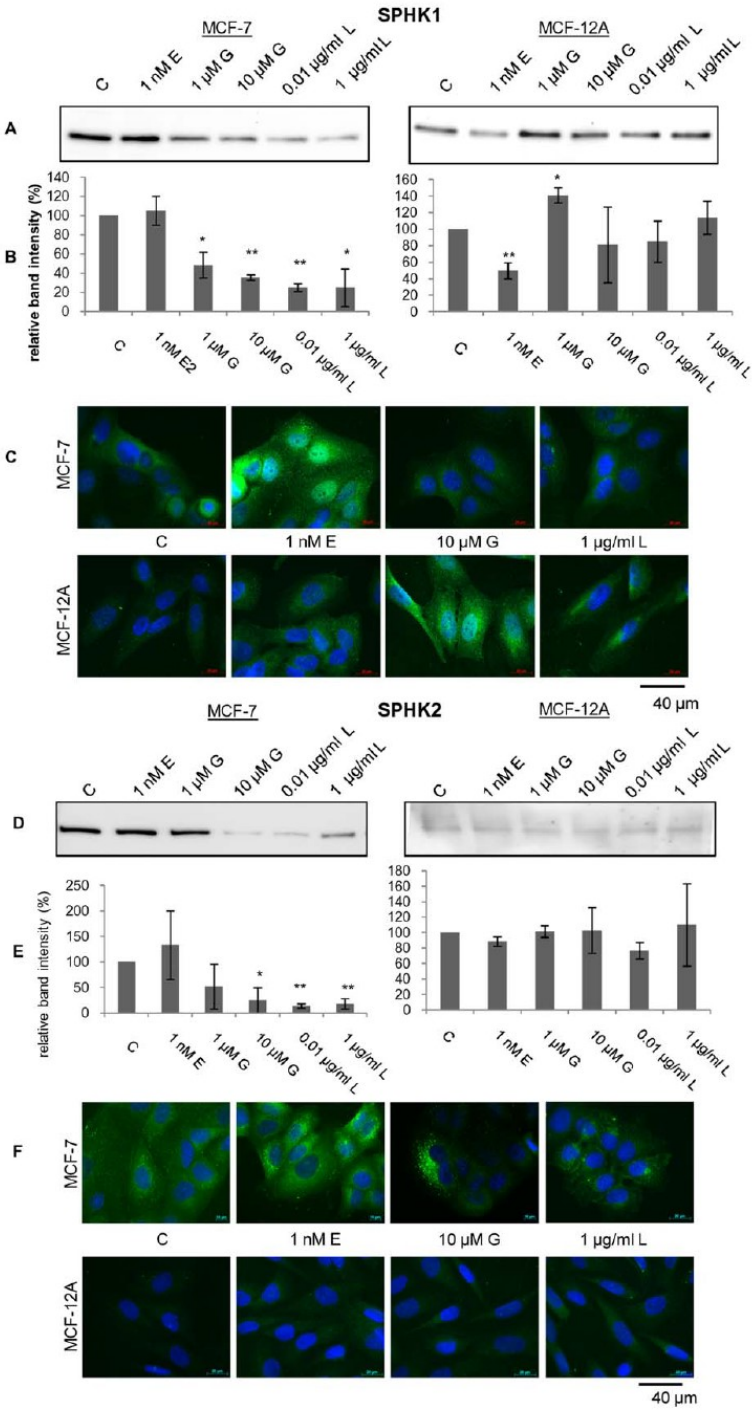

Figure 4. Expression regulation of Sphk1 and Sphk2. Western blotting (**A**, **D**), quantification of western blotting results (**B**, **E**) and immunofluorescence staining (**C**, **F**) of the sphingosine-1-phosphate kinase isoform 1 and 2 (Sphk1; Sphk2) expression level after 48 h exposure to 17ß-estradiol (E), genistein (G) and the root flax extract (L) at different concentration in the cell lines MCF-7 and MCF-12A. Western blotting and immunofluorescence staining were carried out with same primary antibody and were repeated at least three times with individual passaged cells.

Single representative western blot and fluorescence images were displayed. SPHK expression in the immunofluorescence pictures was taken with a constant exposure time of 5.6 s for Sphk1 and 2.0 s Sphk2 (green); nucleus (blue). Mean ± SD values (n = 3−5). * = $p<0.01$; ** = $p<0.001$ as compared to EtOH control (unpaired *t* test).
doi:10.1371/journal.pone.0047833.g004

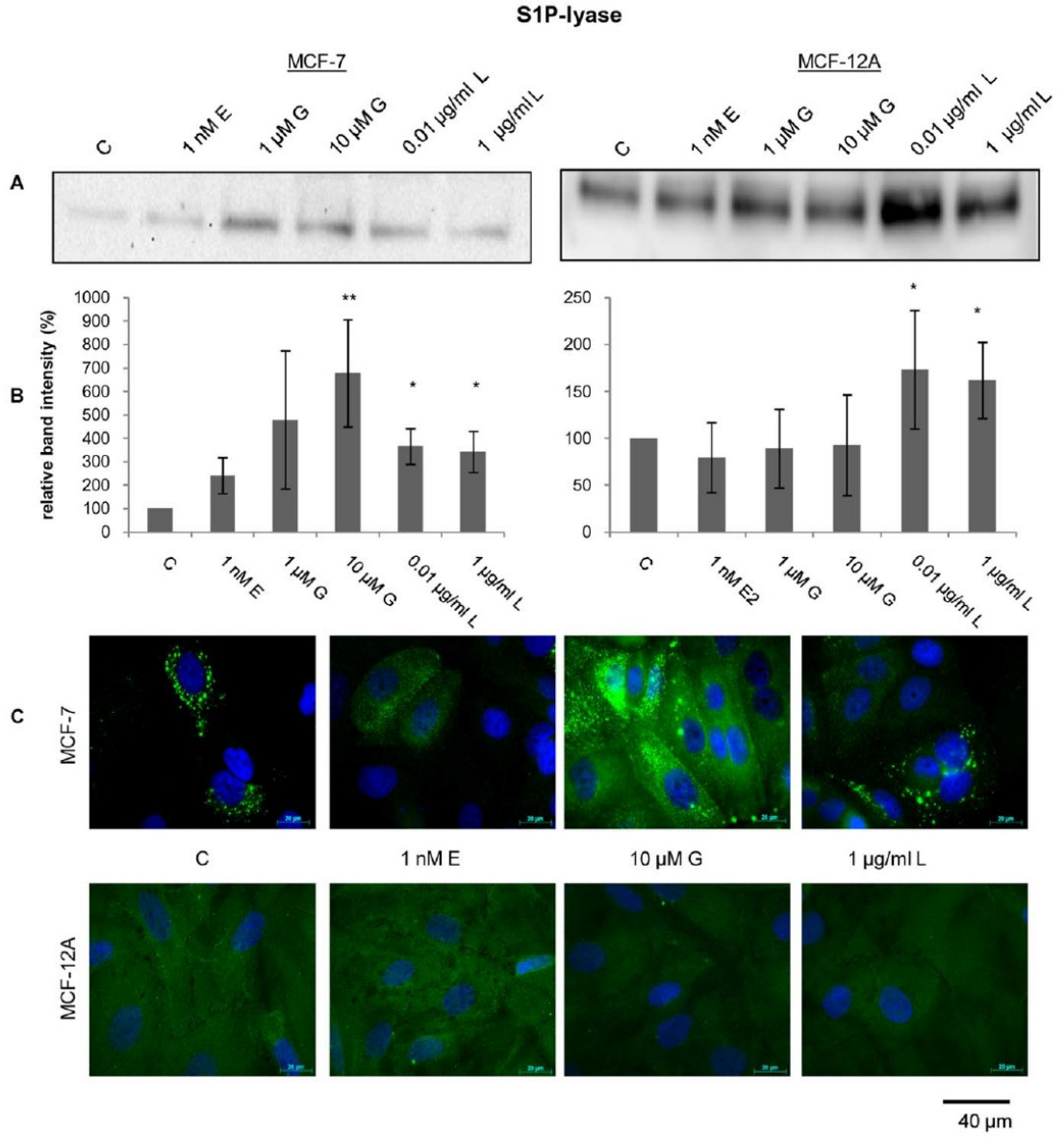

Figure 5. Expression regulation of Sphingosine lyase. Western blotting (**A**), quantification of western blotting results (**B**) and immunofluorescence staining (**C**) of the sphingosine-1-phosphate lyase (S1P lyase) expression level after 48 h exposure to 17ß-estradiol (E), genistein (G) and the root flax extract (L) at different concentration in the cell lines MCF-7 and MCF-12A. Western blotting and immunofluorescence staining were carried out with same primary antibody and were repeated at least three times with individual passaged cells. Single representative western blot and fluorescence images were displayed. S1P lyase expression in the immunofluorescence pictures was taken with a constant exposure time of 2.3 s. S1P lyase (green); nucleus (blue).Mean ± SD values (n = 3−5). * = $p<0.01$; ** = $p<0.001$ as compared to EtOH control (unpaired *t* test).
doi:10.1371/journal.pone.0047833.g005

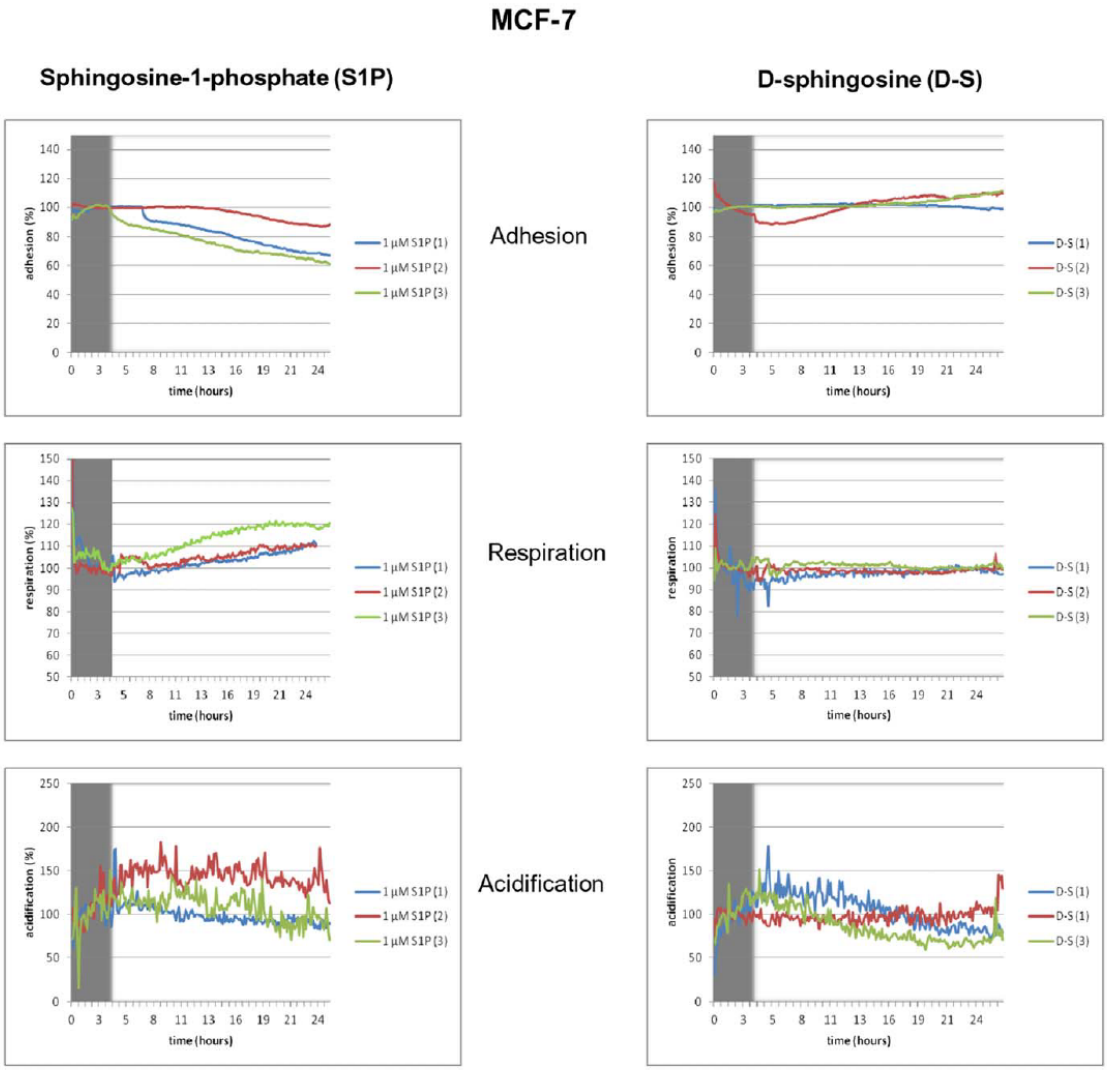

Figure 6. Online monitoring of cell metabolism. Online monitoring of cell metabolism in the cancerous cell line MCF-7 after exposure with 1 µM sphingosine-1-phosphate and 1 µM D-sphingosine. Displayed were the percentage of the standardized and normalized rates of cell adhesion (impedance), respiration (O_2 consumption) and extracellular acidification in a period of 24 h. Displayed were three individual replicates. Grey shadowed area marks the adaption phase (4 h) of the cells to the new conditions.
doi:10.1371/journal.pone.0047833.g006

increased the expression of Sphks in the cancerous cell lines MCF-7, the expression in non-tumorigenic cell line MCF-12A was lowered. The phytoestrogens react in the opposite way: higher expression in MCF-12A und significant decrease in MCF-7. This finding let us draw the conclusion that the exposure with phytoestrogens in higher concentration (genistein >10 µM; root flax extract >1 µg/ml) decreases tumor progression signaling via sphingolipids while normal tissue was not or positively stimulated. Furthermore, the degrading pathway of S1P to phosphoethanolamine by the reaction of the S1P lyase was primarily promoted by the addition of phytoestrogens in tumorigenic cell line MCF-7. The enhanced conversion to phosphoethanolamine could let to evaluated antitumor activity so that phytoestrogens have the ability to influence both, the enzymatic anabolic as well as the degrading step of S1P [31]. In addition, the expression of S1P lyase in the non-tumorigenic cell line MCF-12A was significantly up regulated under control conditions. It seems likely that normal mammary epithelial cells prevent extracellular S1P signaling by degrading this lipid before it reaches the receptors at the cell surface or the intracellular space, respectively [32]. Consequently, S1P lyase emerged as a possible target for anti-cancer research and production of effective chemotherapeutic agents.

Supporting Information

Figure S1 Histograms of Bonferroni corrected P-values obtained in a two way ANOVA with the factors genotype and treatment for absolute values of all 106 metabolic traits. The upper panel shows the number of P-values significant at $\alpha = 0.05$ for each factor and the interaction term, respectively, while the lower panel indicates the strength of the observed effects by presenting the data in log-scale. To this end, a comparable number of metabolic levels is significantly altered due to genotype or treatment, with genotypic effects showing generally lower P-values. However, this is partly due to the different number of levels for the factors (genotype: 2, treatment: 6).
(TIF)

Figure S2 Overview of all mentioned metabolite boxplots. Boxplots of all metabolites mentioned the ranking (Table 1) under the treatment of 17ß-estradiol (E), genistein (G) and flax extract (L) in the cell lines MCF-12A and MCF-7. Plot layout and colors are similar to Figure 3.
(TIF)

Figure S3 Sphingolipid pathway in detail. KEGG pathway of the sphingolipid metabolism in *Homo sapiens* (Entry no.: map00600) overlaid with boxplots of the detected metabolites.
(TIF)

Figure S4 Overview of cellular sphingosine-1-phosphate regulation. Scheme highlighting the relationship between regulation mechanisms of sphingosine metabolism in MCF-7 vs. MCF-12A.
(TIF)

Acknowledgments

We acknowledge the technical help of Petra Seidel, Dept. of Cell Biology, University of Rostock, Germany and Änne Eckardt, MPI-MP, Golm-Potsdam, Germany. We like to thank Lothar Willmitzer, MPI-MP, Golm-Potsdam, Germany for supporting this project and fruitful discussions.

Author Contributions

Conceived and designed the experiments: NEL JL. Performed the experiments: NEL JL. Analyzed the data: NEL, JL. Contributed reagents/materials/analysis tools: NEL JL BN BP. Wrote the paper: NEL JL BP BN. NE cultured cell lines, performed metabolic sample preparation, flow cytometry measurements, western blots, immunofluorescence staining, Bionas analysis, interpreted data and drafted the manuscript. JL performed metabolic profiling via GC-MS, statistical analysis, bioinformatics and contributed to the drafting manuscript. BP prepared and analyzed the fax extract. BP and BN critically revised the manuscript. All authors have read and approved the final manuscript.

References

1. Makiewicz L, Garey J, Adlercreutz H, Gurpide E (1993) In vitro bioassays of non-steroidal phytoestrogens. J Steroid Biochem Mol Biol 45: 399–405.
2. Hilakivi-Clarke L, Cabanes A, Olivo S, Kerr L, Bouker KB, et al. (2002) Do estrogens always increase breast cancer risk? J Steroid Biochem Mol Biol 80(2): 163–74.
3. Zava DT, Duwe G (1997) Estrogenic and antiproliferative properties of genistein and other flavonoids in human breast cancer cells in vitro. Nutr Cancer 27: 31–40.
4. Allred CD, Allred KF, Ju YH, Virant SM, Helferich WG (2001) Soy diets containing varying amounts of genistein stimulate growth of estrogen-dependent (MCF-7) tumors in a dose-dependent manner. Cancer Res 61: 5045–5050.
5. Pagliacci MC, Smacchia M, Migliorati G, Grignani F, Riccardi C, et al. (1994) Growth-inhibitory effects of the natural phyto-oestrogen genistein in MCF-7 human breast cancer cells. Eur J Cancer 30A: 1675–1682.
6. Satih S, Chalabi N, Rabiau N, Bosviel R, Fontana L, et al. (2010) Gene expression profiling of breast cancer cell lines in response to soy isoflavones using a pangenomic microarray approach. OMICS 14(3): 231–8.
7. Engel N, Oppermann C, Falodun A, Kragl U (2011) Proliferative effects of five traditional Nigerian medicinal plant extracts on human breast and bone cancer cell lines. J Ethnopharmacol 137(2): 1003–10.
8. Abarzua S, Szewczyk M, Gailus S, Richter DU, Ruth W, et al. (2007) Effects of phytoestrogen extracts from Linum usitatissimum on the Jeg3 human trophoblast tumour cell line. Anticancer Res 27(4A): 2053–8.
9. Abarzua S, Drechsler S, Fischer K, Pietschmann N, Stapel J, et al. (2010)Online monitoring of cellular metabolism in the MCF-7 carcinoma cell line treated with phytoestrogen extracts. Anticancer Res 30(5): 1587–92.
10. Borgan E, Sitter B, Lingjærde OC, Johnsen H, Lundgren S, et al. (2010) Merging transcriptomics and metabolomics–advances in breast cancer profiling. BMC Cancer 10: 628.
11. Schramm G, Surmann EM, Wiesberg S, Oswald M, Reinelt G, et al. (2010) Analyzing the regulation of metabolic pathways in human breast cancer. BMC Med Genomics 3: 39.
12. Pyne NJ, Pyne S (2010) Sphingosine 1-phosphate and cancer. Nat Rev Cancer 10(7): 489–503.
13. Pyne S, Bittman R, Pyne NJ (2011) Sphingosine kinase inhibitors and cancer: seeking the golden sword of hercules. Cancer Res 71(21): 6576–82.
14. Pitson SM (2010) Regulation of sphingosine kinase and sphingolipid signaling. Trends Biochem Sci 36(2): 97–107.
15. Long JS, Edwards J, Watson C, Tovey S, Mair KM, et al. (2010) Sphingosine kinase 1 induces tolerance to human epidermal growth factor receptor 2 and prevents formation of a migratory phenotype in response to sphingosine 1-phosphate in estrogen receptor-positive breast cancer cells. Mol Cell Biol 30(15): 3827–41.
16. Nebe B, Peters A, Duske K, Richter DU, Briese V (2006) Influence of Phytoestrogens on the proliferation and expression of adhesion receptors in human and epithelial cells in vitro. Eur J Cancer Prev 15(5): 405–15.
17. Lisec J, Schauer N, Kopka J, Willmitzer L, Fernie AR (2006) Gas chromatography mass spectrometry-based metabolite profiling in plants. Nat Protoc 1: 387–396
18. Cuadros-Inostroza A, Caldana C, Redestig H, Kusano M, Lisec J, et al. (2009) TargetSearch–a Bioconductor package for the efficient preprocessing of GC-MS metabolite profiling data. BMC Bioinformatics 16 10: 428.
19. Lisec J, Römisch-Margl L, Nikoloski Z, Piepho H.-P, Giavalisco P, et al. (2011) Corn hybrids display lower metabolite variability and complex metabolite inheritance patterns. Plant J 68(2): 326–336.
20. Bradford MM (1976) Rapid and sensitive method for the quantitation of microgram quantities of protein utilizing the principle of protein-dye binding. Anal Biochem 72: 248–54.
21. Meyer TS, Lamberts BL (1965) Use of Coomassie brilliant blue R250 for the electrophoresis of microgram quantities of parotid saliva proteins on acrylamide-gel strips. Biochim Biophys Acta 24;107(1): 144–5.
22. Thedinga E, Kob A, Holst H, Keuer A, Drechsler S, et al. (2007) Online monitoring of cell metabolism for studying pharmacodynamic effects. Toxicol Appl Pharmacol 220(1): 33–44.
23. Rebl H, Finke B, Schroeder K, Nebe JB (2010) Time-dependent metabolic activity and adhesion of human osteoblast-like cells on sensor chips with a plasma polymer nanolayer. Int J Artif Organs 33(10): 738–48.
24. Stacklies W, Redestig H, Scholz M, Walther D, Selbig J (2007) pcaMethods–a bioconductor package providing PCA methods for incomplete data. Bioinformatics 23(9): 1164–1167.
25. Wang C, Kurzer MS (1997) Phytoestrogen concentration determines effects on DNA synthesis in human breast cancer cells. Nutr Cancer 28(3): 236–47.
26. Wang TT, Sathyamoorthy N, Phang JM (1996) Molecular effects of genistein on estrogen receptor mediated pathways. Carcinogenesis 17(2): 271–5.
27. de Lemos ML. (2001) Effects of soy phytoestrogens genistein and daidzein on breast cancer growth. Ann Pharmacother 35(9): 1118–21.
28. Low YL, Taylor JI, Grace PB, Dowsett M, Scollen S, Dunning AM, et al. (2005) Phytoestrogen exposure correlation with plasma estradiol in postmenopausal women in European Prospective Investigation of Cancer and Nutrition-Norfolk may involve diet-gene interactions. Cancer Epidemiol Biomarkers Prev 14(1): 213–20.
29. Kaelin WG Jr, Thompson CB (2010) Q&A: Cancer: clues from cell metabolism. Nature 465(7298): 562–4.
30. Levine AJ, Puzio-Kuter AM (2010) The control of the metabolic switch in cancers by oncogenes and tumor suppressor genes. Science 330(6009): 1340–4.
31. Ferreira AK, Meneguelo R, Neto SC, Chierice GO, Maria DA (2011) Synthetic Phosphoethanolamine Induces Apoptosis Through Caspase-3 Pathway by Decreasing Expression of Bax/Bad Protein and Changes Cell Cycle in Melanoma. J Cancer Sci Ther 3: 053–059.
32. Tani M, Ito M, Igarashi Y (2007) Ceramide/sphingosine/sphingosine 1-phosphate metabolism on the cell surface and in the extracellular space. Cell Signal 19(2): 229–37.

Referenz V

Engel N*, Adamus A, Schauer N, Kühn J, Nebe B, Kraft K. Synergistic action of genistein and calcitriol in immature osteosarcoma MG-63 cells by SGPL1 up-regulation. PLoS ONE. 2017. doi: 10.1371/journal.pone.0169742.

NCBI-Link: https://www.ncbi.nlm.nih.gov/pubmed/28125641

Zusammenfassung:

Erste *in vitro* Untersuchungen belegten, dass die simultane Applikation von Genistein und Vitamin D3 die Proliferationsinduktion bei der Osteosarkomzelllinie MG-63 auf Normalniveau relativieren kann. Ebenso wurde die extrazelluläre Ansäuerung und die Respirationsrate durch eine gleichzeitige Stimulation mit beiden Substanzen additiv bzw. synergistisch reduziert. Um die dafür grundlegenden zellulären Mechanismen zu untersuchen, wurden abermals metabolische Profile mittels Metabolomics angefertigt. Analog zu den Ergebsnissen mit den Brustkrebszelllinien wurde auch bei den Osteosarkomzellen eine signifikante Beeinflussung des Sphingosin-Stoffwechsels ermittelt, die sich in einer signifikant gesteigerten Ethanolamin-Produktion darstellte. Die Sphingosin-1-Phospat-abbauende Lyase (SGPL1) wurde durch die simultane Applikation von Genistein und Vitamin D3 um das 3,5-fache gesteigert (Abb. 7). Diese Untersuchungen belegen erstmals die Synergie von Genistein und Vitamin D3 auf das Expressionsniveau der SGPL1 und deuten darauf hin, dass die SGPL1-Expression vermutlich bei vielen Tumorentitäten im Rahmen der Tumorigensese eine fundamentale Rolle spielt.

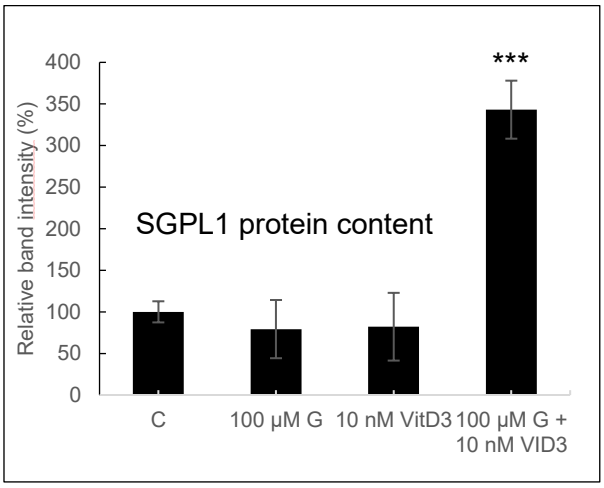

*Abb. 7 Proteinexpressionsanalyse des SGPL1-Gehaltes in der Osteosarkomzelllinie MG-63 nach der Inkubation mit 1, 10, 100 µM Genistein (G), 10 nM Calcitriol (VitD3) und deren Kombination (G +VitD3) im Vergleich zur Kontrolle (C). Mittelwert ± Standardabweichung, n= 3, *** = p < 0.001 im Vergleich zur Kontrolle (ungepaarter t test).*

PLOS ONE

RESEARCH ARTICLE

Synergistic Action of Genistein and Calcitriol in Immature Osteosarcoma MG-63 Cells by SGPL1 Up-Regulation

Nadja Engel[1,2]*, Anna Adamus[1,2], Nicolas Schauer[3], Juliane Kühn[2], Barbara Nebe[2], Guido Seitz[1], Karin Kraft[4]

1 Department of Pediatric Surgery, University Hospital Marburg, Baldingerstraße, Marburg, Germany, 2 Department of Cell Biology, Rostock University Medical Center, Schillingallee, Rostock, Germany, 3 Metabolomic Discoveries GmbH, Am Mühlenberg, Potsdam-Golm, Germany, 4 Complementary Medicine, Center of Internal Medicine, Rostock University Medical Center, Ernst-Heydemann-Straße 6, Rostock, Germany

* nadja.engel-lutz@gmx.de, nadja.engellutz@staff.uni-marburg.de

Citation: Engel N, Adamus A, Schauer N, Kühn J, Nebe B, Seitz G, et al. (2017) Synergistic Action of Genistein and Calcitriol in Immature Osteosarcoma MG-63 Cells by SGPL1 Up-Regulation. PLoS ONE 12(1): e0169742. doi:10.1371/journal.pone.0169742

Editor: Dragana Nikitovic-Tzanakaki, University of Crete, GREECE

Received: March 17, 2016

Accepted: December 21, 2016

Published: January 26, 2017

Data Availability Statement: All relevant data are within the paper and its Supporting Information files.

Funding: This work is supported by fund from Federal Ministry of Education and Research Germany (Women Professors Program) and FORUN program of the University Medical Center Rostock (no. 889025). Women Professors Program provided the salary for author [NE]. Metabolomic Discoveries GmbH, a commercial company, provided support by measuring the

Abstract

Background

Phytoestrogens such as genistein, the most prominent isoflavone from soy, show concentration-dependent anti-estrogenic or estrogenic effects. High genistein concentrations (>10 μM) also promote proliferation of bone cancer cells *in vitro*. On the other hand, the most active component of the vitamin D family, calcitriol, has been shown to be tumor protective *in vitro* and *in vivo*. The purpose of this study was to examine a putative synergism of genistein and calcitriol in two osteosarcoma cell lines MG-63 (early osteoblast), Saos-2 (mature osteoblast) and primary osteoblasts.

Methods

Thus, an initial screening based on cell cycle phase alterations, estrogen (ER) and vitamin D receptor (VDR) expression, live cell metabolic monitoring, and metabolomics were performed.

Results

Exposure to the combination of 100 μM genistein and 10 nM calcitriol reduced the number of proliferative cells to control levels, increased ERß and VDR expression, and reduced extracellular acidification (40%) as well as respiratory activity (70%), primarily in MG-63 cells. In order to identify the underlying cellular mechanisms in the MG-63 cell line, metabolic profiling via GC/MS technology was conducted. Combined treatment significantly influenced lipids and amino acids preferably, whereas metabolites of the energy metabolism were not altered. The comparative analysis of the log2-ratios revealed that after combined treatment only the metabolite ethanolamine was highly up-regulated. This is the result: a strong overexpression (350%) of the enzyme sphingosine-1-phosphate lyase (SGPL1), which irreversibly degrades sphingosine-1-phosphate (S1P), thereby, generating ethanolamine. S1P

metabolomics samples, but did not have any additional role in the study design, data collection and analysis, decision to publish, or preparation of the manuscript. The specific roles of these authors are articulated in the 'author contributions' section.

Competing Interests: There are no patents, products in development or marketed products to declare. This does not alter our adherence to PLOS ONE policies on sharing data and materials.

production and secretion is associated with an increased capability of migration and invasion of cancer cells.

Conclusion

From these results can be concluded that the tumor promoting effect of high concentrations of genistein in immature osteosarcoma cells is reduced by the co-administration of calcitriol, primarily by the breakdown of S1P. It should be tested whether this anti-metastatic pathway can be stimulated by combined treatment also in metastatic xenograft mice models.

Background

Phytoestrogens, e.g. the well investigated isoflavone genistein are able to prevent and to reduce the development of breast cancer *in vitro* and *in vivo* [1, 2]. This effect is due to structural similarities to the endogenous steroid hormone 17ß-estradiol, whereby they can trigger both estrogenic and antiestrogenic effects via binding to the estrogen receptors ERα and/or ERß [3]. This finding has led to intense discussions on the safety of phytoestrogens. *In vitro* as well as *in vivo* studies have demonstrated that genistein enhanced the proliferation of estrogen-dependent human breast cancer cells (MCF-7) already at low concentrations (10 nM), 100 nM achieved proliferative effects similar to those of 1 nM estradiol [4, 5]. However, high concentrations beyond 10 μM inhibited cell proliferation and induced apoptosis of estrogen-sensitive breast cancer cells, most likely by inhibiting the intrinsic tyrosine kinase activity of growth factor receptors [6]. Furthermore, high concentrations of genistein and other soy isoflavones stimulate growth of bone and metastatic breast cancer [7–9]. Due to these effects, isolated phytoestrogens are not recommended for dietary consumption in the case of breast and bone tumors, detected previously.

Despite recent advances in treatment of breast cancer, still substantial numbers of patients develop metastatic disease, especially in the bones up to 70% [10]. Breast cancer is the most common source of bone metastasis which is often characterized by an estrogen-positive phenotype: 65% of the lesions are lytic, 10% are blastic, and 25% consist of both lytic and blastic lesions.

The most biologically active hormonal form of vitamin D3, calcitriol (1α,25$(OH)_2$Vitamin D_3), is synthesized endogenously by a series of reactions, starting with UVB radiation on human skin, and followed by stepwise hydroxylation in liver and kidney. Potential vitamin D target tissues (e.g. colon, prostate, breast, lung, pancreas) can also synthesize and degrade calcitriol. Local production and degradation of calcitriol have been suggested to represent a key factor in several types of human cancer. The function of the vitamin D complex for human body and health is widespread, from effects on cellular differentiation and proliferation and on central nervous system up to the modulation of immune responsiveness [11]. *In vivo* the results are less convincing, often conflicting and show considerable variability [11]. However, the results of *in vivo* studies suggest that the calcitriol precursor cholecalciferol could act as a chemopreventive agent against several malignancies, as an association between low serum levels of the calcitriol precursor calcidiol (25(OH)D) and an increased incidence and mortality of several types of tumors such as non-Hodgkin's lymphoma, melanoma, breast, prostate, colorectal, ovarian, kidney, esophagus, and stomach cancer was confirmed [12–14]. Recently, Keum and Giovannucci [15] have published that supplementation with cholecalciferol at doses of up to 800 IU per day presumably has no substantial effect on cancer incidence within 2–7 years, but is related to a statistically significant 12% reduction in cancer mortality.

Up to now only few studies on the effects of the combination of phytoestrogens with calcitriol have been published. Swami et al. [16] showed that genistein potentiates the action of calcitriol in human prostate cancer cells, and Rao et al. [17] demonstrated that these substances synergistically inhibit the growth of human prostatic epithelial cells. This was achieved by two related important mechanisms: 1) by directly inhibiting CYP24A1 enzyme activity, leading to an increase in the half-life of calcitriol (adults 5–8 h, children 27 h), and 2) by amplifying the homologous up-regulation of the vitamin D receptor (VDR) [18]. However, to our knowledge there are no reports on the effects of a combination of calcitriol and genistein on bone cancer cells. This is of interest, because a synergistic action of both substances is involved in the prevention of osteoporosis and the reduction of hip fracture risk in postmenopausal women [19]. Therefore, we hypothesize that genistein in the presence of calcitriol mediates synergistic antitumor activity in human bone cancer cells by distinct cell biological mechanisms. In the present study these hypotheses were elucidated by focusing on cell cycle analysis, metabolic alterations and signaling cascades.

Material and Methods

Chemicals

Genistein (4′,5,7-Trihydroxyisoflavone) and calcitriol (1α,25-Dihydroxycholecalciferol) were purchased from Sigma Aldrich (Germany) were stored at -20˚C in the dark as single-used aliquots of concentrated stock solutions in dimethylsulfoxide (DMSO, for genistein) or ethanol (EtOH, for calcitriol).

Cell culture conditions

The osteosarcoma cell lines MG-63 (ATCC® CRL-1427™) and Saos-2 (ATCC® HTB-85™) were obtained from the American Type Culture Collection (ATCC, Manassas, VA, USA). The human non-tumorigenic, primary osteoblast cells (POB) were chosen as control cells. Briefly, the primary osteoblast cells were isolated from the spongiosa of the femoral heads of patients undergoing primary total hip replacement. The samples were collected with patient agreement and approval by the Local Ethical Committee named "Ethikkommission an der Medizinischen Fakultät der Universität Rostock", located at St.-Georg-Str. 108, 18055 Rostock, Germany with the registration number: A 2010–10 (see: https://ethik.med.uni-rostock.de/). The participants provide their written consent to participate in this study.

All cells were grown in Dulbecco's modified Eagle's medium (Invitrogen, Germany) with 10% fetal bovine serum (PAN Biotech GmbH, Germany) and 1% gentamycin (Ratiopharm, Germany). Application of genistein (final concentrations: 1, 10, 100 μM) and/or calcitriol (10 nM) was carried out in assay medium: phenol-red-free Dulbecco's modified Eagle's medium (PAA Laboratories GmbH, Germany) with 10% charcoal stripped fetal bovine serum (PAN Biotech GmbH, Germany) for 48 h. Prior treatment cells were adapted to the assay medium for 24 h.

Cell cycle analysis

Cell preparation and cell cycle analysis have been described in detail previously (Engel et al., 2012, 2014). Cells in the cell cycle phases S and G2/M were summarized and defined as proliferative cells. Briefly, the extent of cell cycle progression and apoptosis in the cells was estimated by flow cytometric analysis after propidium iodide (Roche Diagnostics, IN, USA) staining. After treatment cells were trypsinized with 0.05% trypsin–0.02% EDTA for 5–10 min. The reaction was stopped with assay medium. Cells suspension was transferred to FACS tubes (BD

Biosciences, USA) and fixed in 70% ethanol for 12 or more hours at −20˚C. Briefly, after washing with PBS cells were incubated with RNase (1 mg/ml) at 37˚C for 30 min. Finally, cells were re-suspended in propidium iodide (50 mg/ml) for at least 3 h at +2 to +8˚C protected from light until flow-cytometric analysis. The software FlowJo version 10.0.5 (Tree Star Inc., USA) was used for data acquisition.

Live cell metabolism

The live cell metabolic parameters cell impedance, oxygen consumption (respiration), and extracellular acidification were analyzed during stimulation with genistein and/or calcitriol for 24 h with the Bionas Discovery™ 2500 system and the metabolic chip SC 1000 (Bionas GmbH, Rostock, Germany). Measurement conditions were already described [5]. Data sets were normalized to vehicle control treatment and set to 100% using the software Bionas1500[2] Data analyzerV1.07.

Immunofluorescence

The basic procedure for the immunofluorescence staining was described in Engel et al. (2012, 2014). Briefly, the rabbit anti-human estrogen receptor antibodies (ERα: sc-542, ERß: sc-8974), and the VDR (sc-13133, SGPL1: sc-67368), all from Santa Cruz, USA, were applied in a 1:50 dilution for 1 h at room temperature followed by the incubation of 488-labeled secondary goat anti-rabbit antibody (Molecular Probes, USA, 1:100) for 1 h at room temperature in the dark. Nuclei were counterstained with DAPI (Roche Diagnostics GmbH, Germany) for 15 min. Visualization and imaging was investigated with an inverted confocal laser scanning microscope (LSM780, Carl Zeiss, Germany) equipped with a helium/neon-ion laser and a ZEISS 63× oil immersion objective. Notably, photomicrographs stained with the same primary antibody were taken at identical exposure times and laser power to guarantee comparable results.

Western blot

General western blotting procedure using previously described protocols is illustrated in Warsow et al. and Engel et al. [20,21]. The following primary antibodies were used: Hexokinase I (C35C4) Rabbit mAb: #2024; PFKP (D4B2) Rabbit mAb: #8164; LDHA (C4B5) Rabbit mAb: #3582; PDH Pyruvate Dehydrogenase (C54G1) Rabbit: mAb #3205; Fumarase (D9C5) Rabbit mAb: #4567; SDHA (D6J9M) XP® Rabbit mAb: #11998; p-Akt (S473): 9271S; Akt (pan) (C67E7): 4691S; P-p44/42 MAPK (T202/Y204) (D13.14.4E) XP (R): 4370L; p44/42 MAPK (Erk1/2): 9102 (all from cell signaling, USA); and SGPL1: sc-67368, ER alpha (MC-20): sc-542; ER beta (H-150): sc-8974; VDR (D-6): sc-13133; PCNA (PC10): sc-56; beta-Actin (C4): sc-47778; Vinculin (G-11): sc-55465, from Santa Cruz, USA. They were incubated with gentle shaking at 4˚C overnight in a dilution of 1:1000. Secondary antibody (Anti-rabbit or anti-mouse IgG, HRP-linked Antibody #7074 or #7076, from cell signaling, USA) was incubated at room temperature for 1 h. To ensure equal amounts of loaded total soluble proteins on Mini-PROTEAN® TGX Stain-Free™ gels (Bio-Rad, Germany), the band intensities were visualized and calculated by stain-free technology via a ChemiDoc™ MP imager (Bio-Rad, Germany). Normalization and calculation were performed with Image Lab 3.0.1 (Bio-Rad, Germany). Protein signals were visualized by using SuperSignal West Femto Chemiluminescent Substrate (Pierce Biotechnology, Rockford, USA) for detection of peroxidase activity from HRP-conjugated antibodies (Thermo Fisher Scientific Inc., Rockford, USA). Band intensity was analyzed densitometrically with the Molecular Imager ChemiDoc XRS and Image Lab 3.0.1 software (Bio-Rad, USA). Protein detection was repeated at least three to five times with individually prepared cell lysates from independently passaged cells.

Phosphorylation status of signaling proteins

Phosphorylated proteins (Phosph-ERK1/2 (T202/Y204, T185/Y187); No. 5016616, Phospho-Akt (S473); No. 5017459, Phospho-p38 MAPK (T189/Y182); No. 5017183, and Bio-Plex® Phosphoprotein Detection Reagent Kit; No. 310013270, all from Bio-Rad, Germany) were analyzed with the Bio-Plex 200 Array System with Bio-Plex™ Manager 4.1.1. software (Bio-Rad, Germany) according to the manufacturer's recommendations. Total protein lysates (10 μg soluble protein) were prepared with cell lysis kit from Bio-Rad, Germany. Protein lysates were incubated overnight in 96-well plates with fluorescent capturing beads. Then, plates were washed and incubated with biotinylated antibodies against the phosphorylated proteins and final added streptavidin-phycoerythrin solution. The measurement of phosphorylated proteins was performed with the relative mean fluorescence intensity calculated excluding the blank (approach without protein lysates) (n = 3).

Metabolic profiling via GC-MS

Sample preparation was carried out according to the cell sampling protocol of mammalian adherent cells of Metabolomic Discoveries GmbH (Potsdam, Germany). Briefly, approximately 1 x 10^7 cells adherent MG-63 cell were cultivated and treated with the vehicle control, genistein and/or calcitriol in T25 flasks (Greiner, Germany). After 48 h treatment flasks were put on ice, washed three times with ice-cold 0.9% (w/v) NaCl solution (saline) and thereafter cells were quenched with 500 μl ice-cold extraction buffer containing 80% methanol and removed from the flasks with the help of a cell scraper. Additional 500 μl extraction buffer were used to remove all cell remnants. Cell suspension was filled in cryo tubes and shock-frozen in liquid nitrogen. Samples were stored at -80˚C until metabolic measurement. All subsequent steps were carried out at Metabolomic Discoveries GmbH (Potsdam, Germany; www.metabolomicdiscoveries.com)

300 μl of cell extract were used for global metabolite profiling analysis. Derivatization and analyses of metabolites by a GC-MS 7890A mass spectrometer (Agilent, Santa Clara, USA) were carried out as described [22]. Metabolites were identified in comparison to Metabolomic Discoveries' database entries of authentic standards. LC-MS analysis was performed using hydrophilic interaction chromatography with a ZIC-HILIC 3.5 μm, 200 A column (Merck Sequant, Umeå, Sweden), operated by an Agilent 1290 UPLC system (Agilent, Santa Clara, USA). The LC mobile phase was a linear gradient from 90% to 70% acetonitrile over 15 min, followed by linear gradient from 70% to 10% acetonitrile over 1 min, 3 min wash with 10% and 3 min reequilibration with 90% acetonitrile. The flow rate was 400 μl/min, injection volume 1 μl. Mass spectrometry was performed using a 6540 QTOF/MS detector (Agilent, Santa Clara, USA). The measured metabolite concentration was normalized to the internal standard C13-Sorbitol.

Characterization of osteoblastic phenotypes

Alkaline phosphatase (ALP) specific activity was used as an early marker of the osteoblastic phenotype. Therefore, cells were washed in PBS and fixed in 4% paraformaldehyde for 5 min. After washing, cells were incubated with 0.1% naphthol AS-MX phosphate and 0.1% fast red violet LB salt in a 2-amino-2-methyl-1,3-propanediol buffer (56 mM) for 10 min. Alizarin red S staining to visualize calcification was performed according to manufacturer's protocol (Osteogenesis assay kit, #ECM815, Millipore). Matrix mineralization was determined by immunofluorescence labeling with anti-osteocalcin (#AB10911, Millipore). As secondary antibody Alexa 488-labeled secondary goat anti-rabbit antibody (Molecular Probes, USA, 1:100) was used. After staining cells were counterstained with DAPI (Roche Diagnostics GmbH, Germany) for 15 min.

Statistical analysis

All experiments were replicated at least three times with individually passaged cells, and data sets were expressed as means ± standard deviations (SD). Statistical significance was determined by the unpaired student's *t*-test (*** $P<0.001$; ** $P<0.01$; * $P<0.05$). Significant concentration changes of metabolites in different samples were analyzed by appropriate statistical test procedures using the statistical analysis software R-project (www.r-project.org). Results of drug combination experiments (cell proliferation, receptor expression, metabolic alterations, SGPL1 expression) were analyzed for synergistic, additive, or antagonistic effects using primarily the coefficient of drug interaction (CDI) by the method of Chou-Talalay [23]. CDI calculations were done in custom Microsoft Excel templates as follows: CDI = AB/(A6B). According to the measurement values of each group, AB is the ratio of the combination groups to control group; A or B is the ratio of the single agent group to control group. Thus, CDI < 1, CDI = 1, and CDI > 1 indicate synergism, additive effects, and antagonism, respectively.

Results

Characterization of osteoblastic features

For analysis of putative synergistic effects of genistein and calcitriol on bone cancer cells, two tumorigenic osteosarcoma cell lines (MG-63, Saos-2) were compared to non-tumorigenic primary osteoblasts, isolated from patients' cancellous bones (POB). MG-63 represents an early osteoblastic linage characterized by low alkaline phosphatase (ALP) activity and osteocalcin expression, while calcification, determined by Alizarin red staining, was comparable with Saos-2 cells (S1 Fig). In contrast, Saos-2 cells revealed the most mature osteoblastic profile: high ALP activity, calcification and mineralization rates. POBs exhibit the lowest osteoblastic differentiation levels identified by poor rates of ALP activity, calcification and mineralization.

Calcitriol normalizes genistein induced proliferation promotion

Initially, the influence on cell proliferation after 48 h exposure to 10 nM calcitriol and a concentration series of genistein (1, 10, 100 μM), either separately or in combination, was tested via cell cycle analysis (Fig 1). Cells in the cell cycle phases G2/M and S were summed and marked as proliferative cells. The addition of 10 nM calcitriol reduced the proliferation of MG-63 (~ 60% reduction) and Saos-2 (~ 10% reduction) osteosarcoma cells. Treatment with 100 μM genistein only revealed significant proliferation induction in MG-63 (~ 130% induction) and Saos-2 (~ 14% induction) cells. After combined application of 100 μM genistein and 10 nM calcitriol proliferation was not different from untreated controls. This effect is particularly pronounced in MG-63 cells. Proliferation of POBs was not significantly altered after exposure to genistein, calcitriol or their combination, after treatment with genistein alone a trend towards slight proliferation induction was noted.

Overexpression of ERß and VDR after combined treatment

The cellular reactions to genistein are mediated by estrogen receptors (ERα, ERß), and calcitriol signaling is implemented by the VDR, functioning as hormone response elements on DNA resulting in expression or repression of specific gene products. Therefore, expression levels and cellular distribution of these three receptors were determined by immunofluorescence staining (Fig 2A) and Western blotting (Fig 2B). In MG-63, the combination of 100 μM genistein and 10 nM calcitriol caused significantly higher cytoplasmic expression levels of ERß as well as lower of ERα, visible in the immunofluorescence staining as well as in the western blot. While higher VDR expression in MG-63 was clearly visible by the increased fluorescence

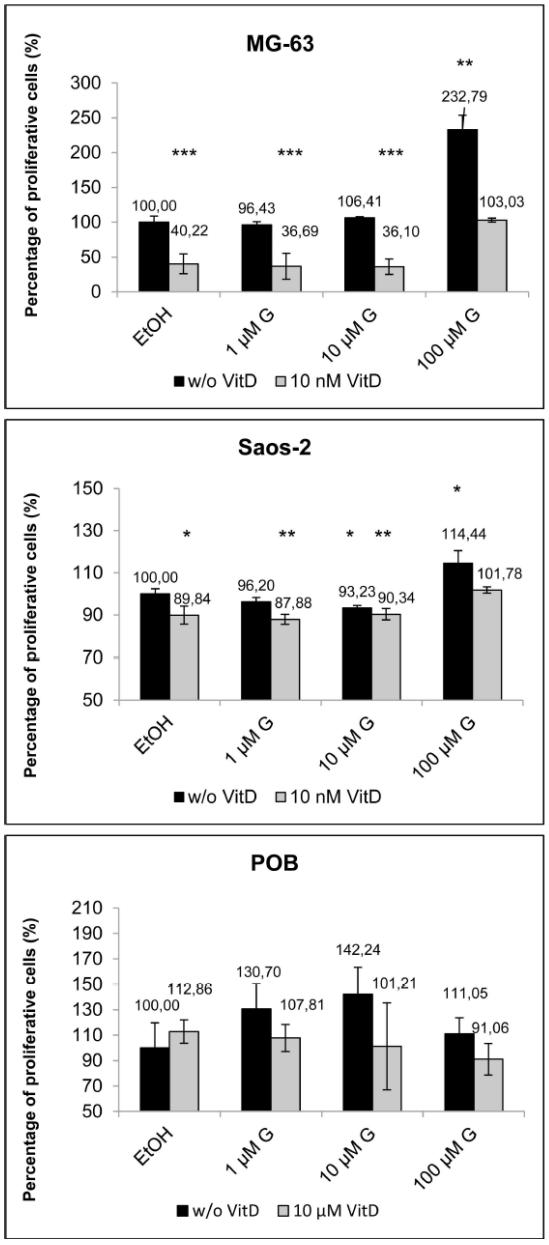

Fig 1. Cell cycle analysis of MG-63, Saos-2 bone cancer cells in comparison with primary osteoblasts (POB) after 48 h treatment with genistein (G; 1, 10, 100 µM; black bars) or in combination with 10 nM calcitriol (VitD; grey bars). Given is the percentage of proliferative cells (G2/M + S phase) whereby the control was set to 100%. Note that 100 µM genistein induces a strong proliferation induction in MG-63 cells

which could be normalized to control levels by the addition of 10 nM calcitriol. Mean ± SD, n = 5, ***P < 0.001, **P < 0.01, *P < 0.5, significantly different compared to control, unpaired *t*-test.

doi:10.1371/journal.pone.0169742.g001

intensity, western blotting results only showed an increase of VDR after treatment with calcitrol. In the mature osteosarcoma cell line Saos-2 as well as in POBs only a slight increase of ERß expression was shown after simultaneous application. In summary, only the simultaneous application of genistein and calcitriol increased the ERß level in MG-63, primarily. This was the first hint, that combined treatment could reduce tumor progression in immature osteosarcoma cells.

Synergistic influence on extracellular acidification and respiration

In order to elucidate this combinatory effects of genistein and calcitriol, metabolic real-time measurements were performed on MG-63 cells for 24 h (Fig 3). The Bionas Discovery^{TM} 2500 system and the metabolic chip SC 1000 enables an online monitoring of three cellular metabolic parameters: extracellular acidification (which is a measure of glycolytic flux in cancer cells), oxygen consumption (a measure of mitochondrial respiration), and cell impedance (a measure of cell adhesion, confluence and morphological alterations). Before treatment with genistein (100 μM), calcitriol (10 nM) or their combination, cells were adapted to the measuring conditions for 2–3 h until constant levels were achieved. The vehicle control values after adaption to the measuring medium were normalized and set to 100%. Extracellular acidification levels showed no alterations after exposure to genistein, a 20% reduction after treatment with calcitriol, and an additive reduction of 40% after combined treatment. A synergistic effect in respiratory levels could be observed after combinatory treatment with a reduction up to 80%. Cell impedance did not alter after any treatment. From this live cell monitoring could be concluded that MG-63 respiration and to a lower extent the glycolysis responded to the combinatory treatment of genistein and calcitriol. Therefore, expression studies of key enzymes of the glycolytic and respiratory pathways, important for cancer progression were conducted (S2 Fig). Protein expression levels of three glycolytic enzymes (hexokinase 1, PFKP: platelet-type phosphofructokinase, LDH: lactate dehydrogenase) and three enzymes of the Krebs cycle (PDH: pyruvate dehydrogenase, fumarase, SHDA: succinate dehydrogenase subunit A) after 48 h exposure to a concentration series of genistein only (1, 10, 100 μM; left panel) or a combined treatment with 10 nM calcitriol (right panel) in MG-63 cells were detected. The protein contents of these six metabolic enzymes changed only slightly (S2 Fig). But these slight alterations in enzyme content did not explain a reduction in respiration of 80% and in glycolysis of 40%. In order to identify the main trigger of the additive or synergistic action of genistein and calcitriol, metabolomic profiling in MG-63 cells was performed after 48 h exposure to the compounds.

Synergistically elevated production of (phospho-) ethanolamine after combined treatment in MG-63 cells

On the basis of the proliferation results (Fig 1) and the live cell metabolic analysis (Fig 3) we decided to use the high concentrations of 100 μM genistein and 10 nM calcitriol for the following metabolomic profiling experiments. Four treatment groups were created: A: untreated control, B: treated with 100 μM genistein, C: treated with 10 nM calcitriol, D: treatment with both 100 μM genistein and 10 nM calcitriol. Subsequently to sample preparation, 186 metabolites were identified in this comprehensive analysis based on retention times, characteristic ions and mass spectra, comprising mainly amino acids, organic acids and lipids. To provide an

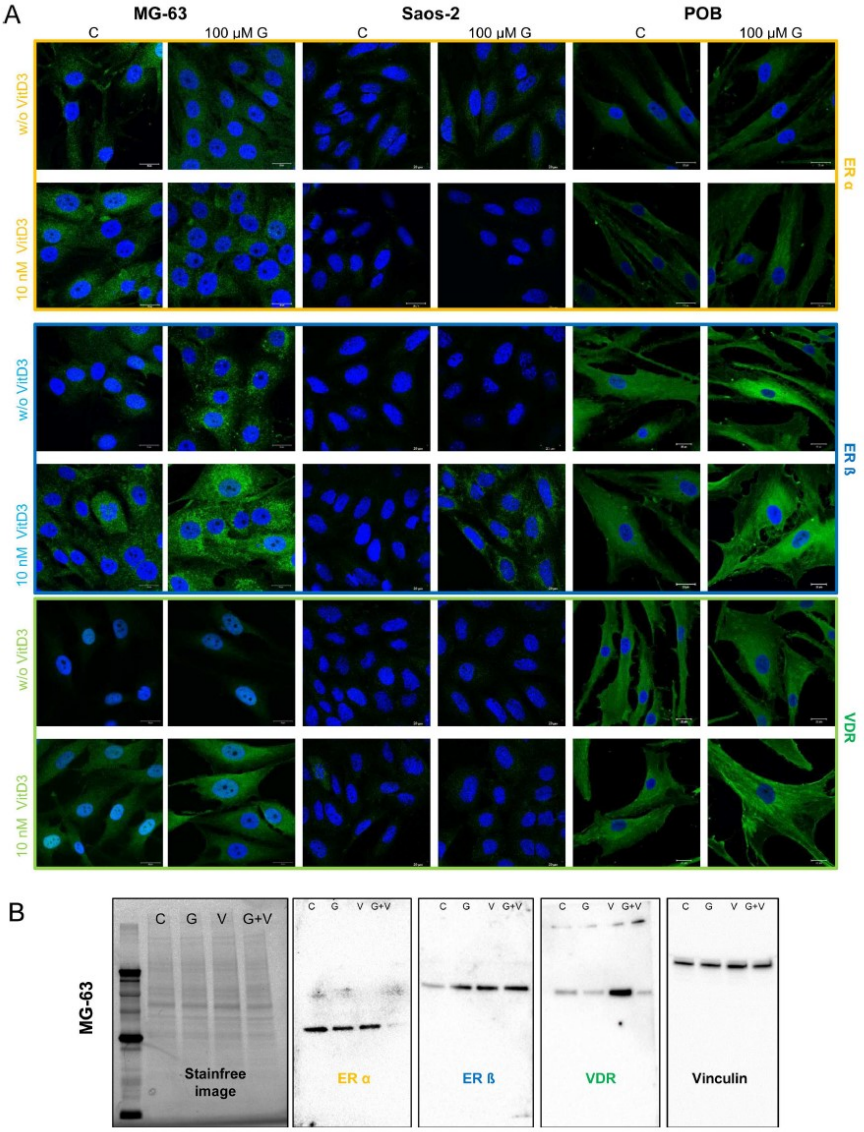

Fig 2. Immunofluorescence staining of ERα, ERß, and VDR in MG-63, Saos-2 and primary osteoblasts (POB) after 48 h exposure to the vehicle control (C), 100 µM genistein (G), 10 nM calcitriol (VitD3) or the simultaneous application of genistein and calcitriol. Receptor expression was secondarily labeled with Alexa488 (green). All samples were counterstained with DAPI to label the cell nucleus (blue). ERß and VDR expression is highly increased in MG-63 and POB cells after combined treatment with genistein and calcitriol. n = 3.

doi:10.1371/journal.pone.0169742.g002

initial overview of all analyzed samples, a principal component analysis (PCA) was calculated (S3 Fig). The PCA depicts 57.8% (46.6% + 11.2%) of all variances in this sample set. PC1

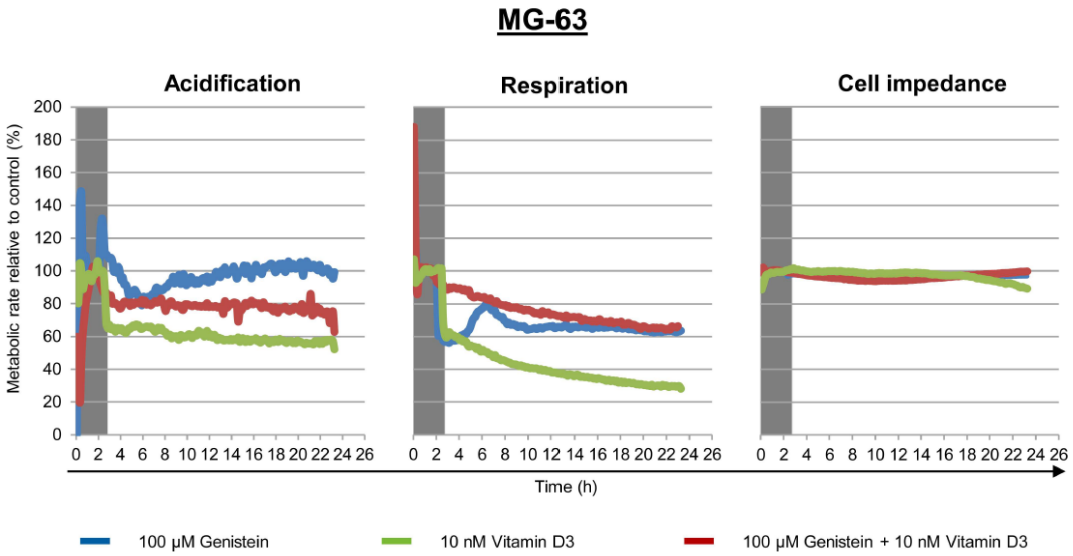

Fig 3. Live cell monitoring of three metabolic parameters (extracellular acidification, mitochondrial respiration, and cell impedance) in MG-63 after exposure to the vehicle control (was set to 100%), 100 µM genistein (blue lines), 10 nM calcitriol (red lines) or the combination of both (green lines) over 24 h. Prior treatment cells were adapted to the flow conditions for at least 2 h (grey shadowed). n = 3.

doi:10.1371/journal.pone.0169742.g003

separates the controls (group A) and calcitriol-treated samples (group C) from the genistein (group B) and double-treated samples (group D). Thus, compared to the controls treatment with 100 µM genistein seems to have a larger influence on the metabolic profiles of the investigated samples than treatment with 10 nM calcitriol. However, potential additive or synergistic effects of individual metabolites caused by the combination of genistein and calcitriol cannot be deduced from the PCA.

To give a more intuitive representation of differences for individual metabolite levels, a heat map based on hierarchical clustering for each metabolite was visualized (Fig 4). Up- and down-regulated metabolites are indicated by red and blue colors, respectively. It is clearly evident that compared to the control many metabolites after genistein or combined treatment are down-regulated (blue). But also a cluster of upregulated (red) metabolites in the left lower quadrant is visible. In the differential analysis, 103 metabolites showed a significant difference between 100 µM genistein and control treatment. Especially, components of various lipids are higher concentrated in the treated samples, whereas various amines and some amino acids show higher concentrations in the control. The comparison between 10 nM calcitriol and control treatment revealed 30 significantly altered metabolites, whereas amines, amino acids and lipids are higher concentrated in the calcitriol group. Compared to the control, 99 metabolites of the 100 µM genistein + 10 nM calcitriol group were significantly altered, this was comparable to the group treated with 100 µM genistein alone. In total, 186 compounds were analyzed with distinct changes in some metabolite classes based upon the treatment, e.g. lipid components, amines and amino acids. In energy metabolites, such as glucose or ATP, no significant changes were observed, strengthening the results of the protein expression analysis of relevant glycolytic and respiratory enzymes (S2 Fig).

To determine the significant altered metabolites, rankings of log2-ratios (treatment vs. control) were calculated (Fig 5). At first glance it is obvious that the single treatments with

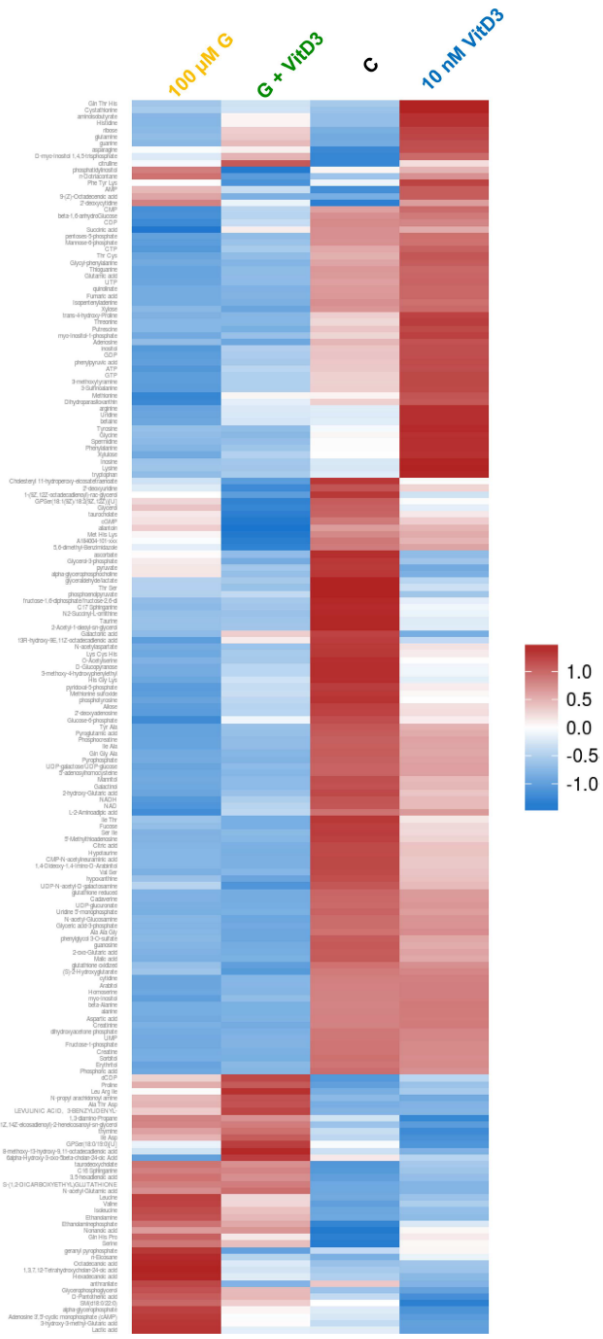
100 µM G
G + VitD3
C
10 nM VitD3
1.0
0.5
0.0
-0.5
-1.0

Fig 4. Heat map presentation of all identified metabolites by global metabolite profiling after 48 h treatment of the vehicle control, 100 μM genistein (G), 10 nM calcitriol (VitD3) and the combination of both in MG-63 cells (see color bar for scale; blue color indicates down regulated metabolites; red color indicates up regulated metabolites).

doi:10.1371/journal.pone.0169742.g004

genistein and calcitriol regulate different metabolites. The application with genistein induces a strong increase in ethanolamine, nonanoic acid, ethanolamine-phosphate, hexadecanoic acid, octadecanoic acid and a boosted decrease in creatinine, aspartic acid, spermidine, taurine, and cadaverine. In contrast, calcitriol regulates the following metabolites: asparagine, ethanolamine-phosphate, spermidine and ethanolamine were up-regulated, and lactic acid, glycerol-3-phosphate, taurine, and α-glycerophosphocholine were down-regulated. The combined treatment revealed a strong increase for ethanolamine, nonanoic acid, and ethanolamine-phosphate whereas aspartic acid, creatinine, glyceric acid-3-phosphate, adenosine and cadavarine were significantly reduced. Synergism was calculated for ethanolamine, ethanolamine-phosphate and nonanoic acid.

Astonishingly, end products of the sphingolipid metabolism—ethanolamine and ethanolamine-phosphate—were upregulated synergistically after co-administration of genistein and calcitriol (Fig 5; highlighted in red). The production of ethanolamine-phosphate is irreversibly mediated by the sphingosine-1-phosphate lyase (SGPL1; UniProtKB—O95470; Gene ID: 8879), an enzyme cleaving the secondary messenger sphingosine-1-phosphate to (2E)-hexadecenal and ethanolamine-phosphate, which thereafter can be dephosphorylated by tissue-nonspecific alkaline phosphatases to ethanolamine. Due to this finding, expression and localization of SGPL1 were examined after stimulation with genistein and calcitriol.

Upregulation of SGPL1 expression after combined treatment

In MG-63 cells, SGPL1 expression studies after treatment with genistein, calcitriol or their combination were performed via western blot and immunofluorescence staining (Fig 6). Both methods revealed a strong up-regulation of SGPL1 protein content only after simultaneous stimulation with genistein and calcitriol, while SGPL1 expression levels were not changed after the single application of either substance. The western blot results indicate an increase of SGPL1 protein up to 350% compared to the control (100%) ($p<0.001$). Immunofluorescence staining of SGPL1 protein confirmed its subcellular localization in the endoplasmic reticulum membrane (http://compartments.jensenlab.org) as well as the overexpression after combined treatment (higher green fluorescence intensity (Fig 6)).

Discussion

In this study for the first time the synergistic antitumor effects of genistein and calcitriol were demonstrated in cancer cells (osteosarcoma cells MG-63), which is associated with the expression up-regulation of sphingosine-1-phosphate lyase (SGPL1). The peculiarity of this finding is that the combination of both substances counteracts the pro-proliferative action of genistein in bone cancer cell lines. In detail, the application of phytoestrogens is discussed controversially because they can convey estrogenic as well as anti-estrogenic responses that thus may affect the growth and tumorigenicity of hormone-dependent tumors. High doses of genistein (>10 μM) can reduce the proliferation of breast cancer cells, but also at the same time they promote the growth of bone cancer cells [9]. We explored the co-administration of genistein and calcitriol because there is preliminary data that they could synergistically inhibit cancer growth [16, 17]. Indeed, the proliferation promotion induced by 100 μM genistein in the bone cancer cell line MG-63 could be normalized to control levels after simultaneous exposure to 10

100 µM G		10 nM VitD3		100 µM G + 10 nM VitD3		
Metabolite	**log2-ratio**	**Metabolite**	**log2-ratio**	**MetaboliteD**	**log2-ratio**	**CDI value**
Ethanolamine	2.65	Asparagine	1.75	Ethanolamine	3.22	0.32
Nonanoic acid	2.34	Ethanolamine-phosphate	1.34	Nonanoic acid	2.23	0.29
Ethanolamine-phosphate	1.92	Spermidine	1.33	Ethanolamine-phosphate	1.88	0.35
Hexadecanoic acid	1.87	Ethanolamine	1.10	Serine	0.91	0.52
Octadecanoic acid	1.82	Cystathionine	0.98	Glycerol-3-phosphate	-1.85	1.24
Glycerophospho-glycerol	1.36	Phenylalanine	0.83	Pyrophosphate	-1.99	1.38
C16 Sphinganine	0.88	Lysine	0.83	Aspartic acid	-2.11	1.19
Creatinine	-2.20	Lactic acid	-0.99	Creatinine	-2.3	0.85
Aspartic acid	-2.50	Glycerol-3-phosphate	-1.44	Glyceric acid-3-phosphate	-2.43	0.89
Taurine	-2.63	Taurine	-1.57	Adenosine	-2,78	0.36
Cadaverine	-3.04	alpha-glycerophosphocholine	-1.92	Cadaverine	-3.33	0.91

Fig 5. Ranking of metabolites which were significantly affected by genistein (G), calcitriol (VitD3) or the combination of both in comparison with control treatment ($p \leq 0.05$; n = 4). Displayed were the log2 ratios. Notably, metabolites of the sphingolipid metabolism like ethanolamine and ethanolamine-phosphate were significantly upregulated. Synergistic effects of genistein and calcitriol were calculated by Chou-Talalay method, and displayed as CDI value. CDI < 1, CDI = 1, and CDI > 1 indicate synergism, additive effects, and antagonism, respectively.

doi:10.1371/journal.pone.0169742.g005

nM calcitriol (Fig 1). Also, a significantly increased expression of the ERß could be observed while the expression levels of the ERα remained unchanged (Fig 2). Similarly, a significant increase of the VDR levels was determined in MG-63 cells and primary osteoblasts. This suggests that the combination of genistein and vitamin D3 stimulates an overexpression of ERß and VDR which are meant to be tumor suppressors and good prognostic markers [24, 25].

Beside the synergistic effects on the proliferation behavior and receptor expression, an influence on the cellular metabolism could be determined by live cell monitoring of three cancer relevant features: extracellular acidification, mitochondrial respiration and cell impedance (Fig 3). Again, synergistic effects could be observed. In MG-63 cells extracellular acidification and respiration were significantly reduced. This may indicate a downregulation of both the

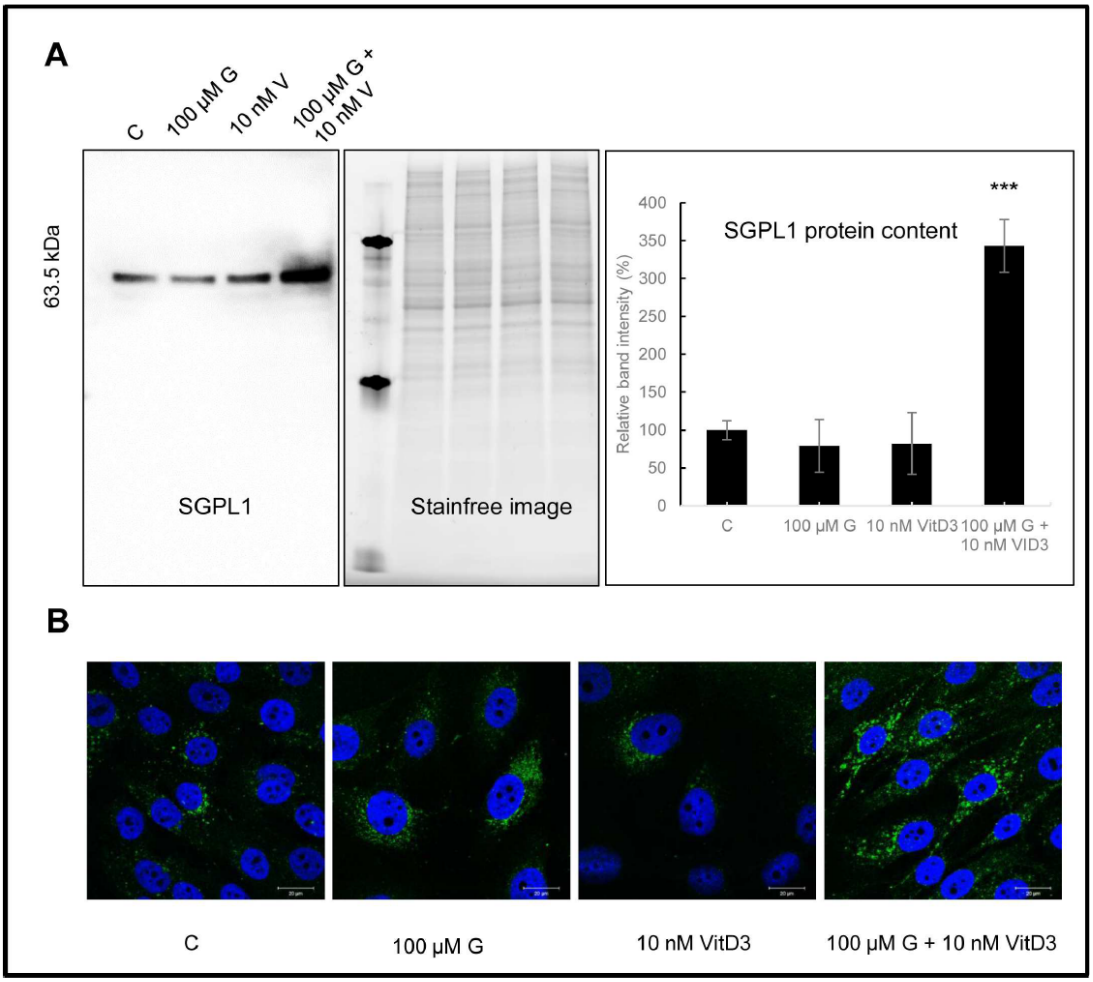

Fig 6. Protein expression analysis of the sphingosine-1-phosphate lyase (SGPL1) in MG-63 cells after treatment with the vehicle control (C), 1, 10, 100 µM genistein (G), 10 nM calcitriol (VitD3) or the combination of both via western blotting and immunofluorescence staining. A: western blot, stain free image as loading control and quantification of the western blotting results. Mean ± SD values (Representative example of 3 independent experiments, n = 3). *** = $p \leq 0.001$ as compared to control (unpaired *t* test). B: Immunofluorescence staining of SGPL1 protein to compare expression levels und subcellular distribution. Green: SGPL1. Blue: cell nucleus. n = 3.

doi:10.1371/journal.pone.0169742.g006

glycolytic activity and the enzymes of the Krebs cycle. This however could not be confirmed by protein expression analysis of cancer-relevant glycolytic and respiratory enzymes in MG-63 (S2 Fig). Distinct alterations of the protein contents of e.g. lactate dehydrogenase, pyruvate dehydrogenase or succinate dehydrogenase, key players in the energy metabolism of cancer cells, were not observed [26]. The lack of a direct impact on the energy metabolism of MG-63 cells by genistein and/or calcitriol was also confirmed by metabolite analysis (Figs 4 and 5). Distinct changes in some metabolite classes based upon the treatment, e.g. lipid components,

amines and amino acids could be detected, but no significant changes were observed in energy metabolites such as glucose or ATP. However, live cell monitoring experiments revealed pronounced synergistic effects of genistein and calcitriol especially for MG-63 and POBs: respiratory and glycolytic activities in MG-63 cells are greatly reduced and in POB respiration they are upregulated strongly. The impact on Saos-2 was moderate, probably because Saos-2 represents a mature osteoblastic phenotype compared to MG-63 and POBs (S1 Fig). Thus, it could be clearly demonstrated that an effect on O_2-consumption and extracellular acidification could be reached although no direct influence on relevant metabolic energy enzymes or metabolites could be determined.

Therefore, a complex metabolic profiling of MG-63 cells was performed (Fig 4). After co-administration of genistein and calcitriol, 99 metabolites, primarily lipids and amino acids, were altered. Comparisons of the log2-ratios of significantly ($p \leq 0.05$) up-regulated metabolites for the three treatment groups revealed, that ethanolamine was synergistically up-regulated after combined exposure to genistein and calcitriol (Fig 5). Schmitt et al. [27] just recently showed that the antitumor agent phorbol-ester stimulates release of ethanolamine from the metastatic basal prostate cancer cell line PC3 suggesting that elevated ethanolamine production could be associated with antitumor activity.

Beside ethanolamine, also high levels of ethanolamine-phosphate were detected. Both metabolites are components of the glycerophospholipid metabolism (KEGG pathway map 00564) and sphingolipid metabolism (KEGG pathway map 00600) and are directly related to each other. Briefly, sphingosine-1-phosphate lyase (SGPL1; KEGG enzyme EC 4.1.2.27) irreversibly cleaves sphingosine-1-phoshate (S1P), a signaling sphingolipid acting as second messenger, into hexadecenal and ethanolamine-phosphate [28]. The latter is dephosphorylated by a phosphoethanolamine/phosphocholine phosphatase (KEGG enzyme EC 3.1.3.75) in the presence of H_2O. Up-regulation of ethanolamine-phosphate and ethanolamine was confirmed by expression analysis of the SGPL1 (Fig 6). Combined treatment with genistein and calcitriol caused a 3.5-fold overexpression of SGPL1 indicating a high breakdown of S1P.

High intracellular S1P levels are associated with increased migration and invasion of cancer cells, and S1P is 5–10 times higher in ovarian cancer patients [29]. A reduction of intracellular S1P levels could be achieved by up-regulating the internal expression and enzyme activity of SGPL1. However, the role of SGPL1 in bone and other cancers has not been directly examined until now. Degagné et al. [30] demonstrated that mice with intestinal epithelium-specific SGPL1 deletion developed phenotypes with pathological evidence of inflammation, colon shortening, high cytokine levels, S1P accumulation, and development of colon tumors. Furthermore, a down-regulation of SGPL1 was detected in most tumors, and over-expression of SGPL1 enhanced sensitivity to cisplatin, carboplatin, daunorubicin and etoposide [31]. Thus, SGPL1 is a potential target for pharmacological manipulation for the treatment of malignant, autoimmune, inflammatory and other diseases [32]. For the first time, synergistic effects by exposure to high doses of genistein in combination with calcitriol were demonstrated in osteosarcoma cells, primarily by a 3 – 4fold up-regulation of the SGPL1 protein content. This up-regulation mediated reduction of proliferation, boosted ERß and VDR expression and altered tumorigenic metabolism. This discovery opens new avenues in the treatment of cancer patients and should be underpinned by *in vivo* studies.

Conclusion

In summary, combined treatment of the immature osteosarcoma cell line MG-63 with genistein and calcitriol results in: (1) a growth normalization of genistein induced proliferation, (2) overexpression of ERß, (3) reduction of extracellular acidification and respiration rates, (4)

synergistically increased ethanolamine production, primarily initiated by a 3 – 4fold overexpression of the sphingosine-1-phosphate lyase. Actually, the co-administration of genistein and calcitriol is investigated in a murine xenograft model.

Supporting Information

S1 Fig. Alkaline phosphate activity (ALP), calcification via Alizarin Red S staining and matrix mineralization with osteocalcin immunofluorescence staining in untreated MG-63, Saos-2 bone cancer cells and in primary osteoblasts (POB). All cells were counterstained with DAPI to visualize cell nuclei.
(TIF)

S2 Fig. Protein expression analysis via western blotting of cancer relevant enzymes of the glycolysis and Krebs cycle in MG-63 cells after 48 h treatment with the vehicle control (C), 1, 10, 100 μM genistein (G), 10 nM calcitriol (VitD3) or the combination of both. Glycolytic enzymes were hexokinase 1, platelet-type phosphofructokinase (PFKP), lactate dehydrogenase (LDH). Pyruvate dehydrogenase (PDH), fumarase and succinate dehydrogenase subunit A (SDHA) were chosen as representative enzyme of the Krebs cycle. n = 3. Stain free images were added to verify that identical soluble protein concentrations were loaded on the polyacrylamid gels.
(TIF)

S3 Fig. Principal component analysis (PCA) of control (A), cells treated with 100 μM genistein (B), 10 nM calcitriol (C) and 100 μM genistein+10 nM calcitriol (D) with four replicates each.
(TIF)

Acknowledgments

This work is supported by fund from Federal Ministry of Education and Research Germany (Women Professors Program) and FORUN program of the University Medical Center Rostock (no. 889025). The funder provided support in the form of salaries for author [NE], but did not have any additional role in the study design, data collection and analysis, decision to publish, or preparation of the manuscript. The specific roles of these authors are articulated in the 'author contributions' section. Metabolomic Discoveries GmbH did not fund this study in any case.

Author Contributions

Conceptualization: NE KK.

Formal analysis: NE NS AA.

Investigation: NE AA JK NS.

Methodology: NE JK AA.

Project administration: NE KK.

Resources: BN KK.

Supervision: NE KK BN GS.

Validation: NE JK AA NS.

Visualization: NE AA.

Writing – original draft: NE KK.

Writing – review & editing: NE KK NS AA GS.

References

1. Hilakivi-Clarke L, Andrade JE, Helferich W. Is soy consumption good or bad for the breast? J Nutr. 2010 Dec; 140(12):2326S–2334S. doi: 10.3945/jn.110.124230 PMID: 20980638
2. Lamartiniere CA, Murrill WB, Manzolillo PA, Zhang JX, Barnes S, Zhang X, et al. Genistein alters the ontogeny of mammary gland development and protects against chemically-induced mammary cancer in rats. Proc Soc Exp Biol Med. 1998; 217:358–364. PMID: 9492348
3. Sirtori CR, Arnoldi A, and Johnson SK: Phytoestrogens: End of a tale? Ann Med. 2005; 37:423–438. doi: 10.1080/07853890510044586 PMID: 16203615
4. Hsieh CY, Santell RC, Haslam SZ, Helferich WG. Estrogenic effects of genistein on the growth of estrogen receptor-positive human breast cancer (MCF-7) cells in vitro and in vivo. Cancer Res. 1998 Sep 1; 58(17):3833–8. PMID: 9731492
5. Engel N, Lisec J, Piechulla B, Nebe B. Metabolic profiling reveals sphingosine-1-phosphate kinase 2 and lyase as key targets of (phyto-) estrogen action in the breast cancer cell line MCF-7 and not in MCF-12A. PLoS One. 2012; 7(10):e47833. doi: 10.1371/journal.pone.0047833 PMID: 23112854
6. Pagliacci MC, Smacchia M, Migliorati G, Grignani F, Riccardi C, et al. Growth-inhibitory effects of the natural phyto-oestrogen genistein in MCF-7 human breast cancer cells. Eur J Cancer. 1994; 30:1675–1682.
7. Yang X, Belosay A, Hartman JA, Song H, Zhang Y, Wang W, et al. Dietary soy isoflavones increase metastasis to lungs in an experimental model of breast cancer with bone micro-tumors. Clin Exp Metastasis. 2015 Apr; 32(4):323–33. doi: 10.1007/s10585-015-9709-2 PMID: 25749878
8. Martinez-Montemayor MM, Otero-Franqui E, Martinez J, De La Mota-Peynado A, Cubano LA, Dharmawardhane S (2010) Individual and combined soy isoflavones exert differential effects on metastatic cancer progression. Clin Exp Metastasis. 27(7):465–480. doi: 10.1007/s10585-010-9336-x PMID: 20517637
9. Engel N, Oppermann C, Falodun A, Kragl U. Proliferative effects of five traditional Nigerian medicinal plant extracts on human breast and bone cancer cell lines. J Ethnopharmacol. 2011 Sep 2; 137 (2):1003–10. doi: 10.1016/j.jep.2011.07.023 PMID: 21782919
10. Braun S, Vogl FD, Naume B, Janni W, Osborne MP, Coombes RC, et al. A pooled analysis of bone marrow micrometastasis in breast cancer. N Engl J Med. 2005; 353(8):793–802. doi: 10.1056/NEJMoa050434 PMID: 16120859
11. Vuolo L, Di Somma C, Faggiano A, Colao A. Vitamin D and cancer. Front Endocrinol (Lausanne). 2012 Apr; 23:3:58.
12. Grant WB, Garland CF. Vitamin D has a greater impact on cancer mortality rates than on cancer incidence rates. BMJ. 2014 Apr 29; 348:g2862. doi: 10.1136/bmj.g2862 PMID: 24780390
13. Hutchinson MS, Grimnes G, Joakimsen RM, Figenschau Y, Jorde R. Low serum 25-hydroxyvitamin D levels are associated with increased all-cause mortality risk in a general population: the Tromsø study. Eur J Endocrinol. 2010 May; 162(5):935–42. doi: 10.1530/EJE-09-1041 PMID: 20185562
14. Grant WB, Juzeniene A, Moan JE. Review Article: Health benefit of increased serum 25(OH)D levels from oral intake and ultraviolet-B irradiance in the Nordic countries. Scand J Public Health. 2011 Feb; 39(1):70–8. doi: 10.1177/1403494810382473 PMID: 20817654
15. Keum N, Giovannucci E. Vitamin D supplements and cancer incidence and mortality: a meta-analysis. Br J Cancer. 2014 Aug 26; 111(5):976–80. doi: 10.1038/bjc.2014.294 PMID: 24918818
16. Swami S, Krishnan AV, Peehl DM, Feldman D. Genistein potentiates the growth inhibitory effects of 1,25-dihydroxyvitamin D(3) in DU145 human prostate cancer cells: role of the direct inhibition of CYP24 enzyme activity. Mol Cell Endocrinol. 2005; 12:12.
17. Rao A, Woodruff RD, Wade WN, Kute TE, Cramer SD. Genistein and vitamin D synergistically inhibit human prostatic epithelial cell growth. J Nutr. 2002; 132:3191–3194. PMID: 12368417
18. Krishnan AV, Swami S, Moreno J, Bhattacharyya RB, Peehl DM, Feldman D. Potentiation of the growth-inhibitory effects of vitamin D in prostate cancer by genistein. Nutr Rev. 2007 Aug; 65(8 Pt 2): S121–3.
19. Lappe J, Kunz I, Bendik I, Prudence K, Weber P, Recker R, et al. Effect of a combination of genistein, polyunsaturated fatty acids and vitamins D3 and K1 on bone mineral density in postmenopausal

women: a randomized, placebo-controlled, double-blind pilot study. Eur J Nutr. 2013 Feb; 52(1):203–215. doi: 10.1007/s00394-012-0304-x PMID: 22302614

20. Warsow G, Struckmann S, Kerkhoff C, Reimer T, Engel N, Fuellen G. Differential network analysis applied to preoperative breast cancer chemotherapy response. PLoS One. 2013 Dec 9; 8(12):e81784. doi: 10.1371/journal.pone.0081784 PMID: 24349128
21. Engel N, Falodun A, Kühn J, Kragl U, Langer P, Nebe B. Pro-apoptotic and anti-adhesive effects of four African plant extracts on the breast cancer cell line MCF-7. BMC Complementary and Alternative Medicine 2014; 14:334. doi: 10.1186/1472-6882-14-334 PMID: 25199565
22. Lisec J, Schauer N, Kopka J, Willmitzer L, Fernie AR. Gas chromatography mass spectrometry-based metabolite profiling in plants. Nat Protoc. 2006; 1(1):387–96. doi: 10.1038/nprot.2006.59 PMID: 17406261
23. Chou TC, Talalay P (1984) Quantitative analysis of dose-effect relationships: the combined effects of multiple drugs or enzyme inhibitors. Adv Enzyme Regul 22:27–55. PMID: 6382953
24. Jarvinen T, Pelto-Huikko M, Holli K & Isola J. Estrogen receptor beta is coexpressed with ERalpha and PR and associated with nodal status, grade, and proliferation rate in breast cancer. American Journal of Pathology. 200; 156:29–35. PMID: 10623650
25. Murphy L & Watson P. Steroid receptors in human breast tumorigenesis and breast cancer progression. Biomedical Pharmacotherapy. 2002; 56:65–77.
26. Kaelin WG Jr, Thompson CB. Q&A: Cancer: clues from cell metabolism. Nature. 2010 Jun 3; 465 (7298):562–4. doi: 10.1038/465562a PMID: 20520704
27. Schmitt J, Noble A, Otsuka M, Berry P, Maitland NJ, Rumsby MG. Phorbol ester stimulates ethanolamine release from the metastatic basal prostate cancer cell line PC3 but not from prostate epithelial cell lines LNCaP and P4E6. Br J Cancer. 2014 Oct 14; 111(8):1646–56. doi: 10.1038/bjc.2014.457 PMID: 25137020
28. Van Veldhoven PP, Gijsbers S, Mannaerts GP, Vermeesch JR, Brys V. Human sphingosine-1-phosphate lyase: cDNA cloning, functional expression studies and mapping to chromosome 10q22(1). Biochim Biophys Acta. 2000 Sep 27; 1487(2–3):128–34. PMID: 11018465
29. Wang D, Zhao Z, Caperell-Grant A, Yang G, Mok SC, Liu J, et al. S1P differentially regulates migration of human ovarian cancer and human ovarian surface epithelial cells. Mol Cancer Ther. 2008 Jul; 7 (7):1993–2002. doi: 10.1158/1535-7163.MCT-08-0088 PMID: 18645009
30. Degagné E, Pandurangan A, Bandhuvula P, Kumar A, Eltanawy A, Zhang M, et al. Sphingosine-1-phosphate lyase downregulation promotes colon carcinogenesis through STAT3-activated microRNAs. J Clin Invest. 2014 Dec; 124(12):5368–84. doi: 10.1172/JCI74188 PMID: 25347472
31. Bandhuvula P, Saba JD. Sphingosine-1-phosphate lyase in immunity and cancer: silencing the siren. Trends Mol Med. 2007 May; 13(5):210–7. doi: 10.1016/j.molmed.2007.03.005 PMID: 17416206
32. Kumar A, Saba JD. Lyase to live by: sphingosine phosphate lyase as a therapeutic target. Expert Opin Ther Targets. 2009 Aug; 13(8):1013–25. doi: 10.1517/14728220903039722 PMID: 19534571

Referenz VI

Engel N*, Adamus A, Frank M, Kraft K, Kühn J, Müller P, Nebe B, Kasten A, Seitz G. First evidence of SGPL1 expression in the cell membrane silencing the extracellular S1P siren in mammary epithelial cells. PLoS One. 2018 May 2;13(5):e0196854. doi: 10.1371/journal.pone.0196854. eCollection 2018

NCBI-Link: https://www.ncbi.nlm.nih.gov/pmc/articles/PMC5931664/

Zusammenfassung:

In dieser Studie konnten wir erstmalig nachweisen, dass nicht-tumorigene Mammaepithelzellen nicht nur eine hohe SGPL1-Expression aufweisen, sondern dass in den gesunden Zellen auch eine SGPL1-Expression in der Zytoplasmamembran darzustellen ist (Abb. 4). Die SGPL1 Lokalisation in der Plasmamembran wurde noch nicht beschrieben.

Insbesondere zur Metastasierung neigende Brustkrebzellen zeigen eine reprimierte oder fehlende SGPL1-Expression in der Zellmembran. Dadurch kann der permanente S1P-Stimulus nicht mehr reguliert werden, und die gerichtete Migration und Invasion wird begünstigt. Durch Restauration der SGPL1-Funktionaliät und -Lokalisation in der Plasmamembran konnte die Motilität der Brustkrebszellen reduziert werden (Abb. 8).

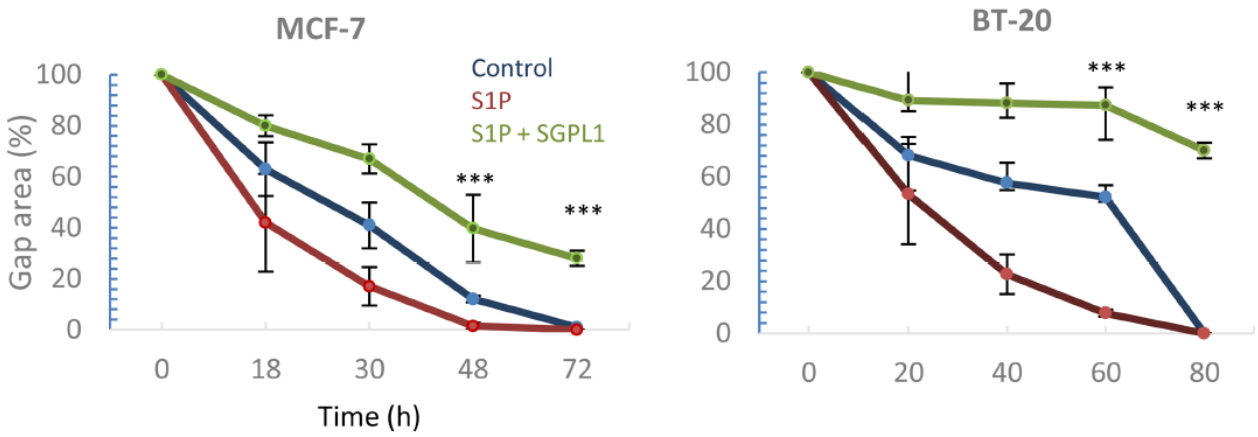

*Abb. 8 Relative Migrationsgeschwindigkeit der Mammakarzinomzelllinien MCF-7 und BT-20 im Scratch-Assay. Ermittelt wird die Migrationsrate in einen definierten Spalt 100 % - der Spalt enthält keine Zellen. O % - der Spalt ist zu 100 % mit Zellen besiedelt. Bei Stimulation der Mammakarzinomzellen mit 1 µM S1P wird die Migrationsgeschwindigkeit deutlich erhöht. Nach Komplementation der Mammakarzinomzelllinien mit der nativen SGPL1.Variante ist die Migrationsgeschwinigkeit signifikant unter das Kontrollniveau gesenkt. Mittelwert ± Standardabweichung, n= 3, *** = p < 0.001 im Vergleich zur Kontrolle (ungepaarter t test).*

PLOS ONE

RESEARCH ARTICLE

First evidence of SGPL1 expression in the cell membrane silencing the extracellular S1P siren in mammary epithelial cells

Nadja Engel[1,2,3]*, Anna Adamus[1,2], Marcus Frank[4], Karin Kraft[5], Juliane Kühn[2,6], Petra Müller[2], Barbara Nebe[2], Annika Kasten[3], Guido Seitz[1]

1 Department of Pediatric Surgery, University Hospital Marburg, Baldingerstraße, Marburg, Germany, **2** Department of Cell Biology, University Medicine Rostock, Schillingallee, Rostock, Germany, **3** Department of Oral and Maxillofacial Surgery, Facial Plastic Surgery, Rostock University Medical Center, Schillingallee, Rostock, Germany, **4** Medical Biology and Electron Microscopy Centre, University Medicine Rostock, Strempelstraße, Rostock, Germany, **5** Complementary Medicine, Center of Internal Medicine, University Medicine Rostock, Ernst-Heydemann-Straße, Rostock, Germany, **6** Institute for Immunology, Friedrich-Loeffler-Institut, Federal Research Institute for Animal Health, Südufer, Greifswald-Insel Riems, Germany

* nadja.engel-lutz@gmx.de, nadja.engel-lutz@med.uni-rostock.de

OPEN ACCESS

Citation: Engel N, Adamus A, Frank M, Kraft K, Kühn J, Müller P, et al. (2018) First evidence of SGPL1 expression in the cell membrane silencing the extracellular S1P siren in mammary epithelial cells. PLoS ONE 13(5): e0196854. https://doi.org/10.1371/journal.pone.0196854

Editor: Rajesh Mohanraj, Faculty of Medicine & Health Science, UNITED ARAB EMIRATES

Received: September 7, 2017

Accepted: April 20, 2018

Published: May 2, 2018

Data Availability Statement: All relevant data are within the paper and its Supporting Information files.

Funding: This work is supported by fund from BMBF habilitation scholarship program of the University of Rostock and FORUN program of the University Medical Center Rostock (no. 889025) (NE). The funders had no role in study design, data collection and analysis, decision to publish, or preparation of the manuscript.

Abstract

The bioactive lipid sphingosine-1-phosphate (S1P) is a main regulator of cell survival, proliferation, motility, and platelet aggregation, and it is essential for angiogenesis and lymphocyte trafficking. In that S1P acts as a second messenger intra- and extracellularly, it might promote cancer progression. The main cause is found in the high S1P concentration in the blood, which encourage cancer cells to migrate through the endothelial barrier into the blood vessels. The irreversible degradation of S1P is solely caused by the sphingosine-1-phosphate lyase (SGPL1). SGPL1 overexpression reduces cancer cell migration and therefore silences the endogenous S1P siren, which promotes cancer cell attraction—the main reason for metastasis. Since our previous metabolomics studies revealed an increased SGPL1 activity in association with successful breast cancer cell treatment *in vitro*, we further investigated expression and localization of SGPL1. Expression analyses confirmed a very low SGPL1 expression in all breast cancer samples, regardless of their subtype. Additionally, we were able to prove a novel SGPL expression in the cytoplasm membrane of non-tumorigenic breast cells by fusing three independent methods. The general SGPL1 downregulation and the loss of the plasma membrane expression resulted in S1P dependent stimulation of migration in the breast cancer cell lines MCF-7 and BT-20. Not only S1P stimulated migration could be repressed by overexpressing the natural SGPL1 variant not but also more general migratory activity was significantly reduced. Here, for the first time, we report on the SGPL1 plasma membrane location in human, non-malignant breast epithelial cell lines silencing the extracellular S1P siren *in vitro*, and thereby regulating pivotal cellular functions. Loss of this plasma membrane distribution as well as low SGPL1 expression levels could be a potential prognostic marker and a viable target for therapy. Therefore, the precise role of SGPL1 for cancer treatment should be evaluated.

Competing interests: The authors have declared that no competing interests exist.

Introduction

The bioactive lipid and second messenger sphingosine-1-phosphate (S1P) has emerged as key regulator in cancer progression by modulating a variety of cellular processes, such as proliferation, migration, platelet aggregation, or angiogenesis [1, 2]. Most studies have focused on S1P-synthesizing enzymes: the two S1P kinases (Sphk1, Sphk2), which are phosphorylating the pro-apoptotic lipid signaling molecule sphingosine. Several growth factors and steroid hormones, such as TGF-ß and 17ß-estradiol could be related to up-regulation of Sphk1 in cancer cells, producing high amounts of SP, which can bind extracellularly to five specific G-protein-coupled receptors, located on the cell surface (named S1P1, 2, 3, 4, 5) or intracellularly stimulate cell survival [3, 4]. Inhibiting the Sphk1 activity leads to a decrease in cancer proliferation and metastasis in mouse models and increases the efficacy of chemotherapy and radiotherapy [2, 5]. Consequently, Sphk1 is announced as a potential prognostic marker and a viable target for therapy, including that of breast cancer [6]. Considerably less attention has been paid to the S1P-degrading enzyme: sphingosine-1-phosphate lyase (SGPL1; EC 4.1.2.27) which irreversibly cleaves S1P into hexadecanal and ethanolamine phosphate and, is thus in a strategic position to regulate these processes by removing available S1P signaling pools, which means silencing the siren in order to prevent cancer cell migration to the blood vessels [7, 8]. Current research has demonstrated that ectopic expression of SGPL1 results in increased sensitivity to stress, including serum starvation [9], to platinum-based drugs, daunorubicin and etoposide [10], and irradiation [11] suggesting that SGPL1 may be a useful target for cancer therapy drugs.

SGPL1 belongs to the PLP (pyridoxal 5'-phosphate) -dependent carbon-carbon lyases and to the family of single-pass type III membrane proteins, and is located in the endoplasmic reticulum [12]. The luminal N-terminal domain is close to the transmembrane segment and the soluble PLP-binding domain. The larger, hydrophilic and catalytic domain faces the cytosol. Several mammalian tissues express SGPL1 in different activity states. While high activity appears in the small intestine, colon, thymus and spleen, moderate activity is found in liver, kidney, lung, stomach and testis. SGPL1 underlies a strict transcriptional and posttranslational regulation, enabling it to respond to environmental changes. Loss of SGPL1 enhances cell resistance to anticancer regimens and increases the ability of cells to acquire a transformed phenotype and become malignant. On the contrary, malignant cancer cells with moderate SGPL1 expression show sensitivity to cisplatin, daunorubicin and etoposide [10]. Inhibition of SGPL1 activity has profound effects on the immune system and lymphocyte trafficking. The sphingosine analog FTY720 is known to inhibit SGPL1 *in vitro* as well as *in vivo* [13]. However, SGPL1 promotes apoptosis through p53 and p38 tumor-suppressor signaling pathways, and therefore indicates that a SGPL1 downregulation in many cancer types is likely. Yet, an upregulation has been observed in some malignant tissues such as ovarian cancer [14]. Hence, the putative role as tumor-suppressor is not yet convincing. For this reason, we explored the SGPL1 expression, location and function in breast cancer cells and tissue in comparison with non-tumorigenic controls with the intent to identify the underlying regulative mechanisms. Thereby, we explored a novel SGPL1 expression in the cytoplasmic membrane of healthy breast cells which could prevent extracellular overstimulation of circulating S1P. Prevention of breast cancer as well as avoidance of breast cancer progression is of the utmost importance since the incidences are still the highest in women worldwide [15]. Effective treatment of this heterogeneous disease is dependent on histological subtype and receptor expression status. The majority (77%) of breast cancers are positive for estrogen, progesterone, and the human epidermal growth factor receptor-2 and therefore suitable for endocrine therapies with Tamoxifen, Anastrozole, or Trastuzumab [16, 17]. However, triple negative breast cancer

(10–17%) lacking the expressions of these three receptors are difficult to treat, due to their multiple drug resistance. Therefore, our research on molecular levels was performed with two triple negative breast cancer cell lines (BT-20, MDA-MB-231) as well as one luminal receptor positive cell line (MCF-7). As non-tumorigenic, epithelial breast cells, MCF-10A as well as MCF-12A were chosen, presenting two immortal, non-transformed cell lines that share characteristics and features of basal progenitor cells [18].

Results

Breast cancer cells harbor low SGPL1 protein contents

Two non-tumorigenic, epithelial breast cell lines MCF-12A and MCF-10A were chosen as control cell lines to compare the SGPL1 features with three conventional available breast cancer cell lines: MCF-7 (representing a luminal, hormone dependent subtype), MDA-MB-231 and BT-20 (representing ~~a~~ the most aggressive, triple-negative subtype with tendency for metastatic invasion). On transcript level, SGPL1 expression was not altered (Fig 1A). Primers, specific for the SGPL1 main coding transcript variant 1 (Tv 1, NCBI Reference Sequence: NM_003901.3) only, and primers for all coding transcript variants (Tv all) were designed for and used in RT-PCR as well as in qPCR. No~~r~~ significant differences occurred on transcript level. In contrast, SGPL1 protein content was significantly lowered in all three breast cancer cell lines, verified by western blotting (Fig 1B). As internal loading controls ß-actin, GAPDH and stainfree imaging of total soluble proteins were used. Furthermore, 10 ng of the recombinant expressed, and affinity chromatography purified human SGPL1 protein was loaded additionally on the immune blot to display the specificity of the SGPL1 antibody used in this study. Uncropped immune blots are shown in S1 Fig. Decreased SGPL1 expression in breast cancer cell lines was verified by immunofluorescence staining (Fig 2A). In addition, confocal imaging of SGPL1 localization revealed the SGPL1 protein in surrounding of the cell nuclei in the non-tumorigenic breast cells, indicating ~~for~~ an association with the endoplasmic reticulum (see S4 Fig). In MCF-7 breast cancer cells a much weaker expression with a more diffuse, cytosolic distribution of the SGPL1 protein was observed. Both invasive breast cancer cells displayed only small spots of aggregated SGPL1 proteins. Surprisingly, in BT-20 cells SGPL1 clusters could primarily be detected in the alveolar structures (oncosomes). The general lowered SGPL1 expression was verified in immunohistochemically stained human breast cancer tissues (Fig 2B). Moderate to high (+2 to +3) scores were detected in normal breast tissue samples whereas the majority of breast cancer samples were weakly stained or negative (Score 0 to +1). Additional immunohistochemical SGPL1 stainings can be found, for example, in the Protein Atlas database (www.proteinsatlas.org, S3A Fig). A few cases of breast cancers displayed moderate immunoreactivity. Normal breast tissue displayed moderate to high SGPL1 contents comparable to liver sections used as positive controls. However, a correlation between overall and relapse-free patients' survival and the SGPL1 expression value was determined significantly by using R2: Genomics Analysis and Visualization Platform (https://hgserver1.amc.nl/cgi-bin/r2/main.cgi) (S3B Fig). Thus, low SGPL1 expression levels are an indication of poor patient' prognosis.

SGPL1 is associated with the cytoplasmic membrane

The SGPL1 subcellular localization in the endoplasmic reticulum membrane was described previously [7, 8] and validated for epithelial breast cells in S4B Fig. By electronic annotations and proteomics approaches a SGPL1 localization in the plasma and mitochondrial membrane is likely (https://compartments.jensenlab.org; http://www.proteinatlas.org/ENSG00000166224-SGPL1/cell; http://www.genecards.org/cgi-bin/carddisp.pl?gene=SGPL1).

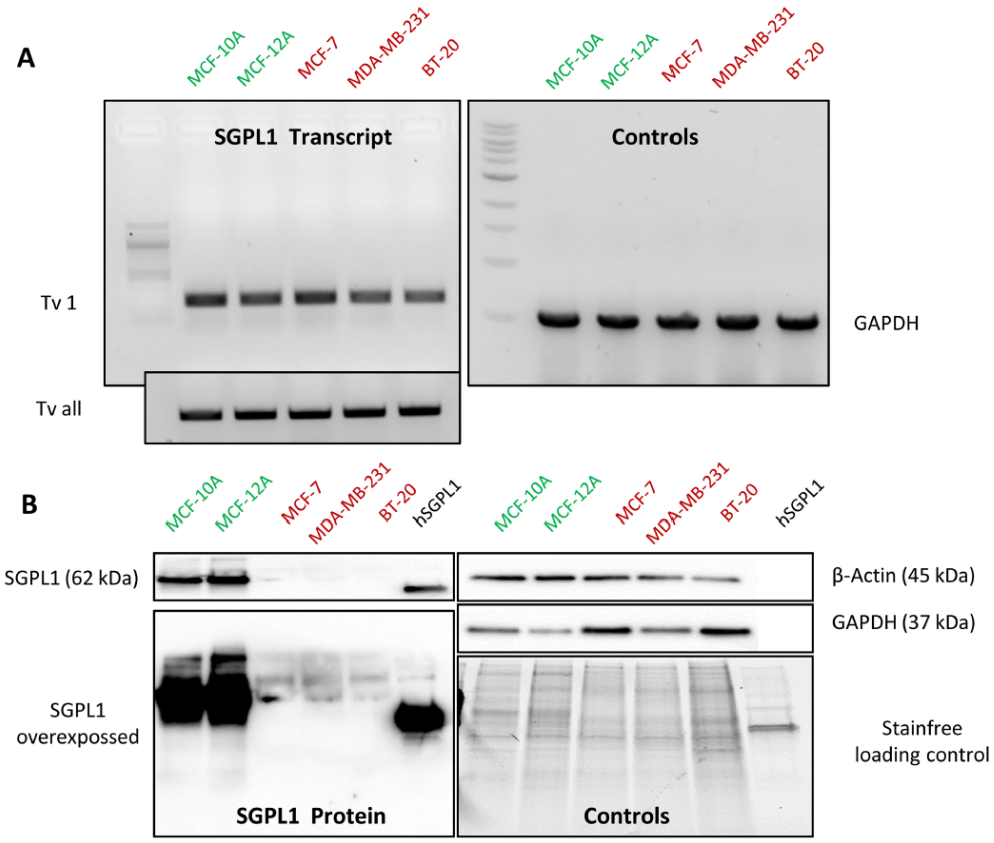

Fig 1. SGPL1 expression analysis. A: RT-PCR with SGPL1 specific primers revealed no significantly altered SGPL1 expression on transcript level for main coding SGPL1 transcript variant 1 (Tv1) as well for the sum of all NCBI annotated SGPL1 transcript variants (Tv all) in comparison with the GAPDH control. B: SGPL1 protein content in the 5 epithelial breast cell lines (20 μg soluble protein) parallel to 10 ng recombinant SGPL1 protein was visualized by western blotting. Non-malignant breast epithelial cell lines MCF-10A and MCF-12A showed strongly elevated SGPL1 protein expression levels. Loading controls were verified by labeling ß-actin and GAPDH proteins as well as by stain-free technology. Uncropped immune blots are shown in S1 Fig.

https://doi.org/10.1371/journal.pone.0196854.g001

Furthermore, the immunohistochemically stained non-malignant breast tissues revealed a SGPL1 association not only with the endoplasmic reticulum but also with the plasma membrane (Personal communication with pathologist Prof. Dr. Erbersdobler (Institute for Pathology, Rostock University Medical Center, Germany). To prove the prediction, live cell labeling with a C-terminal specific SGPL1 antibody was performed (Fig 3). Note that, staining's presented in Fig 2 were performed after cell fixation and cell membrane permeabilization, while the staining's in Fig 3 were done on living cells without fixation and permeabilization. As a result, the antibodies cannot enter the cell interior and thus, no intracellular proteins are labeled. Only cell surface and plasma membrane associated proteins can be marked by this method. 3D confocal imaging and remodeling of the non-tumorigenic breast cells revealed a

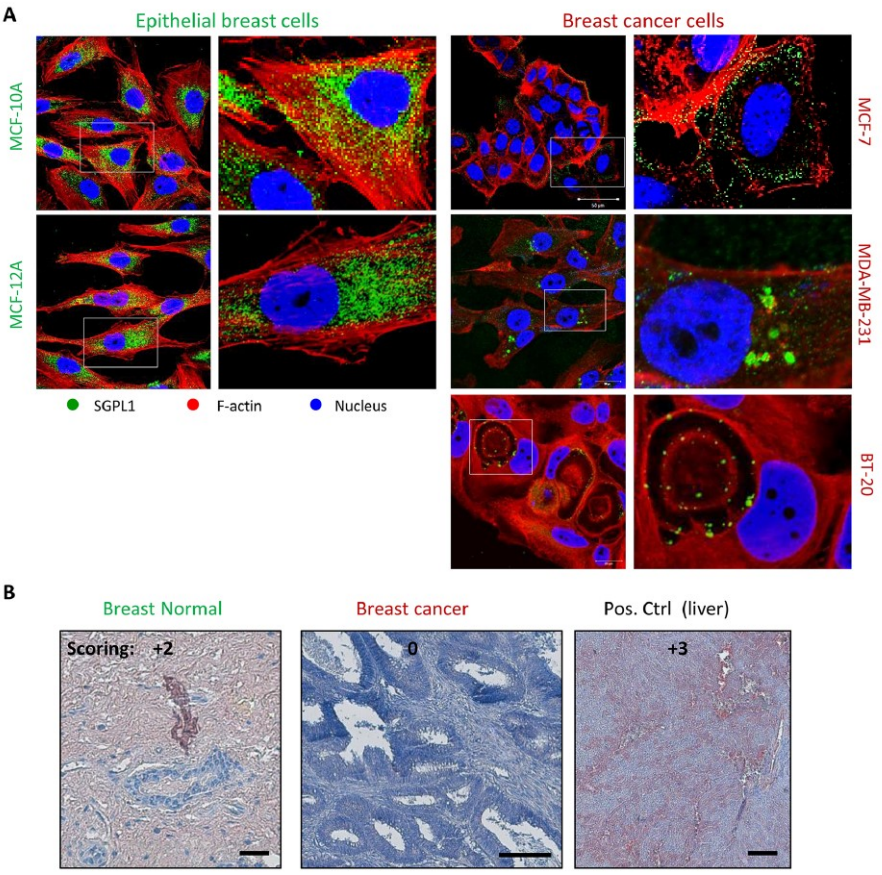

Fig 2. A: Intracellular SGPL1 expression. A: SGPL1 immunofluorescence staining (green) of two non-malignant breast epithelial cell lines (MCF-10A, MCF-12A) in comparison with three established breast cancer cell lines (MCF-7, MDA-MB-231, BT-20) co-localized with ß-Actin (red) and nuclei (blue). B: Representative images of SGPL1 immunohistochemistry staining in normal and breast cancer tissue samples in comparison with positive control organs (liver). SGPL1: reddish brown; Nuclei: blue. Statistical evaluation of *in vivo* SGPL1 protein expression was performed by semi quantitative scoring (0 = no, 1+ = low, 2+ = medium, 3+ = strong expression). Notably, breast cancer tissue and all cancer cell lines displayed SGPL1 downregulation compared to normal breast tissue and non-tumorigenic cell lines.

https://doi.org/10.1371/journal.pone.0196854.g002

green fluorescence signal on top of the actin fibers as it is known from adhesion molecules, for example the great group of integrins, which are anchored in the plasma membrane (Fig 3A). Further, a schematic view of the 3D cell cross sections is given on the right image of Fig 3A. The white arrows point to the green SGPL1 proteins in the cell periphery, which are sitting on the red labeled actin cytoskeleton. This green fluorescence signal at the cell surface was either lowered (MCF-7) or was absent in the triple negative breast cancer cells BT-20 and MDA-MB-231 (Fig 3B). This first evidence of a newly identified SGPL1 association with the plasma membrane was confirmed by additional experiments. By flow cytometry SGPL1 proteins were detected on the surface of the non-tumorigenic cell lines MCF-10A and MCF-12A (Fig 4A)

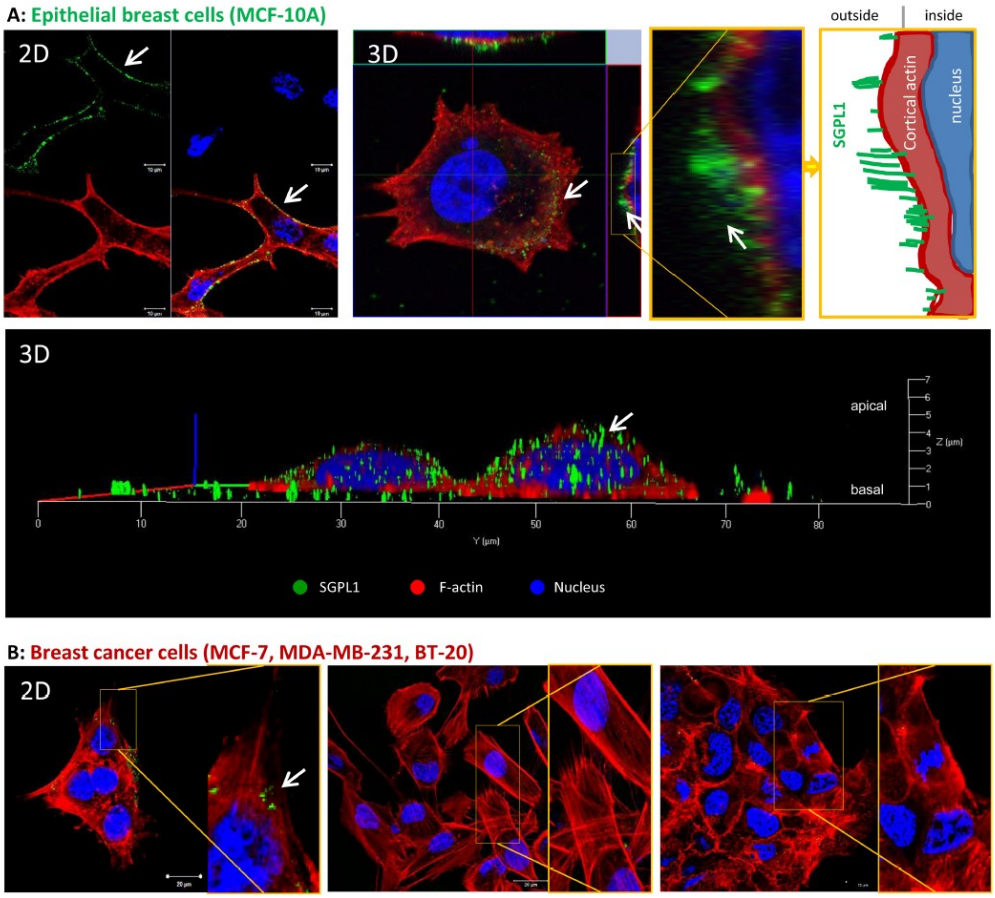

Fig 3. SGPL1 association with the plasma membrane. The living non-tumorigenic breast cell line MCF-10A (**A**) in comparison with the three breast cancer cell lines MCF-7, MDA-MB-231, and BT-20 (**B**) were labeled with a C-terminal anti-SGPL1 antibody without fixation and permeabilization, so that only cell surface and plasma membrane proteins can be labeled. After secondary labeling with Alexa488 dye, cells were fixed and counterstained with Phalloidin and Hoechst. SGPL1: green, F-actin: red, Nuclei: blue. **A**: Images of MCF-10A cells in 2D (upper panel) and 3D (lower panel) to visualize SGPL1 protein signals in direct association with the cell surrounding plasma membrane. 3D images were taken with Zeiss confocal laser scanning microscope. White arrows point to the green SGPL1 protein sitting on the cortical actin cytoskeleton. Additionally, a schematic view of SGPL1 in association with cell periphery is given. **B**: 2D images of SGPL1 expression in the breast cancer cell lines. Note that only non-tumorigenic breast cells show clear SGPL1 expression in cell periphery.

https://doi.org/10.1371/journal.pone.0196854.g003

but not in the breast cancer cells. Also scanning electron microscopy demonstrated a SGPL1 association with the cell surface in healthy breast cells (Fig 4B). Using gold-labeled secondary antibodies, small dots of SGPL1 proteins were detected at the edges of the filopodia in the non-tumorigenic MCF-12A cells, preferentially. No signals could be detected in breast cancer cell lines (S2 Fig). Finally, by co-localization studies with the membrane proteins focal adhesion kinase (FAK) and ß1-integrin the membrane integration of SGPL1 was hedged (Fig 4C and 4D). The green SGPL1 protein partially merged with the red labeled adhesion molecules,

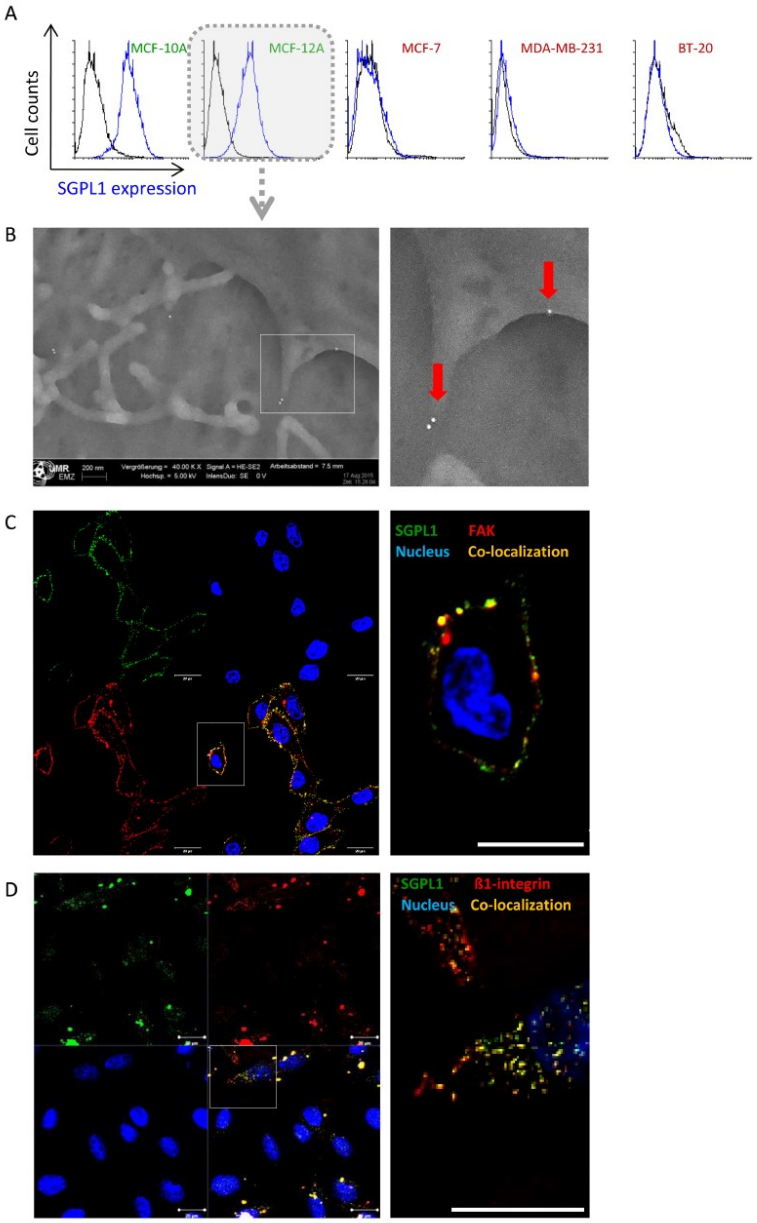

Fig 4. SGLP1 protein in association with the plasma membrane. A: SGPL1 labeling on living breast cells quantitatively measured by flow cytometry. Only the non-tumorigenic breast cells MCF-10A and MCF-12A exhibit SGPL1 signals on the cell surface. B: Scanning electron microscopy of gold-labeled SGPL1 proteins on the cell surface of the non-tumorigenic breast cell line MCF-12A. C/D: Co-localization studies of SGPL1 and known plasma membrane adhesion molecules for MCF-12A C: focal adhesion kinase (FAK) and D: ß1-integrin. SGPL1: green, FAK or ß1-integrin: red, membrane protein overlay: yellow, nuclei: blue. Bar = 20 μm.

https://doi.org/10.1371/journal.pone.0196854.g004

so that 50% fluorescence overlay could be detected. This observation proves that SGPL1 is a plasma membrane associated protein. A functional association with the adhesion protein cannot be assumed.

S1P stimulation was prevented by overexpression of the natural SGPL1 variant

The results of previous studies suggest that the lack of SGPL1 membrane localization and overall lowered SGPL1 content permits uncontrolled extracellular S1P stimulation in the breast cancer cells which could lead to enhanced migratory activity. Though a classical migration assay, an increased migratory force by treatment with 1 μM S1P was verified for the cancer cell lines MCF-7 and BT-20 (Fig 5A). An influence on migration behavior of normal breast cells as

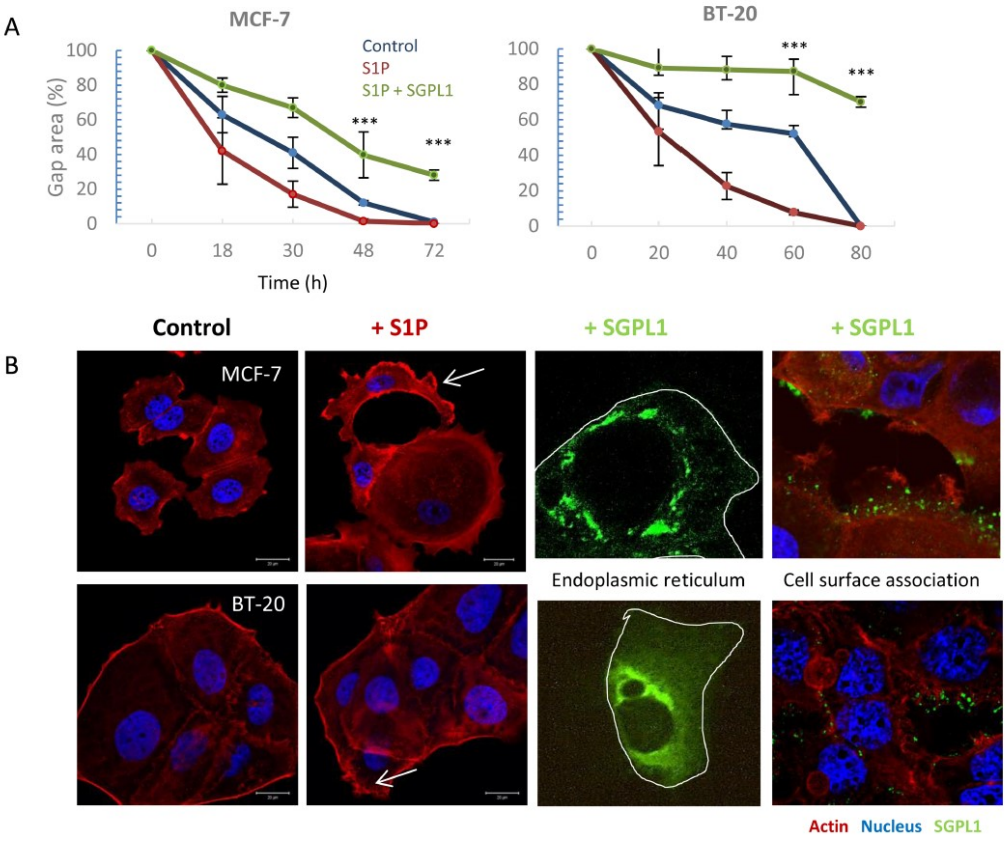

Fig 5. SGPL1 overexpression inhibits S1P induced migration. A: Enhanced migration speed after treatment with 1 μM sphingosine-1-phosphate (S1P) in the breast cancer cell lines MCF-7 and BT-20 (red line). SGPL1 overexpression inhibited the migration ability in the presence of S1P, significantly (green line). Mean ± SD, n = 5, *** $P < 0.001$, significantly different compared to vehicle treated cells, unpaired t-test. B: Morphological alterations of the cytoskeletal protein F-actin (red) after 24 h stimulation with 1 μM S1P. Breast cancer cells MCF-7 and BT-20 show an increased cortical F-actin formation and the formation of filopodia (white arrows). SGPL1 overexpression leads to SGPL1 enrichment within the cell in the surrounding of the nucleus and at the cell surface.

https://doi.org/10.1371/journal.pone.0196854.g005

well as the cell line MDA-MB-231 was not achieved. Additionally, alterations of the actin cytoskeleton were monitored under S1P treatment (Fig 5B). It was obvious that S1P strengthens the cortical actin and filopodia formation (white arrows). So far, we were able to conclude that low SGPL1 content and the missing SGPL1 expression in the outer membrane leads to migratory stimulation of the breast cancer cell lines MCF-7 and BT-20. By restoring the SGPL1 activity in these cancer cells, we checked if the S1P induced migration stimulation could be reverted (Fig 5A). Therefore, the SGPL1 cDNA of the healthy breast cells in frame with a constitutive promoter was stably transfected into MCF-7 and BT-20 cells (Fig 5B). Indeed, SGPL1 overexpression not only repressed the migration behavior to control levels but decreased the general motility of the cancer cells. Astonishingly, BT-20 cell migration ability was almost completely suppressed by SGPL1 overexpression. MCF-7 and BT-20 cells, which were transfected with a SGPL1-cDNA-GFP fusion plasmid revealed a strong co-localization with the endoplasmic reticulum and weak cytosolic and plasma membrane association (Fig 5B). Co-localization of SGPL1 with endoplasmic reticulum (ER) is presented in S4B Fig.

Discussion

Under physiological conditions, high S1P concentrations (200 nM– 1 μM) circulate throughout in the bloodstream, and thus influence a variety of cellular processes: proliferation, migration, invasion, inflammation, and angiogenesis [19]. Tumor cells benefit from this circumstance, either by overexpressing the S1P synthesizing kinases (Sphk1, 2) or by repressing of the irreversible degrading lyase (SGPL1). Thereby, high S1P concentrations in the tumor environment are guaranteed and a continuous stimulation of the cancer cells is achieved. Several research groups have focused on the suppression of the Sphks (S1P generating kinases) activity or on the interception of the circulating S1P contents by the application of FTY720.

But high S1P concentrations are also needed to keep many cellular processes running, for example maturation of the vascular system, immune cell egress, stem cell survival, and cytokine production [20–24]. Systemic downregulation of S1P content in the human body leads to serious side effects. So, it is more likely that human cells control the continuous extracellular S1P stimulation by its degradation mediated by the SGPL1, which is localized in the endoplasmic reticulum. This consideration and the fact that our previously performed metabolome studies revealed an increased SGPL1 activity in association with successful cancer cell treatment *in vitro*, lead to more profound SGPL1 investigations in breast cancer cells [25, 4].

By western blotting and immunofluorescence staining (Fig 1) very low SGPL1 protein levels were found in all breast cancer samples, which correlates with other cancer studies. For example, SGPL1 is downregulated during intestinal tumorigenesis in the ApcMin/+ mouse model and in human colon cancer specimens compared to adjacent uninvolved tissues [10]. The loss of SGPL1 activity may contribute to tumorigenesis. This hypothesis is strengthened by the finding that SGPL1 is significantly downregulated in metastatic tumor tissues compared to primary tumors from the same patients [26]. Kaplan-Meier curves show a stringent correlation between low SGPL1 expression and poorer overall and relapse-free survival (S3B Fig)The low S1P contents could additionally be confirmed by immunofluorescence which also indicates an atypical expression particular in the two triple-negative breast cancer cell lines. MDA-MB-231 showed widely clustered SGPL1 proteins. BT-20 cells revealed an ectopic SGPL1 expression in the alveolar structures; the association with the endoplasmic reticulum was diminished. Since SGPL1 is a single-pass type III membrane protein, integration into other cellular membranes is conceivable. Free available databases (UniProtKB, Reactome) also affirmed the plasma membrane as potential subcellular localization. The co-localization of the SGPL1 protein with the plasma membrane was confirmed by immunofluorescence labeling of living epithelial

breast cells (Fig 3). The highest SGPL1 expression in association with the plasma membrane was detected in the non-malignant breast cell lines MCF-10A and MCF-12A. Here, the SGPL1 proteins are sitting, like most of the adhesion molecules, on the F-actin fibers. Therefore, we decided to perform co-localization staining's with both, the plasma membrane integrated protein ß1-integrin and the focal adhesion kinase (FAK) which connects the integrins with actin fibers. Indeed, co-localization of SGPL1 with adhesion molecules could be achieved (Fig 4). The newly identified SGPL1 plasma membrane localization was further verified by flow cytometry and scanning electron microscopy. The influence of the plasma membrane association on tumor physiology was estimated in two experiments: a) stimulation of the migration by the application of extracellular S1P and b) restoration of the SGPL1 function by a stable overexpression of the natural SGPL1 variant. The migration speed of the breast cancer cell could be increased during the incubation of 1 μM S1P. Overexpression of the native SGPL1 isoform not only neutralized the S1P effects, it also significantly inhibited the migration (Fig 5). These results proved the theory that a functional SGPL1 expression in plasma membrane combined with a high intracellular SGPL1 expression can silence the S1P siren, in the luminal breast cancer cell line MCF-7 and the triple-negative one, BT-20. To this end, we could demonstrate the first evidence of SGPL1 plasma membrane location in non-malignant breast epithelial cells, silencing the extracellular S1P siren *in vitro*, and thereby regulating pivotal cellular functions. Loss of this plasma membrane distribution as well as low SGPL1 expression levels could be a potential prognostic marker and a viable target for therapy. Therefore, the precise role of SGPL1 for cancer treatment should be further evaluated.

Material and methods

SGPL1 antibodies

Several SGPL1 (NCBI Accession: NM_003901, NP_003892.2) antibodies were verified for western blotting, immunofluorescence staining and flow cytometric analysis. Anti-SGPL1 specificity was enabled by specific binding to a recombinant expressed human SGPL1 protein. For western blotting experiments the rabbit anti-SGPL1 antibody (MaxPab®; ABIN948744 from www.antikoerper-online.de), raised against the full length SGPL1 amino acid sequence (AA 1–568), was chosen. For cytoplasmic membrane association, the polyclonal rabbit anti-SGPL1 antibody, recognizing a C-terminal epitope: amino acid 131–430 (cytoplasmic domain) sc-67368, Santa Cruz, USA was used.

Cell culture conditions

All cell lines were purchased from ATCC (www.atcc.org) and maintained at 37 ˚C and in a 5% CO_2 atmosphere. The non-tumorigenic mammary epithelial control cell lines MCF-10A (ATCC® CRL-10317™) and MCF-12A (ATCC® CRL-10782™) were grown in Dulbecco's modified Eagle's medium Ham's F12 without phenol red (Invitrogen, Darmstadt, Germany) containing 10% horse serum (PAA Laboratories GmbH, Munich, Germany), and the Mammary Epithelial Cell Growth Medium Supplement Pack (Promo Cell, Heidelberg, Germany) including 0.004 ml/ml bovine pituitary extract, 10 ng/ml epidermal growth factor (recombinant human), 5 mg/ml insulin (recombinant human), 0.5 mg/ml hydrocortisone and 1% gentamycin (Ratiopharm GmbH, Ulm, Germany). The breast cancer cell lines MCF-7 (ATCC® HTB-22™; estrogen and progesterone receptor positive), BT-20 (ATCC® HTB-19™) and MDA-MB-231 (ATCC® HTB-26™), both triple negative cancer cell lines were cultured in Dulbecco's modified Eagle's medium (Gibco, Paisly, UK) with 10% fetal bovine serum (PAN Biotech GmbH, Aidenbach, Germany) and 1% gentamicin (Ratiopharm GmbH, Ulm, Germany). Confluent cells were treated with 0.05% trypsin– 0.02% EDTA. The medium was changed

every 2 days. Cell line authentication was performed by Seqlab Sequencing Laboratories (Göttingen, Germany).

Transcript analysis

Total RNA from cultured cells was extracted with the NucleoSpin® RNA II Kit (Machery-Nagel, Düren, Germany) and cDNA was produced from 2.5 μg of RNA with the First Strand cDNA Synthesis Kit (Thermo Fisher Scientific Inc., Rockford, IL, USA). qRT and RT-PCR was performed with the SGPL1 primer pair for transcript variant 1 (Tv1) fw: 5′-ATGCCTAG CACAGACCTTCT-3‘ and rv: 5′-CTTCCTGGTGAGCTTAAAACA-3′ amplifying a 240 bp fragment in the C-terminal region of the SGPL1 coding sequence. Primers flanking Tv1, Tv2 and all other NCBI annotated transcript variants were fw: 5′-ACTGCTCGCTTCCTCAAGTC-3′ and rv: 5′-GTGACAGTGTCGGTGCTGTA-3′ producing a 392 bp fragment. cDNA was mixed with iTaq™ SYBR® Green Supermix (Bio-Rad Laboratories Inc., Hercules, USA) and analyzed on iQ™5 Multicolor Real-Time PCR Detection System (Bio-Rad, München, Germany). Relative gene expression was normalized by using two housekeeping genes: GAPDH fw: 5′-CAAGGTCATCCATGACAACTTTG-3′ and rv: 5′-GTCCACCACCCTGTTGCTGTAG-3′, and ß-actin fw: 5´-GGGCATGGGTCAGAAGGATT-3´ and rv: 5´-GAGGCGTACAGGGA TAGCAC-3´.

Protein analysis

Western blotting procedure was performed as described previously [27]. Recombinant protein of human sphingosine-1-phosphate lyase 1 (SGPL1) was produced with TrueORF clone, RC208705 encoding the full-length human SGPL1 with C-terminal DDK tag, from human HEK293 cells (GenBank accession: NM_003901, Predicted molecular weight: 63.3 kDa, purchased from OriGene Technologies, Inc.Rockville, USA; CAT#: TP308705. For protein detection, primary antibodies (MaxPab®; ABIN948744, USA; β-Actin #4970: Cell Signaling, USA; GAPDH: sc-137179, Santa Cruz, USA) were incubated overnight at 4˚C followed by labeling with a horseradish peroxidase (HPR)-conjugated secondary antibody (Cell Signaling, USA) for 1 hour at room temperature. Protein signals were visualized by using SuperSignal West Femto Chemiluminescent Substrate (Pierce Biotechnology, Rockford, USA) for detection of peroxidase activity from HRP-conjugated antibodies. Band intensity was analyzed densitometrically with the Molecular Imager ChemiDoc XRS and Image Lab 3.0.1 software (Bio-Rad, USA). Protein detection was repeated at least three times with individually prepared cell lysates from independent passaged cells.

Immunofluorescence and immunohistochemistry

The basic procedure for the immunofluorescence staining was described in Engel et al. 2012, 2014 [28, 29]. Cells grown on Menzel-Gläser coverslips (Thermo Fisher Scientific Inc., Schwerte, Germany) or in Ibidi dishes/ slides (Ibidi GmbH, Martinsried, Germany) with glass bottoms were fixed in 4% paraformaldehyde (Santa Cruz, Dallas, USA), permeabilized with 0.1% Triton X-100 (Santa Cruz, Dallas, USA) and labeled with anti-SGPL1 primary antibody (SGPL1: sc-67368, Santa Cruz, USA) and Alexa Fluor 488 dye secondary antibody (Thermo Fisher Scientific Inc., USA). Co-localization experiments were performed with Phalloidin-Alexa 596 (Invitrogen), focal adhesion kinase (FAK) primary antibody (#3285, cell signaling, USA), ß1-integrin (#9699, cell signaling, USA) or with cell-permanent ER-Tracker™ Green dye (BODIPY® FL glibenclamide, Molecular Probes, USA) for live cell imaging. Finally, all samples were counter-stained with Hoechst (PanReacAppliChem, Darmstadt, Germany). Stainings were investigated with an inverted confocal laser-scanning microscope (LSM780, Carl

Zeiss, Jena Germany). Notably, images were taken at identical device settings to guarantee comparable results. The image processing was carried out using ZEN 2011 (Carl Zeiss Jena GmbH, Jena, Germany). The expression intensity and distribution of SGPL1 protein was determined in healthy (GTX24324, GeneTex, Irvine, USA) and tumorigenic (GTX24701, GeneTex, Irvine, USA) human breast tissue. Murine liver served as control. Tissues were formalin-fixed, paraffin-embedded, cut, labeled with a SGPL1 primary antibody (SGPL1: sc-67368, Santa Cruz, USA) in a 2% BSA solution followed by a secondary antibody—labeled, polymer —horseradish peroxidase (HRP) (Dako Envision+ Kit; Dako, Glostrup, Denmark). AEC (3-amino-9-ethylcarbazol) served as chromogenic agent. All sections were counterstained with Mayer's hemalum solution (Merck KGaA, Darmstadt, Germany). Each section was digitalized by using an AxioImager. M2 equipped with an integrated XY-scanning device and a MRc camera (all from Carl Zeiss Microscopy GmbH, Göttingen, Germany). Statistical evaluation of *in vivo* SGPL1 protein expression was performed by semi quantitative scoring (0 = no, 1+ = low, 2+ = medium, 3+ = strong and 4+ = very strong expression).

Scanning electron microscopy

General scanning electron microscopy method was described previously in Engel et al., 2016 [28]. For the visualization of SGPL1 cell membrane association, cells were grown on coverslips to a confluency of 80%. After washing with PBS with Ca^{2+} and Mg^{2+}, unspecific binding sites were blocked with 5% goat serum (PAN Biotech, Germany). Primary labeling with SGPL1 antibody (1:100 dilution of SGPL1 in 5% goat-PBS; sc-67368, Santa Cruz, USA) was performed at room temperature for 1 h. Secondary labeling with BBI gold anti-mouse antibody (1:200 dilution in 5% goat-PBS, 0.1% fish skin gelatin (BBI), 0,1% Tween (VWR, Germany); EM GMHL, 15 nm, BBI Solutions Cardiff, UK) was also performed for 1 h. After washing, cells were fixed with 2.5% glutaraldehyde in 0.05 M HEPES buffer. Samples were dehydrated in an ascending ethanol series and critical point dried using CO_2 as an intermedium with the EMITECH 850 critical point dryer (Emitech Ltd. Ashford, UK). Carbon coating was done with the carbon coater SCD500 (Leica, Germany). Images were taken with a field emission scanning electron microscope (Zeiss Merlin VP Compact) using an acceleration voltage of 5 kV for imaging.

Surface expression by flow cytometry

SGPL1 surface expression was measured by flow cytometry according to the measurements of other cell surface markers e.g. ß1-integrin, already described [29]. Briefly, after trypsinization, cells were washed with PBS (with 0.133 g/l $CaCl_2 \bullet 2H_2O$ and 0.1 g/l $MgCl_2 \bullet 2H_2O$, Sigma, Germany) and then incubated with 100 µl of the rabbit anti-SGPL1 antibody, recognizing a C-terminal epitope: amino acid 131–430 (cytoplasmic domain) sc-67368, Santa Cruz, USA for 1 h at room temperature. Thereafter, cells were washed and secondarily labeled with Alexa Fluor 488 dye secondary antibody (Thermo Fisher Scientific Inc., USA) for 1 h at room temperature in the dark. After a final washing step with PBS, cells were diluted in 300 µl CellFix (Beckman Coulter, USA). As control the whole staining procedure was carried out without the primary antibody—PBS was used instead. 10,000 events were recorded for each measurement of SGPL1 surface expression and repeated three times. Results were calculated with the software FlowJo (https://www.flowjo.com).

Migration analysis

Influence on migration was conducted on all five cell lines and stable SGPL1-transfected MCF-7 and BT-20 sorted cells, pre-incubated in assay medium for 48 h adaption in 6-well

plates (Greiner, Germany). A defined gap was made by Ibidi culture inserts (μ-Dish 35 mm; Ibidi GmbH, Martinsried, Germany) following the instructor's recommendations. When cell layers reached confluence, the culture insert was removed and cells were treated with 1 μM S1P or control (vehicle, MeOH) in assay medium (DMEM, 10% charcoal stripped fetal bovine serum (PAN BiotechGmbH, Germany). Medium was changed every day. Gap closure was analyzed as described previously [28].

SGLP1 expression clones

A SGPL1-cDNA-GFP-tagged clone (NCBI Accession: NM_003901, NP_003892.2) was purchased from OriGene (#RG208705, Rockville, USA). Plasmid map is shown in Fig 4B: Sequencing of the full-length transcript variant was carried out with two vector sequencing primer by Seqlab Laboratories (Germany). $3x10^6$ cells of breast cancer cell lines MCF-7 and BT-20 were transfected with 1 μg/ml SGPL1-DNA plasmid using the CLB-Transfection System (Amaxa Nucleofection 6097129; Lonza, Cologne, Germany) according to the manufacturer´s instructions. As positive control the Pmax GFP™ vector (Lonza, Cologne, Germany) was used. After 24 h, transfection efficiency was controlled with a confocal laser-scanning microscope. To generate stable transfected cells, GFP negative cells were eliminated by fluorescence-based cell sorting (BD FACSAria, Heidelberg, Germany).

Statistical analysis

All experiments were replicated at least three times with individually passaged cells, and data sets were expressed as means ± standard deviations (SD). Statistical significance was determined by the unpaired student's t-test or one-way ANOVA (*** $P < 0.001$; ** $P < 0.01$; * $P < 0.05$) using the software Graphpad Prism Version 5 (http://www.graphpad.com/scientific-software/prism/) or Excel 2016.

Supporting information

S1 Fig. Uncropped SGPL1 immune blots und the stainfree loading control (A) of Fig 1B. B: Normal exposure time for detection relative to the saturation of the pixel. C: Overexposed SGPL1 immuno blot.
(TIF)

S2 Fig. Verification of SGPL1 association with the plasma membrane of MCF-10A cells by flow cytometry. A: Gating of MCF-10A cells. B: Dilution series of primary (anti-SGPL1; 1:50, 1:100) and secondary (anti-rabbit Alexa488; 1:100, 1:200) antibodies to prove specific binding of the SGPL1 antibody. MCF-10A cells incubated with secondary antibody only, functioned as negative control (red histogramm). All signals with an FITC-A+ signal higher than $log10^3$ were counted as postive events. (Data for the 1:50 prim./ 1:100 sec. Ab. dilution are shown in the blue histogramm; for 1:50 prim./ 1:200 sec. Ab. dilution in the orange histogramm; for 1:100 prim./1:100 sec. Ab. dilution in the green histogramm and 1:100 prim./ 1:200 sec. Ab. dilution in the dark green histogramm.) The 1:50 dilution of the primary (SGPL1) and 1:100 dilution of the secondary Alexa488-labeled antibody were considered as the effective ones and were used for the experiment.
(TIF)

S3 Fig. A: SGPL1 expression status in healthy and cancer breast tissues, e.g. http://www.proteinatlas.org/ENSG00000166224-SGPL1/pathology. **B**: SGPL1 down-regulation is correlated with overall and relapse free survival of breast cancer patients. For example, you can check the online tool R2 for correlation analysis (https://hgserver1.amc.nl/cgi-bin/r2/main.cgi). The

following Kaplan Curves demonstrate impressively that low SGPL1 expression leads to poorer overall and relapse-free survival.
(TIF)

S4 Fig. A: Map of the SGPL1-ORF expression vector. **B**: Co-localization studies of SGPL1 with the endoplasmic reticulum. For further studies see http://www.proteinatlas.org/search/SGPL1. **C**: Scanning electron microscopy of gold-labeled SGPL1-proteins in the breast cancer cell line MCF-7 showed no signals.
(TIF)

Acknowledgments

This work is supported by fund from BMBF habilitation scholarship program of the University of Rostock and FORUN program of the University Medical Center Rostock (no. 889025). We wish to thank Petra Seidel (Dept. of Cell Biology, Rostock University Medical Center) and Daniel Wolter (Dept. of Oral and Maxillofacial Surgery, Facial Plastic Surgery, Rostock University Medical Center) for technical assistance and Dr. Robby Engelmann (Institute of Immunology, Rostock University Medical Center) for cell sorting. We thank Prof. Dr. Erbersdobler (Institute for Pathology, Rostock University Medical Center) for scoring of the IHC stainings. We thank Dr. Iris Hube and Dr. Niki Travis for the English editing service.8765

Author Contributions

Conceptualization: Nadja Engel, Karin Kraft.

Data curation: Nadja Engel, Anna Adamus, Marcus Frank, Juliane Kühn, Petra Müller, Annika Kasten.

Funding acquisition: Nadja Engel, Barbara Nebe.

Investigation: Annika Kasten.

Methodology: Nadja Engel, Anna Adamus.

Project administration: Nadja Engel.

Resources: Marcus Frank, Barbara Nebe.

Supervision: Nadja Engel, Guido Seitz.

Validation: Nadja Engel.

Visualization: Marcus Frank.

Writing – original draft: Nadja Engel.

Writing – review & editing: Anna Adamus, Marcus Frank, Barbara Nebe, Annika Kasten, Guido Seitz.

References

1. Spiegel S, Milstien S. Sphingosine-1-phosphate: an enigmatic signaling lipid. Nat Rev Mol Cell Biol 2003; 4:397–407. https://doi.org/10.1038/nrm1103 PMID: 12728273
2. Pyne NJ, Pyne S. Sphingosine 1-phosphate and cancer. Nat Rev Cancer 2010; 10:489–503. https://doi.org/10.1038/nrc2875 PMID: 20555359
3. Pitson SM. Regulation of sphingosine kinase and sphingolipid signaling. Trends Biochem Sci 2011; 36:97–107. https://doi.org/10.1016/j.tibs.2010.08.001 PMID: 20870412

4. Engel N, Lisec J, Piechulla B, Nebe B. Metabolic profiling reveals sphingosine-1-phosphate kinase 2 and lyase as key targets of (phyto-) estrogen action in the breast cancer cell line MCF-7 and not in MCF-12A. PLoS One. 2012; 7(10):e47833. https://doi.org/10.1371/journal.pone.0047833 Epub 2012 Oct 24. PMID: 23112854
5. Pchejetski D, Doumerc N, Golzio M, Naymark M, Teissie J, Kohama T, et al. Chemosensitizing effects of sphingosine kinase-1 inhibition in prostate cancer cell and animal models. Mol Cancer Ther 2008; 7:1836–45. https://doi.org/10.1158/1535-7163.MCT-07-2322 PMID: 18644996
6. Cuvillier O. Sphingosine kinase-1–a potential therapeutic target in cancer. Anticancer Drugs 2007; 18:105–10. https://doi.org/10.1097/CAD.0b013e328011334d PMID: 17159597
7. van Veldhoven PP, Mannaerts GP. Sphingosine-phosphate lyase. Adv Lipid Res 1993; 26:69–98. PMID: 8379460
8. Bandhuvula P, Saba JD. Sphingosine-1-phosphate lyase in immunity and cancer: silencing the siren. Trends Mol Med. 2007 May; 13(5):210–7. https://doi.org/10.1016/j.molmed.2007.03.005 PMID: 17416206
9. Reiss U, Oskouian B, Zhou J, Gupta V, Sooriyakumaran P, Kelly S, et al. Sphingosine-phosphate lyase enhances stress-induced ceramide generation and apoptosis. J Biol Chem 2004; 279:1281–90. https://doi.org/10.1074/jbc.M309646200 PMID: 14570870
10. Oskouian B, Sooriyakumaran P, Borowsky AD, Crans A, Dillard-Telm L, Tam YY, et al. Sphingosine 1-phosphate lyase potentiates apoptosis via p53- and p38-dependent pathways and is downregulated in colon cancer. Proc Natl Acad Sci U S A 2006; 103:17384–9. https://doi.org/10.1073/pnas.0600050103 PMID: 17090686
11. Kumar A, Oskouian B, Fyrst H, Zhang M, Paris F, Saba JD. S1P lyase regulates DNA damage responses through a novel sphingolipid feedback mechanism. Cell Death Dis 2011; 2:e119. https://doi.org/10.1038/cddis.2011.3 PMID: 21368890
12. Van Veldhoven PP. Sphingosine-1-phosphate lyase. Methods Enzymol. 2000; 311:244–54. PMID: 10563331
13. Bandhuvula P, Tam YY, Oskouian B, Saba JD. The immune modulator FTY720 inhibits sphingosine-1-phosphate lyase activity. J Biol Chem. 2005 Oct 7; 280(40):33697–700. Epub 2005 Aug 23. https://doi.org/10.1074/jbc.C500294200 PMID: 16118221
14. Dai L, Xia P, Di W. Sphingosine 1-phosphate: a potential molecular target for ovarian cancer therapy? Cancer Invest. 2014 Mar; 32(3):71–80. https://doi.org/10.3109/07357907.2013.876646 PMID: 24499107
15. Ferlay J, Soerjomataram I, Dikshit R, Eser S, Mathers C, Rebelo M et al. Cancer incidence and mortality worldwide: Sources, methods and major patterns in globocan 2012. Int. J. Cancer. 2015 Mar 1, 136: 359–386.
16. Maxmen A. The hard facts. Nature. 2012 May 30; 485: 50–51.
17. Den Hollander P, Savage MI, Brown PH Targeted therapy for breast cancer prevention. Front. Oncol. 2013 Sep 23, 3: 250. https://doi.org/10.3389/fonc.2013.00250 PMID: 24069582
18. Neve RM, Chin K, Fridlyand J, Yeh J, Baehner FL, Fevr T et al. A collection of breast cancer cell lines for the study of functionally distinct cancer subtypes. Cancer Cell. 2006 Dec; 10(6): 515–27. https://doi.org/10.1016/j.ccr.2006.10.008 PMID: 17157791
19. Hänel P, Andréani P, Gräler MH: Erythrocytes store and release sphingosine 1-phosphate in blood. FASEB J 2007; 21:1202–1209. https://doi.org/10.1096/fj.06-7433com PMID: 17215483
20. Zhang H, Desai NN, Olivera A, Seki T, Brooker G, Spiegel S. Sphingosine-1-phosphate, a novel lipid, involved in cellular proliferation. J Cell Biol. 1991; 114:155–67. PMID: 2050740
21. Pebay A, Wong RC, Pitson SM, Wolvetang EJ, Peh GS, Filipczyk A, Koh KL, Tellis I, Nguyen LT, Pera MF. Essential roles of sphingosine-1-phosphate and plateletderived growth factor in the maintenance of human embryonic stem cells. Stem Cells. 2005; 23:1541–8. https://doi.org/10.1634/stemcells.2004-0338 PMID: 16081668
22. Skoura A, Hla T. Lysophospholipid receptors in vertebrate development, physiology, and pathology. J Lipid Res. 2009; 50(Suppl):S293–298.
23. Olivera A, Eisner C, Kitamura Y, Dillahunt S, Allende L, Tuymetova G, Watford W, Meylan F, Diesner SC, Li L, Schnermann J, Proia RL, Rivera J. Sphingosine kinase 1 and sphingosine-1-phosphate receptor 2 are vital to recovery from anaphylactic shock in mice. J Clin Invest. 2010; 120:1429–40. https://doi.org/10.1172/JCI40659 PMID: 20407207
24. Ratajczak MZ, Lee H, Wysoczynski M, Wan W, Marlicz W, Laughlin MJ, Kucia M, Janowska-Wieczorek A, Ratajczak J. Novel insight into stem cell mobilization-plasma sphingosine-1-phosphate is a major chemoattractant that directs the egress of hematopoietic stem progenitor cells from the bone marrow and its level in peripheral blood increases during mobilization due to activation of complement cascade/

membrane attack complex. Leukemia. 2010; 24:976–85. https://doi.org/10.1038/leu.2010.53 PMID: 20357827

25. Engel N, Adamus A, Schauer N, Kühn J, Nebe B, Seitz G et al. Synergistic Action of Genistein and Calcitriol in Immature Osteosarcoma MG-63 Cells by SGPL1 Up-Regulation. PLoS One. 2017 Jan 26; 12 (1): e0169742. https://doi.org/10.1371/journal.pone.0169742 PMID: 28125641

26. Ramaswamy S, Ross KN, Lander ES, Golub TR. A molecular signature of metastasis in primary solid tumors. Nat Genet. 2003 Jan; 33(1):49–54. Epub 2002 Dec 9. https://doi.org/10.1038/ng1060 PMID: 12469122

27. Engel N, Falodun A, Kühn J, Kragl U, Langer P, Nebe B. Pro-apoptotic and anti-adhesive effects of four African plant extracts on the breast cancer cell line MCF-7. BMC Complement Altern Med. 2014 Sep 9; 14:334. https://doi.org/10.1186/1472-6882-14-334 PMID: 25199565

28. Engel N, Adamus A, Ali I, Dad A, Ali S, Nebe B, Atif M, Ismail M, Langer P, Ahmad VU. Antitumor evaluation of four selected pakistani plants on human bone and breast cancer cell lines. BMC Complementary and Alternative Medicine.2016, 16:244. https://doi.org/10.1186/s12906-016-1215-9 PMID: 27457235

29. Engel N, Kraft K, Müller P, Duske K, Kühn J, Oppermann C, Nebe B, 2015. Actin cytoskeleton reconstitution in MCF-7 breast cancer cells initiated by a native flax root extract. Adv Med Plant Res, 3(3): 92–105.

Literaturverzeichnis

Alves RC, Fernandes RP, Eloy JO, Salgado HRN, Chorilli. Characteristics, Properties and Analytical Methods of Paclitaxel: A Review. Crit Rev Anal Chem. 2018 Mar 4;48(2):110-118. doi: 10.1080/10408347.2017.1416283. Epub 2018 Feb 2.

Bray F, Ferlay J, Soerjomataram I, Siegel RL, Torre LA, Jemal A. Global cancer statistics 2018: GLOBOCAN estimates of incidence and mortality worldwide for 36 cancers in 185 countries. CA Cancer J Clin. 2018 Nov;68(6):394-424. doi: 10.3322/caac.21492.

Bublak R. PSA-Screening senkt die Krebsmortalität, aber … Artikel zu Schröder et al. mit Kommentar von L. Weißbach, Uro-News 2014; 18: 56.

Dad A, Ali I, Engel N, Atif M, Hussain H, Ahmad VU, Langer P. The Phytochemical Investigation and Biological Activities of Berberis Orthobotrys. Int J Phytomed. 2017 July; 9(2):213-8. doi: 10.5138/09750185.1899.

Engel N, Adamus A, Ali I, Dad A, Ali S, Nebe B, Atif M, Ismail M, Langer P, Ahmad VU. Antitumor evaluation of four selected pakistani plants on human bone and breast cancer cell lines. BMC Complement Altern Med. 2016 Jul 26;16:244. doi: 10.1186/s12906-016-1215-9.

Engel N, Adamus A, Schauer N, Kühn J, Nebe B, Seitz G, Kraft K. Synergistic action of genistein and calcitriol in immature osteosarcoma MG-63 cells by SGPL1 up-regulation. PLoS One. 2017 Jan 26;12(1):e0169742. doi: 10.1371/journal.pone.0169742.

Engel N, Ewald R, Gupta KJ, Zrenner R, Hagemann M, Bauwe H. (2011) The Presequence of Arabidopsis Serine Hydroxymethyltransferase SHM2 Selectively Prevents Import into Mesophyll Mitochondria. Plant Physiol. 2011 Oct 5.PMID: 21976482.

Engel N, Falodun A, Kragl U, Langer P, Nebe JB. Anti-proliferative and anti-adhesive effects of four plant extracts on the breast cancer cell line MCF-7. BMC Complement Altern Med. 2014 Sep 9;14:334. doi: 10.1186/1472-6882-14-334.

Engel N, Lisec J, Piechulla B, Nebe B. (2012) Metabolic profiling reveals sphingosine-1-phosphate kinase 2 and lyase as key targets of (phyto-) estrogen action in the breast cancer cell line MCF-7 and not in MCF-12A. PLoS One. 2012;7(10):e47833. doi:10.1371/journal.pone.0047833. Epub 2012 Oct 24.

Engel N, Müller P, Duske K, Oppermann C, Kraft K, Nebe B. Cytoskeletal remodeling of MCF-7 breast cancer cells under the treatment of the native root extract of Linum usitatissimum. Advancement in Medicinal Plant Research, Vol. 3(3), pp. 92-105, July 2015, ISSN: 2354-2152.

Engel N, Oppermann C, Falodun A, Kragl U. Proliferative effects of traditional Nigerian medicinal plant extracts on human breast and bone cancer cell lines. J Ethnopharmacol. 2011 Sep 2;137(2):1003-10.

Erharuyi O, Engel-Lutz N, Ahomaforb J, Imiejec V, Falodun A, Nebe B, Langer P. Anticancer activity of five Forest crops used in African folklore: antiproliferative and proapoptotic effects. Nat Prod Res. 2014 Feb 26. DOI: 10.1080/14786419.2013.879475.

Falodun A, Engel N, Kragl U, Nebe B, Langer P. Novel anticancer alkene lactone from Persea americana. Pharm Biol. 2013 Jun;51(6):700-6. doi: 10.3109/13880209.2013.764326. Epub 2013 Apr 9.

Harborne B: Phytochemical Dictionary- A Handbook of Bioactive Compounds from Plants. Verlag Taylor & Frost, London 1983.

Jain M, Nilsson R, Sharma S, Madhusudhan N, Kitami T, Souza AL, Kafri R, Kirschner MW, Clish CB, Mootha VK. Metabolite Profiling Identifies a Key Role for Glycine in Rapid Cancer Cell Proliferation. Science. 2012 May 25; 336(6084): 1040–1044. doi:10.1126/science.1218595.

Lisec J, Schauer N, Kopka J, Willmitzer L, Fernie AR. Gas chromatography mass spectrometry-based metabolite profiling in plants. Nat Protoc. 2006;1(1):387-96.

Lou S, Balluff B, de Graaff MA, Cleven AHG, Briaire-de Bruijn I, Bovee J, McDonnel LA. High-grade sarcoma diagnosis and prognosis: Biomarker discovery by mass spectrometry imaiging. Proteomics. 2016 June; 16:1802-1813. doi:10.1002/pmic.201500514.

McGowan EM, Alling N, Jackson EA, Yagoub D, Haass NK, et al. Evaluation of Cell Cycle Arrest in Estrogen Responsive MCF-7 Breast Cancer Cells: Pitfalls of the MTS Assay. PLoS One. 2011;6(6):e20623. doi: 10.1371/journal.pone.0020623.

Oriakhi K, Erharuyi O, Oikeh EI, Engel-Lutz N, Falodun A. Free radical scavenging and cytotoxic effects of methanol extract of Theobroma cacao L. (Sterculiaceae) seed. West Afr J Pharm 2015; 26(2):83-91.

Perkins GL, Slater ED, Sanders GK, et al; Serum tumor markers. Am Fam Physician. 2003 Sep 15;68(6):1075-82.

Taneja SS. Re: Screening and Prostate Cancer Mortality: Results of the European Randomised Study of Screening for Prostate Cancer (ERSPC) at 13 Years of Follow-up. J Urol. 2015 Aug;194(2):392. doi: 10.1016/j.juro.2015.05.064.

Wall ME, Wani MC. Camptothecin and taxol: discovery to clinic--thirteenth Bruce F. Cain Memorial Award Lecture. Cancer Res. 1995 Feb 15;55(4):753-60. Review.

Warsow G, Struckmann S, Kerkhoff C, Reimer T, Engel N, Fuellen G. Differential Network Analysis Applied to Preoperative Breast Cancer Chemotherapy Response. PLoS One. 2013 Dec 9;8(12):e81784. doi: 10.1371/journal.pone.0081784.

Welshons WV, Wolf MF, Murphy CS, Jordan VC. Estrogenic activity of phenol red. Mol Cell Endocrinol. 1988 Jun;57(3):169-78.

Zhang WC, Shyh-Chang N, Yang H, Rai A, Umashankar S, Ma S et al. Glycine Decarboxylase Activity Drives Non-Small Cell Lung Cancer Tumor-Initiating Cells and Tumorigenesis. Cell. 2012 Jan 20;148(1-2):259-72. doi: 10.1016/j.cell.2011.11.050.

Anhang

Übersicht der Veröffentlichungen

(*Korrespondierender Autor) (Impact-Faktor im Erscheinungsjahr)

Engel N, Oppermann C, Falodun A*, Kragl U. Proliferative effects of traditional Nigerian medicinal plant extracts on human breast and bone cancer cell lines. J Ethnopharmacol. 2011 Sep 2;137(2):1003-10. doi: 10.1016/j.jep.2011.07.023. Epub 2011 Jul 18. Impact Factor: 3.014

Engel N, Falodun A*, Kragl U, Langer P, Nebe JB. Anti-proliferative and anti-adhesive effects of four plant extracts on the breast cancer cell line MCF-7. BMC Complement Altern Med. 2014 Sep 9;14:334. doi: 10.1186/1472-6882-14-334. Impact Factor: 2.020

Engel N*, Adamus A, Ali I, Dad A, Ali S, et al. Antitumor evaluation of four selected pakistani plants on human bone and breast cancer cell lines. BMC Complement Altern Med. 2016 Jul 26;16:244. doi: 10.1186/s12906-016-1215-9. Impact factor: 2.94

Engel N*, Lisec J, Piechulla B, Nebe B. Metabolic profiling reveals sphingosine-1-phosphate kinase 2 and lyase as key targets of (phyto-) estrogen action in the breast cancer cell line MCF-7 and not in MCF-12A. PLoS One. 2012;7(10):e47833. doi:10.1371/journal.pone.0047833 Impact Factor: 4.82

Engel N*, Adamus A, Schauer N, Kühn J, Nebe B, Kraft K. Synergistic action of genistein and calcitriol in immature osteosarcoma MG-63 cells by SGPL1 up-regulation. PLoS ONE. 2017. doi: 10.1371/journal.pone.0169742. Impact Factor: 3.54

Engel N*, Adamus A, Frank M, Kraft K, Kühn J, Müller P, Nebe B, Kasten A, Seitz G. First evidence of SGPL1 expression in the cell membrane silencing the extracellular S1P siren in mammary epithelial cells. PLoS One. 2018 May 2;13(5):e0196854. doi: 10.1371/journal.pone.0196854.

Impact factor: 2.80

LEBENSLAUF

Persönliche Informationen:

Name:	Dr. rer. nat. Nadja Engel
Geburtsdatum:	3. September 1979
Geburtsort:	Rostock
Staatsangehörigkeit:	Deutsch
Dienstanschrift:	Klinik und Poliklinik für Mund-, Kiefer- und Plastische Gesichtschirurgie Schillingallee 35, 18057 Rostock
Email:	Nadja. Engel@med.uni-rostock.de

Hochschulstudium:

10/1998-01/2004	Studium der Biologie an der Universität Rostock mit den Schwerpunkten Pflanzenphysiologie, Biochemie und Biotechnologie
02/2004-01/2005	Diplomarbeit in der Pflanzenphysiologie an der Universität Rostock

Promotion:

02/2005-06/2009	Promotionsstudent an der Universität Rostock, Abteilung Pflanzenphysiologie unter der Leitung von Herrn Prof. Bauwe
08/2010	Promotion zum „Dr. rer. nat." an der Universität Rostock, Thema: „Functional characterization of the mitochondrial GDC and SHM gene families in *Arabidopsis thaliana* by complementation with heterologous genes" („Note: magna cum laude")

Postdoc:

09/2009-03/2016	Wissenschaftliche Mitarbeiterin/Postdoc in der Abteilung Zellbiologie der Universitätsmedizin Rostock (Leitung Herr Prof. J. Rychly; Frau Prof. B. Nebe)
07/2016-03/2018	Leitung des onkologischen Labors der Kinderchirurgie an dem Universitätsklinikum Marburg (Leitung Herr Prof. Dr. med. Guido Seitz)
Seit 04/2018	Leitung des Labors der Mund-, Kiefer-, Gesichtschirurgie an dem Universitätsklinikum Rostock (Leitung Herr Prof. Dr. Dr. B. Frerich)

Auszeichnungen:

1997	Gewinn des Landeswettbewerbes Jugend forscht in Mecklenburg-Vorpommern
1997	Gewinn des Spezialpreises des Bundeswettbewerbes Jungend forscht in Berlin und Teilnahme an dem internationalen Treffen "London International Youth Forum" in London, Uk
2006	Gewinn des Reinhold von Sengbusch-Preises in Dabringhausen für die beste Posterpräsentation
2011	Gewinn des BMBF-Habilitationsstipendiums für 36 Monate
2018	Auszeichnung für die beste wissenschaftliche Vortragstätigkeit im Rahmen DÖSAK (Deutsch-Österreichisch-Schweizerischer Arbeitskreis für Tumoren des Kiefer-Gesichtsbereichs) -Tagung vom 16. bis 17. November

Danksagung

Was lange währt, wird endlich gut.

Und dass es gut geworden ist, verdanke ich meiner Familie, meinen Freunden und Herrn Prof. Frerich. Ich bedanke mich bei Euch von ganzem Herzen!

Erklärungen

Hiermit erkläre ich des Eides statt, dass ich diese Habilitationsschrift mit dem Titel „Translationale Ansätze im Screening neuer Anti-Tumor-Wirkstoffe“ selbständig verfasst habe und dabei keine fremden, nicht erwähnten Hilfen verwendet hat.

Darüber hinaus erkläre ich, dass ich noch nie dieses oder eine anderes Habilitationsverfahren an dieser oder einer anderen Fakultät oder Hochschule eingeleitet habe.

Weiter erkläre ich hiermit, dass mir die Bestimmungen der Habilitationsordnung bekannt sind und diese auch anerkenne.

Datum/Ort: Unterschrift: